



Decision-Making Algorithms: Collective, Social, and Individual Learning

DISSERTATION

zur Erlangung des akademischen Grades

Doktoringenieurin (Dr.-Ing.)

angenommen durch die Fakultät für Informatik
der Otto-von-Guericke-Universität Magdeburg

von M. Sc. Palina Bartashevich

geb. am 01.03.1993

in Minsk, Belarus

Gutachterinnen/Gutachter

Prof. Dr.-Ing. Sanaz Mostaghim

Prof. Dr.-Ing. Heiko Hamann

Prof. Dr. Eliseo Ferrante

Magdeburg, den 12.11.2021

Bartashevich, Palina:
*Decision-Making Algorithms:
Collective, Social, and Individual Learning*

Dissertation, Otto von Guericke University
Magdeburg, 2021.

Abstract

Decision-making is considered as a vital mechanism that can allow linking multiple autonomous systems (e.g., agents) together to design a more intelligent and capable artificial system than considering each of them in isolation. To model or to engineer such a successful collective autonomous distributed system is a very challenging task, as the resulting collective behaviour is a self-organised and emergent phenomenon arisen from the local interactions between the agents and their environment. It does not rely upon a particular leader and is based only on incomplete and noisy sensory information acquired by single individuals. In this way, the collective decision-making mechanism and the underlying collective information processing represent one of the means of designing autonomy at the global level. The current thesis focuses on the question of how individuals have to integrate the personal noisy assessments of their physical and social surroundings to make accurate collective decisions.

The existing state-of-the-art collective decision-making strategies are dominated by biologically inspired approaches and generally established opinion-based models of voting. Although they are described as simple and have low computational requirements, they are highly dependent on the environmental context that can limit their performance. This thesis proposes solutions to enhance the accuracy, the speed, and the generality of existing collective decision-making algorithms, which can be generalised across various spatial patterns in the environment. In this regard, the thesis presents models of decision-making based on preferences and beliefs along with opinions. Furthermore, it proposes three mechanisms for sharing evidence to update personal beliefs. These mechanisms are defined as collective, social, and individual learning. The best-of- n problem is considered, where a swarm of artificial agents has to come to a consensus on the best option out of n available alternatives. Specifically, the collective perception scenario as the spatially distributed consensus achievement task is addressed and the issue of scalability for $n > 2$ is studied. For this purpose, the multi-featured benchmark set generator is proposed consisting of nine spatial visual patterns with different characteristics and noise variability.

We introduce an Ising-based binary decision-making model which includes preferences and opinions, generalising the state-of-the-art models of voting such as the majority rule and the voter model. Inspired by the cognitive dissonance theory, the proposed co-adaptation process of preference-opinion dynamics is designed to resolve the inconsistency between the agent's personal preference and an expressed opinion. As a result, the developed collective decision-making mechanism has been shown to be as fast as the majority rule while also being as accurate as the voter model, combining the best of both strategies. Moreover, assigning preferences to the agents initially in the process allows a designer to steer the self-organisation process to a particular outcome. Other strategies for controlling self-organised collective decisions utilising isomorphic transformations of the environment are also proposed in this thesis. The agent-based simulations conducted on a diverse set of environmental patterns show that the spatial distribution and clustering levels of the features, along with their quantitative ratio, define the difficulty of the task and can significantly deteriorate the collective performance. In this regard, we present the belief-based decision-making model employing the evidence theory in the context of the best-of- n framework. The experiments performed on the proposed benchmark set of collective perception scenarios with $n > 2$ options and twelve most com-

mon operators of evidence fusion indicate the viability and generality of the established collective decision-making strategy. Finally, the superiority of social learning over the collective and the individual learning types is highlighted in terms of the accuracy of the produced collective decisions.

Zusammenfassung

Entscheidungsfindung wird als ein wichtiger Mechanismus betrachtet, der es ermöglicht, mehrere autonome Systeme (z. B. Agenten) miteinander zu verbinden, um ein intelligenteres und leistungsfähigeres künstliches System zu entwerfen, als jedes einzelne von ihnen isoliert betrachtet. Ein solches erfolgreiches kollektives autonomes verteiltes System zu modellieren oder zu entwickeln ist eine sehr anspruchsvolle Aufgabe, da das resultierende kollektive Verhalten ein selbstorganisiertes und emergentes Phänomen ist, das aus den lokalen Interaktionen zwischen den Agenten und ihrer Umgebung entsteht. Es ist nicht auf einen bestimmten Anführer angewiesen und basiert nur auf unvollständigen und verrauschten sensorischen Informationen, die von einzelnen Individuen aufgenommen werden. Auf diese Weise stellen der kollektive Entscheidungsfindungsmechanismus und die zugrunde liegende kollektive Informationsverarbeitung eines der Mittel zur Gestaltung der Autonomie auf globaler Ebene dar. Die vorliegende Arbeit beschäftigt sich mit der Frage, wie Individuen die persönlichen verrauschten Einschätzungen ihrer physischen und sozialen Umgebung integrieren müssen, um korrekte kollektive Entscheidungen zu treffen.

Bestehende kollektive State-of-the-Art-Entscheidungsstrategien werden überwiegend von biologisch inspirierten Ansätzen und allgemein etablierten meinungsbasierten Modellen der Abstimmung dominiert. Obwohl sie als einfach beschrieben werden und einen geringen Rechenaufwand haben, sind sie stark vom Umgebungskontext abhängig, was ihre Leistung einschränken kann. Diese Arbeit schlägt Lösungen vor, um die Genauigkeit, die Geschwindigkeit und die Allgemeinheit bestehender kollektiver Entscheidungsalgorithmen zu verbessern, die über verschiedene räumliche Muster in der Umgebung verallgemeinert werden können. In diesem Zusammenhang stellt die Arbeit Modelle der Entscheidungsfindung vor, die auf Präferenzen und Überzeugungen sowie Meinungen basieren. Außerdem schlägt es drei Mechanismen vor, um durch einen Evidenztausch persönliche Überzeugungen zu aktualisieren. Diese Mechanismen werden als kollektives, soziales und individuelles Lernen definiert. Es wird das Best-of- n -Problem betrachtet, bei dem ein Schwarm von künstlichen Agenten einen Konsens über die beste Option aus n verfügbaren Alternativen finden muss. Insbesondere wird das kollektive Wahrnehmungsszenario als räumlich verteilte Konsensleistungsaufgabe behandelt und die Frage der Skalierbarkeit für $n > 2$ untersucht. Zu diesem Zweck wird ein Generator mit mehreren Merkmalen vorgeschlagen, der aus neun räumlichen visuellen Mustern mit unterschiedlichen Eigenschaften und Rauschvariabilität besteht.

Wir stellen ein Ising-basiertes binäres Entscheidungsmodell vor, das Präferenzen und Meinungen berücksichtigt und die State-of-the-Art-Modelle der Abstimmung wie die Mehrheitsregel und das Wählermodell verallgemeinert. Inspiriert von der Theorie der kognitiven Dissonanz ist der vorgeschlagene Co-Anpassungsprozess der Präferenz-Meinungs-Dynamik darauf ausgelegt, die Inkonsistenz zwischen persönlicher Präferenz des Agenten und einer geäußerten Meinung aufzulösen. Ergebnisse zeigen, dass der entwickelte kollektive Entscheidungsfindungsmechanismus so schnell wie die Mehrheitsregel und gleichzeitig so genau wie das Wählermodell ist, wobei es das Beste aus beiden Strategien kombiniert. Darüber hinaus erlaubt die Zuweisung von Präferenzen an die Agenten zu Beginn des Prozesses einem Designer, den Selbstorganisationsprozess auf ein bestimmtes Ergebnis zu lenken. Andere Strategien zur Steuerung selbstorganisierter kollektiver Entscheidungen, die isomorphe Transformationen der Umgebung

nutzen, werden in dieser Arbeit ebenfalls vorgeschlagen. Agentenbasierte Simulationen, die mit einer Vielzahl von Umgebungsmustern in dieser Arbeit durchgeführt wurden, zeigen, dass die räumliche Verteilung und die Clusterungsebenen der Merkmale sowie ihr quantitatives Verhältnis die Schwierigkeit der Aufgabe definieren und die kollektive Leistung erheblich verschlechtern können. In diesem Zusammenhang stellen wir das auf Überzeugungen basierte Entscheidungsfindungsmodell vor, das die Evidenztheorie im Kontext des Best-of- n -Frameworks verwendet. Die Experimente, die mit dem vorgeschlagenen Benchmark-Set von kollektiven Wahrnehmungsszenarien mit $n > 2$ Optionen und zwölf häufigsten Operatoren der Evidenzfusion durchgeführt wurden, zeigen die Durchführbarkeit und Allgemeinheit der etablierten kollektiven Entscheidungsstrategie. Schließlich wird die Überlegenheit des sozialen Lernens gegenüber der kollektiven und der individuellen Lerntypen in Bezug auf die Genauigkeit der produzierten kollektiven Entscheidungen hervorgehoben.

Contents

Contents	1
1 Introduction	1
1.1 Background and Research Topic	1
1.1.1 Preferences, Opinions, and Beliefs	6
1.1.2 Individual, Social, and Collective Learning	7
1.2 Decision-Making as the Best-of- n Problem	9
1.2.1 Overview of the Challenges	9
1.3 Research Goals and Objectives	11
1.4 Thesis Outline	12
2 Collective Perception as the Best-of-n Problem	15
2.1 Formalisation of the Best-of- n Problem	15
2.1.1 Existing Problem Classification	16
2.1.2 Application Scenarios	17
2.2 Collective Perception Scenario	17
2.2.1 Problem Statement	18
2.2.2 Concept of the Task Difficulty	18
2.2.3 Motion Specifications	18
2.3 Overview of the State of the Art	20
2.4 General Framework	23
2.4.1 Opinion-based Decision-Making	25
2.4.2 Evaluation Metrics	27
2.5 Summary	27
3 Preference-based Decision-Making for the Best-of-2 Problem	29
3.1 Problem Statement and Contribution	29
3.2 Mathematical Background	31
3.2.1 Ising Model	31
3.2.2 Social Impact Theory	33
3.3 Proposed Methodology	34
3.3.1 Opinion Dynamics	35
3.3.2 Preference Dynamics	38
3.4 Experimental Study	39
3.4.1 Impact of Indifferent Individuals	41
3.4.2 Influence of the Task Difficulty	43
3.4.3 Role of Opinion Initialisation	48
3.4.4 Physical Distance Dependency	49
3.5 Summary and Discussion	51
4 Influence of the Environment on Collective Decision-Making	54

4.1	Problem Statement and Contribution	54
4.2	Mathematical Background	55
4.2.1	Incidence Structures and Isomorphism	55
4.3	Proposed Methodology	56
4.3.1	Environment Representation and Transformation	56
4.3.2	Binary-Featured Benchmark Set	58
4.3.3	Patterns Metrics	60
4.3.4	Patterns Quantification	60
4.4	Experimental Study	61
4.4.1	Influence of Patterns on Collective Decision-Making	62
4.4.2	Influence of Isomorphic Transformations in the Environment	64
4.5	Summary and Discussion	68
5	Belief-based Decision-Making for the Best-of-many Problem	71
5.1	From Binary to Multi-Featured Collective Perception	71
5.1.1	Proposed Multi-Featured Benchmark Set Generator	72
5.1.2	Benchmarks Characteristics	73
5.2	Problem Statement and Contribution	75
5.3	Mathematical Background	77
5.3.1	Basics of Evidence Theory	77
5.3.2	Mass function types	78
5.3.3	Fusion Rules	79
5.4	Proposed Methodology	85
5.4.1	Belief-based Decision-Making	85
5.4.2	Individual Learning	87
5.4.3	Collective Learning	88
5.4.4	Social Learning	88
5.4.5	Evaluation Metrics	89
5.5	Experimental Study	90
5.5.1	Convergence Analysis - I	90
5.5.2	Convergence Analysis - II	97
5.5.3	Comparison of Individual, Social, and Collective Learning	102
5.5.4	Influence of the Population Size	107
5.5.5	Scalability with the Increased Number of Options	109
5.6	Summary and Discussion	113
6	Conclusion	117
6.1	Research Contributions	117
6.2	Limitations and Future Research Directions	120
	List of Figures	123
	List of Tables	126
	List of Algorithms	129
	Bibliography	130

A Parameters of Collective Perception Scenario	145
B Supplementary Material to Chapter 3	146
C Supplementary Material to Chapter 5	148
C.1 Statistical Analysis of Collective, Social, and Individual Learning . . .	148
C.2 Statistical comparison - I: Collective, Social, and Individual Learning .	154
C.2.1 Collective vs Social Learning, $\rho = 0.67$	160
C.2.2 Collective vs Individual Learning, $\rho = 0.67$	161
C.2.3 Social vs Individual Learning, $\rho = 0.67$	162
C.3 Statistical comparison - II: Collective, Social, and Individual Learning	163
C.3.1 Collective vs Social Learning, $\rho = 0.93$	169
C.3.2 Collective vs Individual Learning, $\rho = 0.93$	170
C.3.3 Social vs Individual Learning, $\rho = 0.93$	171

Introduction

Decisions are a ubiquitous part of daily life. The ability to decide refers to one of the most important aspects of intelligence and is, therefore, considered as the desired property to replicate in an Artificial Intelligence (AI) system. Under the decision, we mean a direct selection between several given alternatives. It is a common assumption that decisions made by a group are more robust than individual ones. Both biological and artificial collectives are constantly faced with making choices based mostly only on *partial* and *noisy information* provided by their *physical* and *social surroundings*. Therefore, to ensure an expected superiority of shared decision-making, special attention should be paid to the exploitation and processing of social and environmental information at the collective level. The current thesis presents contributions in this regard and studies the impact of environmental and social biases on decentralised collective decision-making in spatially distributed discrete consensus achievement tasks.

This chapter provides a general overview of the topic as well as a motivation for the proposed methodology and the key concepts used in the thesis. Afterwards, the decision-making as the *best-of-n problem* is outlined along with the summary of the existing challenges. Finally, the research questions and objectives of the thesis are stated and an outline is given.

1.1 Background and Research Topic

The design of the state-of-the-art collective decision-making algorithms is primarily biologically inspired. Social insects such as ants or honeybees can leverage *environmental bias* based on simple heuristics and perform group decisions, making them one of the most popular models of collective decision-making (Sasaki and Pratt, 2018). In this context, a cognitive aspect of a single individual is often not considered in much detail. Nonetheless, each individual is also a cognitive unit with personal *motivations*, *preferences*, and *beliefs* guiding its individual decisions (Amdam and Hovland, 2012). These are often hidden from an agent itself and formed during the decision-making process, impacting alongside the choices of an agent as well as of the others. As such, they can be considered as a flexible tool to manipulate collective decisions. To that end, the current dissertation endeavours to examine the possible mechanisms underlying collective cognition.

In the following, we briefly consider (1) how decision-making is carried out at different levels of living organisms, (2) factors that can affect the speed and accuracy of decisions in natural systems, and discuss (3) the cognitive approach to modelling decision-making as a philosophy for the methodology developed in this thesis.

Decision-making across scales

While the human brain serves as the common model and an inspiration for AI, it is not considered as a single entity but as a collection of approximately 86 billion neurons (Azevedo *et al.*, 2009) that interact with each other forming a large distributed network. Each neuron performs its own internal computations based on the inputs from the sense organs of the human body and the other neurons from different areas of the brain. The communication between neurons is done by means of sending electrical impulses, where the firing rate of interactions identifies the strength of the connections and, hence, the way an incoming signal is processed and how the human reacts as a whole to the particular external stimulus. Being faced with a choice problem as a cognitive task, the brain areas responsible for decision-making are activated and a decision is assumed to be taken when a firing rate threshold is met by the neurons related to a particular choice (Potemkowski, 2017). In this way, the undertaken decision is considered as an outcome of not a single neuron but of a whole assembly of neurons driven by their multiple inter-individual interactions, which, in turn, identify the end result. Since neurons form a distributed static network with fixed positions in the brain, the way the inner connections between neurons are established is what makes each human being's problem-solving style unique (Smith and Ratcliff, 2004). As a result, *decision intelligence* in this case can be viewed as an emergent property of a human brain, which is arisen from the local interactions of neurons with each other triggered by an input received from the outside physical surrounding.

Similar structures are also observed in biological systems such as insect colonies (e.g., ants), slime mould or the immune system. Each individual in such a system acts in a role of a neuron but in contrast to the "solid" human brain, the created network is characterised by the ability of its nodes (individuals) to change their physical positions in space and time, that is, to move. As a result, the inter-individual connections are not fixed and are not reinforced as much between particular nodes but more conditioned by their movements and the immediate neighbourhood at a certain time. In this scope, Solé *et al.* (2019) has proposed the term "*liquid brain*" for describing the system, which implies the network of dynamic (i.e., non-static) elements with unstable connections. The introduction of the name of the term is not a coincidence, since the behaviour of such systems resembles the behaviour of fluids (liquids) along with the inheritance of similar properties (Tennenbaum *et al.*, 2015). It is assumed that physical movement and dynamic local interactions complicate the system in a non-trivial way compared to a "solid brain", where the positions of the network's elements are fixed (Solé *et al.*, 2019). A number of studies have shown that despite being a brainless organism (e.g., slime mould, fungi), "liquid brain" system as the whole is successful in solving optimisation problems such as finding the shortest path (Bonifaci *et al.*, 2012; Adamatzky, 2014) or performing decision-making tasks related with nutritional decisions (Dussutour *et al.*, 2010; Beekman and Latty, 2015; Reid *et al.*, 2016).

The principle of “acting together as a whole, one can achieve more than the sum of its solitary parts” is also inherent to more sophisticated living organisms like birds, animals, and even human beings themselves. In this instance, a single individual alone already represents a fully functioning autonomous bio-system that is able to solve tasks on its own. However, the emergent phenomenon of interest, in this case, is observed on a higher level of organisation, that is, the society. As most social creatures, the individuals from the corresponding representative group are highly affected by the interactions with each other and their behaviour in the closest physical surroundings, similar to the neurons in “solid” and “liquid” brain. In this way, the decision-making process is also considered to be done in a group, where everyone’s decision is induced by the choices done by the others, forming a “collective mind”. Many animal species (e.g., primates, fish) and social insects (e.g., bees, ants) benefit from such sharing decision-making, which allows them to find better places to nest, feed, and to migrate, keeping them alongside together to enhance their chances on survival before predators (Strandburg-Peshkin *et al.*, 2015; Couzin, 2018). The resulting collective behaviour is referred to as *swarm intelligence* and is considered to be a self-organised and emergent phenomenon arisen from local interactions between individuals.

Speed and accuracy of collective decision-making in natural systems

Swarm intelligence benefits from the inter-individual interactions, allowing a collective to solve complex cognitive tasks unbearable to a single individual unit. Nevertheless, the speed and accuracy trade-off (SAT) during natural decision-making has been traced on all scales of the aforementioned living systems. That is, fast decisions are likely to be unreliable while improving the accuracy requires more information and, hence, more time and costs to perform (Zimmerman, 2011).

Often a connection between the *difficulty of the task* defined by the physical environment and the speed and accuracy with which it is solved is examined. However, the latter is not always concerned with the SAT problem. For instance, the difficulty of natural discrimination tasks, in which it is necessary to distinguish between sensory inputs and to react accordingly, often lies in the similarities between the target alternative and the other options serving as distractors (Franks *et al.*, 2003; Perry and Barron, 2013). In this regard, the evidence from the study on honey-bees foraging behaviour (Dyer and Chittka, 2004a; Dyer and Chittka, 2004b; Skorupski *et al.*, 2006) shows an increase in the decision time but also decrease in the selection success, when the colours of the fruitful sources are not clearly dissimilar from the unfruitful ones.

The SATs are often observed in tasks with *negative stimuli* in the form of a “stressor”, which induces a bias into the system. As such, limiting the time to perform a certain cognitive task often leads to a decrease in the accuracy of human decision-making, while for more difficult tasks in general more time is required to undertake a decision (Pachella, 1973). The choice between food options under the light exposure forces slime mould to make quicker and usually more inaccurate decisions preferring the ones in the shaded areas to avoid the harmful impact threatening its survival (Latty and Beekman, 2011). There, the SAT problem can be further complicated with the setup of less distinguishable options. That is, an incorrect choice between similar options is characterised by less cost (penalty) since their differences are not significant to be harmful to survival relative to the “stress” factor.

Similarly, in spatially distributed decision-making tasks, a *spatial factor* brings additional costs impacting the exploration process. That is, the closer-located options (e.g., new nest sites, food sources) are more preferable than the distant ones, though the latter can turn out to be of better quality. Nevertheless, Franks *et al.* (2008) has found that ants decide on a new nest site based on the quality and not on the distance from the old nest, using the closer options only as an auxiliary step towards more distant and better alternatives. Furthermore, the studies on nest-site selection by honey bees (Passino and Seeley, 2005; Passino *et al.*, 2008; Makinson *et al.*, 2010; Laomettachit *et al.*, 2015) also indicated that bee swarms are able to select high-quality sites regardless of their distance but required more time to reveal them (Janson *et al.*, 2007; Zurbuchen *et al.*, 2010). Overall, time has to be spent to achieve an accurate decision. In this regard, one can suppose that the SATs observed in natural systems often appear as the result of the trade-off between the quality of the options and their costs such as, e.g., the time necessary to explore them. However, exploration time is not the only factor that can affect a group’s performance costs (effort).

To reinforce weak (distanced) signals, social colonies rely on the mechanism of the *positive feedback*¹ (Sasaki and Pratt, 2018). It acts as a means of coordination between group members and controls foraging dynamics, helping them to spread information quickly and reach an agreement. As a result, the number of individuals that favour a given option grows with an increase of the number of individuals already committed to it, creating a *positive cascade*. However, in addition to reaching a consensus with a relative fast speed, it also tends to magnify errors in the system. As a consequence, when many noisy evaluations are coupled with a positive feedback mechanism, the collective outcome can turn out to be highly inaccurate. In this regard, Nicolis *et al.* (2011) claim that the positive feedback is a heuristic that produces quick and effective group decision-making, but is often prone to “irrationality” in specific environmental conditions. Indeed, as a heuristic, it is considered as more *domain-specific* than *domain-general*. According to Gigerenzer and Gaissmaier (2015), it operates successfully in environments in which it is meant to be “ecologically rational”. That is, a chosen heuristic has to match with the structure of an environment and be able to exploit it. In this way, the environment itself can assist the heuristic. Considering this, the accuracy of the collective decisions done by natural systems based on positive feedback should always be assessed in relation to a particular environment and its structure (Nicolis *et al.*, 2011; Sumpter *et al.*, 2012).

A cognitive approach to modelling decision-making

One can draw a parallel between the *positive feedback* loop, which is a mechanism of behavioural ecology, in social insects and the feedbacks between the neurons in the human brain. However, while decision-making models of behavioural ecology (Mangel and Clark, 2019) mainly focus on how individuals interact with their surroundings, they ignore the underlying neurological (psychological) mechanisms that occur in the brain. In this regard, the model of an agent is often oversimplified (DeAngelis and Diaz, 2019), neglecting the fact that it is also a cognitive entity on its own and can possess attitudes along with multiple mental states, such as, e.g., preferences and beliefs.

¹Positive feedback is a force that strengthens a commitment to a particular choice. As an example, pheromone trails left by foraging ants result in a positive feedback allowing to find the best food source.

The behavioural ecology is based on the assumption of the *rational agent model* as in economic theory (Kacelnik, 2006), where the individuals act to maximise their fitness (utility). Nevertheless, the decision-making process can not be viewed as completely rational as it is often based on *objective* and *subjective*² information. Indeed, even when designing rational decision-making in technical systems, one can talk only about *bounded rationality* (Simon, 1990) due to the incomplete and imperfect sensory information, computational capacity, time restrictions, and chosen heuristics. That is, even though an artificial agent can be programmed to make rational decisions, it will be still limited by its technological and design constraints. Overall, the views on the concept of “rationality” vary depending on the research field, be it psychology, biology, economics or neuroscience, and their philosophical discussion is beyond the scope of this thesis.

In this thesis, we refer to the BPC³ model of rationality as defined by Gintis (2005). He postulates that the agents’ choices are driven by their cognitions such as *beliefs* (B) and *preferences* (P), along with *constraints* (C). It is supposed to serve as a general framework unifying the behavioural sciences, avoiding connotations of “rationality”, and, therefore, has been chosen as a motivation for the proposed methodology in the current thesis. In addition, it also encompasses the concept of bounded rationality under incomplete knowledge assumption. Although BPCs are commonly considered in real life, combinations of these cognitive states together are rather understudied in the AI literature (Rouahi *et al.*, 2018) and their definitions are often confused (see Section 1.1.1). The BPC model is commonly considered within a single individual, but there is nothing that can prevent it from also considering the welfare of other individuals in a group setting (Gintis, 2005). However, in the collective context, the interactions between agents with different mental states can complicate the process of achieving a common group decision. In this scope, the mental states of the agents have to evolve together with the choices and to adapt through social interactions respectively (Hoogendoorn *et al.*, 2010).

Considering that the agents can possess heterogeneous mental states, the desire to maintain inclusion in the group and, hence, consensus can lead to a state known as *cognitive dissonance*. According to the theory of cognitive dissonance proposed by Festinger (1957), an individual always seeks alignment (consonance) of its cognitive states. That is, the beliefs, preferences, and choices of an individual have to be consistent with each other. As a typical example of cognitive dissonance, one can consider the case when a person wants to get rid of some habit, but still consciously continues to follow it. In this example, the cognition (preference/belief) of an agent and its choice are in disagreement with each other. It is assumed that being in such a state causes cognitive distress, which motivates actions from an individual aimed at reducing it. As one of the techniques to minimise cognitive dissonance, one can either modify the importance of his/her cognition (e.g., persuade yourself that the habit is harmful) or completely change it (e.g., decide that you did not really want to get rid of this habit). Both approaches aim to rationalise the choice which has been taken in the past and cannot be reversed, but the resulting alteration in cognitions can lead to new behaviours in the future.

When an individual is considered as a member of a social group, the social group can induce as well as reduce cognitive dissonance. Festinger (1957) stated that cognitive

²An agent is subjectively rational when its decisions are consistent with the available evidence and, in the absence of these, with its own subjective estimates.

³BPC is a short form for “beliefs, preferences, and constraints”.

dissonance in a group occurs when its members openly express a disagreement. According to his theory, the fact that another member of a homogeneous group has a different opinion from my own generates *dissonance*, which causes discomfort and triggers individual mechanisms to mitigate it. Indeed, if an agent is in a state of consonance, e.g., its choice and preference are both towards an option *a*, but acquires a new piece of information from its social environment which is towards another option *b*, the agent enters the *dissonance state*. That is, in such a case, the post-decision cognitive alteration will be activated regardless of the agent’s decision to keep its opinion *a* or to change it to *b*. As such, while initial disagreements between agents can be transformed into collective consensus, intra-individual inconsistencies⁴ are resolved over time as well. The latter can also lead to the formation of the shared social cognition in terms of homogeneous attitudes and mental states (Matz and Wood, 2005). Overall, cognitive dissonance has been shown to have a larger impact on the systems with strong self-organisation properties (Colosio *et al.*, 2017). In this regard, it acts as a driving force of *implicit cognitive bias* that alters decision-making and social interactions.

Despite the capacity for cognitive dissonance in human behaviour has long been recognised and researched in the social and cognitive sciences, it has received little attention in the design of artificial (robotic) systems. While there is some research motivated by cognitive dissonance to address the problem of designing intrinsic motivation systems (Kaplan and Oudeyer, 2007), no studies have been found which investigated its impact on the design of bio-inspired collective decision-making strategies.

1.1.1 Preferences, Opinions, and Beliefs

In the following, we discuss the basic terminology used in decision sciences and throughout this thesis. Namely, the definitions of the terms such as “constraints”, “information”, “knowledge”, “beliefs”, “opinions”, and “preferences” are given. According to Corcoran and Hamid (2015), the last four mainly differ in the levels of certitude and are all interdependent on each other (see Figure 1.1).

Constraints introduce limitations that sort out the set of alternatives from which the choice can be done in a given situation due to specific characteristics of the system and, in this way, partially predefine the decisions (Gintis, 2010). *Information* refers to data or a state (not necessarily a true one) which is received or communicated. *Knowledge* is considered as the objective personal state of the highest level of certitude, while beliefs and opinions are representatives of subjective states with relatively higher and lower certitude respectively. *Beliefs*, being subjective states, can be taken as the *knowledge* in case if their true state is justified by the perceived evidence, otherwise they express a certain degree of hesitation. In contrast, *opinions* do not reassure any rate of reliability in any way as they primarily reflect the preferences and the beliefs of the individual rather than the (true) knowledge. It is also said that “a belief not known to be true is considered to be an opinion” (Corcoran and Hamid, 2015). In general, beliefs are associated with the probability of a certain outcome that will result from a predetermined choice, i.e., represent internal representations of the relationship between actions and outcomes (Steele and Stefánsson, 2016). According to Hausman (2012), *preferences*

⁴Under intra-individual inconsistency, we mean the case when the agent holds a cognition towards one option *a* but chooses another option *b*.

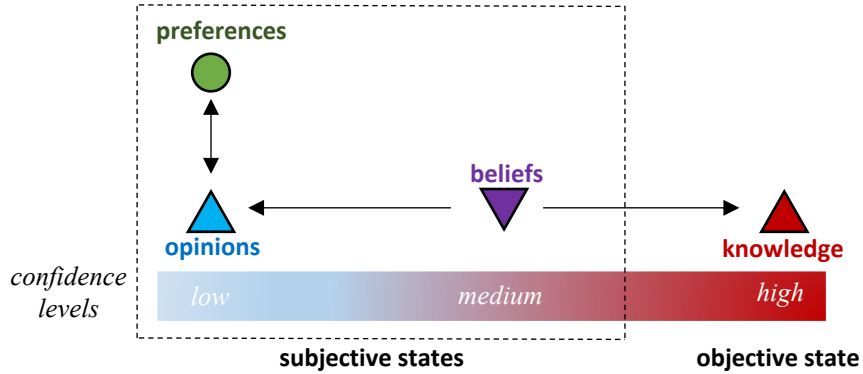


Figure 1.1: Mental states of different confidence levels. *Preferences* represent pre-opinions and coevolve with the opinions themselves together in a closed-loop. Depending on the amount of justification, *beliefs* can pass into *opinions* or *knowledge*. Opinions, beliefs, and knowledge can be considered as *information*.

are subjective states that are defined not only by choices of the individuals but are also considered to be subject to the *beliefs*. As such, *preferences* are the subject of both, opinions and beliefs, and define the individuals' rationality in terms of how the individuals perceive the information. One can expect preferences to be consistent with the choices but not necessarily serving the collective goals (i.e., welfare-enhancing).

1.1.2 Individual, Social, and Collective Learning

Possessing a variety of different mental states can create confusion regarding what kind of information to communicate and, hence, which states to share between individuals. Furthermore, their subjectivity can lead to social biases hindering the success of the group (Bang and Frith, 2017). In the following, we operate with the definition of '*learning*' as an update in the knowledge that results from the experience. In such a setting, we consider *learning* and *decision-making* to be interwoven with each other, since undertaken decisions usually depend on what agents have learned about the state of the world and are, therefore, considered further as a product of learning.

There is evidence that in severe circumstances, individuals count more on their own decisions than on the decisions of other individuals. For instance, Franks *et al.* (2003) observed that individual decision-making prevails over the collective one in ants foraging, when the ants are faced with the wind. Under individual decision-making, one considers a type of *asocial learning* based only on accumulating clues from the environment without communication with other individuals. As a result, agents use only personally obtained information from the environment by observation and their own "reflections". Only recent and past individual information is combined to shape the representation of the environment, subject to the agent's personal mental state.

Situations, when more attention is paid to the accuracy than to the speed, relate to the conditions which do not introduce a threat to the agents' survival, allowing individuals to consider the actions of the others (Franks *et al.*, 2003). Decision-making promoted by observing or interactions with the other individuals as well as the artefacts which they leave (e.g., pheromones) is referred to as a *social* type of learning (Heyes and

Galef, 1996; Huber, 2012). The terms ‘*social*’ and ‘*collective*’ are often interchangeable and confused in the literature, as both imply the exchange of information with other members. In this thesis, we distinguish them based on the content of the transferred information and the way it is integrated with already existing personal information of an individual itself.

One of the easiest social mechanisms to deal with limited cognitive abilities and incomplete information about the environment is considered to be *imitation*, where individuals ignore their personal information and simply copy the behaviour of / or information from a demonstrator (Conlisk, 1980; Hoppitt and Laland, 2013). In a swarm context, each individual can be in the role of a demonstrator and an observer at the same time, creating coupled dynamics between the decisions of the individuals. The resulting emergent phenomenon is also known as *herding*, which is commonly observed in certain species of mammals and birds (Zhao *et al.*, 2011). Though simple, it allows birds to stay together as a flock along the migration routes, maintaining collective consensus on the direction of movement despite the possible negative influence coming from the external environment, e.g., headwinds. It primarily promotes the transfer of navigational information from informed to uninformed individuals in a group and through generations. According to Berdahl *et al.* (2018), such a uni-directional process of passing personal or observed environmental information to other individuals in a swarm is referred to as *social learning*. In this regard, under *social decisions* we mean decisions/actions undertaken by the individuals based on the information received in the scope of the particular social learning procedure driven by imitation or transfer of unprocessed information from informed to uninformed members.

Meanwhile, preserving personal information is considered to be desirable and beneficial in most natural and artificial systems, as the individuals can differ in their decision-making abilities as well as in their access to the information. Marshall *et al.* (2017) argue that the weighted aggregation of individual decisions in a group is usually underestimated in the research on collective animal behaviour, although there is theoretical evidence that it can promote better decisions. However, it is also a more costly procedure than imitation, since it requires communication and combination of different pieces of information. The same holds for enhancing the individuals’ capabilities with more sophisticated learning mechanisms preceding decision-making such as associative learning, i.e., learning with reinforcement and matching environmental cues with rewards, which has shown to be efficient as well in the collective context (Kao *et al.*, 2014). As such, the cumulative incorporation of information from other individuals over multiple social interactions into private individual information within time, including further transfer of the obtained accumulated knowledge, is referred to as *collective learning* (Berdahl *et al.*, 2018). Thus, new knowledge emerges from numerous interactions between individuals, while social learning rather promotes the dissemination of information (evidence) not known to others. In this way, decisions/actions based on the exchanged accumulated acquired partial information from the environment and from other individuals are referred to as *collective decisions*.

As an illustrative example: a student doing coursework performs an *individual type of learning* provided that he/she relies on his/her own gained knowledge; students attending a lecture are subjects of a *social type of learning* passively accumulating information from a lecturer; while the development of the ideas in a research group is already considered

as *collective learning* in the result of which new knowledge can emerge.

1.2 Decision-Making as the Best-of- n Problem

A decision is a choice out of multiple options, carried out by a system based on information gained as a result of learning about the state-of-the-world prior to the decision-making process. Unattached from any kind of scenario, reaching an agreement between multiple system's elements, i.e., agents, over the best choice from a set of available possibilities is classified as the *best-of- n problem*. Under '*the best*' is meant an option that maximises (or minimises, dependent on the *common* goal) a certain given task-related metric or a fitness function of the system. Such type of problem has been primarily studied for many years in a biological context addressing the behaviour of natural systems (Conradt and Roper, 2005) and served later on as an inspiration for the development of the decentralised collective decision-making algorithms for multiple-robot systems (Parker and Zhang, 2004; Parker and Zhang, 2009; Parker and Zhang, 2011).

Artificially replicating collective decision-making of self-organised systems is assumed to be particularly challenging. Without a central control unit, it relies on partial information assessed from local perceptions and local communications between the individuals. As a result, a collective decision is regarded as an outcome of an emergent process that is difficult to predict (Valentini *et al.*, 2014). It is also considered as one of the basic swarm behaviours and the prerequisite in a range of swarm robotics applications (Brambilla *et al.*, 2013; Bose *et al.*, 2017; Schranz *et al.*, 2020). However, the developed algorithms are usually rather problem-specific and designed to address a particular scenario. In this regard, Valentini (2017) has derived the concept of the *best-of- n problem*, which unifies most of these application scenarios, representing itself an abstract model of the consensus achievement task. That is, he has introduced a modular framework for the design of decentralised collective decision-making algorithms based on the work of Parker and Zhang (2009). In comparison to their previous work, it provides the possibility to consider different types of decisions, including individual decision-making of the agents. In this regard, Valentini (2017) has mainly studied opinion-based decision-making strategies for $n = 2$ options, where each agent shares its opinion with other individuals and changes it according to the voting rules. As such, due to the modular structure and supposed generality of the best-of- n framework⁵, it has been also selected as the basis for studying discrete decentralised decision-making in the current thesis.

1.2.1 Overview of the Challenges

The work of Valentini (2017) caused further interest in the swarm robotics community to address the case of multiple options, e.g., Lee *et al.* (2018a), Ebert *et al.* (2018), Talamali *et al.* (2019), although concentrating mainly on the variations of the problem with *asymmetric quality* and *symmetric cost*⁶. Theoretical study of the best-of- n problem by Reina *et al.* (2017) has shown that increasing the number of alternatives can significantly alter the swarm dynamics. The particular attention was paid to the analysis

⁵For more details, we refer the reader to Section 2.4.

⁶The existing classification of the best-of- n problem with respect to the *quality* and *cost* is given later in Section 1.2, where *symmetric* corresponds to equal values and *asymmetric* to differing ones.

of the signalling ratio and, hence, the impact of the strength of positive feedback on the decision process. In this regard, the optimal strength of positive feedback can differ between the number of options. According to Nicolis *et al.* (2011) and Sumpter *et al.* (2012), the feedback rate which generates good decisions for a larger number of options can lead to poor decisions for a smaller one. Nevertheless, the binary variant ($n = 2$) of the best-of- n problem dominates the current research in the field of swarm robotics and requires adaptations of the existing methods for $n > 2$.

The presence of a bias in the physical environment can impose asymmetry in the cost of the options, e.g., expressed as travel distance to the food source during foraging. Previous studies (Passino and Seeley, 2005; Reina *et al.*, 2015) have shown that a swarm that can not compensate for environmental bias selects less costly alternatives regardless of their quality. As a result, the high-quality options which are harder to reach can be overlooked in favour of less costly but lower-quality ones, leading to inaccurate decisions. In this way, an environmental bias induces a negative impact on the collective decision-making process. To the best of our knowledge, after the study of Valentini (2017) only a few works addressing the negative environmental bias in the context of the best- n problem have appeared. Based on the prior work of Reina *et al.* (2015), Cody (2018) has investigated in computer simulation a value-sensitive collective best-of- n decision strategy in the context of the task sequencing framework. Specifically, he proposed mechanisms of interaction delays to control the relative importance of the option's cost and quality. Talamali *et al.* (2020) examined the distance-quality trade-offs within the model of the optimal foraging theory and developed it to address the negative environmental bias. The virtual pheromone trails as observed in ant's colonies were employed. Both studies imply *asymmetric cost* of the options in terms of the distance between the option (source area) and the central gathering depot of the agents (the 'nest'), assuming that the system is well-mixed ⁷ and has access to the global qualities of the sources. In general, violation of the aforementioned assumptions complicates the decision-making process, resulting in poor collective performance (Trabattoni *et al.*, 2018). Indeed, considering that the agents interact only in the 'nest', a longer distance to the source (i.e., a longer exploration time) implies that some individuals interact more often than the others, thereby infringing the well-mixed state. Controlling the time agents spend in the 'nest' by adjusting the direct modulation of positive feedback can thereby even communication chances, helping agents to overcome the *spatial bias* and leading the group towards high-quality decisions (Cody, 2018; Talamali *et al.*, 2020).

While 'nest'-containing scenarios are common for natural systems, in real-world applications, such as, e.g., environmental monitoring, multiple returns to the base can be considered as impractical and energy-consuming, especially when faced with many options ($n > 2$). That is, the physical environment can impose additional challenges (e.g., rough terrain, wind, or water currents), which are often neglected and not taken into consideration during algorithm development. Furthermore, since the environment is assumed to be a priori unknown, the designer (human operator) is unaware of its potential biases. As such, the well-mixed state can be difficult to achieve, in particular without the common gathering point ('nest'). Therefore, there is a need for the development of decentralised decision-making strategies that are robust across various unknown environmental structures.

⁷Each agent in the swarm has the same chance of interacting with any other agent.

1.3 Research Goals and Objectives

The thesis aims to develop and examine how the opinion-based decision-making approaches can be extended to improve the performance and generality of decentralised collective decision-making strategies within the best-of- n framework. Specifically, one of the most important modular blocks to undergo modifications is concerned with the way of how agents make their choices, i.e., individual decision-making. Furthermore, a particular focus is placed on the analysis of the performance in terms of accuracy and speed of the collective decisions (achieving consensus) in relation to the environment and its influence.

We believe that endowing artificial agents with inner motivation and high-level mental states can allow a design of more robust and generic collective decision-making strategies. Therefore, in this thesis, we employ *preferences* and *beliefs* along with *opinions* inspired by the BPC model of rationality and study them coupled with the mechanism of the *positive feedback* within the best-of- n framework.

Our first goal is to obtain a better understanding of how *social* and *physical environments* impact a decentralised consensus process. As mentioned in the previous section, decisions in spatially distributed decision-making tasks are subject to a priori unknown influence imposed by the features of the physical environment. The latter can induce a bias into collective behaviour, inclining the collective towards choices that are easier to discover but not necessarily the best ones. Similarly, a *social environment* can also impose a bias. Namely, the agent’s motivations (preferences) are mostly hidden from others, but they are reflected in the agent’s choices, and, therefore, implicitly bias group decisions. As a consequence, a designer has to develop an understanding of how to manage physical and social spaces to exploit the benefits of collective decision-making.

Our second goal is the design of generic individual decision-making rules to improve the performance of consensus achievement strategies. In essence, a decision-making rule acts based on the accumulated information from the environment and respectively modifies the mental states of an agent. In this regard, there are two main questions to be answered: (i) which information has to be shared between the agents and (ii) how it should be aggregated to get the most reliable collective performance in the shortest amount of time. Besides speed and accuracy, the degree to which individual decision-making rules can be generalised across environments with different spatial structures (patterns) and the number of alternatives is of particular interest to the current study.

To achieve these goals, the specific objectives outlined below will be addressed.

“Vertical” upgrade of the mental model. Assuming that *preferences* do not require any cognitive abilities but induce an inner bias to a certain outcome, we aim to evaluate their impact on opinion dynamics by integrating them as pre-opinions into individual voting rules. This corresponds to the “vertical” change in the agent’s mental model as according to Figure 1.1. Although *preferences* are often shaped by *opinions* and in previous work (Valentini, 2017) are completely defined by the latter, they refer to different mental states and are not necessarily always consistent with each other. Considering that inconsistency in mental states triggers a state of cognitive dissonance at the individual level, one of the objectives is to develop a social mechanism that allows for its reduction. In this regard, the thesis investigates how inner motivation to prevent

cognitive dissonance manipulates social preferences and affects the speed and accuracy of collective decisions (see Chapter 3).

Analysis of the impact of the environment. To ensure the generality of individual decision-making rules across different environments, it is important to understand how particular environmental structures affect collective decision-making and, in particular, bias the *direct modulation of positive feedback*. In this instance, the thesis intends to demonstrate how self-organisation can be facilitated by exclusively manipulating the environment without actual modifications of its global structure and without any changes in the individual decision model (see Chapter 4).

“Horizontal” upgrade of the mental model. Another subjective mental state of a higher level than an *opinion* is a *belief* that seeks the state of *knowledge* and requires more cognitive resources from an agent. A belief oscillates between an opinion and an objective state of the “truth”, corresponding to the “horizontal” change in the mental model (see Figure 1.1). The theory of belief functions (Smets and Kennes, 2008) provides a mathematical basis that allows handling partial and imperfect information. In this regard, the thesis studies how to achieve a state of mutual “knowledge” shared by all individuals through the use of *beliefs*, as well as how to improve collective accuracy despite environmental structure (see Chapter 5).

Analysis of the impact of the information type shared between the individuals. Given that collective decision-making is carried out due to the communication of information between the individuals, it is important to take into consideration what type of information is involved in this exchange process. Therefore, the thesis examines the performance of collective decision-making with respect to *individual*, *social*, and *collective learning* mechanisms of information exchange (see Chapter 5).

Scalability to several alternatives. Another aspect of the generality of individual decision rules is the ability to remain efficient with an increase in the number of alternatives. Therefore, one of the primary objectives is to create a scalable collective decision-making framework that maintains its performance for $n > 2$ (see Chapter 5).

Preserving modularity. To ensure the generality of the developed methods to tackle the best-of- n problem rather than a specific application scenario, a secondary objective is to preserve the modular structure of the existing framework without major modifications.

1.4 Thesis Outline

The thesis is organised in six chapters.

Chapter 2 introduces the collective perception scenario as the best-of- n problem chosen as a case study for the current thesis. The formalisation of the best-of- n in general is given, along with a description of its existing classification and scenarios of application. A choice of the collective perception scenario as a case study is explained. Section 2.2 provides the problem statement and a scenario description including the multi-agent simulation specifications. In Section 2.3, an overview of the state-of-the-art concerning

collective perception is given and the concept of the scenario task difficulty in the current literature is discussed. The general best-of- n modular framework, based on which Chapters 3-5 are developed, is reviewed in Section 2.4. In addition, the most commonly used opinion-based voting methods and standard evaluation metrics to validate the collective performance are described. Finally, Section 2.5 specifies the modular blocks which will undergo modifications in the following chapters.

In Chapter 3, the preferences of individuals are incorporated alongside their opinions and the corresponding preference-based decision-making algorithm is proposed. Dynamic update rules are developed to maintain the dynamic interplay and autonomous adjustment of both mental states, i.e., preferences and opinions, with respect to each other to reduce the cognitive dissonance of the individuals. Sections 3.1 and 3.2 provide motivation and necessary background on the concepts, which are aimed at the development of the proposed methodology. The respective experimental study is conducted on the binary collective perception problem and the obtained results with the following research implications are analysed and discussed in detail. The work presented in this chapter is based on (Bartashevich and Mostaghim, 2019b).

In Chapter 4, a new benchmark set consisting of nine visual pattern generators with different characteristics is designed to assist the study of collective perception and its generality across a variety of environmental structures. All introduced benchmark problems are illustrated and analysed in Section 4.3. To assess the impact of the spatial distributions of the options and the structure of the environment on the collective decision-making, the environment is reconsidered as a combinatorial object and studied under two algebraic transformations. The original best-of- n framework as of Valentini (2017) with opinion-based decision-making is validated on the introduced binary benchmark problems, as well as their counterparts that have undergone algebraic transformations. In this regard, the analysis of the speed and accuracy of collective decisions is performed and the results with and without direct modulation of positive feedback are discussed. The work presented in this chapter is based on (Bartashevich and Mostaghim, 2019c; Bartashevich and Mostaghim, 2019a).

Chapter 5 is based on the findings of Chapter 4 and introduces beliefs into the decision-making process of the agents, offering the framework to tackle collective perception with $n > 2$ options and without any a priori information about the environmental structure. In Section 5.1, the benchmark set introduced in Chapter 4 is scaled up to $n \in \{3, 5, 8, 10\}$ and analysed on the respective pattern characteristics. Section 5.3 provides the necessary mathematical background on the theory of belief functions, while the respective belief-based decision-making framework for the best-of- n problem is proposed in Section 5.4 along with individual, social, and collective learning mechanisms. An extensive experimental study with twelve different fusion rules to combine the beliefs is conducted on the multi-featured benchmark set consisting of seven different environmental patterns to validate the viability of the proposed methodology. Besides the speed and accuracy analysis, this chapter also contains the comparison of the proposed learning mechanisms for sharing information preceding decision-making. The work presented in this chapter has been published in (Bartashevich and Mostaghim, 2021).

Finally, in Chapter 6, we conclude the thesis by summarising the research contributions and proposing future research directions.

Appendix A provides the reader with a table of default settings for collective per-

ception scenario used throughout this dissertation.

Appendix B and Appendix C contain supplementary materials and statistical analysis of the results for Chapters 3 and 5, respectively.

Collective Perception as the Best-of- n Problem

In this chapter, we consider collective perception as a special case of consensus achievement task in collective decision-making. Section 2.1 provides a formalisation of the best-of- n problem as a general collective decision-making task, description of existing problem classification, and application scenarios. Section 2.2 describes in detail a scenario representation of collective perception together with the settings for the simulation model of the multi-agent system. Section 2.3 gives the current overview of the state of the art, which provides the necessary background information. Afterwards, the general best-of- n framework, within which the scenario is considered throughout the thesis, is given in Section 2.4, including the description of the baseline evaluation metrics that are used to assess its performance. Finally, in Section 2.5, we outline the modular blocks of the framework to be modified in order to address the objectives stated in Section 1.3.

2.1 Formalisation of the Best-of- n Problem

The best-of- n problem as a general collective decision-making problem can be formulated as follows. Let us consider a set $\Omega = \{\omega_1, \omega_2, \dots, \omega_n\}$ of n candidate options. Each option ω_i , $i = 1, \dots, n$ is characterised by a certain quality $q_i \in \mathbb{R}$ and by a cost $c_i \in \mathbb{R}$. The corresponding functions $Q, C: \Omega \rightarrow \mathbb{R}$ such that $Q: \omega_i \mapsto q_i$, $C: \omega_i \mapsto c_i$ define the quality and cost values, respectively. Both functions Q, C are initially unknown to the decision-maker and describe the specific properties of the target environment (e.g., light intensity, humidity, shelter size). In general, quality values q_i are either considered as subject to noisy measurements and can not be assessed in their pure form, or are not directly available to single individuals. In the case of more than one environmental attribute of interest, the quality Q is commonly constructed as a weighted aggregation function combining all the attributes under consideration. The cost function C is defined as the time needed for an individual to assess the quality value of the corresponding option. The goal for a group of N individuals is to make a collective decision for the option ω_{best} that maximises the profit expressed in terms of the option's quality $\max_{\omega \in \Omega} Q(\omega)$ while minimising its costs $\min_{\omega \in \Omega} C(\omega)$. When all members of the swarm commit to the same option, a *consensus* is said to be reached.

2.1.1 Existing Problem Classification

Figure 2.1 illustrates different complexities of the best-of- n problem according to Valentini *et al.* (2017), depending on how set of options Ω , quality Q , and cost C are configured in an application scenario.

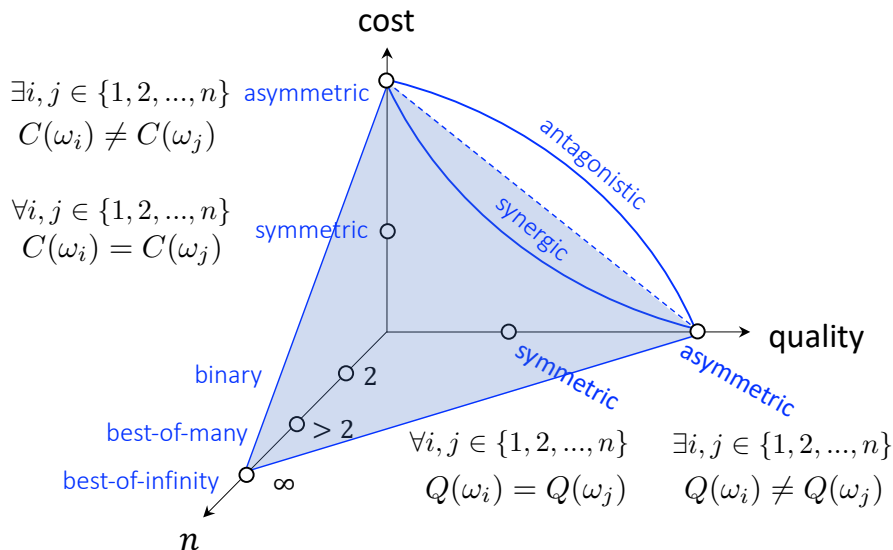


Figure 2.1: Classification of the best-of- n problem.

Taking the number of options $|\Omega| = n$, one can distinguish the binary case $n = 2$ as a particular case of a general discrete case with more than two options $n \geq 2$, which is further called as the *best-of-many* problem. The most complex case in this regard corresponds to the infinitely many (countable or continuum) amount of options, which is called the *best-of-infinity* problem (denoted as the *best-of- ∞*). In terms of quality function Q or cost function C , the problem is classified as either *symmetric* or *asymmetric*. As such, depending on different combinations of quality and cost values of the options, the best-of- n problem can be (1) symmetric concerning both quality and cost, (2) symmetric only concerning quality and asymmetric concerning cost (or vice versa), (3) asymmetric concerning both quality and cost. In terms of quality (or cost), *symmetric* means that all options have the same quality (or cost) values and there is no difference between them, i.e., $Q(\omega_i) = Q(\omega_j)$ (or $C(\omega_i) = C(\omega_j)$) for all $i, j \in \{1, 2, \dots, n\}$. While in the *asymmetric* case with regard to the quality (or to the cost), at least two options exist of different qualities (or costs), i.e., $\exists i, j \in \{1, 2, \dots, n\}$ such that $Q(\omega_i) \neq Q(\omega_j)$ (or $C(\omega_i) \neq C(\omega_j)$). When the cost and the quality are both *asymmetric*, the interaction of these two plays an important role. When the option with the best quality is characterised by the minimum cost, the interaction between cost and quality functions is described as *synergic* and is referred to as the *synergic best-of- n* problem. However, in many real-world problems the considered objectives Q and C can compete against each other, in the sense that the option with the best (i.e., the lowest) cost will be the worst in terms of quality and vice versa the option with the best (i.e., the highest) quality will be very costly to get (i.e., will be the worst concerning the cost). This implies that some features in the environment counterbalance each other by producing opposite effects that

prevent an actual decision-maker from reaching the target. Such type of interactions is described as *antagonistic*, expanding the complexity of the asymmetric problem, and is called as an *antagonistic best-of- n* problem. As an example from nature, foraging path selection can be considered as the antagonistic best-of- n problem if the path to the best food source is also the longest and, as the synergic best-of- n problem, if this path is the shortest one.

Overall, one can think about the complexity of the best-of- n problem as about the volume of the tetraeder (as shown in Figure 2.1) with the vertices on the axes describing the corresponding characteristics (n , Q , C). In this way, with the increase of at least one parameter (described by a dot on the corresponding axis), the complexity of the problem grows as well. For thorough introduction and deep results on the best-of-2 problem, we refer to the monograph of Valentini (2017) dedicated to the case with *asymmetric quality* and *symmetric cost*, as well as containing the profound literature review on the problem of interest according to the provided above classification.

2.1.2 Application Scenarios

Referring to Valentini *et al.* (2017), there are three typical application scenarios in the literature, known as benchmark models for the best-of- n problem: (i) the shortest-path (or double-bridge) scenario, (ii) site selection and (iii) collective perception. The last one is the least studied and is considered as one of the recently introduced scenarios (Valentini *et al.*, 2016). In comparison to (iii), (i)-(ii) are characterised by the presence of a meeting spot, which is referred to as ‘nest’, similar to honey-bees or ants. In this way, the well-mixture of the whole system is obtained, which is considered as one of the strict requirements (limitations) in the current state-of-the-art approaches. However, due to spatial dynamics and established social networks, most populations (natural or artificial) in the real world are inherently not well-mixed (Nowak, 2006). In this respect, the collective perception scenario represents itself as a viable benchmark, where the agents have to operate in the same region of environment, performing the decisions as they move and without guarantee of the well-mixed state. As such, it was chosen as a case study for this dissertation.

2.2 Collective Perception Scenario

According to Schranz *et al.* (2020), collective perception is one of the basic swarm behaviours referred to as *decision-making*, which allows a swarm of agents to come to a common conclusion on the matter of contention, based only on locally gathered information. The concept of collective perception aims at achieving the global awareness about the object of interest through the exchange of the information perceived using local sensors between the agents to assist the others to gain the information about the “blind spots”, i.e., areas which they were not able to observe by themselves. It is widely used in the context of object recognition (Giusti *et al.*, 2012; Stegagno *et al.*, 2014), classification (Kornienko *et al.*, 2005; King and Breedon, 2011), sensor fusion (Elmenreich, 2002; Majcherczyk *et al.*, 2021), surface coverage (Olfati-Saber and Jalalkamali, 2012; Mazdin and Rinner, 2019), where the area/object is too large for a single individual to perceive, and can be considered as one of the aspects of *cognitive intelligence* (Cahen and

Tacca, 2013). In this regard, such a swarm of artificial agents has to be able to merge multiple perception instances of single individuals into one global picture, to collectively assemble an image of a “map” to solve the given task.

In the current work, we study a collective perception scenario as the model of the spatially distributed best-of- n problem proposed by Valentini *et al.* (2016) and describe it more in detail.

2.2.1 Problem Statement

The environment is modelled as a two-dimensional squared grid consisting of Γ regular cells of equal size, i.e., *cell* \times *cell* squared units each. Each such squared cell is coloured in one of the $j = 1, \dots, n$ colours, where colours are considered as spatially distributed options $\omega_j \in \Omega$, specifying a discrete-choice problem (for more details see Section 1.2). The quality $\{q_j\}_{j=1}^n$ of each option is defined as the proportion of the cells with colour j in the grid, i.e., $q_j := \Gamma_j / \Gamma$. Accordingly, the goal in terms of the best-of- n problem is to identify the option with the highest quality. Therefore, if another is not stated, a swarm of N agents distributed over the grid has to come to a consensus on the most prevailing colour ¹ ω_{best} within the environment. Each colour j is also associated with a certain cost c_j , which can be expressed as the time needed to assess and to explore this particular option. Since the colours are distributed randomly over the grid, they have equal opportunities to be discovered by the agents, indicating the symmetric cost of the options. In turn, the qualities of the options are asymmetric and are not directly accessible to single individuals. Each agent can perceive the environment only locally through underneath sensors and, therefore, requires multiple sampling of the environment to assess the profitability of the available options.

2.2.2 Concept of the Task Difficulty

The difficulty of the task is defined by the ratio of options’ qualities ρ expressed as the ratio of the number of cells $\{\Gamma_j\}_{j=1}^n$ with available colours in the environment. According to Valentini (2017), if $\exists k$ such that $\Gamma_k \gg \Gamma_j$ for any $j \neq k$ ($j = 1, \dots, n$), the more noticeable the difference in qualities and, thus, the easier it is to decide. As the colour proportions approach each other, that is, $\rho \rightarrow 1$, the decision-making becomes more challenging. As such, lower values of ρ correspond to the easier difficulty settings of the task, while higher ones to the more difficult.

2.2.3 Motion Specifications

Coordinates and heading directions of the individuals in a swarm are initialised according to a uniform distribution in the ranges of $(x, y) \in [1, \sqrt{\Gamma} + 1] \times [1, \sqrt{\Gamma} + 1]$ and $\phi \in [0, 2\pi]$, respectively. Each agent has a circular shape of the same diameter equals Θ units, which is proportional to the size of the grid’s cells.

¹In the following, the option ω_j and the colour j are considered interchangeable.

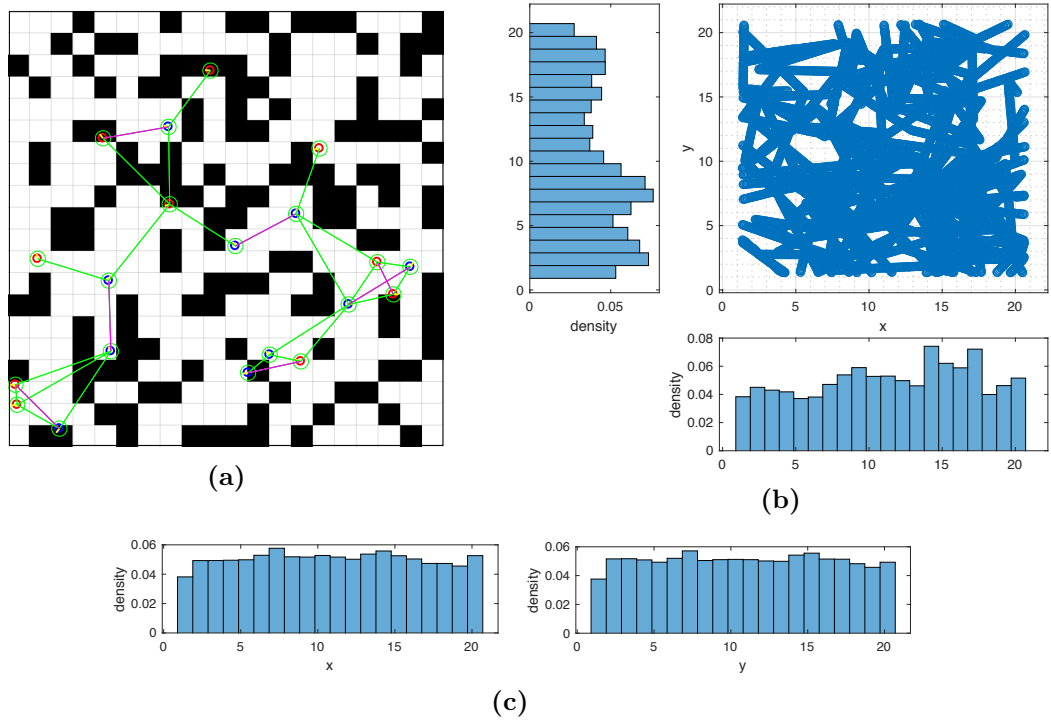


Figure 2.2: (a) Multi-agent simulation: environment and agents, (b) Spatial distribution of 20 individuals resulting from their movements during 400 seconds: result over 1 run, (c) result over 100 runs. Pictures (a) and (c) are taken from (Bartashevich and Mostaghim, 2021).

Individual Movement

Each agent performs a continuous random motion over discrete time steps (further called iterations) so that at each iteration an agent moves. The implemented model of random motion consists of two alternating phases of (1) linear motion with constant speed $|\vec{v}|$ units/s and (2) rotation on the spot with a respective constant angular velocity ω rad/s. The duration of each new movement phase is defined for each individual separately and sampled from a normal distribution with a mean of 40 s and variance of 1 s for linear motion, and from a uniform distribution between 0 and 4.5 s for rotational motion. The direction of rotation (either clockwise or counter-clockwise) is chosen each time at random. Such a motion model can be considered as a *random direction model* (Nain *et al.*, 2005) characterised by a homogeneous uniform distribution of the agents. This differs from another well-known *random waypoint model* of motion (Bettstetter and Wagner, 2002), which results in a high density of agents in the middle of the two-dimensional squared environment and zero probability at its borders. In our case, the former model is more desirable than the latter, since it is not biased to any specific locations and, hence, ensures better coverage and exploration of the space by the agents without control of their positions.

Collision Avoidance

As a collision between the agents is detected, the individuals' current motion phases are switched to the rotation on the spot in opposite directions to their respective opponent. That is, one of the agents rotates clockwise and another one counter-clockwise, to accelerate a "traffic congestion" resolution. The respective collision rotation phase of each individual lasts until its heading direction allows it to resume an instantaneous, free from collision, linear motion. When the agent hits the borders of the environment, it enters the rotation phase (in a random direction) until it is turned around on 180° from its initial collision direction. Such an approach is supposed to prevent a pileup of agents at the borders and to return them quickly to the main area.

Spatial distribution of individuals' trajectories

Figure 2.2b illustrates the resulting density histograms for x - and y -positions of $N = 20$ agents moving simultaneously over 400 seconds, corresponding to the maximum duration T of one trial, where each agent's position is plotted every 10^{th} iteration. The spatial distribution depicted in Figure 2.2b is characterised by some peaks at the places of collisions and prolonged stays of the agents due to the rotation on the spot. The probability that an agent is located at the borders is similar to the other free-from-collisions places of the simulation arena due to the specifics of the introduced before border avoidance mechanism. Depending on the time drawn for the following after-collision linear motion phase and the initial collision-direction with the border, an agent can come back to the inside area of the arena or hit another adjacent border. Figure 2.2c reveals that the spatial distribution of the whole population over 100 runs can be considered to be almost uniform. In this scope, there is an equal chance for every coloured cell to be visited by the agents within 100 runs.

2.3 Overview of the State of the Art

There are different interpretations of the collective perception such as cooperative or distributed sensing in different fields of research and its applications in vehicular ad-hoc networks (Gunther *et al.*, 2016; Thandavarayan *et al.*, 2020) or the Internet of Things (Simoens *et al.*, 2018), where a group of sensors has to determine the state of the environment through the exchange of the information, which is performed within special communication protocols. Whereas in the swarm intelligence context, collective perception is considered as a self-organised phenomenon arising from the local communication, implying low computational effort and exchange of the messages with a small amount of semantics between simple individuals with limited capabilities.

In this regard, Kornienko *et al.* (2005) studied collective perception as a collaborative object *classification task* using a swarm of micro-robots, where each robot can observe only a limited part of an object from its current point of view such that it is not enough to identify to which class it belongs. Schmickl *et al.* (2007) considered collective perception in the context of the *aggregation* scenario, where a group of robots has to assess and gather at the target areas proportionally to their respective sizes. The size of each area is unknown to the swarm and can not be directly assessed by a single individual, as the agent can only determine whether it is within the target area or not. Morlino *et*

al. (2010) has proposed an environment for collective perception scenario modelled by circular black spots painted on a white ground in a grid-like structure, with the task to identify their density. The agents can perceive the colour of the arena only locally and communicate with the others by emitting the flashing signals with the frequency corresponding to the local density estimate. In this way, a collective flashing signal of the whole swarm encodes the global density of the features of interest.

As a *decision-making task*, a collective perception has been studied by Valentini *et al.* (2016) on the same environment as in (Morlino *et al.*, 2010) but within a voting context, where the agents need to collectively decide in a distributed way which of the two colours on the arena ground, e.g., black or white, is the most frequent one. In their work, particular attention was paid to popular decision-making strategies such as the voter model and majority rule. Later, the same scenario of randomly-generated black and white cells has been used as a benchmark problem for collective decision-making in other studies as well. As such, the security issue and the existence of malicious activity in a swarm were addressed by Strobel *et al.* (2018) using blockchain technology on the top of the collective decision-making algorithms from (Valentini *et al.*, 2016) and within the same binary collective perception benchmark. Ebert *et al.* (2018) examined a randomly-generated multi-featured case with a dynamic task allocation strategy to decide between three different colours in finite time. To the best of the author's knowledge, no more research has been performed for the case with more than two colours in the same context of collective perception. A case with a dynamic binary environment was investigated in (Soorati *et al.*, 2019), where the proportions of the colours in the grid are changing over time such that a swarm has to continually revise its obsolete judgment. The findings of the above investigations revealed that, independently of the used methodology, the most difficult scenario setting is the one with almost identical colours' ratios, where the ratio defines the qualities of the options.

Despite the different nature of the studies (Ebert *et al.*, 2018; Strobel *et al.*, 2020), it was also observed that even the easiest collective perception task difficulty setting is hard to solve if the features (namely, options) are non-homogeneously distributed in the space, e.g., forming a 2-section environment. There, the agents can be heavily biased to one of the outcomes based on their movement areas (exploration), resulting in highly conflicting pieces of evidence obtained by different agents from the environment. The voting rules are admitted to be inadequate in this case, as they are not sufficient to model the conflict between experts (Xu *et al.*, 1992). For this purpose, possibility and probability-based theories are used to address the imprecision and uncertainty of the measurements (Martin *et al.*, 2008). In this regard, Ebert *et al.* (2020) presented a distributed collective decision-making algorithm based on the idea of Bayesian inference and applied it to the randomly-generated binary collective perception scenario. There, each agent employs a Bayesian model of the colour ratio (i.e., option quality) and updates it upon observations. Though, the approach has shown to be successful, achieving fast and accurate decisions regardless of the task difficulty, additional parameters identifying a prior model of the distribution of the features are needed to be defined and tuned accordingly. This can cause complications in practical situations, where there is *no a priori* information available.

In this regard, the belief function-based (evidence) theories such as Dempster-Shafer theory (DST) can provide a more appealing mathematical framework for dealing with un-

certain information without any necessity in a priori distributions of the features (Shafer, 1976). Apart from uncertainty, the theory of evidence also allows expressing a full or partial ignorance, i.e., “unknown” state, which has been shown to be beneficial in several following studies on the consensus formation in multi-agent and natural systems. To note, the further mentioned works are considered in the context of the site-selection selection scenario, i.e., a choice to move together to one of the discrete targets. In animal groups (Couzin *et al.*, 2011; Hartnett *et al.*, 2016), it was observed that uninformed individuals, namely those without any preference to a specific option, can significantly modify the outcome of collective consensus decisions. Reina *et al.* (2015) studied a macroscopic description of the site-selection dynamics, where each agent was in either committed state to one of the options or in the overall uncommitted state in order to discover the new ones, promoting better exploration. Crosscombe and Lawry (2016a; 2016b) considered a three-valued logic to model a middle truth value, i.e., borderline true-false value, as “unknown” state resulting during the combination of conflicting binary truth values. It was shown that such an approach accelerates the consensus with high accuracy in a fully connected network in comparison to a simple binary model, supported also by other studies, e.g., Perron *et al.* (2009). Later, Crosscombe *et al.* (2018) evaluated the same three-valued consensus model in a real robot swarm and demonstrated its robustness to noise compared to the weighted voter model, introduced earlier by Valentini *et al.* (2014), though with an increased convergence time. The conducted experiments in Crosscombe *et al.* (2018) have not addressed any particular best-of- n scenario and concentrated mainly on the propagation of initially predefined binary opinions based on local interactions in a swarm without exploration of the options. There, the agents’ beliefs are represented as vectors of $n = 3$ logical values, i.e., $\{1, 0, \frac{1}{2}\}$, and are updated using solely logical operations. While in the DST, besides incorporated “unknown” state, the beliefs are represented as continuous confidence measures in each option separately as well as in the omnifarious unions of options, e.g., $\{\omega_i, \omega_j\}$.

To integrate the gathered evidence from multiple sources, there exist different combination operators in the DST literature (Sentz and Ferson, 2002; Smets, 2007), to name a few, which aid in achieving a unifying degree of belief that encompasses all the available information into account. In the context of the best-of- n problem, Crosscombe *et al.* (2019) investigated four DST belief combination operators for multi-agent consensus formation on a fully-connected graph within a site-selection model (Valentini, 2017). There are also studies in other domains (Kanjatatarakul and Denoeux, 2017; Zoghby *et al.*, 2014), where DST has been studied as an asynchronous distributed linear consensus mechanism on time-varying networks, though in a different context from the best-of- n problem. Notably, alongside belief combination with other agents, in (Crosscombe *et al.*, 2019) each agent makes also individual updates based on his personal partial knowledge perceived from the environment. In this way, exploration of the options has a direct impact on the formation of the agents’ beliefs. While, for instance, in (Valentini, 2017) perceived evidence influenced the decision-making process only indirectly, defining the time during which the agent can exchange his opinion with other individuals.

Although in a setting as in (Crosscombe *et al.*, 2019) the agents can already assess the problem based on their own personal measurements, a further combination with the beliefs of the other agents has shown to be more beneficial. A similar observation was conducted by Lee *et al.* (2018b) in an agent-based system, where a direct Bayesian

updating along with probability pooling was able to reach a faster and better consensus than based only on solitary personal Bayesian updates. Also, later it was coupled with modulation of the negative feedback to update the opinions and tested in robot-based simulation experiments on the site-selection scenario (Lee *et al.*, 2018a). So far, however, a collective perception scenario has remained still unattended by the aforementioned approaches. In comparison to collective perception, the qualities of the options in site-selection studies are directly accessible to the agents and mostly spatially independent due to the nature of the considered scenario model, where the individuals alternate their visits between the place of common gathering (the ‘nest’) and the sites placed on the same distance around it.

In fact, the accumulation of solely direct evidence from an environment by an individual can be considered as an individual type of learning (IND) in the sense of the way of acquiring the information about the environment. IND mainly concerns isolated agents that interact only with an environment and decide purely based on their own local sensory inputs. While most of the natural organisms are social creatures (Kao *et al.*, 2014), the inter-individual interactions allow them to share and propagate the information in a group resulting in a social and collective types of learning (further denoted respectively as SL and CL, see Section 1.1.2 for definitions). In the same vein, studies in social epistemology (Wenmackers *et al.*, 2014; Goldman and O’Connor, 2019) address the question of how individuals on their own, as well as in the collective, can best seek the truth regarding the given problem with the assistance of others in a social context. Berdahl *et al.* (2018) highlighted how CL and SL drive the emergence of animal culture in the context of migration, where new routes can emerge as a result of gradual information gathering from multiple individuals. Sasaki and Biro (2017) have shown that the accumulation of knowledge within the group through IND and successive SL progressively improves a collective performance. Previous studies on SL in animals (Laland, 2004; Galef and Laland, 2005) have revealed that a combination of several types of learning, such as IND and SL, increases the mean population fitness compared to when only one learning mechanism is involved. Also, Marshall *et al.* (2017) argued that variance in individual decision-making abilities can promote better decision-making/learning in the group as the whole. In contrast, far too little attention has been paid to this aspect within the collective perception problem.

2.4 General Framework

As mentioned at the beginning of Section 2.3, there are various algorithms in the literature addressing the problem of collective perception. However, they are mainly difficult to compare with each other or to apply to other scenarios due to their diverse nature and the lack of a unifying framework. At the same time, the best-of- n framework proposed by Valentini (2017) is characterised by the modular structure, which supports its application and re-implementation on different scenarios, belonging to the general class of discrete consensus achievement problems. Such an approach allows studying the underlying concepts of collective decision-making systematically, without rigid reference to the concrete task, promoting their generalisability and transparency. For that reason, a design framework of Valentini (2017) has been selected as the base for the current study as well.

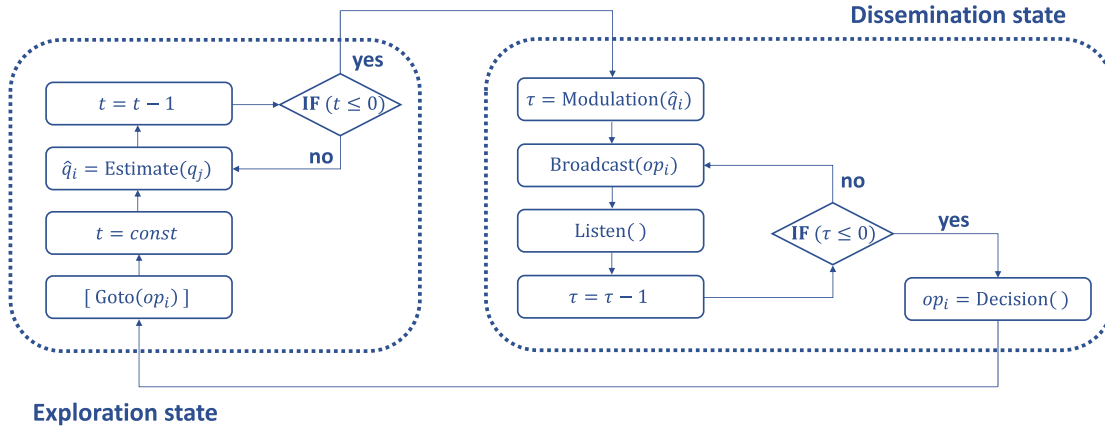


Figure 2.3: General framework. Figure adapted from (Valentini, 2017).

A general modular structure of a collective decision-making algorithm as of Valentini (2017) is illustrated in Figure 2.3 and represented by a behaviour-based approach. Each agent can have one or several mental states (e.g., see Section 1.1.1) and behaves accordingly, taking into account the external information. The motion routine of the agents, as defined in Section 2.2.3, remains unaffected by their current behavioural or mental state. The set of possible options Ω is assumed to be given. In original framework (Valentini, 2017), the mental state of each agent i in a swarm is performed by the opinion op_i , reflecting its subjective judgment on the best option.

There are two main individual behavioural states essential for tackling the best-of- n problem and referred to as (i) exploration and (ii) dissemination states.

- **Exploration state** is responsible for the discovery of the potential options and the individual gathering of the information exclusively from the environment, including a personal assessment of the received input, without interaction with the other agents. Even if the set of options (e.g., colours) present in the environment is given to the swarm, the options' attributes (e.g., their location, quality characteristics) remain unknown to the agents and, therefore, have to be explored.
- **Dissemination state** corresponds to the process of *information pooling* (Campo *et al.*, 2011), implying the propagation of the information through the swarm and the reconsideration of personal decisions, i.e., an individual decision-making mechanism based on the information obtained from the other agents.

Initially, each agent i chooses an option $\omega_j \in \Omega$ uniformly at random as its primary opinion op_i with which it enters the **exploration state**. The goal of the agent in this state is to explore the option corresponding to its current opinion, i.e., $[Goto(op_i)]$ ². The duration of the exploration $t = const$ is fixed during the whole decision-making process and set by a designer. During this time, each agent samples the quality of its own opinion op_i by interacting with the environment through the “ground sensor”. The quality of the options $\{q_j\}_{j=1}^n$ ($q_j \in \mathbb{R}$) is defined as the ratio of cells with colour j to the

²In this context, the colour j selected by the agent i as the option $\omega_j \in \Omega$ and his opinion op_i are interchangeable.

total amount of cells in the environment. Since it is an unknown parameter, the quality estimate \hat{q}_i of the agent i is taken as the ratio of the time during which it perceived the colour j corresponding to his op_i to the total amount of the given exploration time t , that is, “Estimate(q_j)”. As such, every iteration the agent i counts the perception of the option $\omega_j =: op_i$ as a valid observation and takes a proportion of such observations to its total amount of perceptions during this state as its $\hat{q}_i \in \mathbb{R}$ value.

When the time of the exploration state t is over, the agent enters the **dissemination state**. One of the agent’s goals in this state is to broadcast its current opinion and to collect the opinions of its local neighbours while continuing its motion. The communication is carried out with frequency $\Delta\tau_C$ and the channel is established only with one agent at a time, which is randomly selected within the interaction radius of d_{max} units. In Figure 2.2a, thin (green) lines between the agents illustrate possible communication channels, while bold (magenta) ones state for the actual communication between two agents at the given time. The information received twice in a row from one and the same neighbour is not registered by the agent in order to prevent multiple records of identical data. For this, the agents also exchange their IDs along with the main information message. The duration of dissemination τ is different for each individual i in a swarm and depends on its personal quality estimate \hat{q}_i , obtained in the agent’s preceding exploration state. The time τ is defined by the *direct modulation* of a positive feedback loop performed by the linear function positively correlated with the option’s quality estimate, i.e., $\text{Modulation}(\hat{q}_i) = \hat{q}_i * t$. The essence of the positive feedback is to amplify the propagation of the opinions with high quality, such that a swarm can have a higher probability to converge on the best option. For the same reason, the agent listens only to those who are also in the dissemination state, gathering in this way the fittest opinions, and ignoring the ones in the exploration state. If all the necessary conditions are met and a pairwise communication channel is established, the agent i saves the received package of the information if and only if it is currently in the last $\delta\tau$ iterations of its own time τ . This is believed to facilitate effective population mixing and to guarantee that the agent collects the latest up-to-date information.

At the end of the dissemination state, the agent i enters the **decision-making state**, i.e., $\text{Decision}()$, where it reconsiders its committed option $\omega_j \in \Omega$. Afterwards, it gets back in the exploration state to re-evaluate its updated judgment op_i . The entire process repeats until the whole population comes to a consensus on the same option or the given time is run out.

2.4.1 Opinion-based Decision-Making

A decision-making rule, corresponding to the block “Decision()” in Figure 2.3, represents the “brain” of an agent. This rule is used by each individual in a swarm to revise its particular mental state, e.g., opinion. In this case, a decision rule is performed by a function $h: \Omega^k \rightarrow \Omega$ such that

$$h: \{op_1, \dots, op_k\} \mapsto op_i, \quad (2.1)$$

taking k collected opinions by the agent i during its dissemination state as an input and giving back a new opinion $op_i \in \Omega$ as an output. To avoid potential delays in implementing the function h and the impact of the outdated information, the input set

is shortened to the last L perceived opinions to ensure that only the latest ones shape a new decision of an agent. The input can also include the current opinion of an agent itself, depending on the selected strategy. The construction of the function h greatly affects the efficiency of the collective decision-making algorithm, identifying its speed and accuracy (Franks *et al.*, 2003) along with the type of the consensus, i.e., full or partial.

Below we give three of the most popular decision-making strategies studied in (Valentini, 2017) and provide explicit definitions of the corresponding functions h from Equation (2.1).

Voter Model

The voter-based decision-making mechanism is defined by the function h as follows:

$$h: \{op_{k-L+1}, \dots, op_k\} \mapsto rand(\{op_{k-L+1}, \dots, op_k\}), \quad (2.2)$$

such that an agent i selects the opinion of a random neighbour j from the pool of the last L collected ones, ignoring its own current opinion op_i .

Majority Rule

Let $C(op_j)$ denote the frequency of the opinion op_j in the set $\{op_{k-L+1}, \dots, op_k\} \cup \{op_i\}$ and s be the index of an opinion with the maximum frequency in this set. The majority-based decision-making mechanism is defined by the function h as follows:

$$h: \{op_{k-L+1}, \dots, op_k\} \cup \{op_i\} \mapsto \begin{cases} op_s, & \text{if } C(op_s) \geq \frac{L+1}{2} \\ op_i, & \text{otherwise.} \end{cases} \quad (2.3)$$

That is, if the index s is unique and op_s is shared by at least half of the observed neighbours of the agent i , including itself, the op_s is adopted by the agent i as its new opinion. In the other case or in case of a tie, i.e., if there exist several such indexes s , the agent i keeps its current opinion op_i .

Direct Comparison

The direct comparison rule was introduced in (Valentini *et al.*, 2016) and implies that agents besides the opinions also exchange their quality estimates. Let op_r denote a randomly chosen opinion from the set of $\{op_{k-L+1}, \dots, op_k\}$. Then, a direct comparison mechanism is defined by the function h as follows:

$$h: \{op_{k-L+1}, \dots, op_k\} \mapsto \begin{cases} op_r, & \text{if } \hat{q}_r > \hat{q}_i \\ op_i, & \text{otherwise.} \end{cases} \quad (2.4)$$

That is, the agent i adopts the opinion op_r of a randomly selected neighbour r if the quality of this opinion \hat{q}_r is better than its own \hat{q}_i .

In comparison to the voter- and majority-based decision-making, direct comparison is characterised by the absence of the modulation of a positive feedback loop in the

dissemination state, i.e., such that $\tau = t$. It also requires more capable individuals to accurately differentiate between the alternatives based on the qualities, while the other methods operate only based on the agents' opinions.

2.4.2 Evaluation Metrics

The performance of a particular decision-making rule is determined by the general agreement of the whole swarm (full consensus) on the best option $\omega_{best} \in \Omega$. Depending on the type of mental state, different metrics (e.g., degree of belief, confidence level) can be introduced to evaluate the welfare of an agent, hence, of a swarm, and will be identified where necessary in the corresponding chapters of the thesis. While the time and accuracy of the undertaken collective decisions constitute two major characteristics of a collective decision-making algorithm, regardless of its underlying mental model. In the following, these universal metrics are given in the context of the opinion-based decision-making model.

Consensus Time

Consensus time $T_N^{correct}$ is considered as the number of iterations of the whole decision-making process until all members of a group share the same opinion op_i corresponding to the $\omega_{best} \in \Omega$.

Exit Probability

Exit probability E_N defines the accuracy of collective decision-making and is calculated as the ratio of successful trials. A trial is taken as “successful” if a swarm has converged to a consensus on the right alternative, i.e., the ω_{best} .

2.5 Summary

In the following we highlight the connection between several objectives stated in Section 1.3 and the modular blocks of the best-of- n framework as of Figure 2.3.

- Both “vertical” and “horizontal” upgrades of the agent’s mental model require modifications of the function h from Equation (2.1), which determines the “Decision()” block.
- The structure of the environment and the spatial distribution of the options define the values of the individual estimates and, as such, are handled in the “Estimate()” block.

Modular Blocks	Chapter 3	Chapter 4	Chapter 5
Decision()	×		×
Estimate()		×	
Broadcast()/ Listen()			×

Table 2.1: Research design.

- The type of information that agents transmit to each other and based on which decisions are taken is handled by “Broadcast()” and “Listen()”.

In Table 2.1 we specify which modular blocks are the focus of modifications (denoted by cross) in which chapter of the thesis. As such, by introducing modifications in separate blocks of the framework, we intend to preserve its current structure.

Preference-based Decision-Making for the Best-of-2 Problem

In this chapter, we propose a decision-making model, which can be considered as a combination of both voting models aforementioned in the previous chapter, namely, the majority rule and the voter model. The developed decision-making mechanism is based on the “vertical” upgrade of the mental model within the collective perception framework and, therefore, additionally incorporates the personal preferences of the individuals in a collective. In this regard, the research questions to be considered are: (i) how to dynamically co-evolve preferences with the opinions of the agents to be consistent with each other and (ii) how such inclusion of the low-level mental states affects the performance of the collective decision-making system as a whole. For this purpose, we suggest the mechanism of the preference update based on the undertaken decisions of the individual and validate it in the collective setting on the collective perception scenario as a binary collective decision-making problem. In this way, the current chapter focuses on the introduction of modifications in the “Decision()” block as of Figure 2.3.

The chapter is organised as follows. Section 3.1 outlines the problem statement and motivation of this chapter, followed by Section 3.2 with the necessary mathematical background. Section 3.3 describes the proposed methodology along with the designed opinion-preference dynamics, defining the preference-based decision-making mechanism. To verify the upgraded framework, the experiments are conducted in Section 3.4 on the collective perception scenario with randomly distributed black and white colours. The chapter is concluded with a summary and discussion of the results in Section 3.5. The presented concepts and findings of this chapter were previously published by the current author in (Bartashevich and Mostaghim, 2019b).

3.1 Problem Statement and Contribution

As it was mentioned in Chapter 2, popular opinion-based decision-making mechanisms such as the majority voting (MR) (Galam, 2008) and the voter models (VM) (Liggett, 1999) have been extensively studied in the literature, e.g., (Valentini, 2017; Strobel *et al.*, 2018) to name a few, using simulated artificial agents as well as robot swarms. They are also widely used in our daily lives. Let us imagine the situation that a group of friends is going to select whether they are going tonight to a pizzeria or a sushi bar, i.e.,

binary decision-making problem. Every person in a group has his/her own opinion on where to go, but they all need to come to a consensus on one option as a group to stay together. The two common ways of approaching this problem are either to select the opinion of the majority, namely MR, or to flip a coin and select a random one, namely VM. The dilemma is which of these approaches is a better one such that the outcome (final decision) satisfies everyone at most and in the shortest possible time. Another issue is that neither of the approaches is taking explicitly into account the personal preferences of the individuals. That is, under the preference we mean what I usually like more than something else, e.g., “*I prefer pizza more than sushi*”. While opinion is my point of view on a matter in a current situation, e.g., “*I take pizza*”. In such interpretation, one can have certain preferences but not necessarily have their own opinions. In the beginning, the opinions and the preferences can coincide with each other but, as soon as the collective decision-making is started, they can become contradicting under the influence of the other members or based on some preliminary acquired knowledge, for example, that the pizzerias are not good in this region. However, the latter does not mean that you do not like pizza more than sushi but implies that in this particular situation you can have an opinion that does not correspond to your common preference. In this regard, the preferences can also change over time to fit more with opinions. It is considered that one’s preferences are unknown a priori and have to be discovered by experience, therefore they are not considered permanent (Jacobs, 2016). Nevertheless, people’s preferences and opinions attempt to be consistent with each other to reduce a personal cognitive dissonance (Jacobs, 2016). As such, the research question is how one can design such a co-adaptation process of two mental states, preferences and opinions, given constantly incoming information from the surrounding (other agents, environment) and how it affects the collective decision-making process.

Drawing an analogy with the previous example, one can consider a swarm of artificial agents (e.g., robots) which has to collectively identify the abundance or the scarcity of the hazardous materials in a certain unknown area, which is hard to reach and dangerous for exploration by human beings. The applied decision rule is suggested to be chosen by the designer in advance before the artificial system is deployed in the environment (Khaluf *et al.*, 2019), while the further collective decision-making process is considered to be running without human intervention and assumed to be self-organised (Valentini *et al.*, 2014). The environment is unknown a priori to the agents, however, a human operator (the designer) can have some preliminary information based on which the conjecture about the possible correct outcome can be formulated. Referring back to the previous example with sushi and pizza, one can consider this additional information similar to the knowledge that “*the pizzerias are not good in this region*”. Therefore, we intend to integrate this information into agents before they begin the decision-making process in the form of their initial pre-opinions (i.e., preferences) and propose a preference-based decision-making mechanism, which in particular cases includes the majority rule and the voter model, allowing the collective to take into account individuals’ preferences along with opinions during the process of undertaking decisions.

In this chapter, we describe collective perception as the collective decision-making using a family of spin system models, taking inspiration from (Hartnett *et al.*, 2016), where a two-choice decision task was studied on the 2D square static lattice of individuals with and/or without a steady bias regarding the particular option. In (Hartnett

et al., 2016), the dynamics of the agents' opinions were studied only within local interactions predefined by the lattice structure, while, in our case, the agents also acquire information from the environment, driven by the modulation of the positive feedback and dynamic interactions with the others (see Section 2.4). In this regard, following previous works (Berdahl *et al.*, 2013; Torney *et al.*, 2009), where the interdependence between social and environmental influence on the decision-making of a moving group of individuals has been studied, we expect to observe an adaptive group decision-making process in our case. Besides that, we also integrate a learning mechanism for preferences, which allows agents to maintain consistent correspondence between preferences and opinions within themselves over time, to avoid individuals' cognitive dissonance.

3.2 Mathematical Background

To study the behaviour of spin models, in which spins can have only two possible states, one can refer to the Ising model, which is widely used in statistical physics to study ferromagnetism, the phenomenon of spin alignment with each other under the influence of a strong magnetic field. Considering the resulting emergent phenomenon, it has been also used to study opinion formation in the collective systems, including consensus decision-making, and in the application to social sciences (Galam, 1997; Stauffer, 2008). As a common assumption, the Ising model is defined on a static lattice such that the neighbouring spins (i.e., the neighbourhood of each agent on a lattice) stay fixed over time. While natural systems (such as colonies of insects, flocks of birds, etc.) are characterised by dynamic topologies, where individuals constantly change their positions in space over time, creating dynamic networks. In this regard, we consider social application of the two-dimensional Ising model on the dynamic random geometric graph of agents to address the collective perception problem as described in Section 2.2.

In the following, we briefly introduce a theoretical background, including the description of the original Ising model and an overview of the concepts from the social impact theory, needed in this chapter.

3.2.1 Ising Model

The Ising model is one of the basic models in statistical physics to study ferromagnetism and to describe phase transition (i.e., change from one state to another). It is named after Ernst Ising (1925), who was the first to solve the one-dimensional version of the model and has shown that it does not have phase transition to an ordered ferromagnetic state, what, however, does not apply for its higher dimensions.

Originally, it is defined on a d -dimensional lattice, i.e., $\mathbb{Z}^d \subseteq \mathbb{R}^d$, with the coordinates as integer numbers. A finite lattice $\Lambda_\ell \subset \mathbb{Z}^d$ of size ℓ consists of the elements i called *sites* and is defined as follows:

$$\Lambda_L = \{i = (i_1, i_2, \dots, i_d) : 1 \leq i_j \leq \ell, j = 1, 2, \dots, d\}.$$

As such, in the case of $d = 2$, each point of the lattice (i.e., site) is connected to the other four adjacent ones, forming a static square lattice with the shape of a virtual torus (periodic boundary conditions) in relation to the neighbourhood (see Figure 3.1). In addition, each site $i \in \Lambda_\ell$ is characterised by a discrete variable $\sigma_i \in \{+1, -1\}$, which is

called *spin*. That is, in Figure 3.1, a spin pointed “up” corresponds to $\sigma_i = +1$ and a spin pointed “down” to $\sigma_i = -1$, respectively. The assignment of a spin value σ_i to each lattice site $i \in \Lambda_\ell$ represents a *spin configuration* $\sigma := \{\sigma_i\}_{i \in \Lambda_\ell}$.

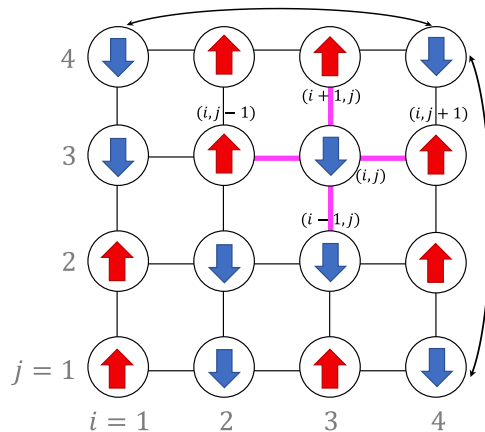


Figure 3.1: Example of a two-dimensional Ising model configuration on a square lattice Λ_4 . Each spin is interacting with its neighbouring spins in the von Neumann neighbourhood (depicted in magenta colour).

In this way, the Ising model is defined by the total energy of its current spin configuration σ and is computed by the Hamiltonian H as follows:

$$H(\sigma) = - \sum_{\langle ij \rangle} w_{ij} \sigma_i \sigma_j - h \sum_i \sigma_i, \quad (3.1)$$

where $\langle ij \rangle$ is a pair of neighbouring sites on a lattice Λ_ℓ such that $\langle ij \rangle = \{i, j \in \Lambda_\ell : |i - j| = 1\}$, i.e., the Euclidean distance between two adjacent points equals 1. The interaction between corresponding neighbouring spins σ_i and σ_j is specified by parameter w_{ij} . The sign of w_{ij} identifies whether the spins prefer to align ($w_{ij} > 0$) or to anti-align ($w_{ij} < 0$), while its absolute value determines the strength of the interaction. As such, to calculate the energy of the interactions between spins in the system, one has to sum over all pairs of neighbouring sites, while longer range interactions are neglected. In the case of the presence of an external magnetic field, which tries to align all the spins in one direction, one has to define the term $h > 0$. Here, we consider the case with $h = 0$ such that

$$H(\sigma) = - \sum_{\langle ij \rangle} w_{ij} \sigma_i \sigma_j. \quad (3.2)$$

The probability that the system is in a state with configuration σ is called the configuration probability $\mu_\ell(\sigma)$ and is calculated as follows:

$$\mu_\ell(\sigma) = \exp(-\beta H(\sigma)) / \sum_{\sigma} \exp(-\beta H(\sigma)), \quad (3.3)$$

where $\beta = 1/kT$ with temperature T and Boltzmann constant k . The denominator sums over all possible 2^ℓ spin configurations of a given finite lattice Λ_ℓ and defines the *partition function* of the model, which describes the statistical properties of a system.

To simulate the two-dimensional Ising model, one can use a modified Monte Carlo method, namely the Metropolis algorithm (Newman and Barkema, 1999). It follows the concept of *single-spin-flip* dynamics and is aimed at total energy minimisation, being established as follows:

- (1) Given the configuration σ , a lattice site is selected at random with probability $1/\ell$ and its respective spin is flipped.
- (2) The energy $H(\sigma')$ of a new configuration σ' is calculated according to Equation 3.2.
- (3) If $H(\sigma') < H(\sigma)$ the flip performed at step (1) is accepted, otherwise it is accepted with probability $\exp(-\beta(H(\sigma') - H(\sigma)))$.
- (4) Return to the step (1).

The process is repeated until all spins of a lattice are aligned. The evidence exists that the system converges in the case of $d = 2$ (Peierls, 1936). In such a setting, the temperature T is responsible for the exploitation-exploration trade-off, since high values of T increase the probability to accept the flip, which does not minimise the total energy of the system, and, as such, promote explorative behaviour, while lower values of T decrease the chance of accepting not energy-minimising flips and, therefore, enhance the exploitation.

The average value of all the spins on a lattice Λ_ℓ defines the level of model's magnetization such that

$$M(\sigma) = \frac{1}{\ell} \sum_{i=1}^{\ell} \sigma_i. \quad (3.4)$$

While one is usually interested in the study of the system's dynamics in the thermodynamic limit, i.e., $\ell \rightarrow \infty$, it was also shown that spontaneous magnetization is observed already on relatively small lattices, although characterised by the smoothed singularities due to the finite size (Bonati, 2014).

3.2.2 Social Impact Theory

Social impact theory (SIT) was proposed by Latané (1981) to model and predict how the social environment affects an individual. It is based on the concepts, attempting to cover a range of emotions, perceptions, attitudes, and physiological states of the individuals and their impact on the others within a society. The impact of a social group on a focal ¹ individual is modelled by a social force field I and represents a multiplicative function of the strength of the assertiveness s , proximity d_E , and the number of the individuals N , that is, $I = f(N \cdot s \cdot d_E)$. It is considered that these three parameters have a significant effect on the exerted influence, such as if one of them approaches zero, the whole impact is neglected. In particular, assertiveness is aimed to describe the aspect of the psychological coupling between the individuals, encompassing different interpersonal and situation-specific factors.

To observe the spread and change in the attitudes of individuals in the group, Nowak *et al.* (1990) refined the static model of Latané (1981) and suggested using a type of Ising

¹Selected person under consideration.

model to model the dynamics of social interactions like spin dynamics, following the principles of SIT. The same as in the case of the Ising model, the individuals in (Nowak *et al.*, 1990) do not move in space and have fixed positions on a lattice. The psychological coupling between the individuals is expressed by two parameters, persuasiveness, p_{ij} , and supportiveness, s_{ij} . The former indicates the degree to which the individual j can convince the individual i to change the opinion, while the latter sets the degree to which the individual j supports the individual i to keep the opinion. In this regard, the social impact I_i of a group consisting of N members on the individual i is calculated in the following way:

$$I_i = \left[\sum_{j=1}^N \frac{p_{ij}}{d_E^\alpha(i, j)} (1 - \sigma_i \sigma_j) \right] - \left[\sum_{j=1}^N \frac{s_{ij}}{d_E^\alpha(i, j)} (1 + \sigma_i \sigma_j) \right], \quad (3.5)$$

where $\sigma_i \in \{-1, +1\}$ represents a binary opinion of the individual i and $d_E(i, j)$ is the Euclidean distance between two individuals i and j in the physical space along with the parameter $\alpha \geq 0$, regulating the degree of a decline in the influence of distant individuals j from the individual i . The parameters $s_{ij}, p_{ij} \geq 0$ are reassigned to random positive values each time an individual changes its opinion.

The persuasive component (the first sum of Equation 3.5) equals zero, if the agents hold the same opinions, resulting in $I_i < 0$, and $I_i > 0$ otherwise. As such, the opinion dynamics of the individual i depends on the sign of the I_i^t at time t and is defined as follows:

$$\sigma_i^{t+1} = -\sigma_i^t \operatorname{sgn}(I_i^t). \quad (3.6)$$

That is, the individual i changes its opinion if $I_i > 0$, and keeps it if $I_i < 0$. Equation 3.6 is applied synchronously to every individual. To simulate possible “misunderstandings” that can arise between the individuals during communication, one can introduce noise $\beta > 0$ into Equation (3.6). As such, the individual will change its opinion with the probability proportional to $\exp(\beta I_i^t)$.

Based on the extensive computer simulations in (Nowak *et al.*, 1990), clustering and polarization of opinions were noted as the most typical collective behaviours using Equations 3.5 and 3.6, depending on the initial distribution of opinions. Also, Lewenstein *et al.* (1992) studied these equations theoretically using a mean-field approach, considering a fully connected system of agents, and obtained the results confirming the simulations. The considered above opinion dynamics can be modified by introducing the learning procedure for the parameters p_{ij} and s_{ij} such that their variations with time are adjusted to be correlated with the opinions of the individuals. For a review of learning effects in SIT, we refer to Kohring (1996) and Holyst *et al.* (2001).

3.3 Proposed Methodology

In this section we propose an adaptation of the Ising model complemented with the principles of the dynamic SIT to be applied to the binary scenario of collective perception.

In the collective perception scenario, instead of fixed lattice sites, we consider N individuals which are moving in the physical space, changing their local neighbourhoods, and receiving information not only from their immediate neighbours (subject to the fulfilment of certain conditions, see Section 2.4) but also from the environment. Unlike the

models in Section 3.2, where the analysis of convergence is focused solely on the relations between the agents given initial population configuration, here the agents must agree on the most dominant feature in an unknown environment. Thus, these features have to be additionally explored. Considering this, we keep the exploration as in Figure 2.3 and concentrate on modifications to the “Decision()” block. Different from the classical opinion-based decision-making approaches considered in Section 2.4.1, along with opinions we endow the agents with the preferences representing a bias towards one of the possible outcomes. In the following, we describe our developed model of coupled opinion and preference dynamics.

3.3.1 Opinion Dynamics

Considering a binary scenario, we assume that each member i of a swarm can share one of two opposing opinions on a subject of matter, i.e., the most frequently met colour in the environment, denoted as $\sigma_i = \pm 1, i = 1, 2 \dots N$, black or white (analogue of “up” and “down” spins). Besides, we also assume that each individual i possesses an inner preference for a particular outcome, denoted as $\zeta_i = \pm 1$. To note, the agents keep their preferences solely to themselves and do not communicate them to others.

The idea is that the individuals can directly affect each other’s decisions with different strengths, depending on whether the opinions held by the others are in correspondence with the preference of the agent under consideration or not. As such, each agent in a group favours the evidence from the others supporting its own preference and represents a subject of *confirmation bias*.

Example 3.1 *Let us consider an agent z , which holds a preference for black colour, i.e., $\zeta_z = +1$. Whenever this agent encounters another agent j with opinion “black”, i.e., $\sigma_j = +1$, it places greater importance on this “evidence” than on the one from the agent i corresponding to the white colour, i.e., $\sigma_i = -1$.*

To define the social field of agent z to fit the aforementioned concept, as the first step, we rewrite Equation 3.2 as follows:

$$I_z^* = - \sum_{\langle zj \rangle} w_{zj} \sigma_z \sigma_j = \frac{1}{2} \sum_{\langle zj \rangle} w_{zj} (1 - \sigma_z \sigma_j) - \frac{1}{2} \sum_{\langle zj \rangle} w_{zj} (1 + \sigma_z \sigma_j), \quad (3.7)$$

where $\langle zj \rangle$ denotes a pair of neighbouring individuals in communication mode and the value of $|w_{zj}|$ indicates the intensity of their “psychological impact” on each other, holding opinions σ_z and σ_j , respectively. As such, if agents z and j share the same mental states, then Equation 3.7 consists only of the second sum and of the first sum otherwise.

As the second step, we incorporate preferences in Equation 3.7. According to our Example 3.1, within one interaction, when the opinion of the neighbouring agent j , i.e., σ_j , coincides with the preference ζ_z of the focal agent z , the social field of the agent z has to amplify the role of such neighbours before those whose opinions are in contradiction with the preference ζ_z . In the following, we introduce the parameter w_z to describe the degree of confirmation needed for the agent to be confident in its own preference. This means that if we consider in Equation 3.7 the mental state σ_z as the preference of the individual z , i.e., ζ_z , then the second term of Equation 3.7 has to be w_z times

greater than the first one. As such, when the preference σ_z and the opinion σ_j are opposing each other, Equation 3.7 consists only of the first term, which in turn has to be w_z times smaller than when Equation 3.7 is represented only by the second one. As such, if the agent has low value of w_z , he needs to seek for more evidence from the others to become confident in itself (i.e., “self-doubting” agent) than the one with higher value of w_z (i.e., “self-confident” agent). That is, in the classical model of social impact, as of Equations 3.5 and 3.6, the agents are “attentive” to others in the sense that the psychological coupling w_{zj} is expressed via two parameters p_{zj} and s_{zj} , which indicate the particular influence exerted by the individual j on the individual z and as such is defined mainly by the influencing individual j . While in our case, as in Example 3.1, the strength of impact coming from others is controlled by the agent z itself from “inside”, i.e., self-centred influence on the contrary to the socio-centric one as in Equation 3.5.

In this way, considering that agent z puts in $w_z > 1$ times more weight on the opinions of its neighbours j that correlate with its own preference ζ_z than on the opinions of those that do not, we redefine Equation 3.7 as follows:

$$I_z = \frac{1}{2} \sum_{j=1}^{\mathcal{N}_z} w_z \zeta_z (1 + \zeta_z \cdot \sigma_j) - \frac{1}{2} \sum_{j=1}^{\mathcal{N}_z} \zeta_z (1 - \zeta_z \cdot \sigma_j) = \quad (3.8)$$

$$= \begin{cases} w_z n_z^+ - n_z^-, & \text{if } \zeta_z = +1 \\ n_z^+ - w_z n_z^-, & \text{if } \zeta_z = -1. \end{cases}$$

As such, the weight w_z is applied as an enhancement of the impact of neighbours that identify with an individual’s internal preference. In other words, it acts as an “inner” supportive parameter $s_{zj} := w_z$, which is the same for all neighbours j in the neighbourhood \mathcal{N}_z of the individual z , while a persuasive parameter is omitted (or $p_{zj} := 1$). One should also take into account the sign of I_z^* and respectively of its sum parts in Equation 3.7. That is, if $\zeta_z = -1$ then the respective weighted sum with neighbouring individuals of opinion $\sigma_j = -1$ has to bias the value of I_z to be negative, while in the case of $\zeta_z = +1$ and $\sigma_j = +1$ – to be a positive one. Therefore, to control the sign of the sums in Equation 3.7 to correlate with the preference of the individual z , we multiply each of them on the value ζ_z such that the non-zero sum over the neighbouring individuals with opinion $\sigma_j = -1$ gets always the negative sign. As a result, one can distinguish two cases depending on the preference ζ_z as shown in Equation 3.8, where n_z^+ and n_z^- depict the number of neighbouring agents with opinion $\sigma_j = +1$ and $\sigma_j = -1$, respectively. We assume that if $w_z = 1$, the individual does not have any preference for the outcomes, i.e., it is *indifferent*.

To generalise the case distinction considered in Equation 3.8, we introduce in Equation 3.9 the parameter w'_z such that $w'_z = w_z$ if $\zeta_z = +1$ and $w'_z = \frac{1}{w_z}$ if $\zeta_z = -1$. That is, $w'_z \in (0, 1)$ if $\zeta_z = -1$ and $w'_z > 1$ if $\zeta_z = +1$, while $w'_z = 1$ if there is no preference. After normalisation, we get the following:

$$\hat{I}_z = \frac{w'_z n_z^+ - n_z^-}{w'_z n_z^+ + n_z^-} \in [-1, 1]. \quad (3.9)$$

To incorporate the impact of the spatial distances between the neighbouring individuals z and j such that the closer individuals to the agent z have greater influence than

the farther ones, following SIT principle one can modify Equation 3.9 as follows:

$$\hat{I}_z = \frac{w'_z \sum_{j \in \mathcal{N}_z^+} (1/d_E^\alpha(z, j)) - \sum_{j \in \mathcal{N}_z^-} (1/d_E^\alpha(z, j))}{w'_z \sum_{j \in \mathcal{N}_z^+} (1/d_E^\alpha(z, j)) + \sum_{j \in \mathcal{N}_z^-} (1/d_E^\alpha(z, j))} \in [-1, 1], \quad (3.10)$$

where \mathcal{N}_z^+ and \mathcal{N}_z^- represent the neighbourhoods of the agent z with the agents of opinion $\sigma_j = +1$ and $\sigma_j = -1$, respectively. In case $\alpha = 0$, Equation 3.9 is the particular case of Equation 3.10.

Given a normalised social field \hat{I}_z of the individual z , we define the opinion dynamics based on the probability values obtained from the following sigmoid activation function according to (Hartnett *et al.*, 2016):

$$p_\beta(\hat{I}_z) = \frac{1}{2} \left(1 + \frac{\tanh(\beta \hat{I}_z)}{\tanh(\beta)} \right) \in [0, 1], \quad (3.11)$$

where $\beta \in (0, \infty)$ describes the nonlinearity of the model. Changing the parameter β from 0 to ∞ one can get a range of voting behaviours between the voter model and the majority rule (Drouffe and Godrèche, 1999). Indeed, when $\beta \rightarrow 0$, p_β is approximated by the linear function which equals 0 and 1 at the corresponding ends of a given segment $\hat{I}_z \in [-1, 1]$ (see Figure 3.2). As a result, the probability to switch the opinion is proportional to the difference between the number of agents with $\sigma_j = +1$ and $\sigma_j = -1$ (given $w'_z = 1$ in Equation 3.9), what corresponds to the likelihood defined by the voter model. While, when $\beta \rightarrow \infty$, p_β represents a step function such that $p_\beta = 1$ if $\hat{I}_z > 0$ and $p_\beta = 0$ if $\hat{I}_z < 0$ along with $p_\beta = 0.5$ at $\hat{I}_z = 0$. In this way, the switch is determined by the sign of the majority, i.e., for $\hat{I}_z > 0$ individuals with $\sigma_j = +1$ are in majority and, therefore,

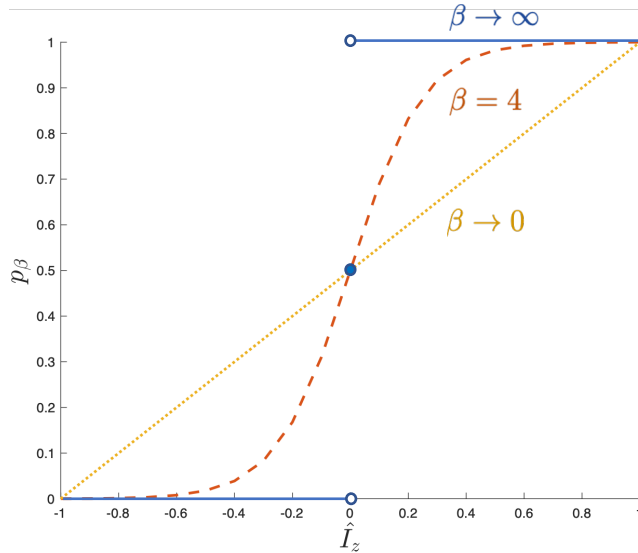


Figure 3.2: Activation function according to Equation 3.11.

$\sigma_j = +1$ will be selected as the new opinion, while for $\hat{I}_z < 0 - \sigma_j = -1$ (given $w'_z = 1$ in Equation 3.9). As such, the model is correspondent to the majority rule for $\beta \rightarrow \infty$.

Decision-making

Finally, the agent z changes its opinion from σ_z^t at discrete time t to σ_z^{t+1} at $t+1$ according to the following function $h: \Omega \rightarrow \Omega$:

$$h: \sigma_z^t \mapsto \sigma_z^{t+1} := \begin{cases} +1 & \text{with probability } p_\beta(\hat{I}_z), \text{ if } \sigma_z^t = -1 \\ -1 & \text{with probability } 1 - p_\beta(\hat{I}_z), \text{ if } \sigma_z^t = +1. \end{cases} \quad (3.12)$$

3.3.2 Preference Dynamics

The decision of an individual z to change its current opinion σ_z^t is based on its social field \hat{I}_z calculated according to Equation 3.10, which is mainly defined by the individual's preference ζ_z and its strength w'_z . While one can assume that the preference keeps static, in the following, we adjust the introduced above opinion dynamics by incorporating the learning procedure for the preferences as originally proposed by the current author in (Bartashevich and Mostaghim, 2019b).

The purpose of the proposed Algorithm 3.1 is to balance the opinions and preferences of an individual such that they are in consonance with each other in order to avoid cognitive dissonance. The state of *cognitive dissonance* can be considered as a state of inner disagreement within an individual, when its opinion σ_z (visible to everyone) does not correspond to its inner cognition/preference ζ_z (not visible to others), e.g., $\sigma_z = -1$ and $\zeta_z = +1$. Since the value of the preference strength w'_z and the preference itself ζ_z are correlated by definition, we do not operate explicitly with the parameter ζ_z but with w'_z . As such, by controlling the value of w'_z one can dynamically adjust the preference

Algorithm 3.1: Preference Dynamics (Bartashevich and Mostaghim, 2019b)

<p>1: if $w'_z > 1$ & $\sigma_z^t = +1$ then</p> <p>2: if $\sigma_z^{t+1} = -1$ then</p> <p>3: $w'_z = w'_z - \Delta w'$</p> <p>4: end if</p> <p>5: if $\sigma_z^{t+1} = +1$ then</p> <p>6: $w'_z = w'_z$</p> <p>7: end if</p> <p>8: end if</p> <p>9: if $w'_z > 1$ & $\sigma_z^t = -1$ then</p> <p>10: if $\sigma_z^{t+1} = -1$ then</p> <p>11: $w'_z = w'_z - 2\Delta w'$</p> <p>12: end if</p> <p>13: if $\sigma_z^{t+1} = +1$ then</p> <p>14: $w'_z = w'_z + \Delta w'$</p> <p>15: end if</p> <p>16: end if</p>	<p>17: if $w'_z < 1$ & $\sigma_z^t = +1$ then</p> <p>18: if $\sigma_z^{t+1} = -1$ then</p> <p>19: $w'_z = w'_z - \Delta w'$</p> <p>20: end if</p> <p>21: if $\sigma_z^{t+1} = +1$ then</p> <p>22: $w'_z = w'_z + 2\Delta w'$</p> <p>23: end if</p> <p>24: end if</p> <p>25: if $w'_z < 1$ & $\sigma_z^t = -1$ then</p> <p>26: if $\sigma_z^{t+1} = -1$ then</p> <p>27: $w'_z = w'_z$</p> <p>28: end if</p> <p>29: if $\sigma_z^{t+1} = +1$ then</p> <p>30: $w'_z = w'_z + \Delta w'$</p> <p>31: end if</p> <p>32: end if</p>
---	--

of the respective individual z . That is, as soon as the value of w'_z becomes greater or less than 1, its corresponding preference value ζ_z changes accordingly, i.e., becomes +1 or -1, respectively. In this regard, at the transition phase (Equation 3.12), depending on the current opinion σ_z^t and the new opinion σ_z^{t+1} of an agent z as well as its current preference (defined by w'_z), we either decrease or increase the preference strength w'_z . That is, if after interaction with social and physical environment the agent z changes its opinion to σ_z^{t+1} such that

- a) the agent gets into cognitive dissonance at $t+1$, we reduce the strength of its preference on $\Delta w'$ to incline the preference towards a new opinion σ_z^{t+1} (lines 3 and 30 in Algorithm 3.1).
- b) the agent remains in the cognitive dissonance at $t+1$, we perform a double decline in the preference strength to accelerate the corresponding change of the preference (lines 11 and 22 in Algorithm 3.1).
- c) the agent gets out of cognitive dissonance at $t+1$, we enhance its preference by reinforcing the preference strength on $\Delta w'$ to the respective side (lines 14 and 19 in Algorithm 3.1).
- d) the agent stays in the cognitive consonance at $t+1$, the preference and its strength do not change (lines 6 and 27 in Algorithm 3.1)

Thus, the proposed preference decision-making mechanism is performed by the composition of the function $h: \Omega \rightarrow \Omega$ given in Equation 3.12 and Algorithm 3.1, in the result of which opinions and preferences “co-evolve” together by means of social experiences and interactions with the environment.

3.4 Experimental Study

The experimental study of this chapter is designed to provide the proof-of-concept for the proposed methodology and, hence, to address the first objective set in Section 1.3. In particular, the impact of the preferences on the opinion-based collective decision-making process is investigated along with the nonlinearity of the proposed model in Section 3.3.

The multi-agent simulation setup and the model of the collective perception environment are provided in Sections 2.2 and 2.4. The prevailing colour in the environment is set to “white”. That is, we assume that a swarm of $N = 20$ agents reached the consensus on the correct outcome, when any individual z in a swarm holds the opinion $\sigma_z = -1$ (i.e., “white”). The opinion and the preference updates are done at the end of the dissemination state of a given agent before its new exploration state (i.e., “Decision()” block in Figure 2.3) based on its last $L_{max} = 4$ neighbours with whom the agent has communicated (as described in Section 2.4) during its last $\delta\tau = 0.3$ seconds (s) of the dissemination state. The period of each individual’s exploration state is constant and lasts $t = 10$ s. If another is not stated, the simulation configuration parameters can be found in Appendix A.

To validate the proposed methodology, we investigate the following preference-based decision-making strategies:

- without preference update:
 - **Static** policy is defined by the function h in Equation 3.12 and does not follow Algorithm 3.1 such that the initial preferences of the individuals are kept stable and do not change within time as well as their respective preference strength. In this regard, we set the preference ζ_z of each individual z in a swarm to coincide with its initial opinion σ_z and define $w'_z := 1.5$ for $\zeta_z = +1$ (preference for “black”) and $w'_z := 1/1.5$ for $\zeta_z = -1$ (preference for “white”), respectively.
 - **W-Static** policy is the variation of the **Static** one but with the initial guess concerning the correct outcome provided by a designer (a capital letter of the policy name indicates an expected outcome, i.e., “W”-white). In this vein, the initial preference for a swarm is given by a designer/human as a conjecture (e.g., “white is correct” as in the considered case) based on some information sources not available to the agents. In this sense, the given conjecture represents only one hypothesis, which is given to all individuals in a swarm to test it in a distributive manner. As such, each individual in a swarm independent of its initial opinion is initialised with the global value $w'_z < 1$ (i.e., the same for each individual) sampled uniformly at random in the interval $(0, 1)$ at each simulation run.
 - **B-Static** is based on the same principle as W-Static, with the difference that initial conjecture set by a designer is wrong and corresponds to the incorrect outcome. That is, the agents assume that “black is correct”. Therefore, each agent is initialised with the global value $w'_z > 1$ sampled uniformly at random in the interval $(1, 2)$.
- with preference update:
 - **Adaptive** policy is defined by the composition of the function h in Equation 3.12 and Algorithm 3.1 such that the preferences of the individuals and their respective strengths are changing within time. We initialise preferences in the agreement with agents’ initial opinions and set the global preference strength for each member z in the swarm, which is sampled uniformly at random in the range of $(0, 1)$ and in the range of $(1, 2)$ for $\zeta_z = -1$ and for $\zeta_z = +1$, respectively. In this way, w'_z values are initially the same for the agents with the same preference. To note, the value of w'_z for $\zeta_z = -1$ is not an inverse value of w'_z for $\zeta_z = +1$ as in Static policy.
 - **W-Adaptive** represents the counterpart of W-Static but with dynamic preferences following Algorithm 3.1.
 - **B-Adaptive** is the counterpart of B-Static with adaptive policy following Algorithm 3.1.

In the following, we summarise considered above policies in Table 3.1. To note, the value of the preference strength w'_z is set globally to a swarm each simulation run. If not stated otherwise, we set $\Delta w' = 0.1$ in Algorithm 3.1 and $\alpha = 0$ in Equation 3.10.

Besides, a swarm can contain **unbiased individuals**, that is, those who do not have a preference for any of the options, and, hence, are defined by $w'_z = 1$. We assume that if

	Static	W-Static	B-Static	Adaptive	W-Adaptive	B-Adaptive
agents with $\sigma_z = -1$	$w'_z = 1/1.5$	$w'_z = rand(0,1)$	$w'_z = rand(1,2)$	$w'_z = rand(0,1)$	$w'_z = rand(0,1)$	$w'_z = rand(1,2)$
agents with $\sigma_z = +1$	$w'_z = 1.5$			$w'_z = rand(1,2)$		
use of Alg. 3.1	no	no	no	yes	yes	yes

Table 3.1: Preference initialisation of six preference-based decision-making strategies with respect to the agents' initial opinions $\sigma_z \in \{+1, -1\}$.

such individuals are present in the swarm, they do not update their preferences regardless of the applied policy, as such remaining indifferent during the entire simulation time of $T = 40000$ iterations.

The opinions of the individuals are initialised in equal proportions, favouring correct and incorrect outcomes. That is, the initial densities of the individuals in the population with opinion $\sigma_z = -1$ and $\sigma_z = +1$ are equal and correspond to $\rho_{wh} = \rho_{bl} = 0.5$, respectively. As such, depending on the density of unbiased individuals in the population $\rho_{un} \in [0, 1]$, the agents' preferences in the case of **Static** and **Adaptive** policies are distributed in the following way. Given a swarm of N agents, $N * \rho_{un}$ individuals are assigned $w'_z = 1$, whereas $\rho_{wh} = \rho_{bl} = (1 - \rho_{un}) * 0.5$ such that the remaining $N * \rho_{wh}$ and $N * \rho_{wb}$ individuals with corresponding opinions $\sigma_z = -1$ and $\sigma_z = +1$ are assigned the preference strengths $w'_z < 1$ and $w'_z > 1$, respectively.

The experimental study is organised as follows. Section 3.4.1 aims to give an insight into the influence of the nonlinearity parameter β in Equation 3.11 on the behaviour of the model introduced in Section 3.3 along with the impact of unbiased individuals on the collective decision-making. Section 3.4.2 investigates the performance of static and adaptive preference-based decision-making policies with respect to the given preference for the whole swarm (see Table 3.1) over different colour ratios in the environment, while Section 3.4.3 examines the influence of initial opinion distribution. Finally, Section 3.4.4 sheds some light on the weight of physical distance between the agents in Equation 3.10 regarding the collective performance in the given context.

3.4.1 Impact of Indifferent Individuals

The goal of the first experiment is to investigate how density ρ_{un} of indifferent individuals (those who have no inherent preference, i.e., $w_z = 1$) affects the consensus time and the exit probability of a swarm on the correct outcome with regard to the nonlinearity parameter β . For this purpose, three preference-based decision-making policies, namely, Static, Adaptive, and W-Adaptive, are evaluated on the binary collective perception scenario with a random distribution of black and white cells being almost in equal proportions in the environment, i.e., $\rho_b^* = 0.92$ ².

In Figure 3.3, for each parameter $\beta \in \{0.5, 1.0, 1.5, 2.0, 2.5, 3.0, 3.5, 4.0, 4.5, 5.0\}$, we analyse the consensus time on the correct outcome as a function of $\rho_{un} \in \{0, 0.1, \dots, 1.0\}$ using a local weighted regression (LOESS) and a generalised linear model (GLM) with a binomial distribution for the exit probability, respectively, to show trends in the data gathered over 40 simulation runs. Regardless of the parameter β , the performance of W-Adaptive drops significantly in both metrics with the increase in the number of in-

²The value of ρ_b^* indicates the ratio of black Γ_{bl} and white Γ_{wh} cells on the grid such that $\rho_b^* = \Gamma_{bl}/\Gamma_{wh}$, given $\Gamma_{wh} > \Gamma_{bl}$.

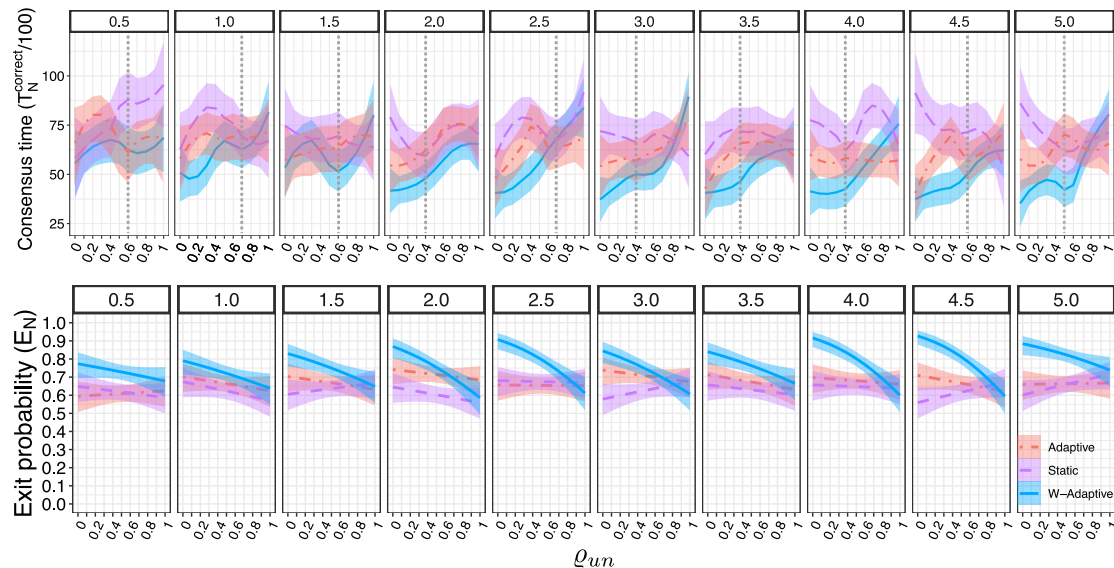


Figure 3.3: Consensus time ($T_N^{correct}$) and exit probability (E_N) over density ρ_{un} of unbiased individuals in the swarm for each value of the nonlinearity parameter β (top headings). Shaded areas represent the 95% confidence interval. Task difficulty: $\rho_b^* = 0.92$. Top plot is from (Bartashevich and Mostaghim, 2019b).

different individuals in the population. As expected, in the case of $\rho_{un} = 0$, it is the best decision-making policy (DM) among others with the lowest consensus time and the highest exit probability rate, reaching its peak performance for $\beta \in \{4.0, 4.5\}$. The results provide evidence that being initially biased towards the correct outcome, individuals following W-Adaptive policy can maintain their preferences, i.e., $w'_z \in (0, 1)$, despite almost equal proportions of the colours in the environment. However, as indifferent agents are integrated into the group, the accuracy of the W-Adaptive swarm degrades steadily along with the increase in the consensus time, while Adaptive and Static policies are less affected by the presence of unbiased sub-groups, preserving the exit probability around (0.6, 0.7) across examined values of ρ_{un} and β . In general, Adaptive and Static policies are described by the similar accuracy (exit probability) but differ in the consensus speed, where the former is primarily faster than the latter for lower densities ρ_{un} . Overall, the best results in terms of speed and accuracy are mainly observed for both adaptive policies at $\rho_{un} = 0$ with $\beta \in (2.0, 5.0)$.

Interestingly to note, for Static policy, the presence of indifferent agents in the population facilitates a decrease in the consensus time without deteriorating accuracy for some values of β , i.e., at $\rho_{un} = 0.4$ for $\beta = \{3.0, 4.0\}$ and at $\rho_{un} = 0.5$ for $\beta = \{4.5, 5.0\}$, respectively. In the case of $\beta = 4.0$, a steady rate in the consensus time for both W-Adaptive and Adaptive is observed up to $\rho_{un} = 0.4$, while Static consensus time drops by this point. Generally, the consensus speed for W-Adaptive and Adaptive raises with the number of unbiased individuals for most of the considered values of β , accompanied by some non-significant decline around $\rho_{un} = 0.6$ for lower values of $\beta \in (0.5, 1.5)$. Nevertheless, the best performance for both adaptive strategies in terms of consensus speed and the accuracy is observed at $\rho_{un} = 0$ for $\beta = 4.5$. As such, in the following experiments of

this chapter, we set $\beta = 4.5$.

The observed results for Static policy, in particular, in the case of $\beta = \{4.5, 5.0\}$, are consistent with the findings in (Hartnett *et al.*, 2016), where it was shown that the individuals without a preference (i.e., indifferent ones) reduce the time to reach a consensus state in a collective placed on a two-dimensional square lattice with fixed positions and without environmental stimuli. Our finding suggests that in the case of static preferences, being coupled with a positive feedback loop and interactions with the environment, indifferent members in a dynamic geometric graph of agents assist in the propagation of opinions reflecting the correct outcome and of the highest quality. While this does not apply in the case of adaptive preferences, where the unbiased individuals, particularly in the case of W-Adaptive, deteriorate the collective performance. The latter can be explained by the fact that the preference strength of indifferent agents, i.e., $w_z = 1$, remains constant over time without undergoing individual adaptation, thereby attenuating the adaptation process as a whole at the collective level, resulting in longer periods of consensus time.

3.4.2 Influence of the Task Difficulty

The goal of the second experiment is to determine how preferences alone impact the opinion dynamics and, hence, the collective outcome in comparison to the classical preference-free opinion-based decision-making strategies such as majority rule and the voter model coupled together with direct modulation of the positive feedback, namely DMMD and DMVD, as in (Valentini, 2017). To do this, we vary the task difficulty ρ_b^* and evaluate the performance of three static (Static, W-Static, B-Static) and three adaptive (Adaptive, W-Adaptive, B-Adaptive) preference-based decision-making policies with regard to different preference initialisation without the presence of indifferent individuals, as indicated in Table 3.1, relative to the performance of DMMD and DMVD.

Figures 3.4 and 3.5 show the exit probability using a GLM with binomial distribution and the consensus time on the correct outcome smoothed using LOESS over eight task difficulty variations and 100 simulation runs for each difficulty and decision-making policy. As one can observe from the figures, the performance primarily drops with the increase of the task difficulty, regardless of the applied strategy. The results for the DMVD and the DMMD strategies are consistent with those presented in (Strobel *et al.*, 2018), where the updated simulation implementation of Valentini *et al.* (2016) was used. That is, the DMVD strategy is more accurate than the DMMD, i.e., characterised by a higher exit probability at all difficulty settings (Figure 3.4), while the DMMD is below 1.0 exit probability even on $\rho_b^* = 0.52$. However, the DMVD has higher consensus time ($T_N^{correct}$) and higher variability than the DMMD, especially for higher difficulties, i.e., $\rho_b^* \geq 0.67$ (Figure 3.5).

As shown in Figure 3.4, the exit probability (E_N) of Static and Adaptive policies share a similar pattern with the DMVD strategy along with the decrease for higher ρ_b^* , although Adaptive is characterised by slightly higher E_N values for the most difficult setting. At the same time, according to Figure 3.5, Adaptive is significantly faster than both DMVD and Static, especially for $\rho_b^* \geq 0.67$. It is even faster than the DMMD strategy at almost all difficulty configurations, reaching the same $T_N^{correct}$ only at $\rho_b^* = 0.92$, along with a higher accuracy E_N . While $T_N^{correct}$ of the Static is in-between the

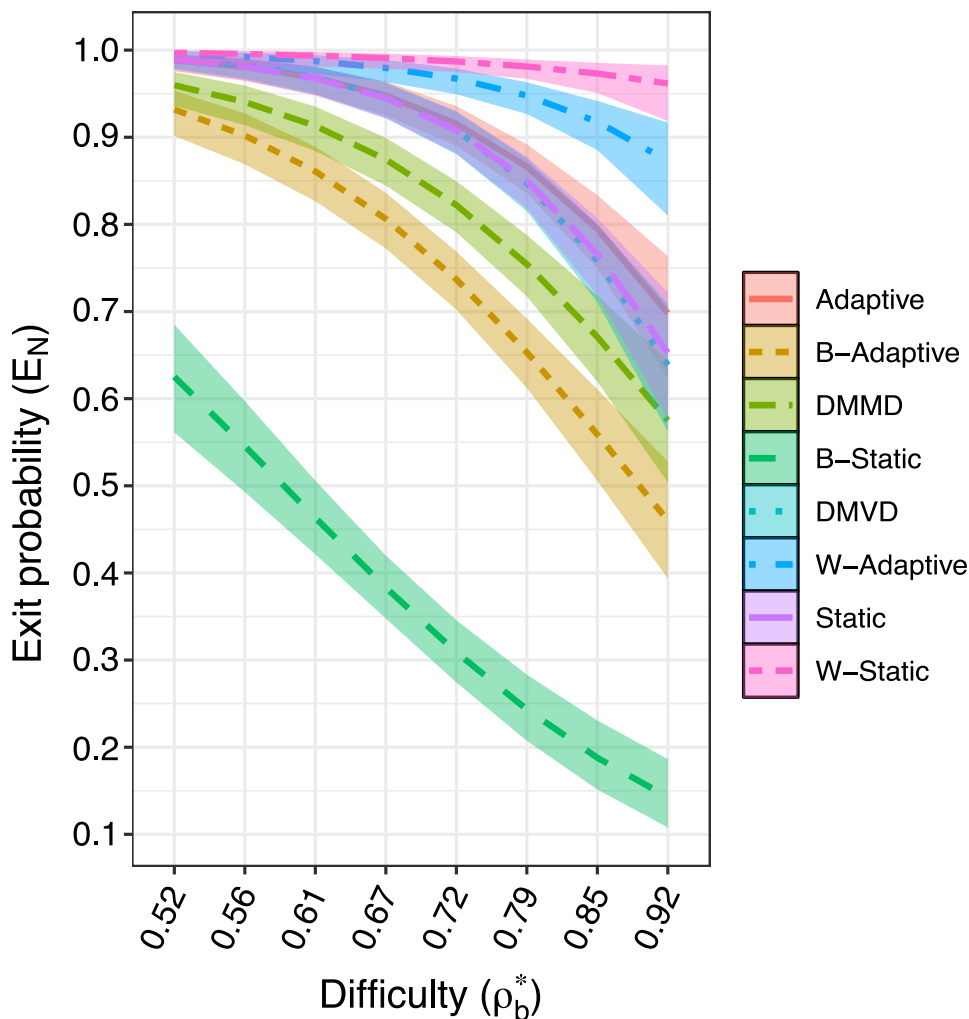


Figure 3.4: Exit probability (E_N) as a function of the task difficulty ρ_b^* . Configuration of parameters: $\rho_{un} = 0$, $\beta = 4.5$. Shaded areas represent the 95% confidence interval.

DMVD and the Adaptive for $\rho_b^* < 0.67$, reaching the same $T_N^{correct}$ as the DMMD at $\rho_b^* \in \{0.67, 0.72\}$, and increases for $\rho_b^* > 0.72$ at the same speed as the DMVD.

Indeed, the results obtained using W-Static and W-Adaptive are the best among others in both metrics E_N and $T_N^{correct}$. However, the exit probabilities of both policies are also characterised by a decline for higher difficulty settings, although W-Static drops only to $E_N \approx 0.95$ at $\rho_b^* = 0.92$, while the E_N of the W-Adaptive is already decreased for $\rho_b^* \geq 0.72$ reaching $E_N \approx 0.87$ at $\rho_b^* = 0.92$. The consensus time using the W-Static policy is unaffected by the task difficulty and remains stable around $T_N^{correct} \approx 30$ s. even at the highest difficulty. Interestingly to note, the W-Adaptive is characterised by lower consensus time than W-Static up to $\rho_b^* = 0.67$, the same $T_N^{correct}$ for $\rho_b^* \in \{0.67, 0.72\}$ and higher $T_N^{correct}$ for $\rho_b^* > 0.72$.

As expected, the performance of the B-Static policy is the worst among others. It has $E_N \approx 0.6$ at the easiest difficulty setting and drops to $E_N \approx 0.15$ at the hardest

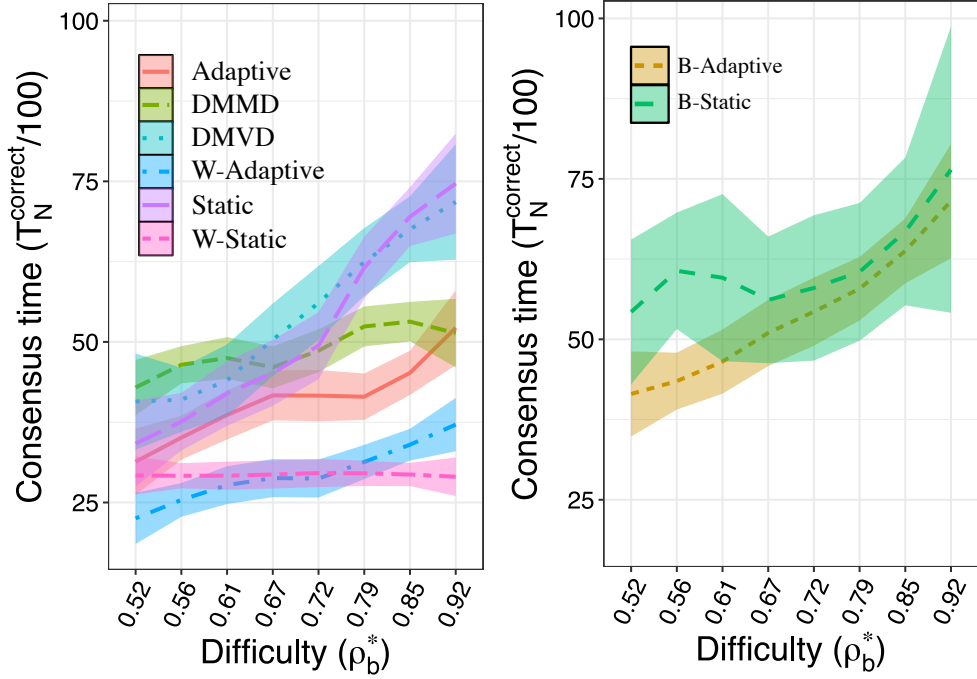


Figure 3.5: Consensus time (T_N^{correct}) as a function of the task difficulty ρ_b^* . Configuration of parameters: $\rho_{un} = 0$, $\beta = 4.5$. Shaded areas represent the 95% confidence interval.

one, accompanied by the longest consensus time T_N^{correct} also increasing with the task difficulty along with high variability. By analogy with W-Static and W-Adaptive, one could expect that the results obtained with the B-Adaptive policy should go aligned with the B-Static with a slightly better performance due to the dynamic update of the preferences, especially on the easier settings. Indeed, we observe a significantly better performance of the B-Adaptive policy in comparison to the B-Static in both metrics E_N and T_N^{correct} , although it is still worse than the other strategies under consideration. That is, the consensus time (T_N^{correct}) of the B-Adaptive policy resembles the pattern of the DMVD strategy, reaching similar T_N^{correct} on average as the B-Static with less variability for higher difficulties. While the exit probability of the B-Adaptive goes close to the exit probability of the DMMD strategy, especially for the easiest difficulty of the task, it drops below the E_N of the DMMD at the hardest setting, i.e., $E_N \approx 0.45$. Nevertheless, such a significant improvement of the B-Adaptive policy in terms of accuracy (E_N) compared to the B-Static indicates that the learning procedure 3.1 with the chosen reward $\Delta w'$ allows agents with the initial preferences in the range of (1,2) to reach the range of (0,1) with the probability of $E_N \approx 0.93$ for $\rho_b^* = 0.52$.

In summary, the results indicate that the Static policy driven by direct modulation of positive feedback resembles the DMVD strategy, but with a faster consensus speed for easier difficulty settings, owing to local noise-induced amplifications caused by the nonlinearity parameter β . Due to the preference dynamics, the resulting Adaptive policy is significantly faster in the consensus speed than both the DMVD and the DMMD

strategies, reaching only the similar consensus time as the DMMD at the highest difficulty, while keeping the high exit probability rates as the DMVD. The performance of the static policies is the best among the others in both metrics $T_N^{correct}$ and E_N when the agents' initial preferences are correlated with the actual correct outcome. On the other hand, these policies are the least reliable and the slowest ones when the agents' preferences are associated with a non-dominant colour (incorrect outcome). A similar pattern in performance is observed for the adaptive policies with the respective initialisation of preferences as well. However, adaptive policies are generally faster than their static counterparts. Moreover, in the case of the "non-appropriate"³ preference initialisation, the Adaptive policy is significantly more accurate relative to the Static one with the same initialisation.

The incorporation of the global preference towards the correct outcome in the Static policy leads to the expected almost 100% exit probability with the constant low consensus time unaffected by the task difficulty ρ_b^* . However, when the swarm is globally biased towards the incorrect outcome (as in the B-Static), the collective performance significantly deteriorates, although the B-Static is still able to keep the exit probability rate above the chance level for $\rho_b^* < 0.61$. It seems possible that the latter result is due to the numerical bias hidden in the values of the preference strength w'_z of the individuals. Indeed, the preference strength w'_z in Equation 3.9 advocates for both biases towards black and white outcomes, that is, leaving the weight of 1.0 and additionally the weight greater than 1.0, depending on the agent's z preference. Let us consider the following example. Even if we pretend that $w'_z = 2$, which is outside the initialisation range of the B-Static, it means that "the agent z prefers 'black' two times stronger than 'white' " or "the agent z prefers 'white' with 0.5 of the strength as it prefers 'black' ". As such, an initialisation with other values below 2 in the range of (1,2) leads even to a weaker preference strength in the black outcome and, hence, to a stronger than 0.5 preference strength in white. As a result, in the case of the easier difficulty settings and the direct modulation of the positive feedback, it shows itself as not strong enough to keep the agent's opinions biased towards black preference. To verify the latter, in the following, we provide additional experiments in the environment with the prevailing colour set to 'black'.

Figure 3.6 shows the exit probability for six preference-based decision-making policies using a GLM with binomial distribution over eight task difficulty configurations based on the data gathered in 100 simulation runs for the environments E^{wh} and E^{bl} with correct outcomes 'white' and 'black', respectively. While one can expect symmetrical results for both environments, we observe that this holds only for the Static policy, whereas the performance of the others in the case of the E^{bl} : 'black is correct' has deteriorated in comparison to their counterparts in the case of the E^{wh} : 'white is correct'. Compared to the B-Static policy on the E^{wh} , the exit probability of the W-Static on the E^{bl} drops below the chance level already for the easiest difficulty of the task. Indeed, in the case of the W-Static, the preference strength of an agent z is initially set in the range (0,1) such that considering, for instance, $w'_z = 0.2$ means that "the agent z prefers 'white' five times stronger than 'black' " or "the agent z prefers 'black' with 0.2 of the strength as it prefers 'white' ". As such, one can see that the initial relative preference strength

³Under "non-appropriate" preference initialisation, we mean the case when initial preferences of the agents are correlated with a non-dominant colour (incorrect outcome).

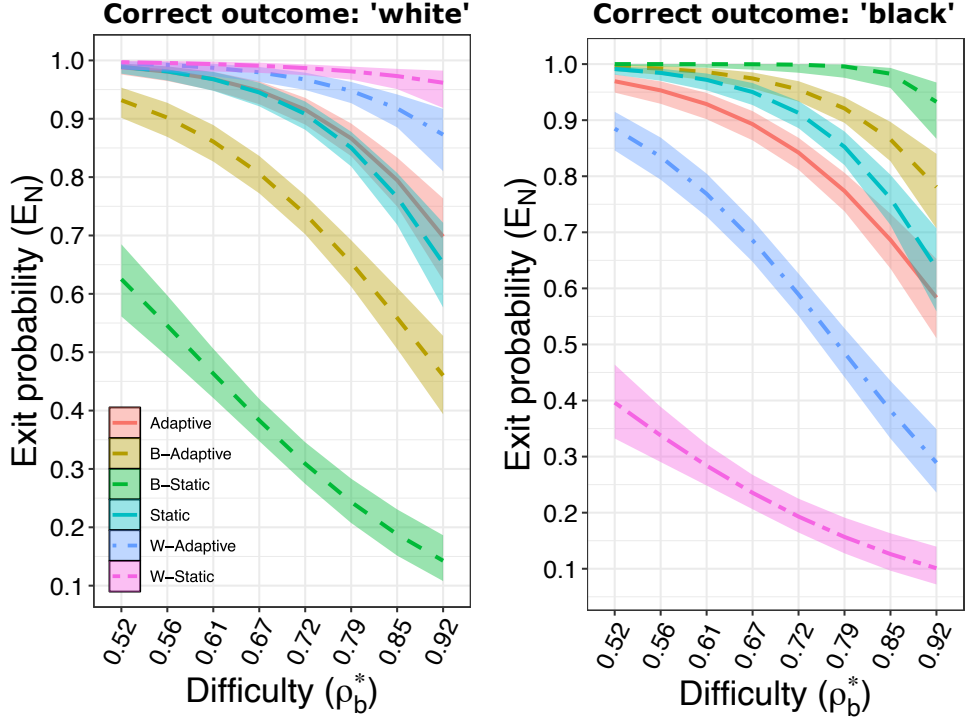


Figure 3.6: Exit probability (E_N) as a function of the task difficulty ρ_b^* for the environments with the prevailing colour ‘black’ and ‘white’ on the left-hand and on the right-hand side, respectively. Shaded areas represent the 95% confidence interval.

of the agents with the preference towards white can be much stronger than of the ones with the preference towards black. That is, as it was shown in the example with $w'_z \approx 2$, the maximum relative possible strength of the agents’ preference for the B-Static equals 2, while in the case of the W-Static it can go much above this value, e.g., it equals 5 in the case of $w'_z = 0.2$. Therefore, the agents with the white preference are in general less biased towards ‘black’ in comparison to the ‘white’ bias for the agents with the black preference. That is, the lowest possible initial bias towards ‘white’ in the case of the black preference equals 0.5 (due to the maximum value of 2 for w'_z), while the initial bias towards ‘black’ in the case of the white preference can go below 0.5, as in the example here, it equals 0.2. In this way, the applied numerical initialisation of the preference strengths is biased to supply individuals with relatively stronger preference towards ‘white’ compared with ‘black’ regardless of the agent preference. As a result, the agents with black preference are easier prone to switch to the white than those with the white preference to the black. The latter is also confirmed by the results of the Adaptive policy and its biased counterparts (W- and B-Adaptive) shown in Figure 3.6. That is, the exit probability of the Adaptive strategy on the E^{bl} is lower than on the E^{wh} for all difficulties and has an exit probability below 1.0 even at the easiest setting on the E^{bl} . This is expected since half of the population with the preference towards white is stronger in their social field than the ones with the black preference, resulting in the better performance on the E^{wh} and the worse one on the E^{bl} . For the same reason,

endowing agents with an initial preference towards the black outcome (i.e., B-Static, B-Adaptive) leads to higher exit probability rates on the E^{wh} than for the ones endowed towards white (i.e., W-Static, W-Adaptive) on the E^{bl} . Overall, the relative performance of the most decision-making policies in relation to each other primarily remains the same regardless of the disclosed numerical bias on both E^{wh} and E^{bl} . That is, those initially biased to the correct outcome are the best among all the others, while those biased to the wrong are the worst, for both static and adaptive policies. The exception holds only for the Adaptive policy alone, where its performance comes closer to the DMMD strategy on the E^{bl} than to the DMVD as on the E^{wh} , indicating no superiority before the Static policy on the E^{bl} .

3.4.3 Role of Opinion Initialisation

According to the preliminary experiments, in order to ensure a consensus on any option in a finite time T_N^{any} , the initial agents' opinions have to coincide with their initial preferences. That is, at the beginning when the agent is not receiving any information from the surrounding, its opinion simply reflects its preference. After interactions with others and the environment, the opinions start to evolve with respect to the personal preferences of the individuals. In this regard, we investigate how the performance of the introduced preference-based decision-making policies, namely Static and Adaptive, depends on the initialisation of the opinions and, hence, of the preferences compared to the DMVD and the DMMD strategies.

Figure 3.7 shows the regression with the 95% confidence interval for the consensus time T_N^{any} using a generalised additive model and the exact values of the exit probability (E_N) with the standard error over the initial number of agents $E_a(0)$, which prefer the option $a = 'black'$, while the option $b = 'white'$ being a correct one, for $\rho_b^* \in \{0.52, 0.92\}$. We consider the population of $N = 20$ agents without indifferent individuals, i.e., $\rho_{un} = 0$, and $\beta = 4.5$, conducting 100 simulation runs for each $E_a(0) \in \{1, 2, \dots, 19\}$. The observed results confirm the ones obtained in the previous section for $E_a(0) = 10$. For all policies, E_N decreases with increasing values of the initial individuals $E_a(0)$ preferring the incorrect outcome, i.e., 'black'. On the easiest scenario ($\rho_b^* = 0.52$), the exit probabilities of the Static and the Adaptive policies share similar patterns to the DMVD strategy, with the Adaptive being in-between of the Static and the DMVD due to the dynamic adjustments of the preferences. Additionally, the Adaptive policy is the fastest policy for all initial settings $E_a(0)$, while the Static is characterised by a similar consensus speed as the DMVD. The consensus time T_N^{any} of the DMMD strategy declines for $E_a(0) > 13$, which is explained by the decreasing E_N (i.e., $E_N < 0.5$ for $E_a(0) > 13$), while the T_N^{any} of other strategies drops only for $E_a(0) > 17$ also being accompanied by the downward change of the E_N below the chance level. On the hardest scenario ($\rho_b^* = 0.92$), the DMVD is the slowest policy with the highest T_N^{any} values for all initial settings $E_a(0)$ but being the most accurate one for $E_a(0) > 12$. While the DMMD strategy is described by the lowest consensus time T_N^{any} , it is also the least accurate, especially for $E_a(0) > 10$. As in the case of $\rho_b^* = 0.52$, the performance of the Static and the Adaptive policies is between the DMMD and the DMVD strategies. The preference-based decision-making policies take the best from both, the DMMD and the DMVD strategies. That is, the decision accuracy of the Static and the Adaptive until $E_a(0) < 10$ is as high as of the DMMD, while for $E_a(0) > 10$ it decreases slower than the DMMD strategy, approaching the accuracy

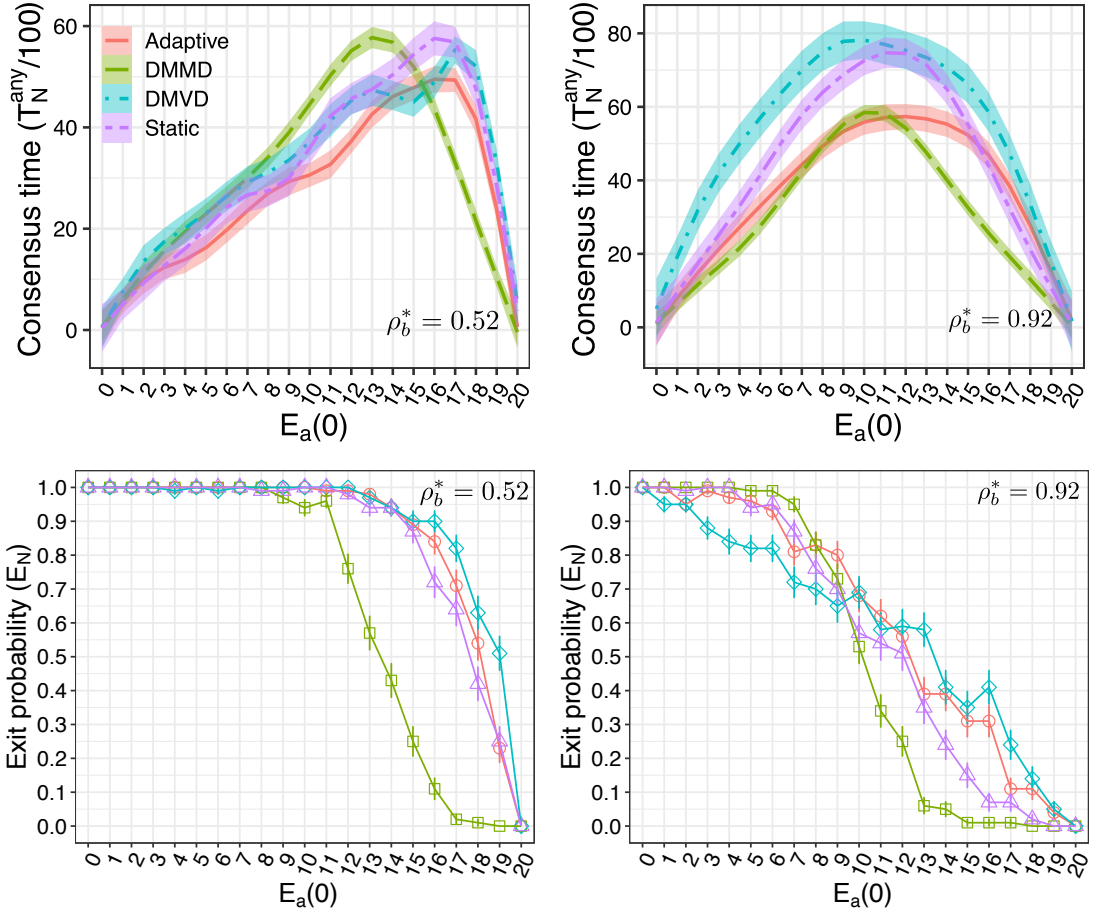


Figure 3.7: Consensus time ($T_N^{correct}$) and exit probability (E_N) as a function of the initial number $E_a(0)$ of individuals with opinion a for $\rho_b^* \in \{0.52, 0.92\}$. Bottom plots: DMMD - \square , DMVD - \diamond , Static - \triangle , Adaptive - \circ . Error bars indicate the standard error for the E_N , considering sample as binomial random variables.

of the DMVD. In general, the Static policy is inferior to the Adaptive policy for all $E_a(0)$ in both metrics T_N^{any} and E_N . The pattern of the consensus speed for the Static approaches the DMVD, while the Adaptive is as fast in the consensus time T_N^{any} as the DMMD, although with higher T_N^{any} values for $E_a(0) > 10$ due to its higher E_N , which is as accurate as for the DMVD.

3.4.4 Physical Distance Dependency

In the following, we analyse the impact of the spatial Euclidean distance d_E between the agents during communication on the preference-based decision-making process by varying the parameter α in Equation 3.10. For this purpose, we conduct the experiments over 40 simulation runs on the hardest binary scenario ($\rho_b^* = 0.92$) with $\alpha \in \{0, 1, 2\}$ and $\beta = 4.5$ using the Static and the Adaptive policies along with their best counterparts, namely, the W-Static and the W-Adaptive, respectively, for different proportions of the

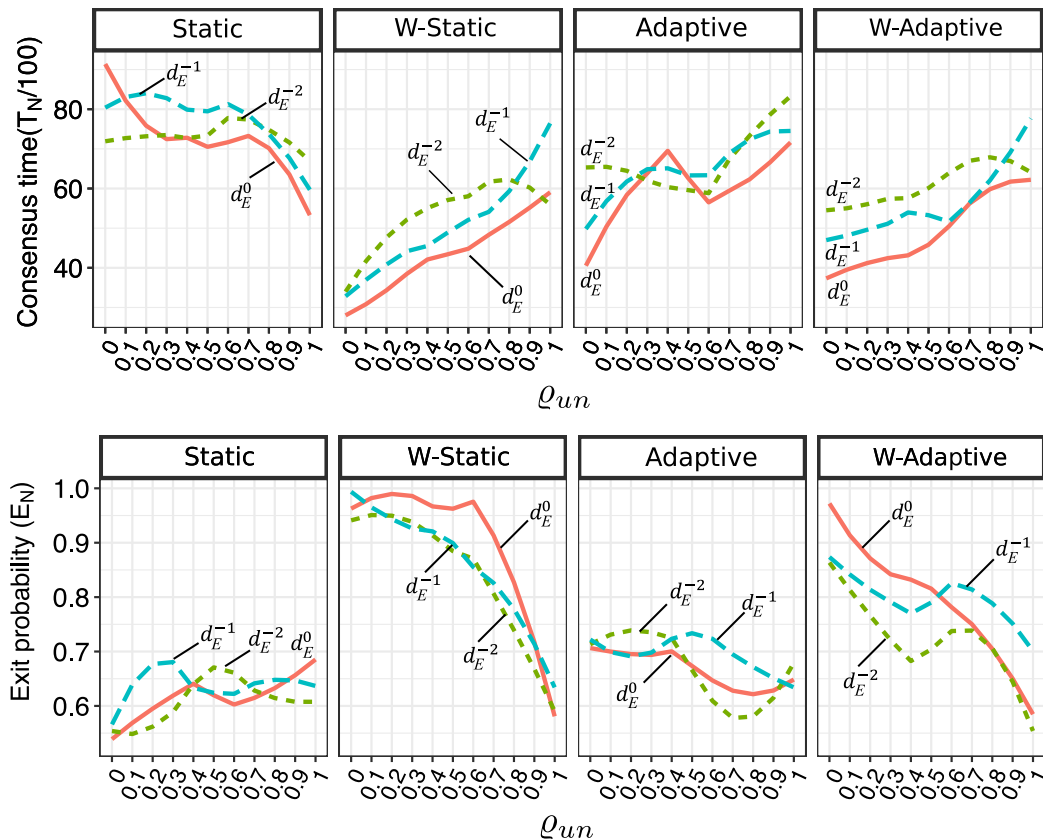


Figure 3.8: Smoothed conditional means of consensus time ($T_N^{correct}$) and exit probability (E_N) as a function of the proportion of unbiased individuals in the swarm for different distance-weightings, i.e., $\{d_E^{-1}, d_E^{-2}\}$. The notion of d_E^0 (solid line) corresponds to the non-distance-based case. Configuration of parameters: $\rho_b^* = 0.92$, $\beta = 4.5$.

indifferent individuals in a swarm, i.e., $\rho_{un} \in \{0, 0.1, \dots, 1.0\}$.

The obtained results in Figure 3.8 regarding the impact of ρ_{un} confirm the ones in Section 3.4.1. That is, the Static policy is improving its performance with the increase of ρ_{un} , while the Adaptive is deteriorating as more indifferent individuals are introduced in the population, the same as for the W-Static and the W-Adaptive policies. As such, the results for $\rho_{un} = 0$ are also the best among the others regardless of the distance-weighting factor (except for the Static policy). Overall, for a swarm of size $N = 20$ with the maximum communication distance of $d_{max} = 5$ units between the agents, we observe that primarily the best results in terms of the mean of both consensus time ($T_N^{correct}$) and exit probability (E_N) are obtained for $\alpha = 0$, indicating that the inclusion of the spatial distance between the agents does not significantly affect the collective performance. The experiments with the increased d_{max} up to 10 units (see Supplementary material Appendix B, Figures B.1 and B.2) also confirm this observation. They demonstrate no significant difference in the performance between considered distance-weighting factors for the Static as well as for the Adaptive policies, where the latter with $\alpha = 0$ is better for higher difficulties ρ_b^* in terms of the $T_N^{correct}$ than its distance-weighted counterparts.

Indeed, since the agents are constantly moving and switching their modes from exploration to communication, it can occur that the neighbours of the focal agent are holding opinions that do not reflect the information (i.e., colour) of this local area as they are already jumbled. In this case, the amplification of the influence of the physically closest neighbours does not necessarily follow the concept that the closer individuals hold similar opinions, as in the case of the classical SIT, therefore resulting in the non-significant numerical corrections in the calculation of the individuals' social fields in the regard of the collective perception.

3.5 Summary and Discussion

In this chapter, we have presented an Ising-based approach for collective decision-making that corresponds to the “vertical” upgrade of the mental model and integrates both opinions and preferences of the group members, following the principles of the social impact theory. The proposed preference-based decision-making model is inspired by the model of the physical spin systems studied by Hartnett *et al.* (2016). The main difference between our and their work is threefold. First, we introduce the learning procedure for the preferences into the model, meaning that the personal preferences are varying with time along with opinions. Secondly, we consider different problems. They focused only on the consensus depending on the initial configuration of opinions, while we require the social system to converge on a particular environmental state. The latter is expressed as the dominant colour in the environment and has to be explored by the agents. In this respect, our model includes direct modulation of positive feedback, implying interaction of the agents with the physical environment. Whereas in their work, the physical environment is considered to be absent. Thirdly, in our work, the individuals are not fixed on the lattice but continuously move. This results in dynamically changing communication topologies, which are intensified by behaviour phases, exploration and dissemination.

The main goal of this chapter was to investigate how the inclusion of an initial *inner personal bias* into individual decision-making towards one of the options can affect the outcome of the decision-making process at a collective level. In particular, the main focus was put on the interplay between two mental states of an agent, namely, preferences and opinions. While initially, the agents are in inner “harmony” with themselves, interactions with others and the environment during the decision-making process can lead to intermediate inner disagreements of an agent within its personal mental states, i.e., opposing preferences and opinions of an agent. We refer to the latter as the agent's state of *cognitive dissonance*. According to Festinger (1957), it is supposed to be an undesirable state of an individual which triggers motivation to reduce it. In its turn, we assume that mitigating the state of inner disagreement by the dynamic re-adjustment of individuals' initial preferences can also help to eliminate a potential socially negative bias on the undertaken decisions (i.e., towards incorrect outcome). In this regard, along with the static approach, where the preferences remain stable, this chapter proposes the adaptation procedure for the individuals' preferences such that their variation is correlated with the individual's opinion dynamics.

One can also think about preferences as an initial conjecture of the agents about how the environment looks like, i.e., what a correct outcome can be. Thus, an initial

conjecture can be also considered as a designer's choice, communicated to the swarm before the start of the decision-making process, based on some information sources not available to the agents. In this sense, it will represent a single hypothesis, given in the form of an initial global preference, the same for all individuals (i.e., homogeneous swarm concerning preferences), to test it in a distributed manner. In case, when there is no available evidence to decide on the initial preference, one can let a collective figure it out on its own by assigning equal proportions of the population with preferences towards one or another option under consideration. As such, we have evaluated swarm configurations with and without initial conjectures to understand the possible implications on the collective decision-making process.

The experiments without a particular initial conjecture have shown that the proposed preference-based decision-making model behaves primarily similar to the voter model (DMVD) and majority rule (DMMD) with direct modulation of the positive feedback. Considering that the voter model is generally more accurate but slower than the majority rule, the adaptive decision-making policy with introduced dynamic preferences leverages the best of both, namely, being as accurate as the voter model and as fast (or even faster on the easier scenarios) than the majority rule. While the static policy with fixed preferences mainly resembles the DMVD strategy in both accuracy and consensus speed. As such, the introduced learning procedure for the preferences allows speeding up the consensus compared to the static policy without deprivation of the accuracy, confirming our research hypothesis. This observation is also supported by similar trends for different initialisation of opinions and, hence, preferences. Especially, in the case of the hardest scenario ($\rho_b^* = 0.92$), the adaptive policy shows superiority before other strategies in the consensus speed for up to 75% of the initial population biased towards the wrong outcome, while remaining as accurate as the DMVD.

The results for the preference-based decision-making policies with correct and wrong initial conjecture have shown the best and the worst performance among all considered policy variations, respectively. In this regard, the adaptive policy with correct initial guess is faster than its static counterpart for easier scenarios maintaining 100% of accuracy, although degrading in both for higher difficulties compared to the static one. In the case of the wrong initial conjecture, the dynamic adaptation of the preferences in the adaptive policy allows a collective to achieve a significantly better performance in both speed and accuracy than its static counterpart, achieving around 90% of accuracy on the easiest scenario. Taken together with the results obtained without a specific initial conjecture, the latter also provides the evidence to confirm our research hypothesis, indicating that the co-evolution of the preference-opinion dynamics avoiding inner states of disagreement within the individuals (i.e., personal cognitive dissonance) promotes faster and more precise undertaking of the collective decisions.

However, the experiments have also demonstrated that the proposed preference-based decision-making model has an asymmetric behaviour concerning the correct outcome. This is mainly caused by the unequal strength of the preferences' initialisation due to the different ranges of strength values defining the preferences. Further research should be done to investigate more equal preference strength's initialisation concerning the potential options to ensure symmetric results with respect to the correct outcome. In future work on this subject, the learning procedure for the preferences can be modified to follow the principle of "cumulative advantage" (Kohring, 1996). In this way, an increase

in one's preference strength will be done proportionally to its current level, thereby bringing more balanced numerical updates to the system with regard to the preference strength ranges. It can also be possible to define the model using separate strength parameters for each option in Equation 3.7 instead of relative preference strength w'_z . As such, both strengths will belong to the same numerical interval, similar to persuasive and supportive parameters, which should be easier to control in equal proportions. Additionally, in the future, it might also be worth investigating the use of social proximity in Equation 3.10 derived from socially spatial information. It was shown to be more influential on decision-making than that from physically spatial information (Angst *et al.*, 2010), such that the agents would exchange opinions only with those they trusted.

Overall, the presented Ising-based approach for collective decision-making can be considered as a generalisation of the voting strategies, incorporating processes ranging from voter to plurality models, regulated by the nonlinearity parameter. The addition of preferences into the model enables a designer to manipulate the undertaken decisions of the individuals based on a presumption of the right outcome, as such, giving the possibility to steer and to take control over the self-organisation process to some degree. The latter is referred to as one of the attributes of the human-collective interaction strategies, which aim to provide operators with the means to influence and to better inform collective decisions, increasing in this way the fault tolerance of the autonomous system (Cody *et al.*, 2021). Indeed, in the case of the correct initial conjecture imposed in the developed preference-based decision-making model, one can observe fast consensus achievement with high accuracy even in the case of a small difference between the options.

Influence of the Environment on Collective Decision-Making

The following chapter analyses the impact of the environmental structure on collective decision-making in the context of the binary collective perception scenario, addressing the second objective posed in Section 1.3. The interaction of individuals with the physical environment, as expressed in the “Estimate()” block in Figure 2.3, is another aspect determining the efficiency of a collective decision-making system in addition to individual decision-making mechanism. When there is some bias hidden in the environment, the agents are the object of its indirect influence, which is often not under their control. Therefore, the goal of this chapter is to build an understanding of what features or characteristics of the environment make it really difficult for distributed collective perception.

The chapter is organised as follows. Section 4.1 introduces the problem statement and motivation of the chapter, followed by Section 4.2 with the necessary mathematical background. Section 4.3 describes the proposed methodology including the considered representation of the environment. In Section 4.3.2, we suggest a binary-featured benchmark set consisting of nine spatial patterns and define their distinctive characteristics in Sections 4.3.3 and 4.3.4. The proposed benchmarks are evaluated in Section 4.4 within the state-of-the-art opinion-based decision-making strategies, which were described previously in Section 2.4. Finally, in Section 4.5, the summary and the interpretation of the obtained results are given, refining the existing concept of the task difficulty for the collective perception scenario. The presented ideas in this chapter and the respective experiments were published in the previous works of the author of this thesis (Bartashevich and Mostaghim, 2019c; Bartashevich and Mostaghim, 2019a).

4.1 Problem Statement and Contribution

Looking at Figure 2.2a, the reader can perceive the picture as the whole, having access to the global information about the environment, based on which one can decide about the prevailing colour. In this regard, collective perception can be thought of as a cognitive process that occurs in human brains while viewing the images, with agents representing neurons of the prefrontal cortex of the brain (Libedinsky and Livingstone, 2011). Nigel (2018) points out that some visuals are easier to perceive than others, depending on “the

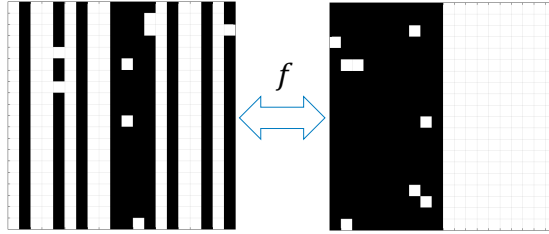


Figure 4.1: Example of two collective perception scenarios with the same colour proportions $\rho = 0.92$ (52% white and 48% black cells in the grids).

spatial properties of the imagery”. In particular, he highlights that the visual perception of the image features that are relatively close to each other occurs faster than those that are sparse. Indeed, if we look at the images in Figure 4.1, it is easier to infer the predominant colour in the image on the right-hand side than on the left-hand side. Both images in Figure 4.1 have the same amount of black (48%) and white cells (52%) but differ in the relative positions of the colours to each other. Previous research (Shepard and Metzler, 1971) has shown that spatial manipulations in the brain, such as e.g., “mental rotation” described as the brain rotating objects while the characteristics of the object remain unchanged, can aid in the recognition of the objects or their particular features in the environment. The Rubik’s Cube, for example, is a common puzzle that requires three-dimensional mental rotation. By drawing on this concept, one can also manipulate the mental representation of the grid on the left in Figure 4.1 to match the one on the right, thereby facilitating the decision-making.

The question arises whether the same observations are valid for a collective of artificial agents spatially distributed over the environment and operating with state-of-the-art decision-making strategies in the context of the considered collective perception task. As such, this chapter aims to focus on the customised environmental transformations f , as in Figure 4.1, that presumably can have a positive effect on the collective behaviour, while maintaining the global structure of the environment intact. To test our hypothesis, we investigate the performance of the opinion-based decision-making described in Section 2.4 on different representations of the environment using a particular type of transformation known in discrete mathematics as *isomorphism*, which is used in mathematical as well as biological studies to obtain a deeper understanding of the objects with similar connections (Kulvicki, 2004).

4.2 Mathematical Background

In the following, we introduce mathematical definitions and concepts from (Beth *et al.*, 1999), which are necessary for the methodology of this chapter.

4.2.1 Incidence Structures and Isomorphism

Definition 1. An **incidence structure** is a pair $S = (\mathcal{P}, \mathcal{B})$, where \mathcal{P} is a finite set called the *point set* of S and \mathcal{B} is a collection of subsets of \mathcal{P} called the *block set* of S . The elements of the point set are called *points* and denoted by $p_i \in \mathcal{P}$. The elements of the block set are called *blocks* and denoted by $B_j \in \mathcal{B}$.

Definition 2. Let $S = (\mathcal{P}, \mathcal{B})$ be an incidence structure with points $\mathcal{P} = \{p_1, \dots, p_k\}$ and blocks $\mathcal{B} = \{B_1, \dots, B_r\}$. An **incidence matrix** $M = (m_{ij})$ of the incidence structure S is a $k \times r$ binary matrix defined by $m_{ij} = 1$ if $p_i \in B_j$ and $m_{ij} = 0$ otherwise.

As a primary method for determining the similarities between two incidence structures, one refers to an **isomorphism relation** (Beth *et al.*, 1999), which can be defined in terms of the respective incidence matrices as follows.

Definition 3. Two incidence structures $S = (\mathcal{P}, \mathcal{B})$ and $S' = (\mathcal{P}', \mathcal{B}')$ with incidence matrices M and M' are called **isomorphic** if there exist *permutation matrices* H and Q such that $HMQ = M'$, where H permutes the rows (i.e., points of S) and Q permutes the columns (i.e., blocks of S).

Definition 4. A **permutation matrix** is a square binary matrix each row and column of which contains exactly one entry 1.

That is, by permuting the rows and columns of the incidence matrix M of an incidence structure S one can get another representation of this incidence structure S' , although the *incidence relation* (i.e., the set inclusion) between its points and blocks remains the same. In general, it is a difficult problem to differentiate between different incidence structures. The following invariant¹ distinguishes different incidence structures independently of the representation.

Definition 5. Let $A \in \mathbb{Z}^{k \times r}$ be given. There exist unimodular matrices² $U \in \mathbb{Z}^{k \times k}$, $V \in \mathbb{Z}^{r \times r}$ and a diagonal matrix $D \in \mathbb{Z}^{k \times r}$ such that $A = UDV$, where the diagonal entries of D are $d_1, d_2, \dots, d_s, 0, \dots, 0$, such that each d_i is a positive integer and $d_i | d_{i+1}$ (that is, d_i divides d_{i+1}) for $i = 1, 2, \dots, s-1$. Then the diagonal matrix D is called **the Smith normal form (SNF)** of A .

As such, the SNF is a natural choice of an invariant³ for an incidence relation, since its computation requires only the methods of elementary linear algebra, which makes it easy to compute. We will use the SNF in the subsequent sections to distinguish different incidence structures.

4.3 Proposed Methodology

In the following, we introduce the equivalence relation on the set of grids by identifying them with the equivalence structures.

4.3.1 Environment Representation and Transformation

A randomly created square grid of black and white cells is typically used to provide the environmental setting for the collective perception scenario (Valentini *et al.*, 2016; Strobel *et al.*, 2018; Ebert *et al.*, 2020). In this respect, one can encode the grid as the binary matrix $M \in \mathbb{Z}_2^{k \times k}$, where 0's of the matrix M correspond to the white cells and 1's to the black ones in the grid. As such, we set values of the matrix $M = (m_{ij})$ to determine the relationship $\mathcal{S} \subseteq \mathcal{V} \times \mathcal{E}$ between columns of the grid as the set of blocks

¹Under “invariant”, we mean a certain characteristic of an incidence structure that does not change after applying equivalence relation, i.e., isomorphism.

²Matrices which determinants are equal to 1 or -1 are called unimodular.

³The SNF does not depend on an arbitrary ordering of the sets, that is, the matrix D is the same for all possible incidence matrices of the incidence structure.

Algorithm 4.1: New isomorphic matrix

Input: $M \in \mathbb{Z}_2^{k \times k}$;
Output: M_{new} , where $M_{new} \cong M, M_{new} \neq M$;

- 1 **begin**
- 2 Generate two random permutations: H, Q , where $H \neq I_k, Q \neq I_k$, and I_k is the identity matrix of order k .
- 3 $M_{new} = H \cdot M \cdot Q$
- 4 **return** M_{new}

$\mathcal{E} = \{e_1, e_2, \dots, e_k\}$ and its rows as the set of points $\mathcal{V} = \{v_1, v_2, \dots, v_k\}$ such that $v_i \in e_j$ for each pair of indices (i, j) if and only if $m_{ij} = 1$, meaning that the corresponding cell of the grid $c_{i,j}$ has a black colour. One can also associate the obtained incidence structure $S = (\mathcal{V}, \mathcal{E})$ with an undirected hypergraph, where the set of points \mathcal{V} forms the vertices of the graph and the set of blocks \mathcal{E} forms its edges, while the values m_{ij} of the respective incidence matrix M denote that a vertex v_i belongs to the edge e_j if $m_{ij} = 1$.

Further, we use Algorithm 4.1 to produce isomorphic grids from a given one. In this way, new grids isomorphic to a specified one are created and defined by the obtained matrices M_{new} . Figure 4.2 shows an example of different representations of the environment under consideration as an incidence structure, where the objects in the top and in the bottom rows are isomorphic to each other. In particular, the ones at the bottom were obtained from the top ones using Algorithm 4.1. It is important to note that a transformation induced by Algorithm 4.1 does not alter incidence relation on the grid, i.e., $\mathcal{I} \subseteq \mathcal{V} \times \mathcal{E}$, such that the combinatorial structure of the environment remains the same, although the visual representation of the incidence relation can change. Furthermore, the global task characteristic such as the ratio of the colours ρ stays intact.

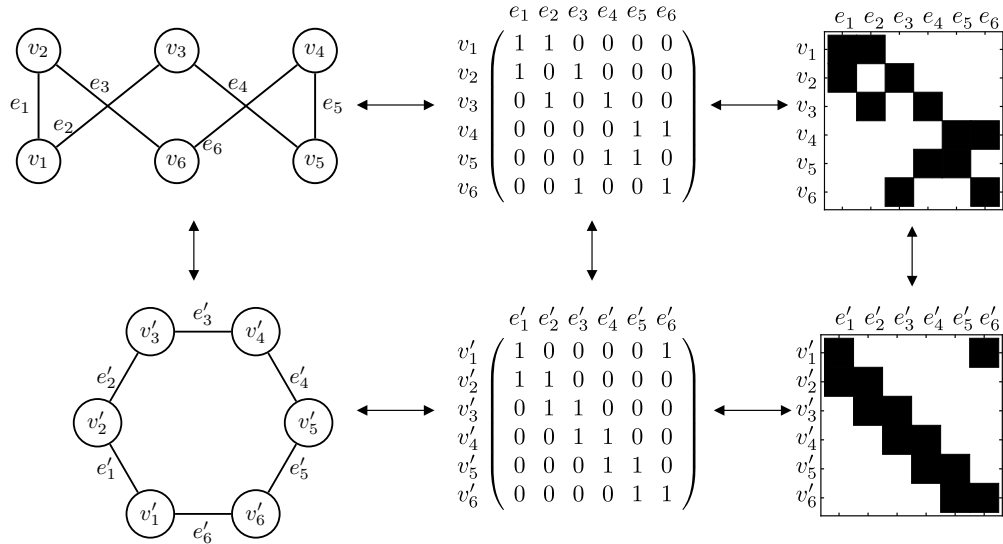


Figure 4.2: Example of different environment representations as isomorphic incidence structures (Bartashevich and Mostaghim, 2019c).

Algorithm 4.2: New non-isomorphic matrix (but with the same amount of 0s and 1s)

Input: $M \in \mathbb{Z}_2^{k \times k}$; $l \in \mathbb{N}$ - number of replaced points;
Output: M_{new} , where $M_{new} \not\equiv M$;

- 1 **begin**
- 2 Compute Smith’s Normal Form of M ;
- 3 $\{U, D, V\} = SNF(M)$
- 4 **repeat**
- 5 Get M_{new} : Replace l random black points by white and l white by black
- 6 Compute: $\{U_{new}, D_{new}, V_{new}\} = SNF(M_{new})$
- 7 **until** $D_{new} \neq D$
- 8 **return** M_{new}

Albeit it is difficult to determine whether two given incidence structures are isomorphic (neither known to be P nor known to be NP-complete problem (Toran, 2004)), one can get a numerical validation that two of them are not isomorphic based on the SNFs of their respective incidence matrices. In Algorithm 4.2 we define the procedure for constructing non-isomorphic matrices M_{new} to a given one M by ensuring that the Smith Normal Forms of M and M_{new} are not identical. There, by replacing certain 0’s with 1’s or vice versa in the matrix M , one can destroy the old incidence relations and sets the new ones, thus altering the combinatorial properties of the object. In this regard, the manipulations with the colour ratio parameter ρ relate to the non-isomorphic transformations of the environment as well, modifying the global task characteristics. The parameter ρ has shown to have a great impact on the state-of-the-art collective decision-making strategies (Valentini, 2017), identifying the concept of the difficulty for the collective perception task. Inspired by human brain capabilities such as “mental rotation” (Nigel, 2018), we aim to explore how the introduced isomorphic transformations of the environment alter the distributed collective perception, while keeping the combinatorial and global characteristics of the environment intact.

4.3.2 Binary-Featured Benchmark Set

Based on the concepts of visual patterns in matrices, considered in the literature on matrix visualisation (Behrisch *et al.*, 2016; Behrisch *et al.*, 2017; Behrisch *et al.*, 2018), we construct binary grids as a new benchmark set for the collective perception scenario. There, under a *visual pattern*, one means a “visual structure in the matrix that exposes information about the underlying graph topology”. The latter is in agreement with our environment representation as illustrated in Figure 4.2. Therefore, for our study, we consider in the following nine of the most common visual patterns retrieved from the binary matrices, which are illustrated at the top of Figure 4.3, where, without loss of generality, black colour forms the pattern, that is:

- “*Random*”: A random pattern is a common benchmark scenario used in collective perception (Morlino *et al.*, 2010; Valentini, 2017), described by a random distribution of black and white cells in the matrix.

- “*Block*”: A block pattern is designed by blocks consisting of at least 2×2 black cells going along the main diagonal of the matrix and two blocks at the corners of its minor diagonal.
- “*Off-diagonal*”: An off-diagonal pattern is similar to the “*Block*” but is described only by two big black blocks placed at the corners of the minor diagonal of the matrix.
- “*Star*”: A star pattern consists of horizontal and vertical black lines that do not necessarily run the entire width or length of the matrix, respectively.
- “*Stripe*”: A stripe pattern is performed by a wide horizontal or vertical black band stretching along the entire width or length of the matrix, respectively.
- “*Band*”: A band pattern consists of black lines parallel to the main diagonal of the matrix but not lying on it.
- “*Band-Stripe*”: A band-striped pattern is similar to the “*Band*” but is, instead of lines, characterised by two wide black parallel bands, placed on the opposite sides relative to the main diagonal of the matrix.
- “*Bandwidth*”: A bandwidth pattern resembles a black frame around a rhombus packed with white cells such that one of the rhombus diagonals runs along the matrix’s main diagonal while the length of the other one is randomly defined.
- “*Bandwidth-Rand*”: A bandwidth-rand is essentially a bandwidth pattern with both rhombus diagonals of random lengths.

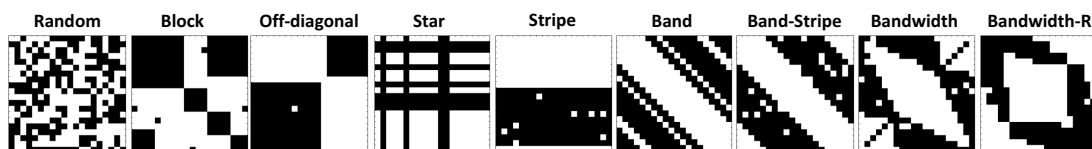


Figure 4.3: Binary-feathered pattern samples with $\rho_b^* = 0.92$ (Bartashevich and Mostaghim, 2019a).

A binary-feathered benchmark generator based on the types of the aforementioned visual patterns, matrix (grid) size, and the ratio of the black and white cells $\rho_b^* = \Gamma_{bl}/\Gamma_{wh}$, $\Gamma_{bl} < \Gamma_{wh}$ was implemented in MATLAB (2018) by the current author. In this way, each newly generated environment with the same input differs in spatial configuration while maintaining the same visual structure. That is, the respective visuals of the patterns, such as blocks or lines, are not fixed and vary in their size and positions on the grid within the same pattern type. If there are not enough empty cells in the grid to be filled in with the specific colour without interfering with the pattern, the pattern’s visuals can contain “artefacts” which are represented by cells of another colour disrupting the pattern. To that end, one can observe randomly placed white or black cells obstructing some patterns (see Figure 4.3).

4.3.3 Patterns Metrics

We introduce the following metrics to quantify spatial characteristics of visual patterns, in addition to the colour ratio ρ in a grid (matrix):

- *Entropy* (\mathcal{E}) is used to define the density of the cells' patches with the same colour (i.e., clusters) in a pattern P .

Assuming that black colour defines the visuals of the pattern, let $|C_i|$ denote the number of black cells in the cluster C_i and Γ_{bl} denote the total number of black cells in P . As such, \mathcal{E} is calculated in the following way:

$$\mathcal{E} = \frac{H_c^{max} - H_c}{H_c^{max}} \quad (4.1)$$

$$H_c = - \sum_{i=1}^M \frac{|C_i|}{\Gamma_{bl}} \log_2 \frac{|C_i|}{\Gamma_{bl}} \quad (4.2)$$

$$H_c^{max} = - \sum_{\Gamma_{bl}} \frac{1}{\Gamma_{bl}} \log_2 \frac{1}{\Gamma_{bl}}, \quad (4.3)$$

where M is the number of clusters, H_c^{max} is the maximum entropy. The value of \mathcal{E} increases as the number of clusters decreases. That is, a value of \mathcal{E} close to 1 indicates an ordered colour state in the environment, whereas a value of \mathcal{E} close to 0 points out its random distribution. Nevertheless, the value of \mathcal{E} provides no information about the appearance of the cluster(s), that is, whether it is dense like a "block" or sparse like a "chain". In this regard, another metric is considered together with \mathcal{E} , namely:

- *Moran Index* (MI) is used to characterise the degree of correlation in colours among nearby cells in a pattern P . In other words, it defines the degree of connectivity between clusters (if any).

Let c_i and c_j denote the colours (1 is 'black' and 0 is 'white') of two adjacent cells in a pattern P and Γ is the total number of cells in a matrix. As such, MI is defined as follows:

$$MI = \frac{\Gamma}{\sum_{ij} w_{ij}} \cdot \frac{\sum_{ij} w_{ij} (c_i - \bar{c})(c_j - \bar{c})}{\sum_i (c_i - \bar{c})^2}, \quad (4.4)$$

where \bar{c} is the mean of all cell values in P , that is, $\bar{c} = \Gamma_{bl}/\Gamma$. If cells c_i and c_j are neighbours in the von Neumann neighbourhood \dagger (see as in Figure 3.1), then $w_{ij} = 1$ and $w_{ij} = 0$ otherwise. In this way, the values of $w_{ij} = w_{ji}$ and determine the degree of spatial proximity of the cells c_i and c_j , respectively. As such, $MI \rightarrow 1$ if P has many \dagger -linked black cells, $MI \rightarrow 0$ if they are sparsely located to each other (randomly distributed), and $MI \rightarrow -1$ if the colours alternate like on a chessboard.

4.3.4 Patterns Quantification

Based on the described above metrics, we analyse how the pattern instances of the proposed binary-featured benchmark set quantitatively differ from one another. The

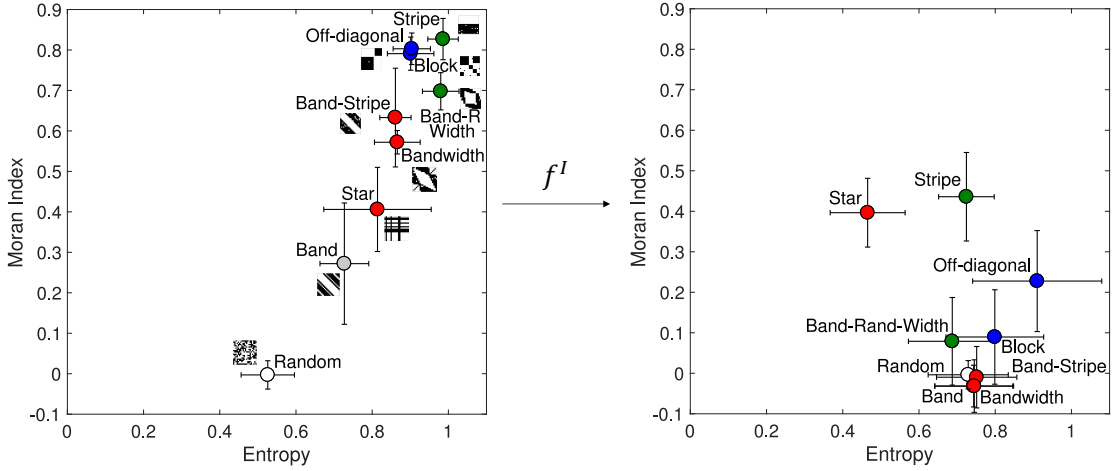


Figure 4.4: Scatter diagrams of the patterns’ metrics’ statistics over 100 generations “before” (left-hand side) and “after” applying isomorphism (right-hand side). The figure is adapted from (Bartashevich and Mostaghim, 2019a). The same colour of points denotes that they belong to the same pattern group.

metrics’ values vary mostly between the patterns and are unaffected by the colour ratio parameter ρ .

Figure 4.4-left shows the mean (points) and the standard deviation (bars) of the Moran Index MI and Entropy \mathcal{E} evaluated over 100 generations of each pattern instance. According to the Kruskal-Wallis ANOVA analysis (Hollander *et al.*, 2013), there is a statistically significant difference ($p < 0.01$) between all the patterns in MI , except for “Block” and “Off-diagonal”, while in \mathcal{E} some patterns indicate no statistically significant difference. That is, the same colour of the points in Figure 4.4-left represents the patterns that are not statistically significantly different ($p > 0.01$) between each other in \mathcal{E} . As such, they form the following groups: (1) “Band-Stripe”, “Bandwidth” and “Star” (in red); (2) “Stripe” and “Band-Random-Width” (in green); (3) “Off-diagonal” and “Block” (in blue). In this regard, we assume that the performance of the collective decision-making strategies on the benchmarks from the same group will be similar. To note, “Band” and “Random” are not associated with any of the defined categories, as they are significantly different ($p < 0.01$) from all other pattern instances in both \mathcal{E} and MI characteristics. Figure 4.4-right shows the statistics for the Entropy \mathcal{E} and Moran Index MI of the benchmark instances isomorphic to the respective patterns. While the isomorphic transformations f^I do not modify the pattern instance’s combinatorial properties, they alter its visual representation (see an example of two isomorphic patterns in Figure 4.1), which is reflected in the shift of \mathcal{E} and MI values.

4.4 Experimental Study

The experiments in this chapter were carried out to determine the impact of the environment on the distributed collective perception in the context of the best-of-2 problem, addressing the second objective defined in Section 1.3. Three state-of-the-art opinion-based decision-making strategies listed in Section 2.4.1, namely DMVD (voter model),

DMMD (majority rule), and DC (direct comparison), are evaluated on the proposed above binary-featured benchmark set in the multi-agent setting as described in Sections 2.2 and 2.4. The following experimental design was originally reported in (Bartashevich and Mostaghim, 2019a). However, in the current study, we employ a different implementation of the DMVD and DC strategies. In particular, the DMVD strategy is driven by direct modulation of positive feedback and the DC is not, while in our previous work this was done vice versa. Therefore, the results provided in this section differ from those presented in our prior work.

4.4.1 Influence of Patterns on Collective Decision-Making

The first experiment aims to demonstrate how different pattern configurations and colour ratios ρ_b^* affect collective perception in terms of consensus time on the correct outcome ($T_N^{correct}$) and exit probability (E_N) as defined in Section 2.4.2. In Figure 4.5, we analyse the $T_N^{correct}$ as a function of $\rho_b^* \in \{0.52, 0.56, 0.61, 0.67, 0.72, 0.79, 0.85, 0.92\}$ using a local weighted regression (LOESS) and a generalised linear model (GLM) with a binomial distribution for the E_N . The results are based on the data gathered over 40 simulation runs for each benchmark instance and each ρ_b^* with a maximum simulation time of $T = 400$ sec (where 1 simulated second corresponds to 100 iterations). As such, if a swarm has not converged to the correct outcome during the time T , the trial is taken as a failed one. For each pattern, we also provide quantitative characteristics (mean \pm std) of MI and \mathcal{E} calculated over 100 generated instances.

P1-Random ($MI = -0.003 \pm 0.035$, $\mathcal{E} = 0.526 \pm 0.07$) has been a main focus of the previous studies. We observe similar results for the DMVD, DMMD, and DC strategies as in (Strobel *et al.*, 2018). That is, the DMVD is more accurate than the DMMD strategy but is slower for higher difficulties ρ_b^* , while the DC strategy is the fastest and the most accurate among all three for any ρ_b^* .

P4-Star ($MI = 0.406 \pm 0.104$, $\mathcal{E} = 0.814 \pm 0.141$) and *P6-Band* ($MI = 0.272 \pm 0.15$, $\mathcal{E} = 0.727 \pm 0.064$) seem to deteriorate the performance of collective perception compared to *P1*. The DMVD and the DMMD on *P4* are described by the same indicators of consensus time with the DMVD being more accurate over ρ_b^* . On *P6*, the accuracy as well as the speed of the DMVD become significantly worse such that the DMVD and the DMMD are comparable in the accuracy but the DMVD is slower over ρ_b^* . The DC still keeps the highest performance among all three, although its performance starts to decline earlier than on *P1*, i.e., at $\rho_b^* = 0.67$, and reaches comparable performance to the others at $\rho_b^* = 0.92$.

P8-Bandwidth ($MI = 0.572 \pm 0.029$, $\mathcal{E} = 0.866 \pm 0.06$) and *P9-Bandwidth-Rand* ($MI = 0.698 \pm 0.046$, $\mathcal{E} = 0.98 \pm 0.048$) are characterised by controversial results in the performance of the DMVD and the DMMD strategies. That is, the DMMD strategy is more accurate and faster than the DMVD, although both reach the same indicators of consensus time at the highest difficulty $\rho_b^* = 0.92$. The accuracy of both strategies on *P9* declines faster than on *P8* with the E_N for the DMVD falling below the chance level by $\rho_b^* = 0.92$. While the exit probability of the DC strategy $E_N = 1.0$ for all $\rho_b^* \leq 0.79$ and drops to $E_N \approx 0.8$ at $\rho_b^* = 0.92$. The consensus time ($T_N^{correct}$) of the DC increases with the increase of ρ_b^* similar as on *P1* and *P6*, reaching the same $T_N^{correct}$ as the DMVD and the DMMD by $\rho_b^* = 0.92$.

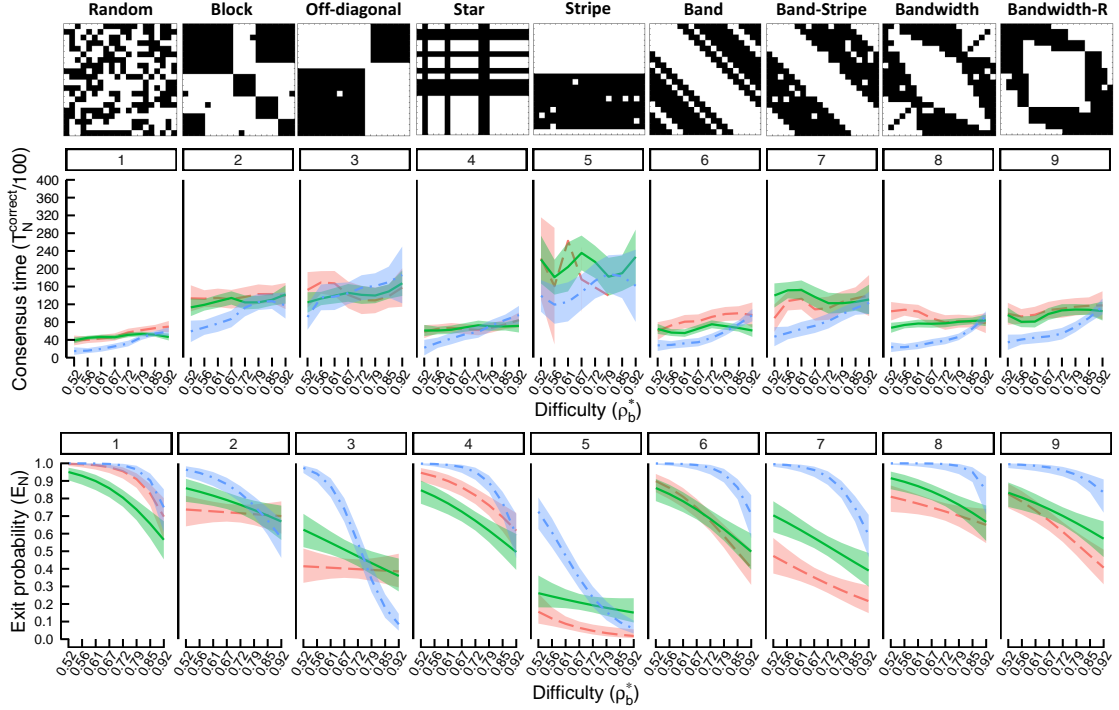


Figure 4.5: Consensus time ($T_N^{correct}$) and exit probability (E_N) as a function of task difficulty ρ_b^* for each pattern. Dashed (red), solid (green) and dash-dotted (blue) lines correspond to the DMVD, DMMD and DC strategies, respectively. Shaded areas represent 95% confidence interval.

P7-Band-Stripe ($MI = 0.633 \pm 0.122, \mathcal{E} = 0.861 \pm 0.041$) is visually similar to *P6*, but the performance of the strategies differs significantly between these patterns, indicating that *P7* is more challenging for collective perception. The consensus time using the DMVD as well as the DMMD strategies is higher than for the already aforementioned patterns over all levels of the task difficulty. The exit probability of the DMVD is below the chance level even at the easiest difficulty setting and is worse than the E_N for the DMMD, which is also significantly lower than on previous benchmarks. The consensus time ($T_N^{correct}$) of the DC strategy is the smallest among all three but increasing with the rise of ρ_b^* , reaching the same $T_N^{correct}$ as the DMMD and the DMVD by $\rho_b^* = 0.92$. Its exit probability $E_N = 1.0$ for $\rho_b^* \leq 0.61$ and drops to $E_N \approx 0.65$ at $\rho_b^* = 0.92$.

P2-Block ($MI = 0.791 \pm 0.041, \mathcal{E} = 0.901 \pm 0.061$) and *P3-Off-diagonal* ($MI = 0.803 \pm 0.039, \mathcal{E} = 0.904 \pm 0.049$) share similar visuals but are described by different results in the performance of collective decision-making. The exit probabilities on *P3* are significantly lower than on *P2* and other aforementioned benchmarks for all decision-making strategies. That is, the exit probability of the DMVD is $E_N \approx 0.4$ on *P3* and does not change with ρ_b^* , while the E_N of the DMMD is higher for easier settings but declining to the same level as the DMVD by $\rho_b^* = 0.92$. There, the consensus time ($T_N^{correct}$) of both the DMVD and the DMMD strategies are the same and higher than on the other patterns considered above. The performance of the DC significantly deteriorates on *P3*. Its exit probability $E_N = 1.0$ only at the easiest difficulty and drops to $E_N \approx 0.1$ by $\rho_b^* = 0.92$.

The consensus time of the DC is as high as the other strategies and increases with the rise of ρ_b^* . As such, the DC is the worst among others at the highest difficulty setting on *P3*. The results on *P2* are characterised by similar trends in the performance of the strategies relative to each other, but with quantitatively higher exit probabilities rates over ρ_b^* .

P5-Stripe ($MI = 0.827 \pm 0.051$, $\mathcal{E} = 0.986 \pm 0.04$) is shown to be the most difficult pattern in the benchmark set. All decision-making strategies under consideration are characterised by long consensus times ($T_N^{correct}$), whereas the DMVD strategy completely fails, being unable to perform for $\rho_b^* > 0.79$. The exit probability rates (E_N) of the DMMD and the DMVD are significantly below the chance level already at the easiest task difficulty setting, decreasing further to $E_N \approx 0.2$ and $E_N = 0$ by $\rho_b^* = 0.92$, respectively. While on the other patterns, the DC strategy was able to maintain $E_N = 1.0$ for the easier settings, on *P5*, it is described by $E_N \approx 0.7$ at $\rho_b^* = 0.52$ which also drops to zero by $\rho_b^* = 0.92$.

Summary. The obtained findings indicate that the speed and accuracy performance of the state-of-the-art opinion-based decision-making strategies (Valentini *et al.*, 2016), namely the DMVD, DMMD, and DC, significantly varies across different visual patterns of the collective perception scenario. Overall, it is reasonable to claim that the complexity of the collective perception task is determined not only by the ratio ρ_b^* of one colour to another but also by the *spatial distribution* of each colour. That is, although the DMVD is known to be more accurate than the DMMD strategy in a setting with a random distribution of the features, our results show that this is not the case when the features are spatially correlated. While the DC strategy does not make use of the direct modulation of positive feedback, compared to the DMVD and the DMMD, it appears to be more robust in its outcome across the patterns with a lower degree of spatial correlations, that is $MI \leq 0.6$ and $\mathcal{E} \approx 0.8$ (*P1*, *P4*, *P6*, *P8*), although its performance also significantly deteriorates on the patterns with $0.6 < MI \leq 0.8$ and with \mathcal{E} value close to 1 (*P2*, *P3*, *P5*, *P7*, *P9*). As such, since the environment is a priori unknown to the agents, one can conclude that clustered patches of the features induce a *negative environmental bias*, distorting the quality of the agents' estimates, regardless of the global quality of the features ρ_b^* . After all, the decisions of all three strategies are guided by individuals' estimates of the option qualities, which are used either implicitly, i.e., in the direct modulation of the positive feedback, as for the DMVD and the DMMD strategies, or directly in the individual decision-making mechanism as in the case of the DC.

4.4.2 Influence of Isomorphic Transformations in the Environment

In the second experiment, we assess the generalizability of the opinion-based collective decision-making strategies on the benchmark set consisting of the isomorphic patterns to the ones considered in the previous experiment. For this purpose, we apply isomorphic transformations, as described in Section 4.3.1, to the nine visual patterns under consideration. In this way, we aim to examine the performance of collective decision-making on a broader range of environment configurations sharing the same combinatorial structure, i.e., the same number of features and the same connectivity relations to each other. As such, in Figures 4.6-4.7, we analyse the impact of the isomorphic transformations of the environment on the consensus time ($T_N^{correct}$) and exit probability (E_N) of the DMVD,

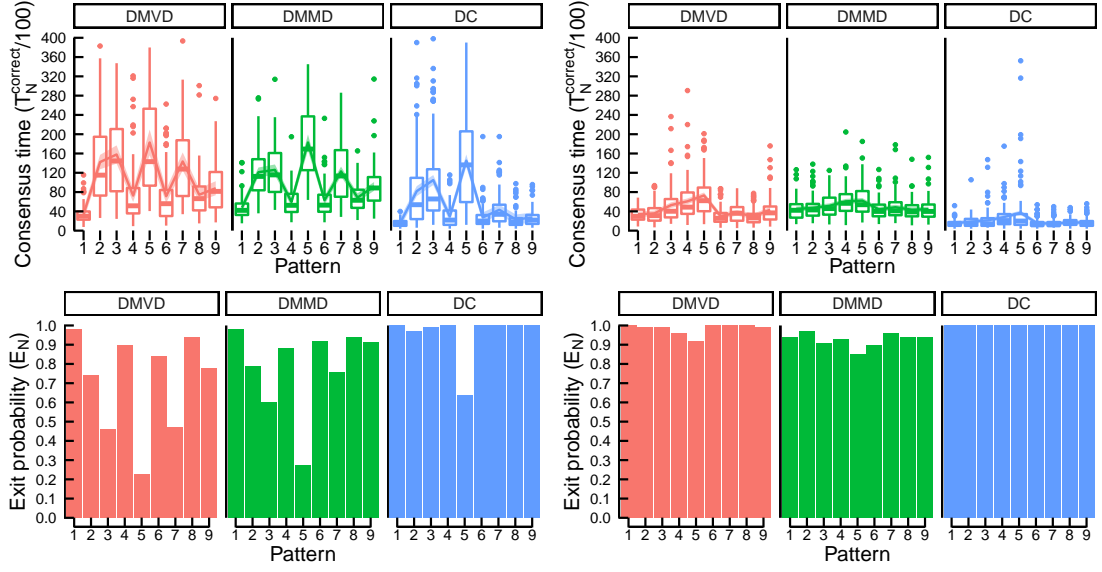


Figure 4.6: Consensus time ($T_N^{correct}$) and exit probability (E_N) within patterns “before” (left-hand side) and “after” applying isomorphism (right-hand side) for $\rho_b^* = 0.52$. The curves over box-plots are fitted via local weighted regression. Shaded areas represent 95% confidence interval.

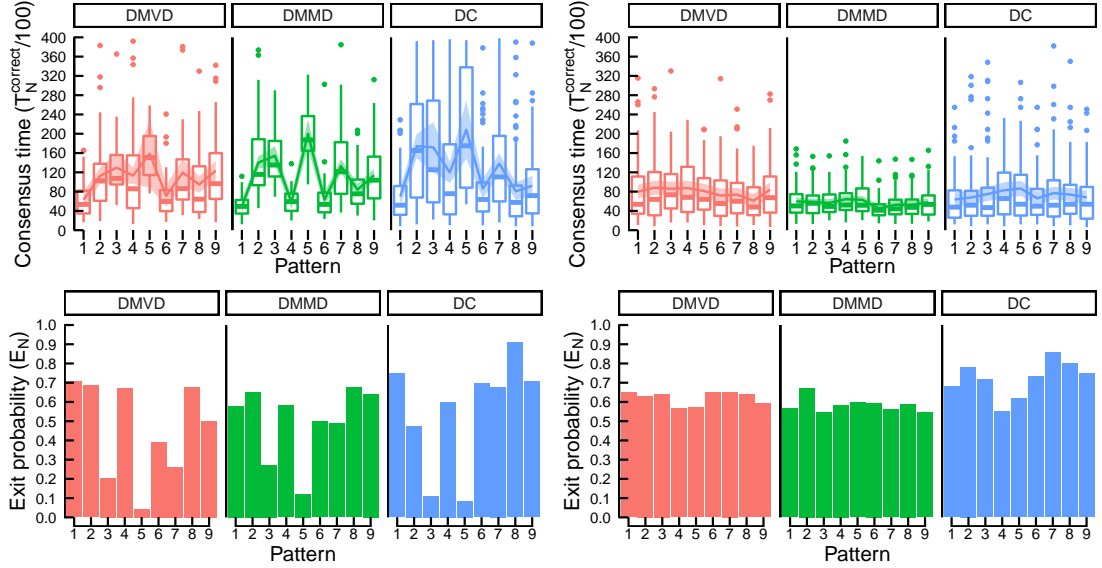


Figure 4.7: The same analysis as in Figure 4.6 but for the “task difficulty” of $\rho_b^* = 0.92$.

DMMD, and DC strategies over 100 simulation runs for the easiest and the most difficult settings, i.e., $\rho_b^* \in \{0.52, 0.92\}$, respectively.

The findings reveal a significant difference in the collective output in terms of $T_N^{correct}$ as well as of E_N on the patterns “before” (Figures 4.6 and 4.7 on the left-hand side) and “after” (Figures 4.6 and 4.7 on the right-hand side) isomorphic transformations of the environment. The statistical comparison in the performance, according to the Mann-

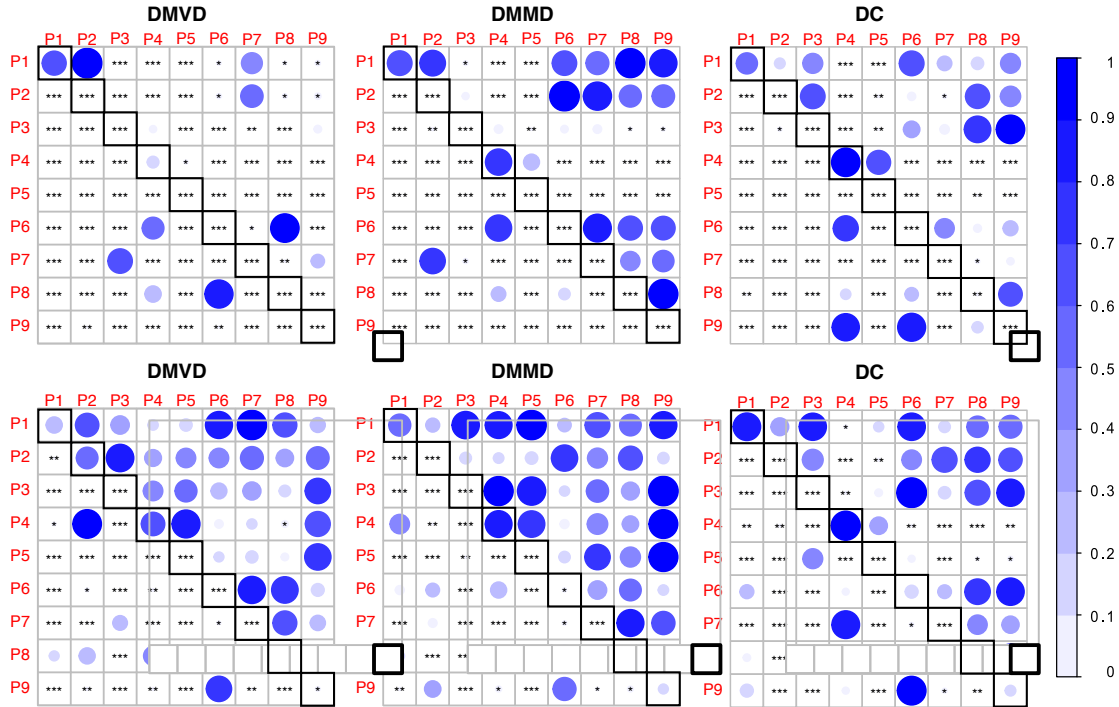


Figure 4.8: The heatmaps of significance levels (denoted by asterisks * – $p < .05$, ** – $p < .01$, *** – $p < .001$) according to the Mann-Whitney U-test for the difference in the performance of the decision policies across the patterns. The lower (LT) and the upper triangular (UT) parts of the matrices correspond to the performance on the patterns “before” and “after” isomorphic changes, respectively (top row: $\rho_b^* = 0.52$; bottom row: $\rho_b^* = 0.92$). The diagonal elements demonstrate how isomorphism affects the performance of a given policy on a single pattern. Non-significant results are denoted by circles of varying sizes and colours that depict the exact p -values.

Whitney U-test (Mann and Whitney, 1947), between the decision-making strategies on the same benchmark instances as well as across the patterns and their isomorphic counterparts is illustrated in Figures 4.9-4.10. As Figure 4.8 shows, there is a significant difference between each strategy on one and the same “before” and “after” patterns, except “P1: Random” and “P4: Star” for $\rho_b^* = 0.52$ (top row: diagonal elements). That is, the performance of each strategy is significantly improved on the constructed isomorphic patterns relative to their basic counterparts. While on the basic patterns, the results of each decision-making policy were significantly different from the ones on “P1: Random”, after their isomorphic transformations one can observe that there is no more statistical significance between the outcome on most of the patterns and “P1: Random”. The exceptions are P3-P5 for the DMMD and P4-P5 for the DC, where the performance on these patterns remains to be worse than on P1 also after applying isomorphism. For the DMVD, the performance on the “after”-patterns differs from P1 on most of the patterns. In general, for the DMMD and the DC there is no statistical difference in the performance across the “after”-patterns, except for “P4: Star” and “P5: Stripe” (see UT-parts of the matrices in Figure 4.8-top). Further analysis for $\rho_b^* = 0.92$ showed

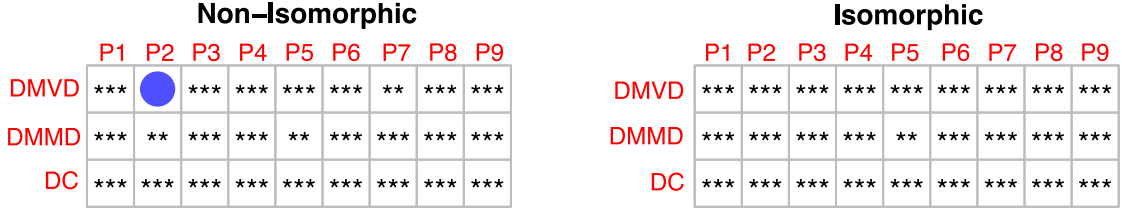


Figure 4.9: The heatmaps of significance levels (denoted by asterisks * – $p < .05$, ** – $p < .01$, *** – $p < .001$) according to the Mann-Whitney U-test for the difference in the performance of the decision policy with itself between the easiest and the hardest settings of ρ_b^* on each pattern. The circle indicates a statistically non-significant result.

no statistical significance difference across all “after”-patterns for the DMVD and the DMMD strategies, while for the DC patterns P4 and P5 still remain the exceptions (see UT-parts of the matrices in Figure 4.8-bottom).

As Figure 4.9 shows, there is a significant difference in the performance of a single decision-making strategy with itself between respective pattern configuration with $\rho_b^* = 0.52$ and $\rho_b^* = 0.92$ “before” applying the isomorphism (non-isomorphic) as well as “after” (isomorphic). The exception is only for the DMVD on the non-transformed “P2: Block”, for which outcome there is no statistically significant difference between the easiest and the hardest pattern configurations ρ_b^* , although its isomorphic counterparts are statistically significant ($p < .001$) between $\rho_b^* = 0.52$ and $\rho_b^* = 0.92$. Overall, the increase of the difficulty ρ_b^* diminishes the performance of collective decision-making regardless of the pattern type and the applied transformation of the environment. However, the isomorphic transformations of the respective patterns significantly improve the performance of the strategies relative to the non-transformed ones in the case of $\rho_b^* = 0.92$ as well as in the case of $\rho_b^* = 0.52$ (see Figure 4.8-bottom).

On the original patterns with $\rho_b^* = 0.52$ (see LT-parts of the matrices in Figure 4.10-top), the DMMD is statistically significantly faster than the DMVD on P3 and P7 along

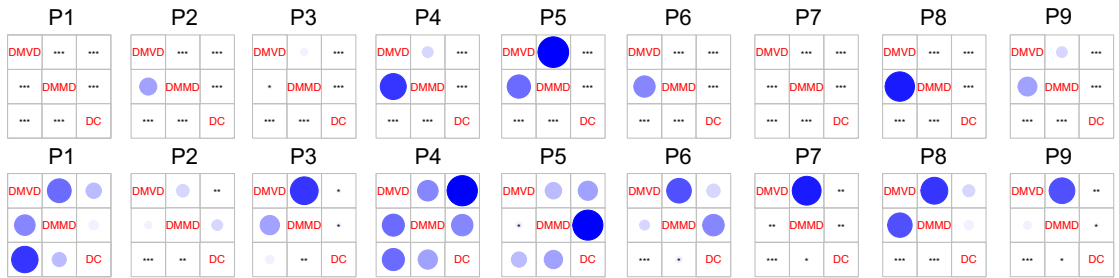


Figure 4.10: The heatmaps of significance levels (denoted by asterisks * – $p < .05$, ** – $p < .01$, *** – $p < .001$) according to the Mann-Whitney U-test for the pairwise comparison in the performance of the decision policies. The lower triangular (LT) part of the matrices corresponds to the results on the given pattern “before”, and the upper one – to the results “after” applying isomorphism, respectively (top row: $\rho_b^* = 0.52$; bottom row: $\rho_b^* = 0.92$). Non-significant results are denoted by circles of varying sizes and colours that depict the exact p -values.

with higher rates of exit probability E_N , while on the other patterns (except classical P1) there is no statistically significant difference in the performance between the DMMD and the DMVD strategies. However, on their isomorphic counterparts (see UT-parts of the matrices in Figure 4.10-top), there is a statistically significant difference in the $T_N^{correct}$ between the DMVD and the DMMD on P1-P2, P6-P8, such that the DMVD strategy is faster and more accurate than the DMMD at the easiest difficulty setting ρ_b^* . In turn, the DC strategy in the case of $\rho_b^* = 0.52$ is statistically significantly better than the others in $T_N^{correct}$ and E_N on the patterns “before” as well as “after” applying isomorphism. For $\rho_b^* = 0.92$ (see LT-parts of the matrices in Figure 4.10-bottom), there is no statistically significant difference in the consensus time ($T_N^{correct}$) between the DMVD and the DMMD strategies on the non-transformed patterns, except for the two striped scenarios, namely P5 and P7. There, one can also observe controversial results, that is, the DMVD is less accurate but faster than the DMMD strategy. Further analysis after isomorphic transformations of the respective patterns indicates no statistically significant difference in the performance between both of the voting strategies. While the DC is statistically significantly different from the DMVD and the DMMD on most of the patterns, no significant differences in the performance were found between the DC and two other strategies on the “before”-P1, P4-P5. While “after” isomorphic transformations of the environment in the case of $\rho_b^* = 0.92$, there is primarily no statistically significant difference observed in the $T_N^{correct}$ between the DC and the voting strategies on most of the patterns, except for P2 (for DMVD vs. DC) and P3, P7-P9 (for both DMVD, DMMD vs. DC), where the DC strategy is appeared to be more accurate than the others.

Summary. Whilst an isomorphism retains the environment’s overall structure, the properties of patterns with high clustering density after applying isomorphic mappings f^I have been modified (see Figure 4.4). Specifically, the values of MI are decreased for most of the patterns to the range of $[-0.1, 0.1]$, while the entropy E_c is primarily kept in the range of $[0.7, 0.8]$. The exceptions are P3 (“*Off-diagonal*”), P4 (“*Star*”), and P5 (“*Stripe*”), which are characterised by $MI \in [0.2, 0.5]$ and $E_c \in [0.4, 0.9]$ after undergoing isomorphic transformations. Notably, exactly on these patterns, one observes an increase in the consensus time ($T_N^{correct}$) relative to the other transformed benchmarks for the easiest difficulty setting ($\rho_b^* = 0.52$). This matches with the results obtained in the first experiment, indicating that the environments with a higher density of clustering between the features deteriorate the performance of the considered collective decision-making strategies. Overall, the difference in the collective performance between voting mechanisms is levelled off on the respective isomorphic patterns regardless of the colour ratio ρ_b^* , thereby emphasising the generality of the proposed benchmarks.

4.5 Summary and Discussion

In this chapter, we have introduced a benchmark suite for collective decision-making as a set of collective perception scenarios to investigate the generality and robustness of collective decision-making strategies across a variety of environments with different spatial patterns. Specifically, we quantified the scenarios according to the entropy (\mathcal{E}) and Moran index (MI) of the options in the environment, proposing these metrics as

another measures of the “task difficulty” in addition to the classically considered ratio of the features. Our benchmark analysis shows that spatial distribution of the features with high degree of correlations induces negative environmental bias that significantly distorts the direct modulation of majority (DMMD) and voter-based decision (DMVD) strategies, regardless of the relative amount of the features. The same decline in the performance was observed for the strategy of the direct comparison of options’ qualities (DC), that does not have direct modulation mechanism.

Inspired by the ability of the human brain to solve problems by performing mental transformations of the visuals, we explored the performance of the aforementioned decision-making strategies on the *isomorphic* set of patterns to the proposed benchmarks. Previously, isomorphism has been demonstrated to be an effective tool for creating a complex range of computer cognitive games (Sedig and Haworth, 2012). Similarly, we used isomorphic transformations of the environment to broaden the proposed suite of benchmarks without changing the combinatorial structure of the respective instances. It can also be thought of as a process of rearranging elements of the picture using brains to aid problem-solving (Bilge and Taylor, 2017).

The results indicate that isomorphic changes in the environment lead to faster and more accurate collective decision-making of the examined policies, eliminating the controversial relative performance of the DMVD and the DMMD strategies observed on the patterns other than that of random distribution. In this way, isomorphism allows for the mapping of complex environments into simpler ones in terms of MI and \mathcal{E} , while preserving the global structure of the pattern. In turn, this supports the definitions of MI and \mathcal{E} as the measures of the difficulty of the task along with the quantity of the features, as well as the generality of the proposed benchmark suite. However, direct changes to the environment in the real world appear to be difficult to implement. In this regard, during the exploration phase, one can consider transformations related to the agents’ locations to promote a better mix of their opinions or in the agents’ “inner world” (Ziemke *et al.*, 2005) as a result of collaborative latent learning (Jensen, 2006).

One can draw an analogy between how spatial bias in a site-selection scenario influences the frequency of the agents engaging in the dissemination and how spatial correlations of the features in the collective perception scenario hinder direct modulation of the positive feedback. Compared to site-selection, where the distance from the nest to the site defines the exploration time, the duration of the exploration phase for the agents in the collective perception is set to be the same independently of the chosen option. However, for instance, if an agent holds a ‘white’ opinion and is located in the patched black area, it will undergo several exploration phases, bypassing dissemination, until it reaches the white area. This results in several exploration phases in a row, which can be considered as an artificial increase in exploration time, leading to a lower frequency of interactions with others. In this way, similar to travelling to a more distant site relative to the nest, spatial correlations of the features indirectly affect the time necessary to explore a particular option and, hence, its cost. Such a collective perception scenario can be classified as the best-of-2 problem with *asymmetric* cost and *asymmetric* quality (see Section 2.1.1). Our results indicate that variability in options’ costs depending on the agents’ opinions and their spatial positions deteriorates the collective performance of the considered opinion-based decision-making strategies. In contrast to a random distribution of the features, i.e., the collective perception scenario with symmetric costs,

we observe a significantly slower and less accurate consensus process. To overcome the negative effects of the resulting sample bias, the agents could assess the frequency of the missed dissemination phases to account for in the calculations of their direct modulation, similar to leveraging distance-quality trade-offs. However, such modifications can lead to a general increase in the duration of the decision-making process and still do not guarantee a well-mixed state of the swarm during dissemination (Trabattoni *et al.*, 2018). The latter can require the design of specific adaptive motion patterns to use spatial patterns to an advantage for a decision-maker. This could also potentially assist the DC strategy to obtain more relevant and less noisy quality estimates. Indeed, although the DC strategy does not use a mechanism of direct modulation, its performance is also deteriorated by the presence of spatial correlations resulting in the contradicting estimates of the equally high quality, rendering their direct comparison as idle. Meanwhile, adjustment of the motion routines concerns the low-level controller of the agents, which does not relate to the generality of a decision-making strategy.

Therefore, in the following chapter, we concentrate on the development of individual decision-making mechanisms that can successfully perform across the variety of spatial distribution of the features and despite the negative effects of the spatial correlations.

Belief-based Decision-Making for the Best-of-*many* Problem

As it was shown in the previous chapter, spatial distribution and clustering levels of the features define the complexity of the collective perception alongside the ratio of the global quality of the features. Considering that the environment is a priori unknown, these properties can be viewed as additional hidden characteristics of the options. In such a context, they can not be directly measured by individuals but can induce *sample bias*, hindering decisions. The commonly used opinion-based decision-making strategies, such as voter and majority rules, demonstrated themselves inefficient in this regard and are not robust in their performance with the increase of the number of options. In this chapter, the framework based on the theory of belief functions is introduced and analysed for the case of multiple features $n > 2$, which is referred to as the best-of-*many* problem. The research questions to be answered are: (i) what to exchange and (ii) how to integrate the gathered information in a swarm to get the most reliable collective decision, regardless of the environmental structure. For this purpose, the impact of the communicated information type and the upgrade of the “horizontal” mental model, as the objectives stated in Section 1.3, will be addressed and reflected in the modifications of the three modular blocks, namely, “Decision()”, “Broadcast()” and “Listen()”, as of Figure 2.3.

The chapter is organised as follows. In Section 5.1, we extend the binary-featured benchmark set from the previous chapter for the case of multiple colours, as well as analyse its characteristics. After the problem statement and motivation in Section 5.2, we provide the necessary mathematical background in Section 5.3, including description of the twelve fusion operators to be investigated. Section 5.4 is concerned with the methodology proposed for this study, followed by the experiments in Section 5.5 and the general discussion of the results in Section 5.6. The proposed approach and the findings of this chapter were previously presented by the current author in (Bartashevich and Mostaghim, 2021) as the “Evidence Theory-Based Design Framework”.

5.1 From Binary to Multi-Featured Collective Perception

To examine how a collective perception scenario as the best-of-*many* problem scales with an increasing number of options and concerning different spatial distributions, we

extend the binary benchmark set from the previous chapter to a multi-featured case with $n > 2$ colours.

5.1.1 Proposed Multi-Featured Benchmark Set Generator

The resulted multi-featured benchmark set consists of the following seven environmental patterns, namely “Random”, “Star”, “Stripe”, “Band”, “Band-Stripe”, “Bandwidth”, and “Rectangle”¹. Due to the increasing difficulty to keep the pattern with the increase of the number of colours and the limited number of available cells in the grid, scenarios “Block” and “Off-diagonal” from the binary benchmark set are reduced to the “Rectangle” scenario for the multi-featured case. Similarly, the binary “Bandwidth-Rand” in case $n > 2$ coincides with the “Bandwidth” scenario. Figure 5.1 illustrates the corresponding scenario samples with respect to the number of options $n \in \{3, 5, 8, 10\}$ and $\rho \in \{0.67, 0.93\}$, i.e., the “old” task difficulty metric as defined in Section 2.2.

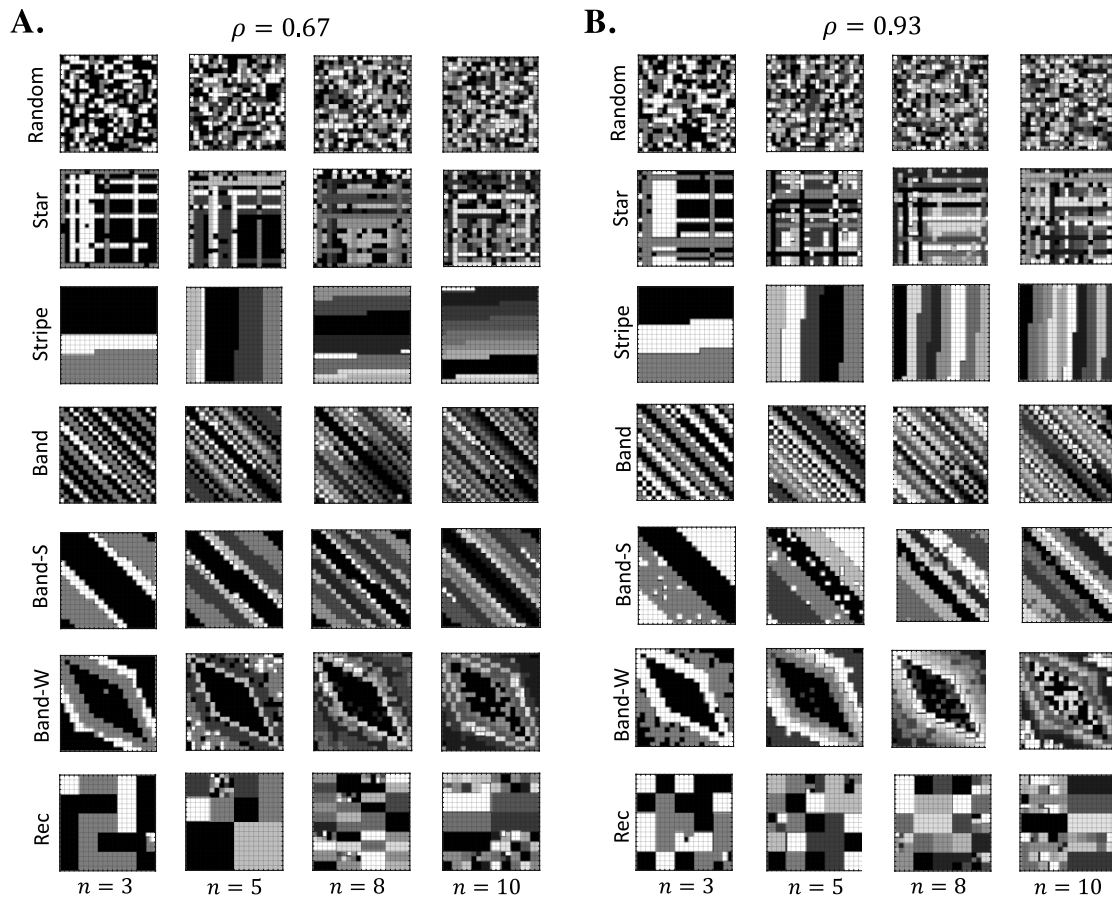


Figure 5.1: Samples of the patterns for different amount of options $n = \{3, 5, 8, 10\}$ and $\rho \in \{0.67, 0.93\}$.

¹In the following, we employ abbreviated forms of “Band-S”, “Band-W”, and “Rec” for “Band-Stripe”, “Bandwidth”, and “Rectangle”, respectively.

To avoid further coupling of the collective decision-making outcome with the particular spatial distribution, the environment is not predefined and is generated each simulation run. The target colour (i.e., the best option $\omega_{best} \in \Omega$) differs each time as the environment is generated, as well as the location of the colours in the grid. If there are not enough cells of a certain colour to shape a particular pattern element, then another colour that is available ² can be used instead. In turn, this can result in some artefacts, i.e., distinct cells of a different colour in respect to most of the neighbourhood. This is particularly observed in the case of $\rho = 0.93$, when the proportions of the colours are nearly the same, e.g., see “*Band-Stripe*” in Figure 5.1b.

As in the binary case, to generate the pattern one has to define the colour ratio parameter ρ . Let $\vec{f}_\Omega = (f_{\omega_1}, \dots, f_{\omega_n})$ be a vector of the proportion of the cells f_{ω_i} with a specific colour $\omega_i \in \Omega$ in the environment, such that $f_{\omega_i} \leq f_{\omega_{i+1}}$ and $\sum_{i=1}^n f_{\omega_i} = 1$. In case of $n > 2$, we calculate the value of $\rho(\vec{f}_\Omega)$ in the following way:

$$\rho(\vec{f}_\Omega) := 1 - \text{gini}(\vec{f}_\Omega) = 1 - \frac{1}{n-1} \left(n+1 - 2 \cdot \left(\sum_{i=1}^n \sum_{j=1}^i f_{\omega_j} \right) \cdot \left(\sum_{i=1}^n f_{\omega_i} \right)^{-1} \right), \quad (5.1)$$

where the Gini coefficient $\text{gini}(\cdot) \in [0,1]$ is a measure of the degree of inequality in a distribution (Gini, 1921). It indicates how the given \vec{f}_Ω differs from the equal distribution of the features’ frequencies, i.e., defines a degree of the colours’ disproportion. That is, $\text{gini}(\vec{f}_\Omega)$ equals zero in the case when there is an equal amount of cells of each feature $\omega_i \in \Omega$, and it equals one when there is a definitive distinction between them, i.e., complete inequality.

To stay consistent with the difficulty levels of ρ as those for the binary case, i.e., $\rho \in \{0.67, 0.93\}$, we need to define colour proportions \vec{f}_Ω also for $n > 2$ in such a way that $\rho(\vec{f}_\Omega)$ keeps its concept regardless of the vector’s length $|\vec{f}_\Omega| = n$. According to our definition of $\rho(\vec{f}_\Omega)$ in Equation 5.1, where $\text{gini}(\vec{f}_\Omega) = 1 - \rho(\vec{f}_\Omega)$, the easiest case of $\rho(\vec{f}_\Omega) = 0.67$ corresponds then to the Gini value of 0.33, indicating some level of colour disproportion. While $\rho(\vec{f}_\Omega) = 0.93$ implies almost equal colour distribution, as intended, since the Gini value is approaching zero in this case, i.e., $\text{gini}(\vec{f}_\Omega) = 0.07$. For instance, in the case of $n = 3$ and $\rho(\vec{f}_\Omega) = 0.67$, the vector of colour ratios is then defined as follows: $\vec{f}_\Omega = (0.17, 0.33, 0.5)$.

5.1.2 Benchmarks Characteristics

The general visual of the pattern is preserved each time it is generated but its quantitative characteristics can vary (see Section 4.3.3). The latter is due to the fact that the positions of the coloured cells forming the pattern are not fixed on the grid. In the following, we perform the analysis of the introduced multi-featured benchmark set for $n \in \{3, 5, 8, 10\}$ and $\rho \in \{0.67, 0.93\}$ with respect to the proposed metrics, Entropy and Moran Index as defined in Section 4.3.3.

Figure 5.2 presents the mean and the standard deviation values of the Moran Index MI and the Entropy parameter \mathcal{E} evaluated over 100 runs for each configuration. The results for both metrics are compared between the patterns to verify whether the data comes from the same distribution or not. According to the Kruskal-Wallis ANOVA

²That is a colour that has not yet reached its ratio in the grid.

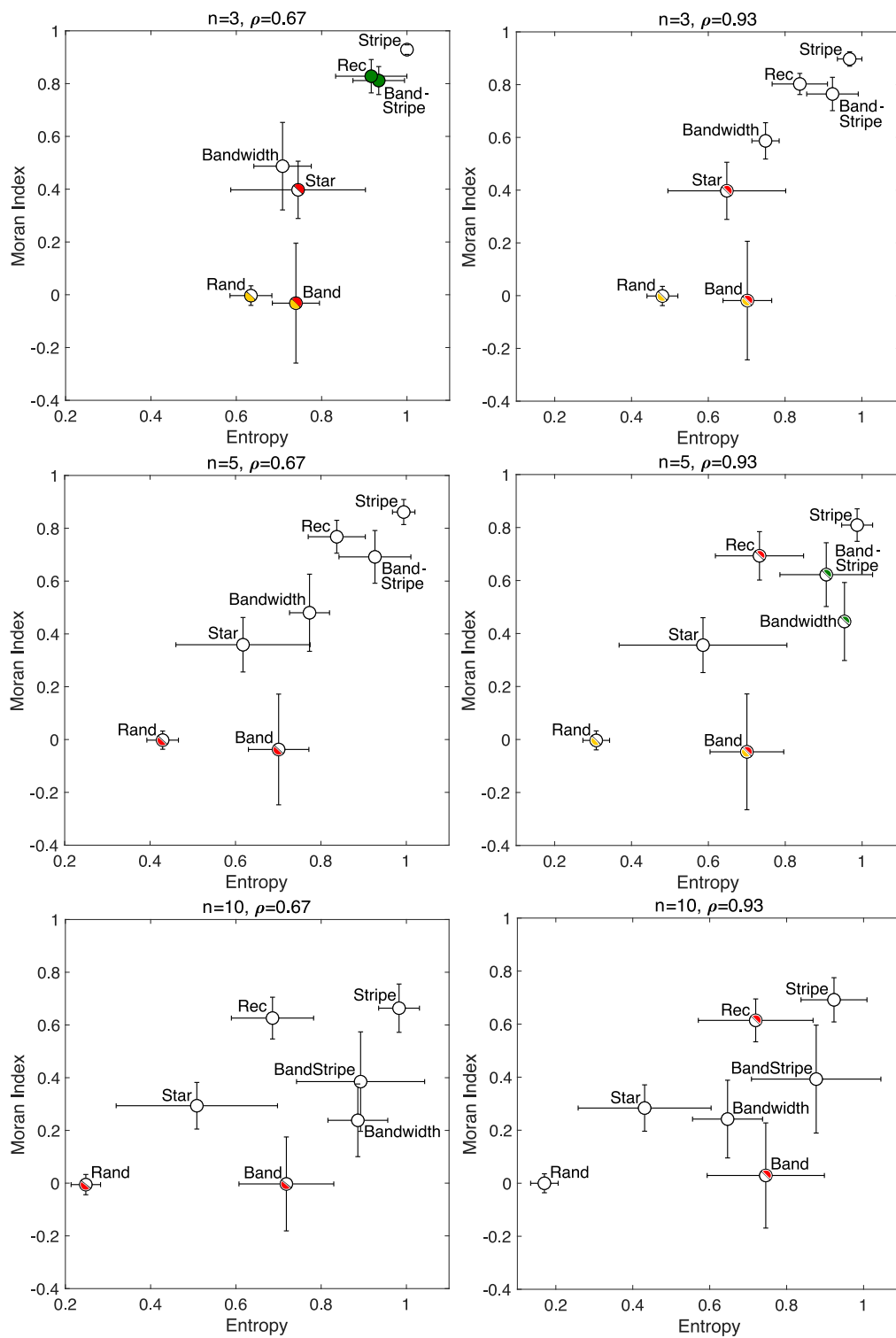


Figure 5.2: Scatter diagrams of the statistics over 100 runs for patterns' characteristics. Left: $\rho = 0.67$. Right: $\rho = 0.93$.

analysis (Hollander *et al.*, 2013), there is a statistically significant difference ($p < 0.01$) between most of the patterns in both MI and \mathcal{E} characteristics, regardless of the n and the ρ configuration. In case of $\rho = 0.67$, the exceptions are mainly for “*Random*”, “*Band*” and “*Star*”. There is no statistical difference in MI for “*Random*” and “*Band*”, despite the n and ρ values. The same holds for “*Band*” and “*Star*” in terms of \mathcal{E} , when $n = 3$ and $\rho \in \{0.67, 0.93\}$. In case of $\rho = 0.93$, there is no statistical difference for “*Band*” and “*Rec*” in terms of \mathcal{E} as well as for “*Bandwidth*” and “*Band-Stripe*”, when $n = 5$ and $\rho = 0.93$. Also, in case of $n = 3$ and $\rho = 0.67$, “*Rec*” and “*Band-Stripe*” are not considered to be statistically different in both MI and \mathcal{E} characteristics.

The same “up-”colour in Figure 5.2 indicates a non-significant difference ($p > 0.01$) in the *Entropy* between the corresponding patterns, while the same “down-”colour states for the non-significance difference in the *Moran Index*. The empty circles of Figure 5.2 imply a significant difference ($p < 0.01$) between each other in both parameters according to the Kruskal-Wallis ANOVA analysis (Hollander *et al.*, 2013).

The complexity of the scenario increases in the diagonal direction from the left-bottom corner to the right-top corner of each plot in Figure 5.2, which is consistent with the results of Chapter 4. That is, from “*Random*” as the easiest scenario case to “*Stripe*” as the most difficult one, together with other patterns in-between. However, with an increase in the number of possible features n , there is also observed a significant drop in the values of characteristics towards easing the complexity in terms of MI and \mathcal{E} . This is primarily due to the limited grid size, which remains constant regardless of the number of options n , making it more difficult to replicate the pattern for a larger n while preserving the proportions of the necessary features $\rho(\vec{f}_\Omega)$. As intended by the construction, the parameter ρ does not significantly affect the characteristics’ values of the patterns with the increase of n (the only exception is “*Bandwidth*” pattern, see Figure 5.2). Similar to the binary case, a negative correlation is expected between the performance of the collective decision-making algorithm and the underlying complexity of the pattern, together with an increase in the number of options.

5.2 Problem Statement and Contribution

In this chapter, we propose the methodology to tackle spatial correlations in an a priori unknown environment in the context of a collective perception scenario. As it was indicated in Chapter 4, the environment with large clusters of cells of the same colour introduces challenges in the decision-making process in comparison to the random scenario. Since the spatial distribution of the features is a priori unknown to the swarm, it can impose *sample bias* into the exploration process, thereby indirectly biasing the collective performance. As a result, the cost (in terms of time) to explore a particular option $\omega_j \in \Omega$ becomes dependent on its spatial setup. This introduces a corresponding disbalance in the estimation process, i.e., “Estimate(q_j)”³, sabotaging exploration of the options due to the spatial arrangements of the features and the movement trajectories of the individuals. That is, the time to discover (reach) areas with certain features is relative to the agent’s initial position and the location of this area.

As it was shown in Chapter 4, the opinion-based decision-making seems to be inefficient in this regard, while the preference-based approach (as introduced in Chapter 3)

³The value q_j corresponds to the actual quality of the option j , i.e., of the $\omega_j \in \Omega$.

has demonstrated itself prone to error already in the case of a random scenario if the agents hold the wrong initial conjecture. Nevertheless, the preference update process of the Algorithm 3.1 can be modified for less impact on the opinion dynamics and, hence, for a slower altering of opinions. The latter can lead to a better exploration of alternatives than in the case of pure opinion-based decision-making strategies. However, the requirement to tune multiple parameters makes it difficult to apply in an unknown environment.

The task becomes even more complicated in the case of multiple options $n > 2$, where the agents require efficient allocation strategies to switch between the estimation of different alternatives $\omega_j \in \Omega$ to ensure sufficient exploration (Ebert *et al.*, 2018). In addition, the latter demands adaptation of the agents' exploration trajectories to a given spatial distribution of the options, which is challenging since the distribution of alternatives is a priori unknown to the swarm (Khaluf *et al.*, 2019). This also implies modifications related to the low-level controller of the agents, which is application-dependent and represents a subject of the domain specifics, e.g., cluttered spaces, rough surfaces, external forces.

Therefore, there is a need to develop decision-making algorithms that are scalable and robust (trustworthy) in a wide range of environments regardless of the spatial distribution of the features. Non-homogeneous distribution together with imperfect and local estimates of the perceived information biases the agents towards gathering highly conflicting pieces of evidence. The Dempster-Shafer theory is well suited for this type of problem as it reflects the uncertainty and provides tools for handling imperfect and conflicting information (Liu and Yager, 2008). This theory is based on the concept of the belief functions and allows combining information from multiple sources into one common shared belief without relying on any prior knowledge. As already mentioned in Section 2.3, four DST belief combination operators have been studied in the case of the site-selection scenario with a fully connected graph of agents, where the global knowledge (quality values of the options) was available to the agents and was not a subject to spatial dependencies (Crosscombe *et al.*, 2019).

In this chapter, the DST framework is exploited to address the collective perception as the best-of-*many* problem, particularly in the presence of sample bias imposed by the environment and expressed in the distribution of the features. In comparison to opinion-based decision-making, DST represents the framework of belief functions that operates with a powerset of options (i.e., a set of all subsets) and not only with n single options $\omega_j \in \Omega$, $j = 1, \dots, n$. In this regard, we hypothesise that the allocation of beliefs to the union of options $\{\omega_i, \omega_j\}$, e.g., either 'black' (ω_1) or 'white' (ω_2) in the case $n = 2$, will slow down the collective consensus. On the other hand, this will give extra time to resolve the potential conflict⁴ between the agents from different clustered areas. Besides, one can expect the agent's choices based on continuous opinion dynamics (as in the DST case) to be more reliable and resulting in a more precise collective outcome than based on the counts of opinions, i.e., discrete opinion dynamics. This also involves that the mechanism for undertaking decisions on its own will be able to provide an adequate exploration of the options' space without adjustments of the agents' low-level controller.

⁴The terms conflict and disagreement are used interchangeably.

5.3 Mathematical Background

Dempster–Shafer theory (DST) is aimed to express the uncertainty under partial knowledge (Kohlas and Monney, 1994). In its probabilistic interpretation, the probabilities are allocated to the set of outcomes and not only to single events. To estimate how close the evidence is to the possibility that a given event is true, the belief intervals are used instead of the classical probability distribution. In the following, we introduce the basic terminology used in this chapter.

5.3.1 Basics of Evidence Theory

A finite set Ω of n mutually exhaustive and exclusive single events (singletons) is called a *frame of discernment*. One and only one element of such set Ω is believed to be true. In this vein, our set of n candidate options (colours) $\Omega = \{\omega_1, \omega_2, \dots, \omega_n\}$ represents a frame of discernment. The set of all possible subsets $\{A_i\}_{i=0}^{2^n-1}$ of Ω , including an empty set and Ω itself, forms the powerset 2^Ω . For example, if $n = 3$, then $2^\Omega = \{\emptyset, \omega_1, \omega_2, \omega_3, \{\omega_1, \omega_2\}, \{\omega_1, \omega_3\}, \{\omega_2, \omega_3\}, \Omega\}$.

The theory of evidence assigns to each subset $A_i \in 2^\Omega$ a non-negative weight called *mass*, which is defined by a *basic belief assignment* or a *mass function* $m: 2^\Omega \rightarrow [0, 1]$, satisfying the conditions $m(\emptyset) = 0$ and $\sum_{A_i \in 2^\Omega} m(A_i) = 1$. The condition $m(\emptyset) = 0$ can be relaxed if one observes that the given set Ω is not complete and a true state can be outside Ω , i.e., not exhaustive assumption. The subsets A_i characterised by $m(A_i) > 0$ are called *focal* elements of m . In the case $m(\Omega) > 0$, the mass function is said to be *non-dogmatic*. A mass function m is considered to be *normalised*, when \emptyset is not its focal element, that is, $m(\emptyset) = 0$.

The value $m(A_i)$ is interpreted as the measure of belief (or degree of confidence), which is entrusted exactly to the set A_i without indicating how it is specifically divided among its separate subsets $A_j \subseteq A_i$. In the case $m(\{\omega_i\}) = 1$ for a singleton $\omega_i \in \Omega$ ($\omega_i \in A_i$ and $|A_i| = 1$), one deals with the state of **full certainty** that the truth lies in ω_i . When it is difficult to discriminate between two single events, e.g., ω_i and ω_j , their union is allocated a certain mass value $m(\{\omega_i, \omega_j\})$. To this extent, unions of options reflect the state of **partial ignorance**, whereas \emptyset implies **impossibility** of the perceived event, meaning that it does not belong to Ω . The state of **full ignorance**, when nothing is known, is described by a *vacuous* mass function such that $\forall A_i \neq \Omega$ hold $m(A_i) = 0$ and $m(\Omega) = 1$.

The total *belief* $Bel(A_i)$ committed to the set A_i is considered as the sum of masses $m(A_j)$ of all its subsets $A_j \subseteq A_i$. As such, $Bel(A_i)$ reflects all provided evidence that approves the truthfulness of A_i . The sum of the mass values not committed to the negation of A_i defines the *plausibility* $Pl(A_i)$, i.e., $Pl(A_i) = 1 - Bel(\neg A_i)$. That is, $Bel(\neg A_i)$ expresses the degree of evidence that contradicts A_i , such that $Pl(A_i)$ specifies then a measure of evidence that potentially supports A_i . Therefore, $Bel(A_i)$ provides the lower and $Pl(A_i)$ the upper bound to the probability that the event A_i is true, such that $0 \leq Bel(A_i) \leq Pl(A_i) \leq 1$. In such terms, the *uncertainty* measure for all $A_i \subseteq \Omega$ is defined as $u(A_i) = Pl(A_i) - Bel(A_i)$. The precise definitions of the respective belief and plausibility

functions $Bel, Pl: 2^\Omega \rightarrow [0, 1]$ are given in the following way:

$$Bel(A_i) := \sum_{\substack{A_j \subseteq A_i, \\ A_j \neq \emptyset}} m(A_j), \quad Pl(A_i) := \sum_{A_j \cap A_i \neq \emptyset} m(A_j). \quad (5.2)$$

In addition, there are several other functions that are used as an analogue for a mass function m , that is, *implicability* $b: 2^\Omega \rightarrow [0, 1]$ and *commonality* $Q: 2^\Omega \rightarrow [0, 1]$ functions, defined respectively as:

$$b(A_i) := Bel(A_i) + m(\emptyset), \quad Q(A_i) := \sum_{\substack{A_j \subset \Omega, \\ A_i \subseteq A_j}} m(A_j). \quad (5.3)$$

The implicability function b is used instead of Bel in the case of an unnormalised mass function m , while the commonality function Q expresses the probability of obtaining a set observation that is consistent with every element of A_i . Function Q is mainly used to simplify the computations. Depending on the application, one can use any of the aforementioned functions, i.e., m, Bel, Pl, b , or Q , since they all can be derived through one another. However, a mass function m is considered as the most fundamental representation of the belief. The term ‘belief’ is ambiguous as it is used as a particular term related to the Bel function as well as in a general sense. In the following, we continue to use it as a general term unless it is stated otherwise.

According to (Smets and Kennes, 2008), in order to make decisions based on mass functions, one has to transform them into probabilities via the *pignistic transformation*:

$$BetP(\{\omega_i\}) := \sum_{A: \omega_i \in A} \frac{1}{|A|} \frac{m(A)}{1 - m(\emptyset)}, \quad (5.4)$$

where $|A|$ is the cardinality of the subset $A \in 2^\Omega$ and $m(\emptyset) \neq 1$. When m is normalised, this transformation evenly redistributes the mass values of focal elements with $|A| > 1$ among the singletons $\omega_i \in A$.

5.3.2 Mass function types

In the following, we provide definitions of the specific types of mass functions, which will be used further in the chapter.

A Bayesian model of uncertainty is also considered as a special case of the theory of evidence (Smets, 1993). When all focal elements of a mass function m are singletons, then such a mass function is called *Bayesian* (Shafer, 1976) and it is equivalent to a probability distribution. In this case, for all $A_i \in 2^\Omega$, we have: $Bel(A_i) = m(A_i) = Pl(A_i)$.

Another special case of a mass function m that assigns a positive value $w(A_i) \in [0, 1]$ to two and only two subsets $A_i \in 2^\Omega$ such that:

$$m(A_j) = \begin{cases} 1 - w & \text{if } A_j = A_i \\ w & \text{if } A_j = \Omega \\ 0 & \text{otherwise,} \end{cases} \quad (5.5)$$

is called a *simple support function* (**SSF**) with focus on A_i (Ke et al., 2014) and denoted

as $w(A_i)$. In other words, it represents a weight of evidence that provides support to one and only one subset $A_i \subset \Omega$. **SSF** represents that there is “a good reason to believe” in a given event A_i and in nothing more. If $w(A_i) \in [0, +\infty)$, then such a support function is called a *generalised simple support function* (**GSSF**) and, respectively, indicates that there are some “good reasons **not** to believe” in a certain event A_i .

In the case when evidence supporting solely one subset is pooled together from several observations, such a combination of two or more **SSF** forms a *separable support function*. Unlike a **SSF**, a *separable support function* focuses on multiple subsets $A_i \subset \Omega$. In comparison to a general mass function, for any of its two focal elements A_i and A_j , if $A_i \cap A_j \neq \emptyset$, then $A_i \cap A_j$ is also a focal element. Decomposition of separable and non-dogmatic mass function (i.e., with $m(\Omega) > 0$) is unique and can be used to decrease the computational complexity (Barnett, 2008), especially in case of combination of a large number of sources (Zhou *et al.*, 2017). As stated by Smets (1995), any non-separable, non-dogmatic mass function can be decomposed using **GSSF**. Both, separable and non-separable functions, can be also extended to the case of dogmatic mass function (i.e., with $m(\Omega) = 0$) by assigning a small value $\epsilon \rightarrow 0$ to the Ω set and redistributing it over the rest subsets.

With respect to the canonical decomposition as proposed by Smets (1995), the weights $w(A_i) \in [0, +\infty)$ for every $A_i \subset \Omega$ can be obtained from the values of commonality function $Q: 2^\Omega \rightarrow [0, 1]$ as follows:

$$\begin{aligned} w(A_i) &= \prod_{A_j \supseteq A_i} Q(A_j)^{(-1)^{|A_j|-|A_i|+1}} \quad \text{or equivalently} \\ \ln w(A_i) &= - \sum_{A_j \supseteq A_i} (-1)^{|A_j|-|A_i|} \ln Q(A_j). \end{aligned} \tag{5.6}$$

The Fast Möbius Transformation (Kennes and Smets, 1990) can be used to compute $\ln w$ from $-\ln Q$.

5.3.3 Fusion Rules

Dempster-Shafer theory suggests that each piece of evidence is represented by a separate function of a given belief representation (see Section 5.3), e.g., a mass function $m: 2^\Omega \rightarrow [0, 1]$. The idea is that evidence gathered from multiple distinct sources s can be further combined by fusing their corresponding mass functions m_1, m_2, \dots, m_s to get certainty about the state of the world Ω . There are different types of belief fusion rules in the literature (Smets, 2007), which mainly differ in the way how they handle conflicting pieces of evidence. The degree of disagreement K between two pieces of evidence is allocated to the empty set of their resulting mass function combination, which has to be re-distributed in a particular way among the remaining subsets $A_i \in 2^\Omega \setminus \{\emptyset\}$. Within the framework of this thesis, we work under the “closed-world” (exhaustive) assumption, meaning that there no piece of evidence exists which is out of the a priori defined set Ω . This also implies that $m(\emptyset)$ has to be equal to zero for any considered mass function m .

In the following, we introduce the twelve most well-known fusion rules from the literature on evidence theory, which are used in this thesis to address the hypotheses defined in Section 5.2.

1. **Dempster's Rule (DR)** is known as the original combination rule in Dempster-Shafer evidence theory. It strongly emphasizes the agreement between multiple sources (resembles "AND"-operator), ignoring the conflicting evidence through a normalisation factor K , such that a combination of two sources of evidence $m_{1\oplus 2}$ for all $A \in 2^\Omega$ is calculated as:

$$m_{1\oplus 2}^{DR}(A) := \frac{1}{1-K} \sum_{B \cap C = A \neq \emptyset} m_1(B) \cdot m_2(C), \quad (5.7)$$

where $K = \sum_{B \cap C = \emptyset} m_1(B) \cdot m_2(C)$. The normalisation redistributes conflicting masses to non-conflicting ones, and thereby tends to eliminate any conflict in the resulting mass distribution, keeping $m_{1\oplus 2}(\emptyset) = 0$. However, when the pieces of evidence are highly conflicting, this rule tends to produce illogical results known as Zadeh's paradox (Shafer, 1976). That is, the greater is the conflict between pieces of evidence, the greater is the certainty in the combination. Dempster's rule is undefined for $K = 1$. As another limitation, it is assumed that the sources of evidence to be combined should be independent, i.e., distinct (Dempster, 1967). Classical Bayes's rule is considered as a special case of Dempster's rule (Dezert *et al.*, 2013).

2. **Dubois-Prade's Rule (DP)** assigns the mass associated with the empty set in combination (i.e., conflict) to the disjunction of conflicting evidences (resembles "OR"-operator). As a result, it does not generate any conflict and does not reject any of the information asserted by the sources. No normalisation procedure is required. Formally, it is expressed as:

$$m_{1\oplus 2}^{DP}(A) := \sum_{B \cap C = A \neq \emptyset} m_1(B) \cdot m_2(C) + \sum_{\substack{B \cap C = \emptyset, \\ B \cup C = A}} m_1(B) \cdot m_2(C) \quad (5.8)$$

In the absence of conflict, it is equivalent to the Dempster's rule. While if $K = 1$, it consists only of the disjunctive part. In this way, the behaviour of this rule is considered as adaptive between conjunctive (i.e., "AND") and disjunctive (i.e., "OR") modes. Thus, it is supposed to maintain a reasonable trade-off between precision and reliability.

3. **Yager's Rule (YR)** is an analogue of the Dempster's Rule without normalisation. The conflict K is added up to the set of full ignorance Ω (Sentz and Ferson, 2002). If $K = 0$, this rule yields the same result as the Dempster's one.

$$m_{1\oplus 2}^{YR}(A) := \begin{cases} \sum_{B \cap C = A \neq \emptyset} m_1(B) \cdot m_2(C) & \forall A \subseteq \Omega, A \neq \Omega, A \neq \emptyset \\ m_1(\Omega) \cdot m_2(\Omega) + K & \text{if } A = \Omega \end{cases} \quad (5.9)$$

4. **Averaging (Avg)** of all the pieces of evidence instead of applying a specific combination rule can be used to eliminate the influence of any strongly conflicting single belief. To this extent, no evidence is lost but the rule lacks convergence towards certainty.

$$m_{1\oplus 2}^{Avg}(A) := \frac{1}{2}(m_1(A) + m_2(A)) \quad (5.10)$$

5. **PCR5/6** is based on a proportional conflict redistribution (in short form PCR) principle for combining highly conflicting independent (i.e., distinct and non-interacting) sources of evidence. It implies that the conflicting mass is passed only to the elements involved in the conflict and proportionally to their particular individual masses, such that the specificity of the information is predominantly retained. Firstly, the conjunctive rule is applied and then total or partial conflicting masses are redistributed proportionally as follows:

$$\begin{aligned}
 m_{1\oplus 2}^{PCR5/6}(A) &:= \sum_{\substack{X, Y \in 2^\Omega, \\ X \cap Y = A}} m_1(X) \cdot m_2(Y) + \\
 &+ \sum_{\substack{Z \in 2^\Omega \setminus \{A\}, \\ A \cap Z = \emptyset}} \left[\frac{m_1(A)^2 \cdot m_2(Z)}{m_1(A) + m_2(Z)} + \frac{m_2(A)^2 \cdot m_1(Z)}{m_2(A) + m_1(Z)} \right]
 \end{aligned} \tag{5.11}$$

The fraction in Equation 5.12 is discarded, if its respective denominator equals zero. In the case of only two sources of information $s = 2$, this rule is known as PCR5, and for $s > 2$ as PCR6 (Smarandache and Dezert, 2005). Detailed numerical examples, as well as implementation code in MATLAB (2018), could be found in (Smarandache *et al.*, 2010).

Moreover, the following statement was shown by Smarandache and Dezert (2013).

Theorem 1 *If $s \geq 2$ sources of evidences provide binary mass functions (i.e., which contain only two numerical values 0 and 1) on 2^Ω and their total conflicting mass $K = 1$, then PCR5/6 fusion rule coincides with the averaging fusion rule.*

6. **Murphy's Rule (MR)** allows pieces of evidence from s sources that are in agreement to reinforce each other while dropping those which disagree. It provides convergence to the averaging method by combining it with the Dempster's rule (Murphy, 2000). Initially, the evidence of all s sources is averaged, reducing the possible dominance of a single one, i.e., $m_{1\oplus 2\oplus \dots \oplus s}^{Avg}$. Afterwards, the Dempster's rule is applied for $s - 1$ times to the obtained before average combination.

$$m_{1,2..s}^{Murphy}(A) := m_{1\oplus 2\oplus \dots \oplus s}^{DS}(A), \tag{5.12}$$

where $m_{1'} = m_{2'} = \dots = m_{s'} = m_{1\oplus 2\oplus \dots \oplus s}^{Avg}$. Since the evidence is averaged prior to combination, Zadeh's paradox is eliminated. While all the methods mentioned above assume that the sources of evidence are independent of each other, the Murphy's rule can be applied to the situations where the sources of evidence are either dependent (i.e., coming from the same source) or independent (i.e., coming from distinct sources).

7. **Normalised Cautious Conjunctive Rule (NCCR)** is not related to conflict minimisation but solves the *data incest problem*, which appears when the information from a given source is taken into account several times or when the considered sources are dependent (Dencœux, 2008). It is based on the minimum of the weights

obtained from the canonical decomposition of mass functions (see Equation 5.6) as the conjunctive combination of GSSF. That is, for two non-dogmatic mass functions m_1, m_2 , their cautious combination is denoted by $m_{1\otimes 2}$ and defined as:

$$m_{1\otimes 2} := \bigodot_{A \subseteq \Omega} A^{w_1(A) \wedge w_2(A)}, \quad (5.13)$$

for all $A \subseteq \Omega$ such that $w_1(A) \wedge w_2(A) \neq 1$, where \wedge denotes the minimum operator, i.e., $w_1(A) \wedge w_2(A) = \min(\{w_1, w_2\})$. $A^{w_j(A)}$ is the GSSF focused on A with the weight function $w_j(A)$ issued from the canonical decomposition of m_j and \bigodot is the unnormalised Dempster's rule. A normalised version of this operator, i.e., $m_{1\otimes^* 2}$, is defined by replacing the conjunctive operator \bigodot by the Dempster's rule \bigoplus or simply through introducing the normalisation factor $K = m_{1\otimes 2}(\emptyset)$ as follows:

$$m_{1\otimes^* 2} := \bigoplus_{A \subseteq \Omega} A^{w_1(A) \wedge w_2(A)} = \begin{cases} \frac{1}{1-K} \cdot m_{1\otimes 2}(A) & \forall A \in 2^\Omega \setminus \{\emptyset\} \\ 0 & \text{if } A = \emptyset \end{cases}. \quad (5.14)$$

Note that we can never have $K = 1$, because the cautious combination of two non-dogmatic (i.e., with $m(\Omega) > 0$) mass functions can never be dogmatic (i.e., with $m(\Omega) = 0$).

8. **Neighbourhood confidence algorithm (NCA)** was proposed in (Ducourthial *et al.*, 2012) mainly for distributed information fusion in communication networks based on the adapted Dempster's rule, which performs on weight functions instead of masses (see Equation 5.6), denoted by $w_{1\boxplus 2}$ and defined for any $A \in 2^\Omega \setminus \{\Omega, \emptyset\}$:

$$w_{1\boxplus 2}(A) := w_1(A) \cdot w_2(A). \quad (5.15)$$

The algorithm itself works as follows. Every node $i \in \{1, 2, \dots, s\}$ of a network has its own *direct confidence* (Inp_i), which is updated regularly by some external sources, e.g., sensors. It also represents a local mass function m_i and is expressed by the corresponding weight function w_i (see Equation 5.6). At certain time steps, each node sends its *direct confidence* to its neighbours (ancestors). Nodes are not synchronised and act according to their own local clocks, such that the frequencies of sending the results can differ between nodes. Upon certain time expiration, each node i computes its *neighbourhood confidence* (Out_i) by combining its direct confidence (Inp_i) with received ones from the neighbours j as: $Out_i = Out_i \boxplus Inp_j$. At the beginning, it is assumed that $Out_i := Inp_i$. Important to note that only direct confidence and not the neighbourhood one is exchanged between the nodes. According to Ducourthial *et al.* (2012), the outputs of the algorithm get stabilised as soon as the topology and the direct confidences stop varying.

9. **Distributed confidence algorithm (DCA)** is an extension of the neighbourhood confidence algorithm (Ducourthial *et al.*, 2012). It assumes an exchange of the *distributed confidence* and its further combination with the current direct confidence of the node using discounting and cautious operator. It works with weights obtained from the commonality functions (see Equation 5.6) in a way that their

cautious combination is denoted by $w_{1\otimes 2}$ and defined as:

$$w_{1\otimes 2}(A) := \min(w_1(A), w_2(A)). \quad (5.16)$$

The forwarded last computed *distributed confidence* (Out_j) of a neighbouring node j is additionally discounted prior its cautious combination with direct confidence (Inp_i) of the receiving node i as: $Out_i = Out_i \otimes \mathbf{r}(Out_j)$, where \mathbf{r} is a *discounting operator* and $Out_i := Inp_i$ initially. The choice of \mathbf{r} is application-dependent. Note that, here, only the distributed confidence and not the direct one is propagating through the network. In (Ducourthial *et al.*, 2012) it was shown that the algorithm converges in finite time from any initialisation as soon as the topology becomes stable (i.e., sending and receiving nodes remain the same). Some application experiments could be found in (Ducourthial and Cherfaoui, 2016).

10. **Florea's Rule (Flo)** defines a compromise between disjunctive \oplus and conjunctive \odot rules in accordance with the global conflict $K = \sum_{B \cap C = \emptyset} m_1(B) \cdot m_2(C)$ for any $A \in 2^\Omega, A \neq \emptyset$ (Florea *et al.*, 2006; Martin and Osswald, 2007).

$$\begin{aligned} m_{1\oplus 2}^{Flo}(A) &:= \beta_K \cdot \sum_{B \cup C = A} m_1(B) \cdot m_2(C) + \\ &+ (1 - \beta_K) \cdot \sum_{B \cap C = A} m_1(B) \cdot m_2(C), \end{aligned} \quad (5.17)$$

where $\beta_K = \frac{K}{1-K+K^2}$. In comparison to the Dubois-Prade's rule, wherein even in the presence of high conflict $K \rightarrow 1$ at least one of the two masses' sources is supposed to be the true outcome, here, the disjunctive rule has more weight than conjunctive one, assuming that both sources are non-reliable. While in the case of absence or low conflict $K \rightarrow 0$, the whole combination turns into a conjunctive mode, supposing the reliability of the sources.

11. **Cautious Florea's Rule (CFlo)** is a counterpart of the **Flo** rule for dependent sources of information. Conjunctive and disjunctive rules used inside **Flo** rule assume the independence of sources, while it can be not the case in the real-world situations. For this, conjunctive and disjunctive parts of **Flo** are replaced by their corresponding cautious counterparts, namely *cautious conjunctive* (without normalisation) and *bold disjunctive* rules (Denœux, 2008), respectively. The cautious conjunctive operator was introduced before by Equation 5.13. In the following, we describe the bold disjunctive rule, denoted by $m_{1\otimes 2}$, for two subnormal mass functions m_1, m_2 such that $m_1(\emptyset) = m_2(\emptyset) > 0$:

$$m_{1\otimes 2} := \bigoplus_{A \neq \emptyset} A_{v_1(A) \wedge v_2(A)}, \quad (5.18)$$

where $A_{v_j(A)}$ is called a **negative GSSF** assigning a mass $v_j(A) > 0$ to \emptyset , and a mass $1 - v_j(A)$ to A for all $A \in 2^\Omega \setminus \{\emptyset\}$. As in the cautious rule, \wedge denotes a minimum operator. The function $v_j : 2^\Omega \setminus \{\emptyset\} \rightarrow (0, +\infty)$ is called a *disjunctive weight function*

and defined through a corresponding implicability function b_j as follows:

$$\begin{aligned} v_j(A) &= \prod_{B \supseteq A} b_j(B)^{(-1)^{|A|-|B|+1}} \quad \text{or equivalently} \\ \ln v_j(A) &= - \sum_{B \supseteq A} (-1)^{|A|-|B|} \ln b_j(B). \end{aligned} \quad (5.19)$$

Finally, the resulting **CFlo** rule with $K = m_{1 \otimes 2}(\emptyset)$ and β_K is defined as:

$$m_{1 \oplus 2}^{CFlo}(A) := \beta_K \cdot m_{1 \otimes 2} + (1 - \beta_K) \cdot m_{1 \otimes 2}. \quad (5.20)$$

12. **Modified Weighted Average Approach (MWA)** is considered as the modification of Murphy's rule (**MR**) and is based on the *evidence distance* (Jousselme *et al.*, 2001) and the *uncertainty measure* (Chen *et al.*, 2018). Instead of simple averaging of s pieces of evidence before applying the classical Dempster's rule for $s-1$ times as it is done in **MR**, the weighted sum of the evidence is considered:

$$m_{1,2,\dots,s}^{MWA} := \sum_{i=1}^s \alpha_i \cdot m_i, \quad (5.21)$$

where α_i is the corresponding weight degree of each mass m_i , such that $\sum_{i=1}^s \alpha_i = 1$. To define the weights $\{\alpha_i\}_{i=1}^s$, evidence distance between two mass functions m_i and m_j is calculated as:

$$d(m_i, m_j) = \sqrt{\frac{1}{2} (m_i - m_j)^T \cdot D \cdot (m_i - m_j)}, \quad (5.22)$$

where D is a $2^n \times 2^n$ matrix, which elements are $D(A_i, A_j) = |A_i \cap A_j| / |A_i \cup A_j|$, $A_i \in 2^\Omega$. The lesser the distance $d(m_i, m_j)$, the more m_i and m_j are similar to each other, that is, $Sim(m_i, m_j) = 1 - d(m_i, m_j)$. In this way, a similarity matrix $Sim \in \mathbb{R}^{s \times s}$ can be constructed between all available pieces of evidence. The support Sup and the credibility Crd degree of their corresponding mass functions $\{m_i\}_{i=1}^s$ are calculated as follows:

$$Sup(m_i) = \sum_{j=1, j \neq i}^s Sim(m_i, m_j) \quad \text{and} \quad Crd(m_i) = \frac{Sup(m_i)}{\sum_{i=1}^s Sup(m_i)}, \quad (5.23)$$

such that $\sum_{i=1}^s Crd(m_i) = 1$. The value of $Crd(m_i)$ reveals the relative importance of a particular piece of evidence in comparison to the all gathered evidence. After it is combined with the uncertainty measure $U_i = \sum_{A_j \in 2^\Omega} u_i(A_j)$ of the respective mass function m_i in a way that $Crd'(m_i) = Crd(m_i) \cdot e^{U_i}$, its normalised value is used as the corresponding weight α_i in Equation 5.21, that is:

$$\alpha_i = \frac{Crd'(m_i)}{\sum_{i=1}^s Crd'(m_i)}. \quad (5.24)$$

Thus, more weight is given to the evidence which is greater supported by others (i.e., high credibility Crd) and which possesses a lesser uncertainty degree, indicating its high quality. While the conflicting evidence (i.e., low credibility Crd) with a

higher uncertainty degree gets less weight and, hence, less influence on the overall result. Lastly, the same as in the **MR**, the classical Dempster’s rule is applied to combine $m_{1,2,\dots,s}^{MWA}$ for $s - 1$ times.

All the operators are defined for one-off combinations between two pieces of evidence (beliefs), which in the context of the collective perception scenario are studied in an iterative setting, therefore it is important to consider their algebraic properties, given in Table 5.1. If the fusion operator possesses the respective property in the table, it is marked by a filled circle and by an empty one otherwise. The *associativity* implies that, given a particular sequence of evidence, the order in which its pairwise standing elements are merged (i.e., rearranging the parentheses in a sequence) does not change the outcome. If the rule is *quasi-associative* (for more details, the reader is referred to Yager (1987)), it can be transformed into an associative one by applying the algorithm proposed by Smarandache and Dezert (2004b). The *commutativity* means that changing the order of the elements in the evidence sequence has no impact on the resulting combination. This property is one of the most preferable ones, as it indicates that the order in which the agent communicates with the others in some temporarily fixed neighbourhood does not affect its evidence fusion. The *idempotence* ensures that no piece of evidence is counted twice, which is an important property in the case of dependent sources, i.e., overlapping, non-distinct items of evidence (Dencœux, 2008). The assumption concerning independence or dependence of the sources, when applying the corresponding fusion operator, is marked by the respectively filled-in side of the circle in the last row of Table 5.1. For instance, **MR** can be applied in both cases, i.e., when the sources are either independent or dependent, and therefore is depicted by a fully-filled circle mark.

The fusion operators (1)-(4) have been studied in (Crosscombe *et al.*, 2019) on the fully connected graph of agents within the site-selection best-of- n problem and later in the work of the current author (Bartashevich and Mostaghim, 2021) along with rules (5), (10)-(12) on the collective perception scenario. The results of this chapter are primarily based on the author’s previous work (Bartashevich and Mostaghim, 2021) and are complemented by the consideration of the operators (6)-(9).

5.4 Proposed Methodology

In this section, we introduce modifications into the general framework described in Chapter 2.4 to adapt it for the application of the DST to handle the collective perception scenario. In particular, “Decision()” and “Broadcast()” blocks in Figure 2.3 are modified, addressing the fourth and the fifth objectives defined in Section 1.3. The described methodology has been previously proposed by the author of the current work in (Bartashevich and Mostaghim, 2021).

5.4.1 Belief-based Decision-Making

In the context of the DST, the mental state of an agent k is modelled by a *belief*, represented in a form of a normalised mass function $m_k : 2^\Omega \rightarrow [0, 1]$, satisfying the exhaustive assumption. That is, the agents form their beliefs about the “world” described by the set Ω , which is assumed to be complete and constant throughout the entire simulation period T , such that $m_k(\emptyset) = 0$, excluding the *impossibility* state. Initially, the agents do

	DR	DP	YR	Avg	MR	PCR5/6	NCCR	NCA	DCA	Flo	CFlo	MWA
associative	●	○	quasi	○	●	○	●	●	●	○	●	●
commutative	●	●	●	●	●	●	●	●	●	●	●	●
idempotent	○	○	○	●	○	○	●	○	●	○	●	○
ind/depn	●	●	●	●	●	●	●	●	●	●	●	●

Table 5.1: Algebraic properties (by rows) of fusion operators (by columns).

not have any information about the environment and, therefore, are characterised by a vacuous mass function such that $m_k(\Omega) = 1$, indicating the state of a *full ignorance*.

To revise its personal mental state m_k , the agent gathers information by interacting either with the environment (in the exploration state) or with the other agents (in the dissemination state). Therefore, the evidence gathered from the external sources (i.e., environment, agents) has to be also recorded in terms of the belief representation, i.e., mass functions. In the following, we distinguish between two masses of evidence, that is, direct evidence from the environment m_{e_k} gathered by the agent k and the agent's personal belief m_k .

In the collective perception scenario, during time t in the exploration state, an agent gathers the evidence supporting its chosen hypothesis $\omega_i \in \Omega$ while moving through the environment. The agent can identify only one colour at a time, meaning that it explores only those subsets $A \in 2^\Omega$ which satisfy $|A| = 1$. In particular, it senses either the respective colour ω_i is underneath it or not. Based on the latter, the quality estimate \hat{q}_i of the option ω_i is built. In this way, if the agent has not perceived the chosen colour ω_i over time t of its exploration state, it has not gathered any evidence supporting that this option is a “true state of the world”, i.e., the dominant colour. Thus, its direct confidence in ω_i corresponds to 0 as well as its current quality estimate, i.e., $\hat{q}_i = 0$. In contrast, if the agent has observed only ω_i and nothing else in its exploration state, it gets the evidence fully supporting its choice along with the maximum quality estimate, i.e., $\hat{q}_i = 1$. As such, the piece of evidence received by an agent directly from the environment can be modelled by a quality estimate \hat{q}_i , regarding the alternative ω_i under the agent's consideration. In this regard, we define the evidence mass m_{e_k} obtained by the agent k in the exploration state through a *simple support function* (as given in Equation 5.5) with a focus on the respectively explored option ω_i , that is, $m_{e_k} := A^{1-\hat{q}_i}$. In this way, the quality estimate \hat{q}_i is allocated to $m_{e_k}(\{\omega_i\})$ as a mass value, implying precisely a degree of confidence in the chosen alternative ω_i and in nothing else, leaving the value $1 - \hat{q}_i$ as a level of uncertainty, i.e., $m_{e_k}(\Omega) = 1 - \hat{q}_i$.

Entering the dissemination state, the agents exchange the pieces of evidence and not the opinions as it was done in Chapter 2.4. Given that each agent k holds two types of the mass functions representing the evidence, that is, m_{e_k} and m_k , one can differentiate different ways of learning about the “world”. Under “learning” we mean the process of updating the mental state through observation (perception) of others and/or the environment. The “learning from the others” is done via establishing communication channels between the agents. As described in Section 2.4, the exchange between the agents is not necessarily performed in a pairwise symmetric manner, unlike in the previous work (Crosscombe *et al.*, 2019).

Learning Mechanism

Let $M^{\mathcal{N}} := \{(m_1, \dots, m_{\mathcal{N}}) \mid m_i : 2^{\Omega} \rightarrow [0, 1]\}$ denote the set of tuples of \mathcal{N} mass functions m_i . Then, the learning mechanism is defined by the function

$$l : M^{\mathcal{N}} \rightarrow M, \quad (5.25)$$

which, depending on the type of its input (i.e., broadcasted mass functions), determines the type of learning: individual, collective or social. As such, the driving mechanism of learning in our case lies in the fusion of beliefs (denoted by \oplus), determined on the basis of one of the combination rules specified in Section 5.3.3.

In Sections 5.4.2-5.4.4, we give explicit definitions of the corresponding functions l describing each learning type in particular.

Decision-Making

Based on the “learned” information during exploration and dissemination states, which is stored in the form of the agent’s belief, each agent k undertakes a decision about the true state of the world Ω . This decision corresponds to its opinion op_k on a certain option $\omega_j \in \Omega$ to be explored in its next exploration state. Thus, the decision-making mechanism is defined by the function $h : M \rightarrow \Omega$ such that

$$h : m_k \mapsto op_k, \quad (5.26)$$

where m_k is the belief of an agent k at the end of its current dissemination state, already representing by itself the accumulative evidence as an outcome of the learning function l from Equation 5.25. That is, the input of the function h represents the result of the fusion of several pieces of evidence gathered by the agent over one or several behaviour cycles (i.e., exploration and dissemination states).

To transit from the belief to opinion, one has to transform the agent’s mass function m_k into probabilities about possible outcomes $\omega_j \in \Omega$ to be true using the pignistic transformation as given in Equation 5.4. A roulette wheel selection is then applied to the set of probabilities obtained as the result of the composition of functions $BetP \circ l : M^{\mathcal{N}} \rightarrow [0, 1]$ to select the best option $\omega_i \in \Omega$, which is further taken as a new opinion of an agent k . As such, the function h in Equation 5.26 is defined by the composition of roulette wheel selection and pignistic probability function $BetP$.

5.4.2 Individual Learning

We define individual learning (IND) for the case that there is no communication between the individuals and, hence, no information exchange. Here, the agent forms its belief m_k based only on its own evidence received directly from the environment. In such a setting, its learning mechanism is given by the following function:

$$l : (m_k, m_{e_k}) \mapsto m_k := m_k \oplus m_{e_k}. \quad (5.27)$$

As soon as time t of the agent’s exploration state is expired, it combines its current mass function m_k with the received evidence in the form of m_{e_k} (since $m_{e_k} \in M$, i.e., $\mathcal{N} = 1$, the brackets for m_{e_k} are omitted in the input notations of the function l). The resulted

mass combination $m_k \oplus m_{e_k}$ is set as a new mass of an agent k at the beginning of the agent's dissemination state.

In this case, the dissemination state serves solely for the better mixing of the group and provides its members the time between two exploration states to reach other locations in the environment to collect new pieces of evidence m_{e_k} .

5.4.3 Collective Learning

We define collective learning (CL) as the case that implies interaction between the individuals and exchange of their personal beliefs m_{k_i} with each other. In this way, an agent k gathers the beliefs of its \mathcal{N} neighbours, satisfying the conditions for communication in the dissemination state. As such, the learning mechanism is defined by the function l as follows:

$$l: (m_k, (m_{k_1}, \dots, m_{k_L})) \mapsto m_k := (((m_k \oplus m_{k_1}) \oplus \dots) \oplus m_{k_L}). \quad (5.28)$$

The agent k combines its current belief m_k with the belief of another agent k_i as soon as it receives the information from it, i.e., $m_k \oplus m_{k_i}$. The resulting accumulative mass function m_k of $\mathcal{N} + 1$ individuals is set as a new belief of the agent k by the end of its dissemination state. The received masses can be also firstly collected and saved by the agents in a separate archive and later combined sequentially by the end of the state. However, this requires extra memory for the agents and can also cause time delays as the final combination of all the collected masses at once takes extra time. Additionally, the preliminary experiments (not reported here) have not indicated a significant influence on the collective outcome in comparison to the direct combination upon the receipt. In this scope, we consider and analyse the results obtained only for the case where the combinations are done as soon as the information becomes available to the agents, i.e., dynamic fusion mechanism.

It is important to note, that this learning mechanism incorporates in itself individual learning as well. That is, the beliefs m_{k_i} shared between agents (including m_k) are already updated with the respective evidence grasped by each agent k_i on its own directly from the environment (following Equation 5.27). It is also the first step, which allows agents to leave their initial state of ignorance, providing them further with meaningful combinations with each other (while a fusion of vacuous mass functions results again in a vacuous mass function).

5.4.4 Social Learning

We define social learning (SL) as passing of the pure information from the environment observed by an agent k to the other agents during communication. Thus, the evidence gathered by the agents in their respective exploration states in the form of $m_{e_{k_i}}$, and not the agents' beliefs m_{k_i} , is broadcasted in the dissemination state, as opposed to CL. The learning mechanism, in this case, is defined by the function l in the following way:

$$l: (m_k, (m_{e_{k_1}}, \dots, m_{e_{k_L}})) \mapsto m_k := (((m_k \oplus m_{e_{k_1}}) \oplus \dots) \oplus m_{e_{k_L}}). \quad (5.29)$$

Similar, as in the case of CL, the agent k combines directly at once its current belief m_k with the received evidence $m_{e_{k_i}}$ from another agent, assigning $m_k \oplus m_{e_{k_i}}$ as its updated belief upon the first reception from the agent k_i . The resulting agent's belief m_k by the

end of its dissemination state represents pure cumulative evidence from the environment, assessed by $\mathcal{N} + 1$ agents during their personal exploration states.

Notably, in SL the agent's belief m_k is primarily updated with its own observation of the environment m_{e_k} and, therefore, in case of zero encounters with the other agents, coincides with Equation 5.27. In general, SL resembles the individual learning (IND) but with additional L pieces of evidence $m_{e_{k_i}}$ acquired from different locations in the environment instead of a single one m_{e_k} . That is, SL is characterised by an increased frequency of receiving direct evidence from the environment.

5.4.5 Evaluation Metrics

As it was previously mentioned in Section 2.4.2, the performance of the collective decision-making mechanism is defined by the consensus of the group on the best alternative $\omega_{best} \in \Omega$. However, the opinion-based metrics (defined in Section 2.4.2) seem to be not reliable for the evaluation of the belief-based decision-making, since in the latter the opinions are formed probabilistically based on the agents' beliefs. In this regard, the convergence of the group on one option, e.g., ω_j , is determined by the achieving of the state of *full certainty* by each agent k in a swarm of size N , that is, $m_k(\{\omega_j\}) = 1$ for all $k = 1 \dots N$. In this case, the group attains the objective state of collective "knowledge" as depicted in Figure 1.1, illustrating the highest degree of confidence in the selected outcome, which also corresponds to the stabilised group opinion dynamics (i.e., $op_k = \omega_j$ for all $k = 1 \dots N$).

To estimate how close is the collective to the state of "knowledge", we introduce the following evaluation metrics.

Average population belief

Average population belief depicts the average mass value in the target option $\omega_{best} \in \Omega$ over all individuals in the group at a given time, that is, $\sum_{k=1}^P m_k(\omega_n)/P$, where P is the size of the population. As such, it shows the average aggregate degree of faith in the hypothesis that ω_{best} is the true state of the world. The state of collective absolute "knowledge" corresponds to the average population belief value of 1.

Population success rate

Population success rate over time specifies the metric of the *average population belief* by indicating the proportions of individuals in a group corresponding to different states of certitude according to their current mass values for the target option, i.e., $m_k(\{\omega_{best}\})$. Given the belief value, one can quantify the confidence level in a certain outcome subdividing it into one of the following categories:

- (a) $m_k(\{\omega_{best}\}) = 0$ corresponds to the state of the absolute disbelief in ω_{best} ;
- (b) $m_k(\{\omega_{best}\}) \in (0, 0.5]$ indicates the degree of uncertainty that ω_{best} is entirely impossible;
- (c) $m_k(\{\omega_{best}\}) \in (0.5, 1)$ indicates that ω_{best} is most likely the correct outcome but there is some degree of uncertainty that it is the only one probable hypothesis;

- (d) $m_k(\{\omega_{best}\}) = 1$ corresponds to the state of full certainty that ω_{best} is the only one correct outcome.

As opposed to the average belief, this metric demonstrates the belief dynamics in the population, in particular, the flow of individuals from one state into another from (a)-(d) over time.

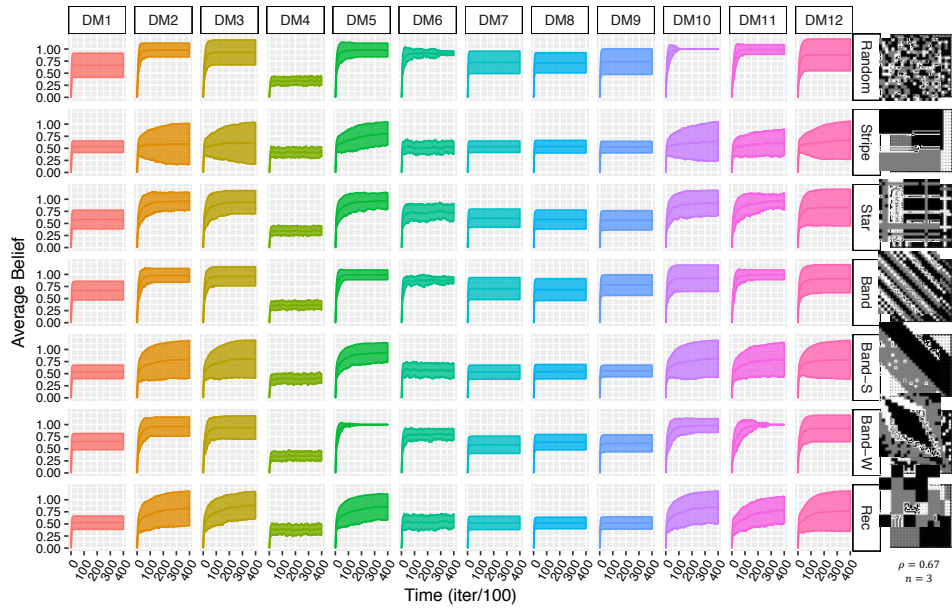
5.5 Experimental Study

In this section, we describe the results of the experiments designed to address the following objectives previously defined in Section 1.3. The first objective is to determine whether the proposed belief-based decision-making could enhance the efficiency of the opinion-based framework mentioned in Section 2.4. The main focus lies in obtaining a higher degree of collective accuracy regardless of the environmental structure. Overall, the proposed decision-making mechanism h from Equation 5.26 is tightly bound with the learning mechanism l from Equation 5.25. In this regard, the second objective is to analyse the impact of the learning type on the performance of decision-making in general. For this, *collective*, *social* and *individual* types of learning are studied coupled together with twelve belief fusion operators outlined in Section 5.3.3. Finally, the third objective is to evaluate the scalability of the proposed methodology with the increased number of options $n > 2$. For the evaluation, the metrics introduced in Section 5.4.5 are used. The description and the results of this section are based on (Bartashevich and Mostaghim, 2021).

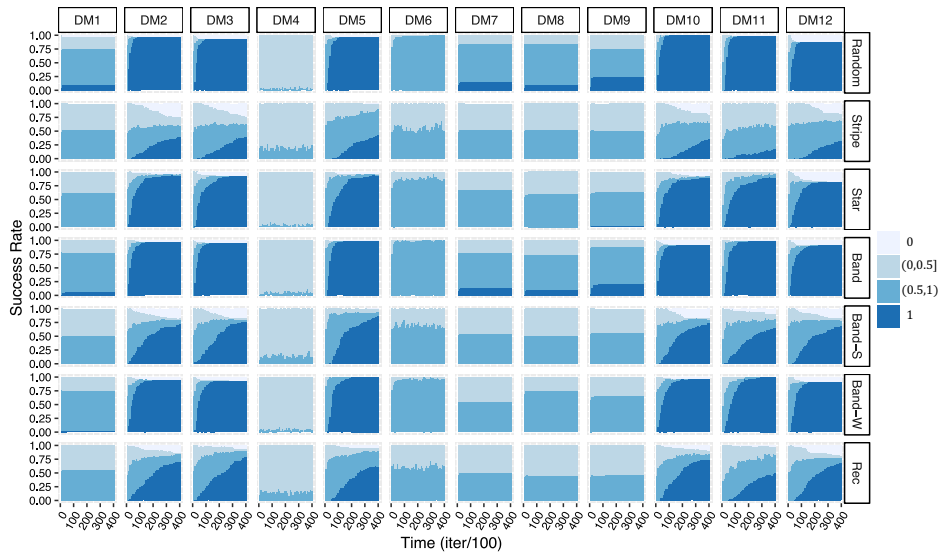
The experimental study is organised as follows. Section 5.5.1 seeks to address the first objective and provides insights on the performance of fusion operators within environments with different characteristics. Section 5.5.3 compares the performance of individual, collective and social learning in the scope of the proposed methodology, fulfilling the second objective. Section 5.5.4 investigates the impact of the population size, while Section 5.5.5 studies the question of scalability with an increase in the number of options.

5.5.1 Convergence Analysis - I

In the following, we perform the set of experiments on seven benchmarks introduced in Section 5.1.1 with $n = 3$ and $\rho = 0.67$ to evaluate the convergence of the swarm to the state of collective global “knowledge” over time for each learning type in particular and within twelve fusion rules from Section 5.3.3. For each configuration, we execute 100 trials with a maximum period of simulation time $T = 400$ s each. The duration of each single agent’s exploration state is fixed and set to $t = 10$ s along with $\delta t = 0.3$ s for each dissemination state, where 1 s is equivalent to 100 iterations, as defined in Section 2.2. While the outcomes and performance analysis for all three learning types (collective, social, and individual learning) are considered in the studies below, the primary purpose of this section is to evaluate how fusion rules from Section 5.3.3 operate in the context of the decentralised collective perception framework across the variety of environments, and to identify which rules are more successful and general than the others.



(a) Average belief over time



(b) Success rate over time

Figure 5.3: The results for collective learning in the population of $N = 20$ agents for $\rho = 0.67$ and $n = 3$ (statistics of 100 runs). Samples of the corresponding patterns are illustrated in (a) on the right.

Collective Learning

Figure 5.3a shows the mean *average population belief* over time T along with standard deviation of twelve fusion rules (by columns, denoted as DM1,...,DM12, where the index number corresponds to the rule mentioned in the same order as in Section 5.3.3) on seven environmental patterns (by rows) using **collective learning** mechanism l from

Equation 5.28.

DM1 and DM7-DM9 exhibit similar trends and are characterised by fast convergence to stable performance independent of the considered pattern. Although, for “*Stripe*”, “*Band-S*”, and “*Rec*”, the population ends up in the uncertain state (i.e., average belief of 0.5) with half of the agents being more in favour of the option ω_{best} , while exactly another half feels less confident about it but without any agents with full or zero confidence (see Figure 5.3b), indicating the collective indecision on average. To note, “*Stripe*”, “*Band-S*” and “*Rec*” belong to the same group of patterns with high \mathcal{E} and MI values and thus relating to the hardest scenarios. For another pattern group, considered as the easiest one, that is, “*Random*” and “*Band*” with the non-statistical difference in MI , DM1 converges faster than DM7-DM9 and reaches the median belief of 0.7 already at the 10th iteration, staying unchangeable, while the performance of DM7-DM8 is slightly improved and stabilised at 0.75 value by the 50th iterations together with the DM9 up to 0.85 of *average belief*. There, on both patterns, DM9 has one-fourth of the population in the state of the full certainty, followed by DM7 and DM8 with around one-tenth part of the fully committed individuals and no single one with complete disbelief. While DM1 is characterised by a much lower proportion of confident agents (5–10%) and also the non-significant presence of disbelieved ones in the case of “*Random*”. In case of middle complexity scenarios, that is, the “*Star*” and the “*Band-W*”, the *average belief* performance for DM1, DM7-DM9 is higher than 0.5 on average (median values of 0.6, 0.65 for DM1,7 and 0.6 for DM8-9 in case of “*Star*”, and 0.65, 0.55, 0.65, 0.6 for DM1, DM7-DM9, respectively, in the case of “*Band-W*”). The results on these patterns are similar to the ones on the hardest group of scenarios, as there are no agents with either complete disbelief or complete certainty that ω_{best} is the true state of the world.

DM6 is characterised by a similar convergence trend across the patterns. However, in comparison to DM1 and DM7-9, it does not converge to a certain value but more oscillates around it. In particular, in case of “*Random*” and “*Band*”, its *average population belief* median values are around 0.91 and 0.893 respectively, along with 100% of the population holding the beliefs in the range of (0.5,1). Although, there are no individuals observed with full confidence as well as full disbelief. This indicates that the whole population is much more confident in ω_{best} than in other options. The latter was not the case for DM1,7-9, where the quarter of the agents was characterised by complete disbelief in ω_{best} . DM6 on “*Random*” is marked by a small standard deviation at the end of the time T , indicating almost full convergence with median *average population belief* value of 0.91, significantly outperforming DM1. However, on “*Stripe*”, “*Band-S*” and “*Rec*”, DM6 is not superior to DM1,7-9 and its *average population belief* oscillates around median value of 0.5 with 50–50% ratio of hesitant individuals, that is, those with beliefs in the ranges of (0,0.5] and (0.5,1), respectively (see Figure 5.3b). While, on “*Star*” and “*Band-W*”, DM6 statistically significantly outperforms DM1,7-9 with 0.789 and 0.825 median average population beliefs and 90–100% of the population inclined towards ω_{best} .

DM4, as expected, is characterised by the lack of convergence towards certainty with low *average population belief* median values around 0.3–0.4 and the prevailing majority of highly uncertain agents with levels of confidence below 0.5, regardless of the considered pattern type. Such a result is also consistent with the one from previous studies (Crosscombe *et al.*, 2019) and corresponds to the worst performance among all

the considered combination rules.

The rest fusion rules DM2-3, DM5, and DM10-12 stands apart from the aforementioned ones and is considered as the one with more successful outcomes in general. The median values of *average population belief* of DM2-3,5,10-12 correspond to 1 and are not statistically significantly different between each other according to the two-sided pairwise Mann-Whitney-U test ⁵ (Mann and Whitney, 1947). However, DM10 has been shown to be the one among all twelve fusion rules which completely converges towards certainty on “*Random*” with 100% success rate over all 100 runs (see Figure 5.3b). Also, for “*Band*” (as a scenario with statistically the same *MI* as “*Random*” but higher \mathcal{E}), there is no statistically significant difference between the medians of the mentioned DMs’ *average population beliefs* values, indicating convergence to the complete certainty. Although, DM5 and DM11 are characterised by the highest success rates, i.e., 99%, among the other rules, along with DM5 being also the fastest one. The convergence speed on “*Star*” slows down significantly at the beginning for DM11 and DM12 with later levelling out again to the high performance by 100 iterations. In addition, the success rate also drops to around 90%, so not every agent is fully convinced in ω_{best} compared to above scenarios. DM12 gets stable by 300 iterations but with the highest fraction (i.e., $\frac{1}{4}th$) of the population among others with zero belief in ω_{best} . While for “*Band-W*”, DM5 and DM11 converge to a full certainty with a 100% success rate with DM5 being the fastest one as in the case of “*Band*”. However, the results for DM2-3,10,12 are not considered as statistically significantly different from DM5 and DM11 by the end of simulation time T . On “*Band-S*”, DM5 is also characterised by the fast convergence speed towards certainty with the highest median *average population belief* up to 200 iterations in comparison to the other rules. Notably, it is the only rule in the considered group with no agents in the state of full disbelief in ω_{best} by the end of time T (see Figure 5.3b). Compared to the aforementioned scenarios, the performance of DM5 and DM11 is significantly slowed down on “*Rec*”. However, DM5 attains the state of collective “knowledge” by 300 iterations with only 5% of the group being in the state of full disbelief. The same non statistically significant different results, according to the two-sided pairwise Mann-Whitney-U test ⁵ (Mann and Whitney, 1947), hold for other DMs (DM2-3,10,12) except DM11 on “*Rec*” (for DM11, the median value of *average belief* equals 0.975). However, in comparison to “*Band-S*”, here, DM2-3,10 are characterised by a lesser amount of completely disbelieved individuals and more by uncertain ones, i.e., those in the range of $(0, 0.5]$. Finally, on “*Stripe*”, DM5 is the best one among the others in both metrics, i.e., the average population belief and the population success rate. In contrast to the other rules, it shows the statistically significant results in the *average population belief* with the highest median value of 0.917 attained by the end of simulation time T . Furthermore, it demonstrates the convergence trend towards certainty almost without disbelieved agents and is characterised by half of the population in the uncertain state biased towards ω_{best} at the end of the given time T , i.e., those with beliefs in the range of $(0.5, 1]$. To shed more light on the convergence behaviour of DM5, a more detailed analysis with a prolonged simulation time T will be performed in Section 5.5.5.

⁵For more details, see supplementary material, Appendix C.

Individual Learning

As shown in Figure 5.4a, DM11 is the fastest and the best one in terms of the *average population belief* among the others, independently of the benchmark scenario. It stabilises already by the 100th iteration, converging to a certain population belief value of 0.65. On “*Band*”, DM11 achieves the highest performance (and statistically significantly different one from the others) with a median *average belief* of 0.7 by the end of the given time T , while on other benchmarks it is around 0.55–0.6. In the case of “*Stripe*”, “*Rec*” and “*Band-S*” (the hardest group of scenarios), the performance of almost all fusion rules (except DM4 and DM6) is statistically significantly the same and mainly converges to the median *average population belief* value of 0.5–0.55, indicating the high level of uncertainty in a swarm. As in the case of collective learning, DM4 shows the worst performance on all considered patterns with the population of uncertain agents with beliefs in the range of (0,0.5] and around 0.2–0.4 median population belief on average. In contrast, DM6 is described by the majority of agents biased towards ω_{best} with beliefs in the range of (0.5,1). That is, except “*Stripe*” and “*Rec*”, on most of the patterns DM6 is characterised by 50% of the agents with beliefs in the range of (0.5,1) and by 100% on “*Random*” and “*Band*”. Besides, on “*Random*”, DM6 indicates the highest and the best performance along with DM11 (DM11 is non statistically significantly different from DM6 by the end of the time T). In general, despite a considered fusion rule or a scenario, with this type of learning there are no extreme individuals observed, that is, either being fully certain or fully disbelieved in ω_{best} .

Social Learning

The results for social learning mechanism in Figure 5.5 resemble the ones for collective learning in Figure 5.4. The performance of DM1 and DM7-9 in case of Equation 5.29 remains similar as in the case of collective learning (Equation 5.28) and is characterised by high collective uncertainty levels with half of the population’s beliefs in the range of (0,0.5] and another half — (0.5,1). The same holds for SL-DM4 and SL-DM6, which are keeping the same trends as in the collective case and both lack the convergence towards certainty. A significant difference is observed for DM12, which in the case of social learning has statistically significantly deteriorated in the performance. In comparison to CL, SL-DM12 lacks individuals fully converged to either 1 or 0 beliefs and mainly consists of the agents in the uncertain states with beliefs in the range of (0.5,1). This leads to unreliable results with median *average population belief* values around 0.7–0.8 on all patterns under consideration. However, for SL-DM2-3, SL-DM5 and SL-DM10-11, the amount of agents in the state of complete disbelief has been reduced. On “*Random*” and “*Band-W*”, SL-DM2, SL-DM5 and SL-DM11 converge to fully certainty with 100% population success rate. In comparison to CL, SL-DM3 on “*Random*” and “*Band-W*” indicates a similar speed of convergence but higher reliability with almost 100% success rate, whereas DM10 keeps statistically significantly the same performance as in CL. Additionally, on “*Band*”, DM5,10-11 are characterised by convergence towards certainty with 100% population of individuals in the state of full certitude on average. In general, SL-DM2 and SL-DM3 display more trustworthy swarms than their collective counterparts. On “*Star*”, DM3 and DM10 have a performance rate of approximately 100% of the population in the state of certainty, while their median average population belief values

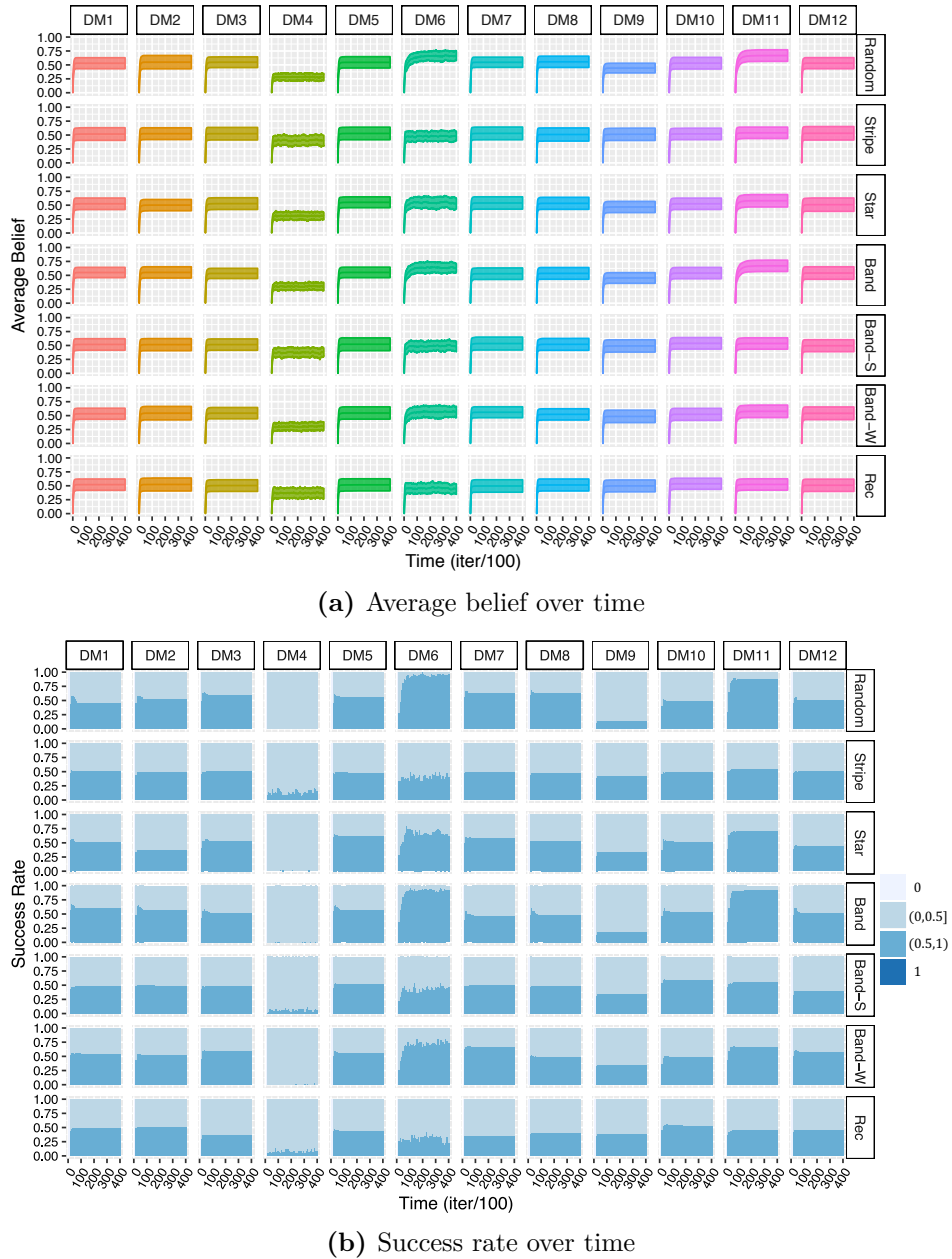
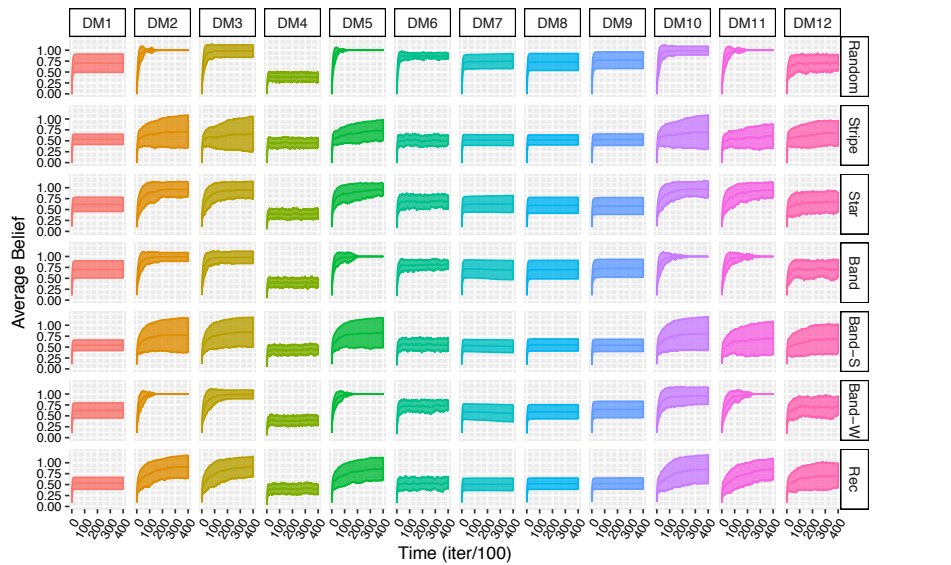
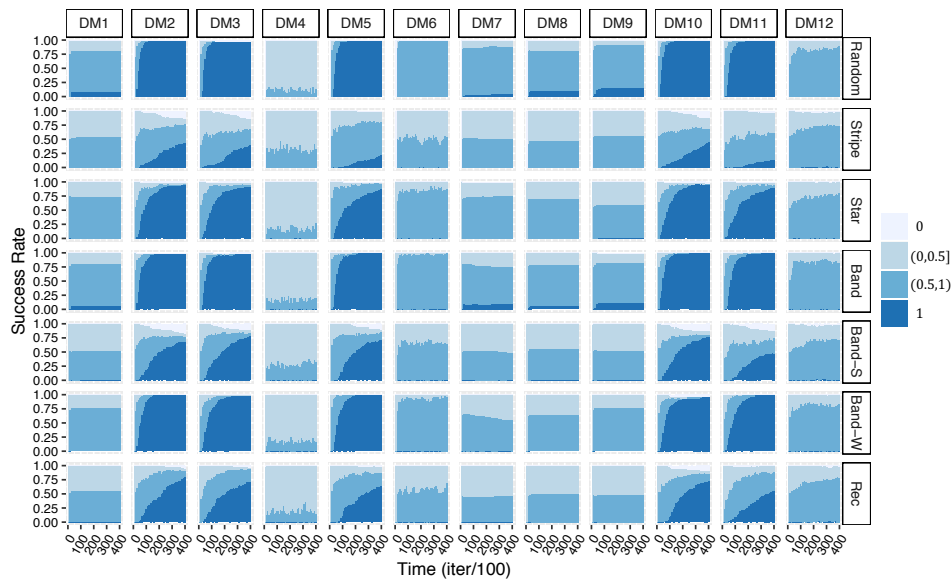


Figure 5.4: The results for individual learning in the population of $N = 20$ agents for $\rho = 0.67$ and $n = 3$ (statistics of 100 runs).

remain statistically significantly the same as in the case of CL. On the hardest scenarios, that is, “*Band-S*”, “*Rec*” and “*Stripe*”, there is no statistically significant difference in performance between DM2-3, DM5 and DM10. These fusion rules are characterised by similar convergence trends in the average population belief but with a decreased amount of fully disbelieved agents (almost in 2 times) by the end of the given time T in comparison to CL. Nevertheless, the performance of SL-DM5 has significantly deteriorated compared to its CL outcomes, where it was statistically significantly the best one among



(a) Average belief over time



(b) Success rate over time

Figure 5.5: The results for social learning in the population of $N = 20$ agents for $\rho = 0.67$ and $n = 3$ (statistics of 100 runs).

the others with a clear trend towards certainty.

Discussion

Independent of the type of learning, certain fusion rules can be grouped according to their similar performance behaviour. That is, a group consisting of **DR**, **NCCR**, **NCA** and **DCA** (i.e., DM1 and DM7-9 respectively) does not aim to conflict minimisation by its nature. Moreover, **DR** serves as the base operator for **NCCR**, **NCA** and **DCA**,

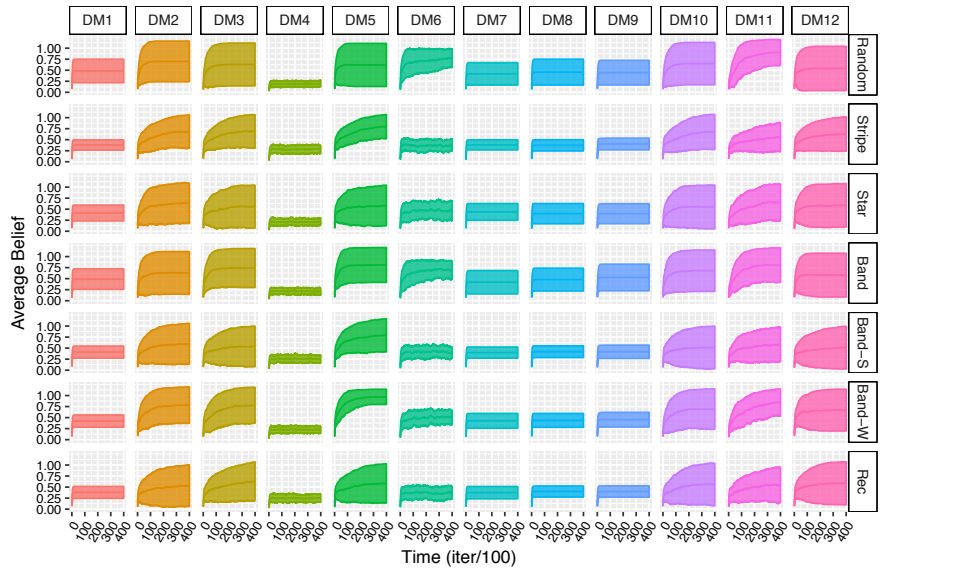
thus a similar performance is expected. Particularly, the case of high conflict ($K = 1$) is not addressed here and the combination of such pieces of evidence is not handled, that is, the corresponding mass of the agent remains unchanged. As a result, this group of combination rules reaches its stable performance (is frozen) as soon as the agents become highly conflicting with each other, lacking reliability and convergence towards certainty. It is especially crucial in scenarios with high values of MI and \mathcal{E} , which imply clustered patches of options in certain areas of the arena that result in the gathering of highly conflicting evidence by the agents. However, **MR** (DM6) is also based on **DR** but before applying **DR** operator it averages the evidence, reducing in this way certain belief's predominance and eliminating Zadeh's paradox (Shafer, 1976). This leads to a significantly better and more reliable performance in case of scenarios with scattered options (i.e., those with lower values of MI and \mathcal{E}), though remains a challenge for the clustered ones (i.e., with higher values of MI and \mathcal{E}). While averaging on its own (DM4) fully lacks convergence towards certainty independent of the environmental characteristics. Fusion rules from another performance group, that is, **DP**, **YR**, **PCR5/6**, **Flo**, **CFlo** and **MWA** (DM2-3, DM5 and DM10-12, respectively), are particularly designed to handle conflicting beliefs and, hence, better results than in aforementioned groups are expected.

Interestingly, the performance of **CFlo** (DM11) is in general (regardless of the learning type, i.e., either collective or social) more reliable than **Flo** (DM10), while both represent the same rule with the only difference that **CFlo** uses cautious counterparts. Although **CFlo** is intended for dependent sources, it still lacks reliability on the scenarios with high MI and \mathcal{E} . In case of the conflict absence ($K = 0$), **YR** (DM3) is considered as a counterpart of **DR** but as soon as the conflict appears it sums up with the full ignorance set. This improves significantly the performance in comparison to **DR**, leading to convergence towards certainty mainly on the scenarios with lower MI and \mathcal{E} parameters. While both **DP** and **Flo** (DM2 and DM10) resolve the conflict differently from **YR** (see Section 5.3.3), all three are characterised by similar convergence trend and not statistical significantly different performance. **MWA** (DM12) represents an updated DM6 based on **DR** and shows similar convergence performance as **DP**, **YR** and **Flo** (i.e., DM2-3 and DM10) but inferiors in reliability. **PCR5/6** (DM5) explicitly redistributes the conflict between involved elements and is shown to be the best rule among others, especially in the case of the scenarios with high MI and \mathcal{E} parameters values. It is the only one fusion rule among twelve considered, which on "Stripe" ($n = 3$, $\mathcal{E} = 0.993 \pm 0.026$, $MI = 0.894 \pm 0.031$) indicates a clear convergence trend towards certainty with a significant decrease of uncertain individuals, i.e., those with the beliefs in the range of $(0, 0.5]$, which in turn are predominantly moving to the category of $(0.5, 1)$ and later to a fully certain state over time.

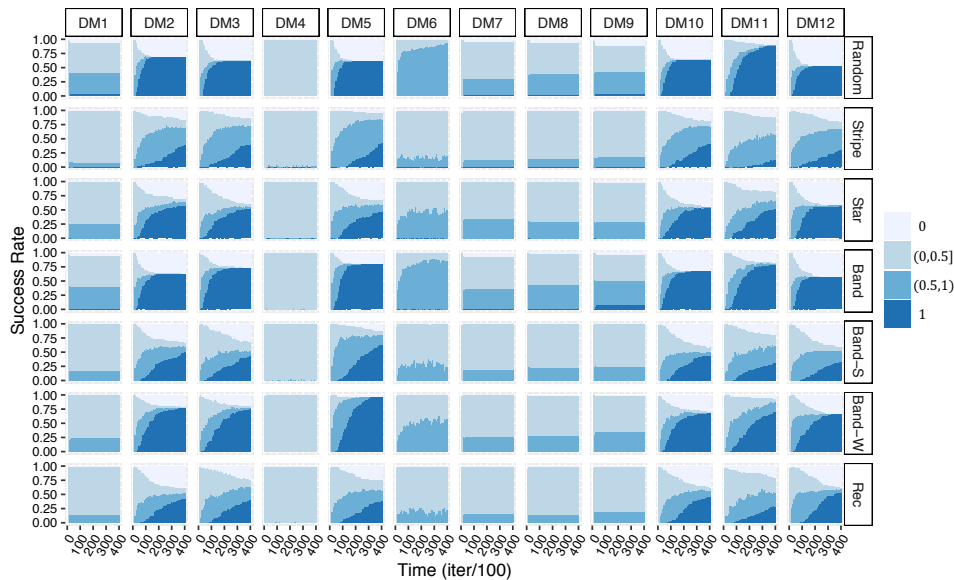
5.5.2 Convergence Analysis - II

In this section, we perform the same set of experiments as in Section 5.5.1 on the benchmarks with $n = 3$ and $\rho = 0.93$. Figures 5.6-5.8 show the results for collective, individual and social learning, respectively.

The environment with $\rho = 0.93$ is characterised by the feature vector corresponding to the almost equal ratios of the colours, i.e., $\vec{f}_\Omega = (0.295, 0.34, 0.365)$. Comparing the results of Figures 5.4-5.5 with Figures 5.6-5.8, one can observe significant deterioration



(a) Average belief over time

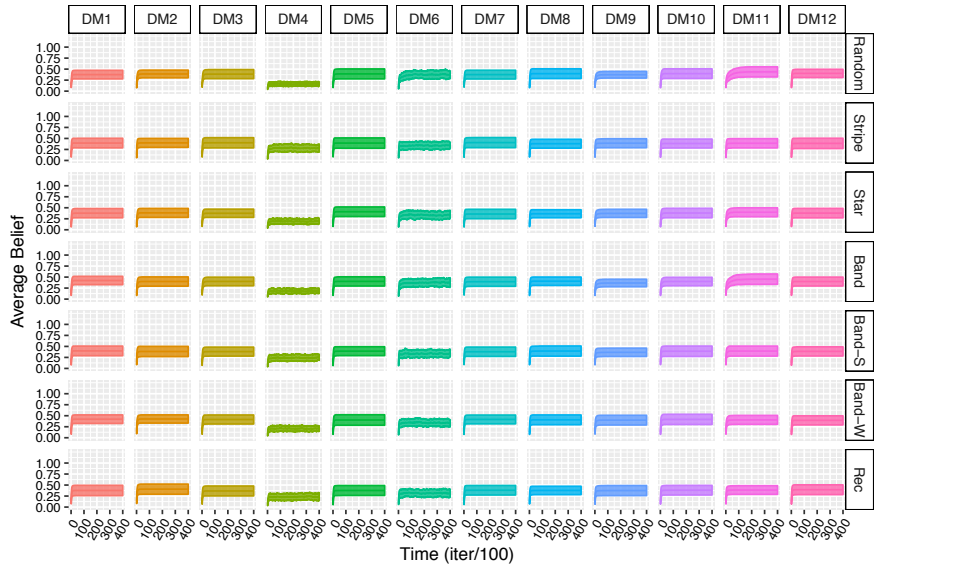


(b) Success rate over time

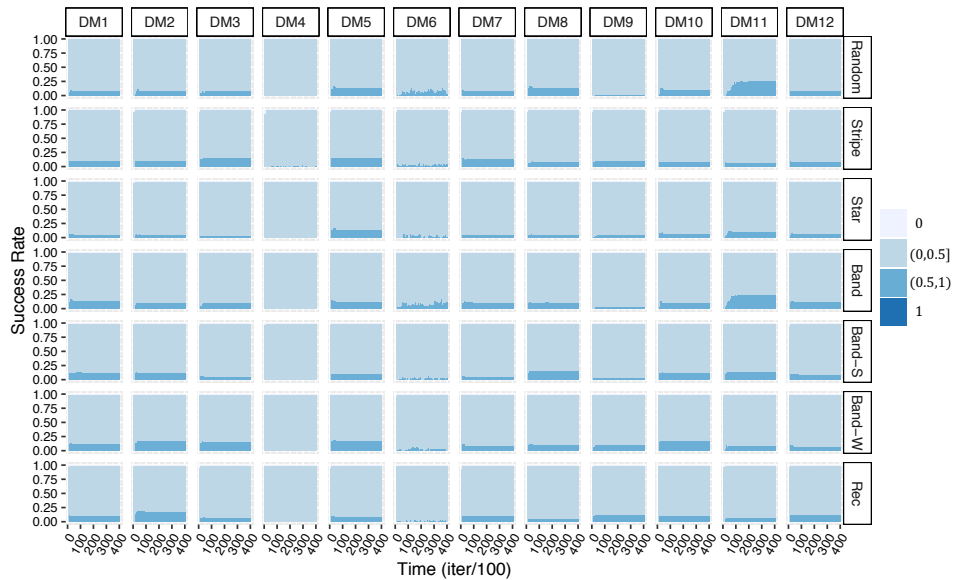
Figure 5.6: The results for collective learning in the population of $N = 20$ agents for $\rho = 0.93$ and $n = 3$ (statistics of 100 runs).

in the accuracy of the fusion rules in the latter, expressed in high standard deviation of the average population belief and increased percentage of the agents in the disbelief state. Nevertheless, the group of operators consisting of DM2-3, DM5, and DM10-12 illustrates the convergence trend towards certainty in the median average population belief for both CL and SL in the case of $\rho = 0.93$ as well.

Considering CL in Figure 5.6, on “Random”, DM11 demonstrates itself as the most reliable rule, characterised by 90% of agents in the state of complete certainty in ω_{best}



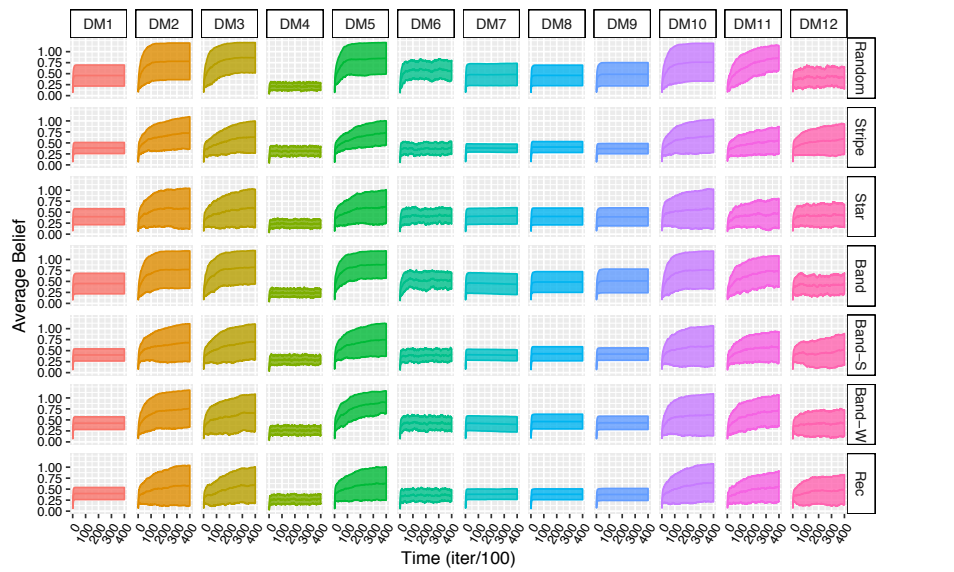
(a) Average belief over time



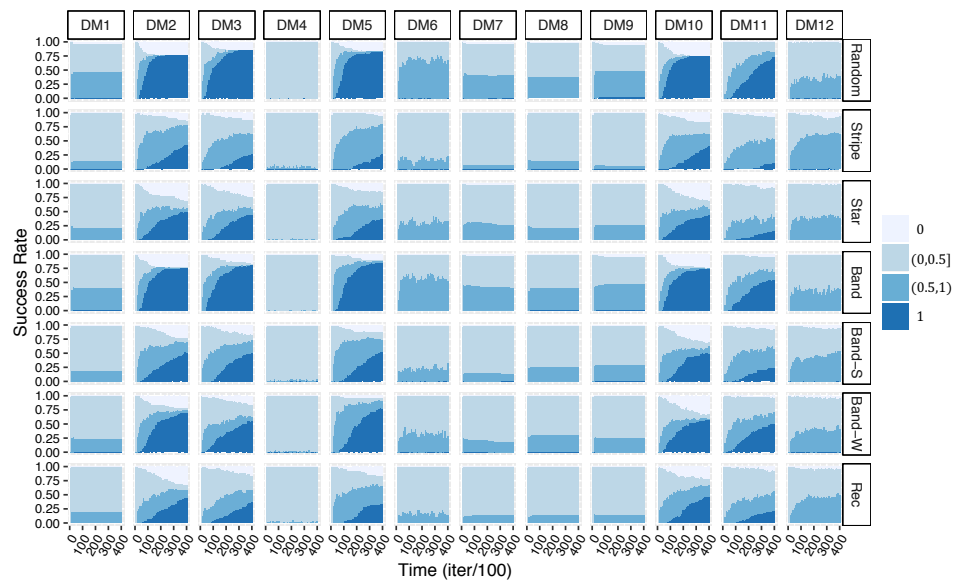
(b) Success rate over time

Figure 5.7: The results for individual learning in the population of $N = 20$ agents for $\rho = 0.93$ and $n = 3$ (statistics of 100 runs).

and the rest ones in the state of absolute disbelief by the end of the given time T . While DM2-3, DM5, DM10,12 converge to the highly polarised population already by 100–200 iterations (see Figure 5.6b). However, on most of the other patterns, excluding “*Star*” and “*Rec*”, DM5 is considered as the one with the majority part of the population in the state of certainty in comparison to the other fusion rules. Interestingly to note, on “*Stripe*”, the aforementioned group of rules is described by the more trustworthy population of agents than in the case of $\rho = 0.67$ (see Figure 5.3b). Nevertheless, CL-



(a) Average belief over time



(b) Success rate over time

Figure 5.8: The results for social learning in the population of $N = 20$ agents for $\rho = 0.93$ and $n = 3$ (statistics of 100 runs).

DM5 remains the best one among the others also in the case of $\rho = 0.93$, although with the increased amount of agents in the uncertain state, i.e., 25% of the population with beliefs in the range of $[0, 0.5]$ versus 10% in the case of $\rho = 0.67$.

The results for SL in Figure 5.8 are characterised by a significant decrease in the percentage of complete disbelievers on average compared to CL, in particular on “*Random*”, “*Band*” and “*Star*”, which belong to a similar scenario group (see Figure 5.2). On “*Stripe*”, the difference between SL-DM2, SL-DM5, and SL-DM10 in the median *aver-*

age population belief is not statistically significant, suggesting that this group of rules is better than the others. However, SL-DM5 is described by more trustworthy swarms than the other rules on the considered benchmarks, indicating its generalisability across different environments.

In the case of IND in Figure 5.7, the convergence performance for any of the considered fusion rules is statistically not significantly different between each other and mainly converges to the median *average population belief* value of 0.4 independently of the benchmark scenario, indicating the state of collective uncertainty.

Discussion

Since the number of cells with a specific colour determines the quality of the corresponding alternative $\omega_i \in \Omega$, it is expected that the proportion of the colours ρ in the benchmark setup will significantly affect the decision-making performance. Although this is supported by the findings presented in Section 5.5.2, it has been also shown that the distribution and the clustering levels of the features significantly impact the decision-making process irrespective of the ratio of the colours. The same observation was done in Chapter 4 on the binary benchmark set within the opinion-based decision-making framework. There, “*Stripe*” corresponds to the hardest pattern type with the highest levels of entropy and Moran index, causing difficulties for collective perception.

In the context of the proposed belief-based decision-making framework, according to the results of Section 5.5.1 and Section 5.5.2 for $n = 3$, **PCR5/6** has shown relative robustness in comparison to the other fusion operators across the diversity of environmental patterns, retaining comparably high collective performance. In particular, on “*Stripe*”, it is the one which is characterised by a clear convergence trend towards the state of collective “knowledge” in ω_{best} , regardless of the ratio of the colours ρ . Such a performance can be explained by the construction of the operator and how it combines the conflicting pieces of evidence (Section 5.3.3). Specifically, it redistributes the arising conflict only over the conflicting propositions proportionally to the values of their respective mass values. In the case of “*Stripe*”, the agents for the most part of the time possess highly conflicting pieces of evidence, primarily in the form of a binary mass function with full certainty in one or another option ω_i and in nothing else. That is, due to the specifics of the underlying spatial distribution of the features and the motion of the agents, the individuals observe for most of the time some certain option ω_i , which results in the environmental evidence $m_{e_k}(\omega_i) = 1$ in case if ω_i was also the opinion under consideration of an agent k or $m_{e_k}(\Omega) = 1$ otherwise. As such, the belief fusion between agents from different feature-locations of the environment is characterised by the high degree of conflict $K = 1$. In such a setting, by Theorem 1, **PCR5/6** operates as the averaging operator. As a result, the beliefs in the conflicting propositions, e.g., ω_i and ω_j , are evened out such that the agent k is set into an uncertain state regarding both of the options, that is, $m_k(\omega_i) = 0.5$ and $m_k(\omega_j) = 0.5$. Later in the decision stage, according to Equation 5.26, an agent equiprobable selects one of these options as its new opinion op_k to explore. In turn, this slows down the entire decision-making process but promotes a more thorough exploration of the most likely outcomes, leading to more accurate collective decision-making. To support this hypothesis, we perform additional experiments with **PCR5/6** in Section 5.5.5 on prolonged period of time T .

5.5.3 Comparison of Individual, Social, and Collective Learning

In this section, we perform the comparison between different learning types within the performance of twelve fusion rules by the end of the simulation time $T = 400$ s on the benchmark set with $n = 3$ and $\rho \in \{0.67, 0.93\}$. Figures 5.9-5.11 show the distribution of the *average population belief* at $T = 400$ s. across 100 trials, respectively illustrating the differences between **collective** and **social** (i), **collective** and **individual** (ii), **social** and **individual** (iii) types of learning for both $\rho = 0.67$ and $\rho = 0.93$. In the following, the results are described by the groups of the fusion operators as in previous sections.

According to Figure 5.9a, for the group consisting of DM1 and DM7-9 the overall shape and distribution of the population beliefs are similar for both CL and SL regardless of the environmental pattern. In case of DM6, CL results are more shifted towards certainty on “*Star*”, “*Band*” and “*Band-W*” (middle-difficulty scenarios). SL-DM4 is represented by a higher median average population belief than its CL counterpart, while both correspond to an uncertain state. On “*Random*” (the easiest scenario), both SL and CL variants of DM2, DM5, and DM11 are characterised by the distribution of beliefs highly concentrating around the median value, which indicates the state of collective certainty in ω_{best} . However, CL is described by more outliers on the ends of the distribution shape (skinny on the ends and wide in the middle). Similar results are demonstrated on “*Band*”, while on “*Band-W*”, DM5 and DM10-11 have identical shapes of the SL and CL belief distributions. On “*Stripe*” (the hardest scenario), DM2-3, DM10, and DM12 are described by bimodal distributions of the population beliefs with two peaks on the opposite ends, corresponding to the states of “complete certainty” and “complete disbelief” that ω_{best} is the true state of the world. The peak of “disbelief” in the case of CL is higher than the one with SL. The latter is also described by a higher median belief value, indicating its bias towards certainty. To note, DM5 (**PCR5/6**) is characterised by similar shapes of CL and SL belief distributions with a higher median value in the case of CL but with more outliers than for SL. On “*Star*”, “*Band-S*” and “*Rec*”, DM2-3, DM5, and DM10-11 have similar shapes of belief distributions with a number of outliers for both CL and SL cases.

From Figure 5.10a, one can see the largest difference in the shape of the distributions between CL and IND as well as in their median population belief values, independent of the pattern type. The median population belief difference is more apparent for the group of fusion operators such as DM2-3, DM5, and DM10-12 on all the patterns, while for DM1, DM4 and DM6-9 this is not always the case. On the hardest set of benchmark scenarios, i.e., “*Stripe*”, “*Band-S*” and “*Rec*”, the median values of the aforementioned fusion group mainly coincide for both learning types and lack convergence towards certainty. In general, IND distribution is concentrated around the 0.5 belief value despite the applied combination operator. Figure 5.11a confirms the same observation for SL and IND, indicating, in the case of DM2-3, DM5, and DM10-12, the striking difference between the two (SL and IND) distributions. While for DM1, DM4, and DM6-9, they are mainly similar on the scenarios with high \mathcal{E} and MI parameters.

According to Figure 5.9b, belief distributions for both CL and SL do not significantly differ, when there are almost equal ratios of the colours in the environment ($\rho = 0.93$). CL and SL counterparts of DM1 share similar shapes of belief distribution with the same median average population belief values, indicating the uncertainty, across the benchmarks. A similar observation holds for the operators DM6-9, with the exception

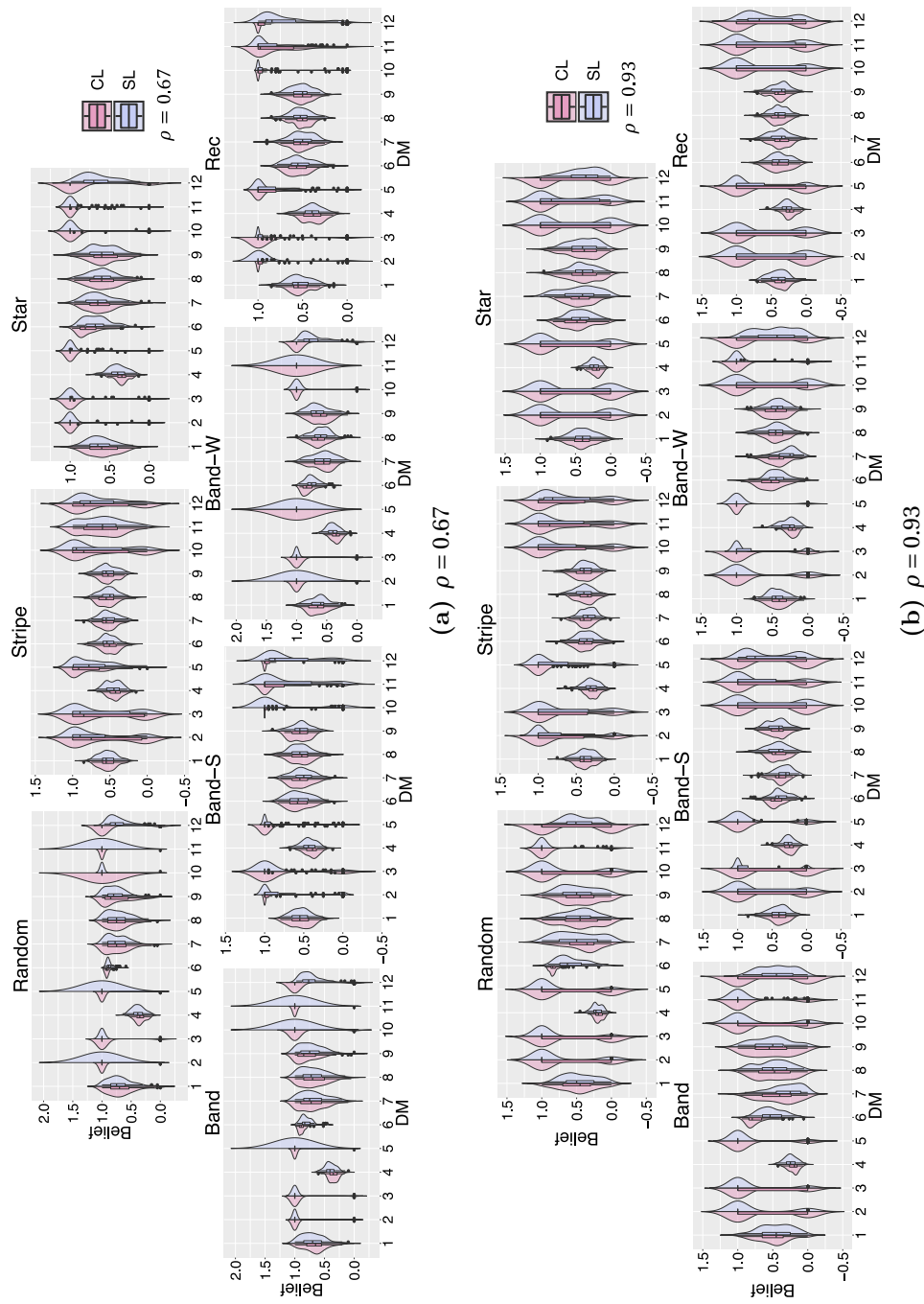


Figure 5.9: Collective vs social learning (left-pink vs right-blue). Split violin plots of the average belief in the population of $N = 20$ agents after 400 iterations over 100 runs.

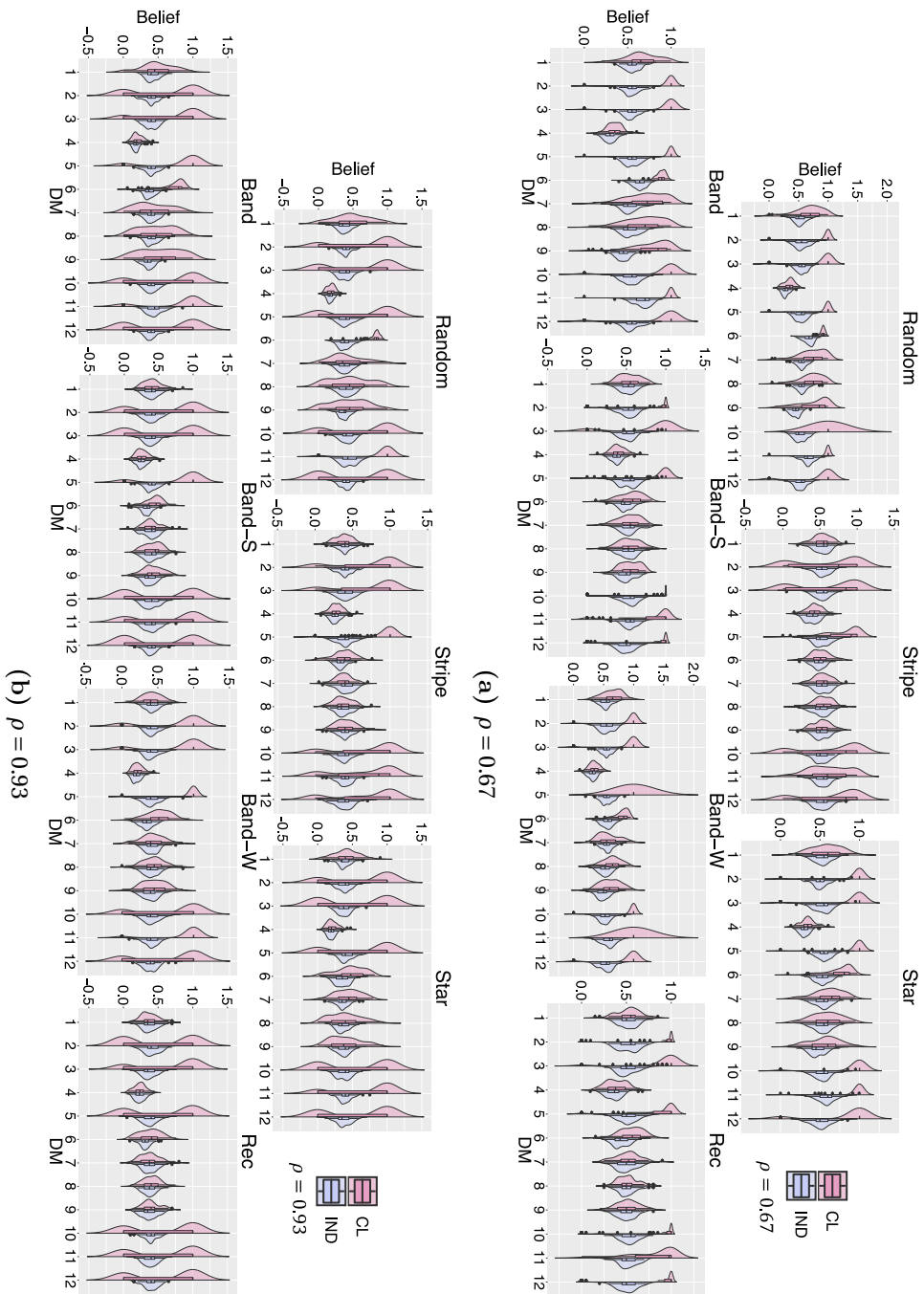


Figure 5.10: Collective vs individual learning (left-pink vs right-blue). Split violin plots of the average belief in the population of $N = 20$ agents after 400 iterations over 100 runs.

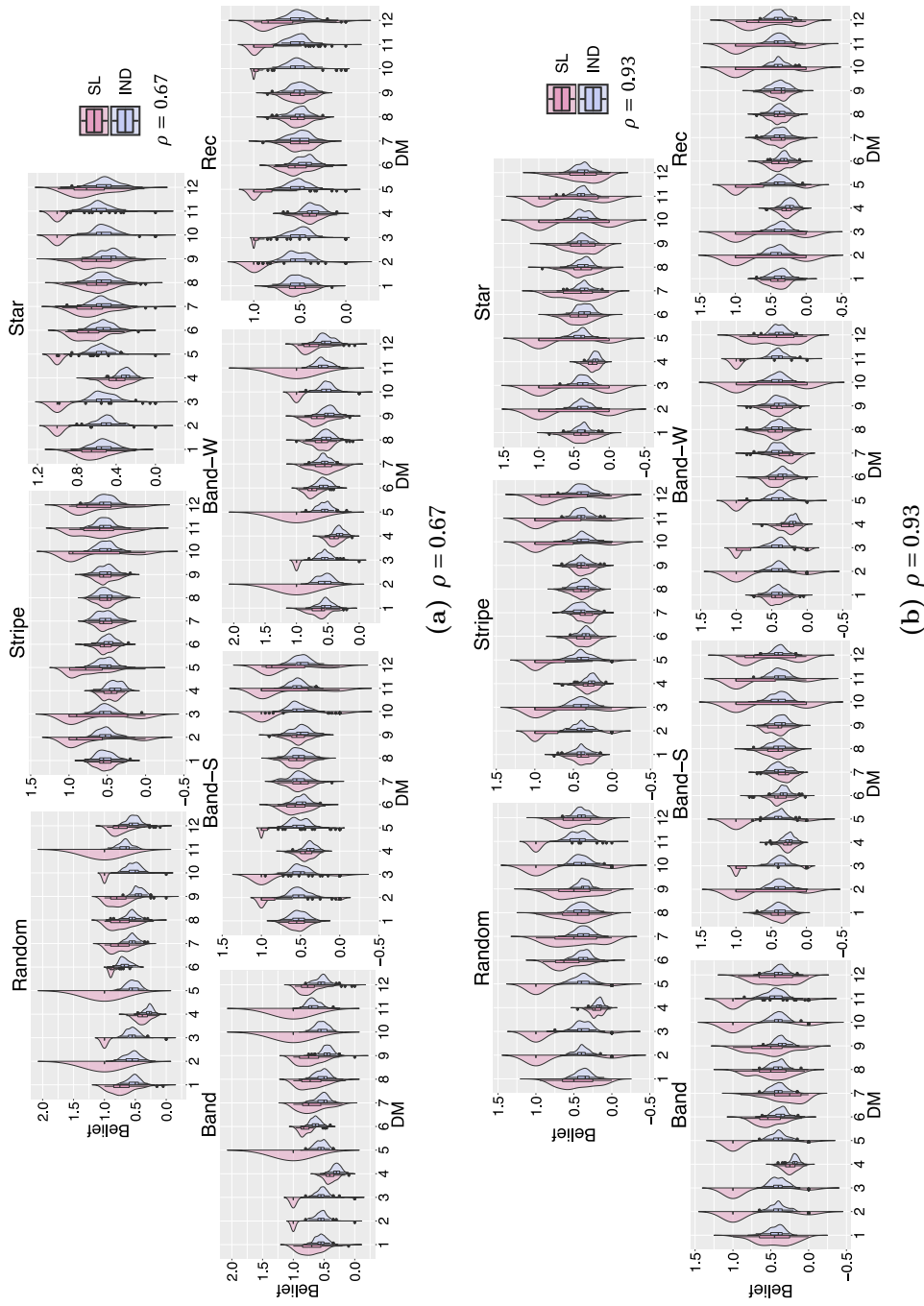


Figure 5.11: Social vs individual learning (left-pink vs right-blue). Split violin plots of the average belief in the population of $N = 20$ agents after 400 iterations over 100 runs.

for DM6 on “*Random*” and “*Band*”. There, beliefs of CL-DM6 are highly concentrated around the median, referring to the state of “complete certainty”, with the increased number of outliers compared to SL-DM6. The most difference in the results between CL and SL is observed for DM12. Except for the hardest benchmark scenarios, that is, “*Stripe*”, “*Band-S*” and “*Rec*”, SL-DM12 is described by uni-modal belief distribution concentrating around the state of uncertainty versus bimodal distribution for CL-DM12 with two peaks around the states of “complete certainty” and “complete disbelief”. While the median population belief of CL-DM12 corresponds to the collective certainty, the SL variant is characterised by a lower median on the hard scenarios, though sharing similar bimodal belief distribution as its CL counterpart. CL and SL for DM2-3, DM5, and DM10-11 also share similar bimodal distributions of the beliefs regardless of the underlying pattern in the environment. To note, CL-DM5 on “*Stripe*” is described by numerous outliers in comparison to SL-DM5, while both have the same median average population belief values and shapes of the belief distributions.

From Figure 5.10b, one can see that IND distribution is highly concentrated around the median value of 0.4, which is, in turn, lower than for the case of $\rho = 0.67$. In case of “*Stripe*”, “*Rec*”, “*Band-S*” and “*Band-W*” (hard scenarios), the shapes of IND and CL distributions coincide for the group of fusion operators such as DM1, DM4 and DM6-9. In the rest scenarios, the median belief’s values of the aforementioned rules are almost the same, while the CL shape distribution is more stretched in both directions and the IND one is more concentrated around the median. Figure 5.11b illustrates the comparison between SL and IND and holds the same relative performance as in the case of CL versus IND in Figure 5.10b.

Discussion

Individual learning alone is characterised by a highly uncertain population of agents lacking any convergence even on easy scenarios, e.g., such as “*Random*”, independently of the applied fusion rule. Nevertheless, additional consideration of the interactions between the agents together with individual updates (resulted in either **social** or **collective** types of learning) leads mainly to a significant improvement in collective performance. However, in this case, the selected combination rule and the scenario complexity have to be taken into account. Specifically, for the group of rules which is not designed for conflict minimisation, that is, DM1, DM7-9, there is no significant difference between considered types of learning (**collective vs individual** or **social vs individual**) on the scenarios with high \mathcal{E} and MI parameters. While another group of rules, that is, DM2-3, DM5 and DM10-12, is mainly able to resolve the conflict in evidence fusion with other agents independent of the type of the exchanged information, either **social** or **collective**, on all the benchmark patterns.

In general, **social** learning promotes the transfer of the information received solely from the environment between the agents, increasing in this way the rate of individual learning. Compared to individual learning, the resulting belief based on social learning is a cumulative environmental estimate of individual estimates performed by the members of the population from different parts of the environment, without requiring additional time for the agent to explore on its own. To note, the results of the experiments in this section indicate that mutual decisions based on **social** learning are more robust to outliers compared to the ones based on the **collective** learning, while both end up with

relatively high performance depending on the applied fusion operator. The reason for this can be attributed to the type of the mass functions which encode one or another type of evidence and which mass functions evolve as the result of the belief fusion due to the specifics of the underlying fusion rule. That is, in the case of SL, the agent combines its current mass m_k only with mass functions in the form of **SSF** focused on one of the options $\omega_i \in \Omega$. While in the case of CL the fusion is done between different types of mass function, which already represent the outcome of previous combinations and, therefore, can have mass values on the subsets $A_i \in 2^\Omega$, depending on the applied combination operator. The latter can lead to higher collective variability in the average population mass in ω_{best} during the decision-making process, which makes the collective result potentially more noisy than in the case of social learning.

Depending on the applied fusion rule, the results on the hardest benchmark scenario, namely, “*Stripe*”, are subdivided into two categories regardless of the learning type, that is, polarisation of the group into extreme states (either “complete certainty” or “complete disbelief” in ω_{best}) or convergence to the state of collective uncertainty. The exception is **PCR5/6**, which is described by the average population beliefs highly concentrated around the state of “complete certainty” and which is free from outliers using **social** learning. In particular, on “*Stripe*” with $\rho = 0.93$, **PCR5/6** is characterised by the numerous amount of outliers based on the collective learning compared to a social one, which remains reliable, maintaining high collective accuracy given almost equal qualities of the options. To note, the performance of the most successful group of fusion operators based on collective learning in the case of $\rho = 0.93$ is primarily featured by the bimodal distribution even on benchmarks with low \mathcal{E} and MI . While **PCR5/6** based on social learning holds population belief distribution condensed around the certainty state independent of the benchmark type.

5.5.4 Influence of the Population Size

In this section, we analyse the influence of the increased size of the population of agents on the collective convergence towards the state of certainty that $\omega_{best} \in \Omega$ is the true state of the world. Following the results of the previous sections, we evaluate the performance of the most successful group of fusion operators, that is, DM2-3, DM5, and DM10-12, on the easiest and the most complex benchmark scenarios, namely, “*Random*” and “*Stripe*”, both with $\rho = 0.67$.

Figure 5.12 shows the average population belief in $\omega_{best} \in \Omega$ (top) and the population success rate (bottom) averaged across 100 runs for the population of $N = 60$ individuals based on (a) collective and (b) social learning using the aforementioned fusion operators. Given the fixed size of the environment and the scale of the agents (see Chapter 2), the total area coverage by the swarm of $N = 60$ homogeneous individuals constitutes 10.5% in contrast to 3.5% when $N = 20$. Comparing the results in Figure 5.12a and Figure 5.12b with Figure 5.4 and Figure 5.5 respectively, one can see a significant change in the performance of considered fusion operators on “*Random*” for both types of learning. In particular, all the aforementioned operators with CL on “*Random*” can reach the global state of complete certainty with the high collective accuracy (100% of the population in the state of “fully certainty”) and are described by increased convergence speed compared to previous experiments. Similar results are observed in the case of SL on “*Random*”, although SL-DM11 and SL-DM12 do not achieve the same convergence performance

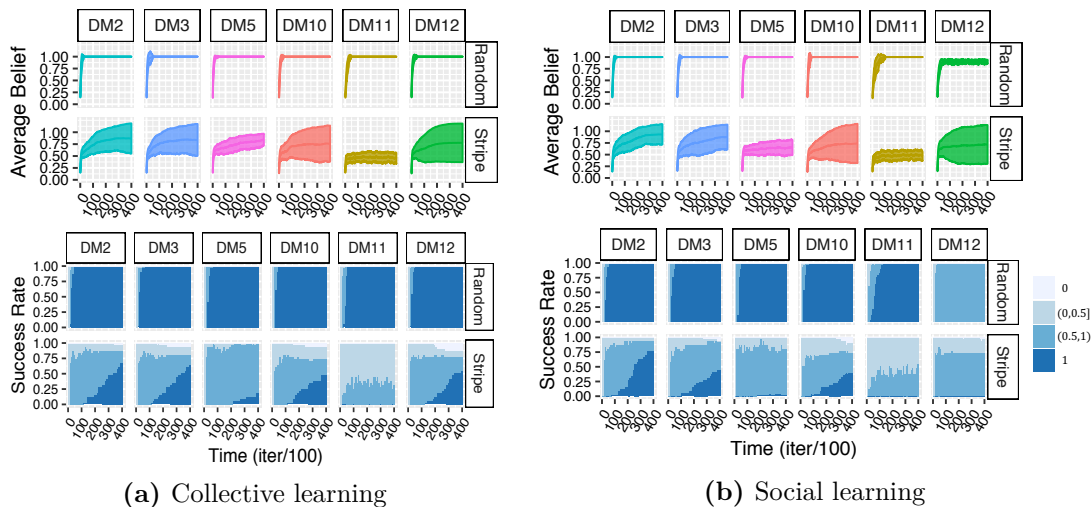


Figure 5.12: Average belief (top) and success rate (bottom) over time in the population of $N = 60$ agents for $\rho = 0.67$ and $n = 3$ (Bartashevich and Mostaghim, 2021).

as the other operators. SL-DM11 is slower than SL counterparts of DM2-3, DM5, and DM10, but still reaches the state of collective certainty, while SL-DM12 oscillates around 0.9 average population belief without any agent able to achieve the certainty state (0% of the population in the state of “fully certainty” w.r.t. population success rate). However, both SL-DM11 and SL-DM12 with $N = 60$ indicate an improvement in their performance compared to the case with $N = 20$.

With the increase of the population size, on “*Stripe*”, the collective accuracy and the average population belief in $\omega_{best} \in \Omega$ are significantly improved for DM2 and DM3, regardless of the learning type. Compared to Figure 5.4 and Figure 5.5, DM2 and DM3 in Figure 5.12 are described by the increased linear growth of the agents achieving the state of complete certainty and significantly decreased amount of the ones in the disbelief state, which result in a more robust global convergence towards certainty than with smaller population. In particular, SL-DM2 and SL-DM3 indicate better performance on “*Stripe*” than their CL counterparts, almost without agents in the state of complete disbelief. To note, DM2 significantly outperforms DM5 on “*Stripe*” with the increased population size ($N = 60$) for both types of learning, while with a smaller population ($N = 20$) DM5 was the best fusion rule among the others. That is, both CL and SL versions of DM5 are primarily characterised by the uncertain population with beliefs in the range of (0.5,1). While CL-DM5 with $N = 60$ is described by a belated transition (starting from 200 s.) of the non-significant amount of agents into a state of confidence, SL-DM5 contains almost no individuals on average in a state of certainty by the end of the whole given time T . Similarly, the performance of DM11 is significantly deteriorated with the increase of the population size for both learning types, resulting in a highly uncertain population of agents with beliefs in the range of (0,0.5]. In case of DM10 and DM12 with $N = 60$ on “*Stripe*”, the results do not significantly differ from the ones with $N = 20$. Nevertheless, both CL and SL counterparts of DM10 and DM12 are characterised by the belated though accelerated afterwards transition of the agents into extreme states, i.e., “fully certainty” and “complete disbelief” in $\omega_{best} \in \Omega$, compared to Figure 5.4 and Figure 5.5.

Specifically, the average population belief of CL-DM12 is higher in the case of $N = 60$ than the one in the case of $N = 20$, due to the transfer of agents into disbelief state only after 200 s. along with rapid linear growth of the ones in the state of certainty.

Discussion

The larger amount of individuals increases the coverage of the arena as well as the amount of collected evidence, however at the same time makes it harder for the agents to move freely through the environment without collisions with their neighbours. In addition, due to the specific collision avoidance mechanism, the agents tend to move together or in proximity to each other for a certain time after the collision is resolved, creating in this way temporary flocks. Together with the increased population size, this leads to a higher probability of the agents' interactions in a limited communication radius and, hence, to a higher rate of the incoming evidence. As a result, the agents can keep stable topological structures in their neighbourhoods for certain periods of time, resulting mainly in a *tree network topology* spanning over the whole swarm. In turn, this leads to a stabilised input from the environment and other agents scattered over the space and, thus, to a faster and less prone to uncertainties collective consensus in the unstructured environments, e.g., such as “*Random*”, than with a smaller amount of individuals. However, due to the high spatial conflict between the options in the case of environments with a particular structure, i.e., with high MI and \mathcal{E} , such as “*Stripe*”, the higher connectivity in the swarm requires more time to propagate the conflict between different areas of the environment, and respectively to resolve it, than in comparison to a sparser swarm of smaller sizes. As a result, a later appearance of the extreme beliefs (i.e., fully convinced or fully unconvinced ones) is observed in the population. In turn, this belated confidence growth leads to more robust results with a lesser amount of fully disbelieved agents and also to a faster, though a later, growth of convinced ones, depending on the way of resolving the conflict.

For social learning, due to the frequent agents' collisions and the tendency to form and move in clusters, the individuals exchange predominantly the same direct evidence perceived from the same area sources as their closest neighbours, specifically in the case of the high spatial conflict between the options. In this way, the conflict can be detected only when the corresponding agents are passing the spatial border between the options during their exploration phase, so that later they can communicate this evidence. While in collective learning, individuals exchange their cumulative beliefs, such that the conflict can be identified from experience and does not depend only on the last exploration trajectory of the agents as in social learning. As a result, SL performance on “*Stripe*” is in general characterised by slower confidence as well as disbelief growth in the population than with respective collective counterparts, resulting in a more accurate collective outcome depending on the applied fusion rule.

5.5.5 Scalability with the Increased Number of Options

In this section, based on the findings of Sections 5.5.1 and 5.5.2, we provide additional experiments to investigate in more detail the performance of the most successful fusion operator, that is, **PCR5/6** (DM5), given an extended period of simulation time $T = 2000$ s., compared to $T = 400$ s. in previous experiments. In particular, the goal of the

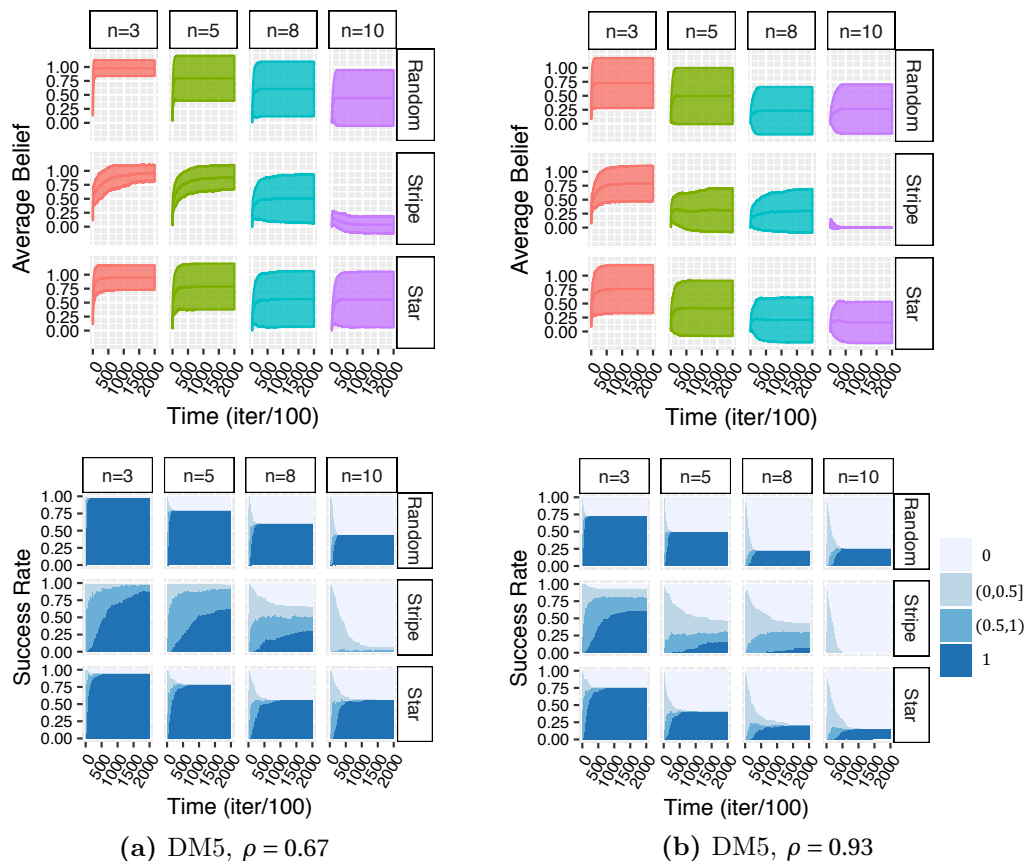


Figure 5.13: Average belief (top) and success rate (bottom) of DM5 (i.e., PCR5/6) over longer period of time (i.e., 2000 iterations) in the population of $N = 20$ agents for a variety of options $n \in \{3, 5, 8, 10\}$. Statistics of 100 runs. Learning type: collective (Bartashevich and Mostaghim, 2021).

following experiments is to evaluate the scalability of the **PCR5/6** to the larger number of options, i.e., $n \in \{3, 5, 8, 10\}$, in the context of collective learning on three benchmark scenarios representing different levels of complexity, i.e., “*Random*” (the easiest), “*Star*” (middle) and “*Stripe*” (the hardest), with $\rho \in \{0.67, 0.93\}$.

In Figure 5.13 there is a clear trend of decreasing the collective performance with increasing the number of alternatives in the environments under consideration, regardless of the options’ quality ratios ρ . The increase of the number of alternatives is primarily accompanied by the increase in the number of agents in the state of “complete disbelief” in $\omega_{best} \in \Omega$. In particular, on “*Random*” and “*Star*” ($\rho = 0.67$), the quarter of the population transfers from the state of “complete certainty” into the state of “complete disbelief” with each increment in the number of possible colours, e.g., from 3 to 5 and then from 5 to 8. This results into high standard deviation values of the average population belief on both “*Random*” and “*Star*” ($\rho = 0.67$) with $n > 3$. In general, **PCR5/6** is characterised by faster convergence to the collective steady state on “*Random*” compared to “*Star*”. That is, on both scenarios with $n \in \{8, 10\}$, the collective performance is characterised by a highly polarised population of agents in two opposing extreme states.

Whereas on “*Stripe*” ($\rho = 0.67$), **PCR5/6** is described by the absence of the individuals in the state of “complete disbelief” in $\omega_{best} \in \Omega$ up to $n = 5$ inclusively. As a result, the overall trend indicates steady convergence towards certainty. The decline in the performance is observed with $n \in \{8, 10\}$. That is, the case of “*Stripe*” ($\rho = 0.67$) with $n = 8$ is characterised by 40% of disbelieved agents along with only 25% in the state of “complete certainty” by the end of the given simulation time T . While the case of “*Stripe*” with $n = 10$ is described by the worst performance of **PCR5/6** for $\rho = 0.67$. There, the swarm completely fails to identify $\omega_{best} \in \Omega$, ending up with almost the whole population of agents in the disbelief state by the end of 2000 s.

The results on the benchmarks with $\rho = 0.93$ are in general worse than the ones with $\rho = 0.67$. According to Figure 5.13b and Figure 5.13a, one can observe a faster decline in the performance with the increase of the number of option n in the case of $\rho = 0.93$, compared to the case of $\rho = 0.67$. The performance on “*Random*” and “*Star*” for $\rho = 0.93$ and $n = 3$ resembles the one for $n = 5$ and $\rho = 0.67$, characterised by the quarter of the population in the state of “complete disbelief”, which is expanding further to more than 50% in the case of more options, creating a highly polarised population for $n \geq 5$. On “*Stripe*” ($\rho = 0.93$) with $n = 3$, **PCR5/6** gets stabilised already by 1000 s. and described by 75% of the population with beliefs biased towards certainty in $\omega_{best} \in \Omega$, i.e., in the range $(0.5, 1]$, among which 50% are in the state of “complete certainty” along with only around 5% in the state of “complete disbelief”. While for $n = 5$ the performance is already significantly deteriorated with the average population belief below the certainty level, i.e., around 50% of the population is in the disbelief state and only 25% possesses the beliefs in the range of $(0.5, 1]$ by the end of the entire given time T . The same holds for $n = 8$. For $n = 10$, the population converges four times quicker to the collective state of “complete disbelief” in contrast to the corresponding case with $\rho = 0.67$, i.e., already by 500 s. the average population belief in $\omega_{best} \in \Omega$ equals zero.

Discussion

The obtained results are consistent with previous work (Crosscombe *et al.*, 2019), where only limited scalability of the DST approach to the best-of- n problem was shown on a fully connected network of agents simulating a spatially independent site-selection scenario with direct access to the global quality of the options. Alongside this, the increase of sensibility to noise was depicted there as well with an increase of n . In the context of the current work, a considered collective perception task is specified by very high noise levels on its own. For instance, scenario “*Stripe*” with $n = 3$ and $\rho = 0.67$ is described by the following vector of global qualities of the options $\vec{q} = (0.17, 0.33, 0.5)$ (where $\sum_{i=1}^n q_i = 1$ and $\max \vec{q}$ is the best option). However, these global quality values are not accessible to the agents and can be only locally estimated based on the time the agent has observed its committed option during its last movement. Due to the spatial characteristics of “*Stripe*”, the estimates are mainly taking extreme values such as 0 and 1, when the agent has not observed the selected colour and when it has seen nothing else except it, respectively. The intermediate estimate in the range of $(0, 1)$ takes place only when the agent crosses the spatial border between the selected colour and any other one. The obtained value, in this case, is far from the corresponding option’s real global quality value q_i and is purely defined by the crossing border trajectory of the agent. As a result, especially in case of lower n , the estimated qualities by the agents

mainly contradict each other, such that one excludes another, i.e., either $q_i = 1$ or $q_j = 1$ (taking into account that $\sum_{i=1}^n q_i = 1$). In such case, i.e., when the degree of conflict $K = 1$, the resulting combination using **PCR5/6** represents the average of the beliefs, providing equal probabilities, i.e., 50%–50% chance, for both of the options ω_i and ω_j to be explored in the next exploration phase. In turn, this prevents agents from the premature convergence on a single option and gives extra time for better mixing of the population, resulting in a longer convergence time but a high success rate for up to $n = 5$, as can be observed in Figure 5.13a. Though for $n > 5$, this does not already hold due to the arising options' exploration difficulties accompanied by a higher frequency of agents' crossing the spatial borders between the options (especially on “*Stripe*”). For instance, considering $n = 8$, the communication between agents k and l with corresponding mass functions $m_k(\omega_1) = 0.67$, $m_k(\Omega) = 0.33$ and $m_l(\omega_2) = 0.45$, $m_l(\Omega) = 0.55$, results in the following combination $m_{k\oplus l}$ using **PCR5/6**, where $m_{k\oplus l}(\omega_1) = 0.5489$, $m_{k\oplus l}(\omega_2) = 0.2696$, $m_{k\oplus l}(\Omega) = 0.1815$, which is further assigned as a new $m_k := m_{k\oplus l}$ and $m_l := m_{k\oplus l}$ of the corresponding agents, subject to the fulfilment of all the necessary communication conditions. As a result, confidence in both options, ω_1 and ω_2 , is preserved but decreased accordingly to their degree of conflict. Later, combining with another more confident neighbour z , e.g., m_k with $m_z(\omega_3) = 1$, brings it up to $m_{k\oplus z}(\omega_1) = 0.1945$, $m_{k\oplus z}(\omega_2) = 0.0573$, $m_{k\oplus z}(\omega_3) = 0.7482$ (being further assigned under other conditions as a new mass for agents k and z , i.e., $m_k := m_{k\oplus z}$ and $m_z := m_{k\oplus z}$), decreasing in this way the confidence in the ω_1 and ω_2 even further but still keeping a small chance for them to be selected for the next exploration phase. Assuming that the true state of the world ω_{best} is the ω_8 , which has not been even explored yet, it would be hard for the agent k to get into corresponding exploration mode for the ω_8 and, hence, to participate in further dissemination phases. That is, as according to the current mass function m_k , the option ω_3 will be highly probable selected and there is zero chance to switch for the exploration of the ω_8 unless the agent changes its mass. In other words, after the agent leaves the environmental area of ω_3 , it will stay in the exploration phase constantly re-selecting the option to explore according to Equation 5.4 until the selected option will be correlated with the agent's current movement trajectory. Hence, until this moment, the agent will be cut off from any sources of information (either other individuals or the environment) and will stick to its old belief, which, in the case of larger n , is very unlikely to reflect the correct state of the world. Thus, the rise of unconvinced individuals in the ω_{best} is primarily observed for $n > 5$, independently of the pattern type (see Figure 5.13).

Notably, since the size of the arena remains the same, with the increasing number of options the area covered by each colour in general decreases. As a consequence, it makes it harder for the agents to enter the dissemination phase and to participate in communication, as they stay locked in an exploration state until they move into the area of their selected colour. Especially, for larger n , this point is crucial at the beginning, where the agents select randomly the option to explore. As it was observed from simulations, dependent on the initial position and choice of the option, the agent can spend a long period of time iterating over n options while it finds the one correlated with its current movement trajectory. In fact, the communication happens then only between agents which have lately observed the selected by them option (what means that this option has the highest mass value among others) and predominantly occurs between either those coming from adjacent areas with conflicting options (e.g., from

adjacent colour stripes) or from the area with the same colour. Accordingly, the agent needs always to stay up-to-date and be updated by the information from its neighbours in order to be successful in the succeeding phase, when he moves to another colour-area. For instance, the agent k with mass function $m_k(\omega_2) = 0.63$, $m_k(\Omega) = 0.37$, crossing the spatial border between ω_2 and ω_5 , connects with the corresponding agent l of $m_l(\omega_5) = 1$, so that their resulting combination $m_{k\oplus l}$ using **PCR5/6** is characterised by $m_{k\oplus l}(\omega_2) = 0.2435$, $m_{k\oplus l}(\omega_5) = 0.7656$, being assigned as a new mass function $m_k := m_{k\oplus l}$ for agent k . Here, the option ω_5 is the most likely to be selected for the next k -th exploration phase and coincides with a new current spatial area of the agent. Thus, the agent gets personal quality update with $m_e(\omega_5) = 1$, which reinforces its confidence in the ω_5 even further. Though, if the agent does not connect with any other individual from the next area (stripe section), it will miss the succeeding dissemination phases until it is back to the area with ω_5 . Therefore, lack of communication, due to the indirect influence of the agent's quality reflected in its dissemination time, leads to poor performance for $n > 5$, as can be observed from Figure 5.13.

5.6 Summary and Discussion

In this chapter, we have proposed a belief-based decision-making framework to model the collective decision process in the context of the collective perception scenario as the best-of- n problem with $n > 2$ options. The main focus was to overcome the potential sample bias induced by the unknown environment through resolving the local conflicts at the level of individuals. For this purpose, we explored the application of evidence theory (or DST) to model the decision-making of the agents. In particular, we compared the performance of the twelve most common belief fusion operators with regard to their robustness across seven spatial patterns in the collective perception scenario as a distributed consensus achievement problem. The DST has been previously applied by Crosscombe *et al.* (2019) in the context of the best-of- n problem, where the macro-level convergence properties of four belief combination operators were studied in a dynamic spatially independent multi-agent setting. The main difference between the current work presented in this chapter and the previous work is threefold: (1) in the collective perception scenario the agents cannot directly access the quality of the features, while in (Crosscombe *et al.*, 2019) the quality was directly measured like in traditional site selection problem; (2) in the previous work, the agents had access to any other agent in the population, forming a fully connected network, while in the current work the communication is subject to the agents' movements and their respective behaviour states; (3) we also consider the modulation of the positive feedback in the decision-making process.

Apart from different mental models compared to the original opinion-based decision-making framework (see Section 2.4), the proposed methodology implies that (1) the evidence from the environment is directly incorporated in the process of forming agents' mental states, that is, involving individual learning; as well as (2) the current belief of an agent (mass function m_k) is necessarily included in the aggregation of the acquired individual's information, while not all voting models take into account the current personal opinion of an agent. As such, our proposed belief-based decision-making framework operates on a dynamic random geometric graph of agents with quantitative belief assignments based on the observation time estimates of the selected options, coupled together

with *direct modulation of positive feedback*.

The research findings of this chapter confirm our hypothesis and show that the re-distribution of beliefs across unions of options allows the mechanism of collective decision-making to successfully overcome inter-individual conflicts as a result of a certain environmental structure, albeit at the expense of the consensus (convergence) speed. In this regard, **PCR5/6** fusion rule has demonstrated itself as the most successful operator among the studied ones in the collective perception task under consideration for smaller swarm size of $N = 20$. It has indicated high collective accuracy across the diverse set of benchmarks (from the ones with low \mathcal{E} and MI to the ones with respectively high values) without any additional modifications, suggesting its generality. As such, the choice of **PCR5/6** becomes advantageous before robots' placement in the scenarios, where there is no a priori information about the features' distributions to be explored. **PCR5/6** has also been noted in the DST literature as the effective tool to resolve the arising conflict during fusion of quantitative beliefs (Smarandache and Dezert, 2004a), as well as demonstrating itself worthwhile in a number of applications, such as, multisensor distributed target tracking (Kirchner *et al.*, 2007), grid occupancy estimation (Dezert *et al.*, 2015), threat assessment in decision support systems (Israel and Blasch, 2016), to name a few. However, according to our results, with an increase of the size of a swarm up to $N = 60$, the performance of **PCR5/6** tends to deteriorate. In particular, the convergence towards the collective state of full confidence is significantly slowed down. A possible explanation for this can be due to the increased frequency of communication and, hence, more accumulated information by individuals. The latter can trigger an early start of the process of conflict redistribution, which facilitates exploration and slows down exploitation. To the best of the author's knowledge, the current work is the first to study the DST fusion operators (including **PCR5/6**) to address the problem of collective perception in the context of the best-of- n framework. Additionally, the impact of the observations' frequency, i.e., time intervals between the observations, can be studied in regard to how they define quality estimates of the agents and, respectively, affect the fusion outcomes. In the current work, a high frequency of agent's observations was considered, which leads to the collection of less spatially distributed evidence, while the lower frequency of observations can be more beneficial in clustered scenarios.

Results obtained on the scenarios with the increased amount of options (i.e., $n \geq 3$) reveal the scalability of **PCR5/6** up to $n = 5$ alternatives, sustaining for $n = 5$ about 75% of the agents in the state of "complete certainty" on the easiest and the middle difficulty benchmarks. On the hardest one, i.e., "*Stripe*", around 90% of the population was skewed towards $\omega_{best} \in \Omega$, among which 62% of the individuals were absolutely convinced in its truth. The reason for the decline in the performance for $n > 5$ can lie in the manifestation of the ineffectiveness of the *positive feedback* mechanism due to the reduced coverage of the area by the features of a certain colour. This results in a lesser likelihood to reach the propagation process by the agent that strongly depends on its initial location and, hence, leading to a reduced number of encounters with the others. As a result, the agent remains stuck with its first evidence update unless it enters again the initial area. In this regard, more effective task allocation mechanisms are required to explore a larger space of options. As another possibility, in the case of **PCR5/6**, a larger set of options can be split into smaller subsets of the size up to $n = 5$, due to its shown reliability on the scenarios with up to five options. By doing so, one can also

prevent the growth of computational complexity with the increasing size of the frame of discernment for a larger number of options n , which is one of the main restrictions of the applying of **PCR5/6** in the real-world applications (Scholte and Norden, 2009).

Noteworthy, with the increase of the number of options, especially on “*Stripe*”, the agents have a tendency to converge on the second-best alternative, resulting in a sub-optimal collective decisions. There, large patches of the same features require longer exploration times along with more energy consumption of the agents. Since the feature’s prevalence is taken as the corresponding option’s quality, the time required to sample the respective alternative can be defined as its associative cost. As such, spatial correlations of the colours can make one options be harder for exploration than the others, i.e., demanding longer exploration times. This can in turn create a negative bias in the collective decision-making process, depending on the quality of the option. The latter is supported by the observed cost-quality trade-off in the results of **PCR5/6** in Section 5.5.5, indicating longer convergence time on the scenarios with clustered features, despite the ratio complexity ρ and the options’ number n .

The impact of learning as the mechanism of “sharing with the others” on the decision-making process has been also investigated, comparing *collective*, *social* and *individual* types of information sharing within the proposed methodology. The obtained results provide the evidence that transfer of the pure (albeit rather noisy) information sampled from the environment (considered as a social way of learning) leads to comparable and even more robust outcomes to those obtained by sharing the full cumulative knowledge of the agents (collective way of learning). That is, *social* learning has demonstrated robustness and effectiveness over a *collective* one, while both confirm the superiority to the solo *individual* accumulation of information. The latter is in the agreement with the findings of other works (Lee *et al.* (2018b); Crosscombe *et al.* (2019), to name a few), while the former has not been studied so far in previous studies to the best of the author’s knowledge.

Social learning implies the broadcast of the information sampled by the individuals directly from the environment, while collective learning means the broadcasting of the entire accumulated knowledge attained by the agent over time from different information sources (i.e., environment, other agents) and retained in the agent’s personal mass function. As such, the evidence obtained by the agent from the environment can be communicated to the other agent as a single value (i.e., $q_i \in \mathbb{R}$ of an option ω_i , $i = 1 \dots n$) in comparison to the whole vector of mass values in the case of the agent’s mass function. The former makes social learning to be more appealing to the application in a robotic system due to the less chance of potential communication delays compared to collective learning. Moreover, the combinations of *simple support functions* (i.e., mass function representation in the case of social learning) are in general performed faster than of the other mass function’s types (Barnett, 2008), giving another advantage to the deployment of social learning in the real-time distributed robotics systems. However, due to the increased rate of the perceptions directly from the environment in social learning, one should also maintain the sufficient mingling of the population to prevent the accumulation of overly repeating pieces of evidence. The latter is supported by the deterioration of the social learning output for the population coverage ratio of 1 : 10 relative to the size of the environment (see Section 5.5.4).

Overall, the results of this chapter indicate the viability and generalisability of the

proposed belief-based decision-making framework to tackle spatial correlations of the features, without modifications of the low-level controller of the individuals (e.g., their movements).

Conclusion

One of the key components of collective cognition is the processing of a large number of local observations, which allows a collective to identify an environmental or social state more accurately than a single individual (Sasaki and Pratt, 2018). In this regard, decision-making as a group cognitive ability is determined by individual behavioural rules that operate on incomplete information assessed through local interactions with others and physical surroundings. As such, one of the challenges in the design of an artificial cognitive system is determining how to aggregate this information and which individual decision-making rules to apply. While these rules are usually referred to as “simple” in the literature on self-organisation (Jeanson *et al.*, 2012), this is rarely the case for the underlying cognitive mechanisms inside an individual that enable them. Indeed, biological systems often rely on simple heuristics such as the mechanism of positive feedback for sharing information and achieving consensus on a single option. However, the performance of such heuristics highly depends on the environmental context.

In this thesis, we have argued that by considering individuals as cognitive entities with multiple personal mental states, one can design generic individual decision-making rules that provide collective accuracy across a variety of environments. To this end, we have introduced *preferences* and *beliefs* along with opinions into the decision-making process and studied the proposed models in a multi-agent setting on the collective perception scenario. In the following, we summarise the corresponding contributions presented in this dissertation and suggest future directions of the research.

6.1 Research Contributions

In this dissertation, we have developed individual decision-making rules which enable more accurate and robust collective decisions across various environments than existing opinion-based decision-making strategies within the best-of- n framework. The main focus lied on the generalisability across different environmental structures (patterns) and scalability for a larger number of options $n > 2$. In this instance, the structure of the *physical environment* can impose bias into the collective system. This is expressed in the corresponding bias in *social space* as some opinions prevail over others due to the particular spatial distribution of the options and, hence, bias the decision-making process. Therefore, in order to improve the performance of collective decision-making

algorithms, our first goal was to understand how *social* and *physical environments* can affect the opinion-based decision-making strategies.

In Chapter 3, we studied the bias in the *social environment* given by preferences. For this purpose, we have proposed a decision-making model based on the Ising model from statistical mechanics that generalises both the majority rule and the voter model, which are referred to as the state-of-the-art opinion-based decision-making strategies. There, setting up the nonlinearity parameter of the model, one can obtain a variety of voting behaviours ranging from the voter to the majority rule. To introduce the bias into the social system, we endowed agents with *preferences* and incorporated them into our Ising-based decision model by following the concepts of social impact theory. Thus, we developed a preference-based decision-making strategy that takes into account the opinions of others in terms of the individual's personal preferences. Simulation experiments have shown that by assigning a global preference, a designer can guide the autonomous collective system towards a particular outcome. In this regard, the consensus speed can serve as an indicator of the successful assignment (i.e., most likely matching the best option) in the case of two alternatives, especially if they are of close quality. Furthermore, we also introduced a mechanism of online preference adaptation such that preferences can co-evolve together with opinions. The latter was inspired by the cognitive dissonance theory of Festinger (1957) according to which an individual is self-driven to reduce the inconsistency between its cognitive representations, which, in our case, are expressed by opinions and preferences. The results on the binary collective perception scenario indicate that such an adaptive strategy takes the best of both, being as fast as the majority and as accurate as the voter model, even on the scenario with close-quality options. Therefore, we confirmed our hypothesis that intrinsic motivation can manipulate social biases and lead to more accurate and faster collective decisions by altering preference dynamics.

To study the bias imposed by the *physical environment*, the collective perception scenario as the best-of-2 problem has been examined in Chapter 4 for benchmarking and generalisability across different distributions of the features (options). For this purpose, we proposed and analysed nine environmental patterns taken from the matrix visualisation literature as scenarios of collective perception task besides commonly used random distribution of the colours. Simulation experiments on a diverse set of problems have shown that the real task difficulty lies not only in the quantity ratio of the features, but also in their distributions and the clustering levels. Two metrics based on the *entropy* and *Moran index* were proposed to characterise a new measure of the difficulty. The experiments with three state-of-the-art collective decision-making mechanisms (majority rule, voter model, and direct comparison) supported their validity. As such, spatial correlations of the features have demonstrated to define the cost of the options with respect to the system driven by the mechanism of positive feedback. That is, similar to the environmental bias imposed by the distance from the site to the nest in the site selection scenarios, spatial patterns induce sample bias into the distributed collective perception system. In this regard, we also analysed how environmental transformations can affect the collective decision-making without modifying the individual decision-making rule. The focus lied on the application of a special kind of equivalence relation, namely isomorphism, to the environment. It introduces local changes in the scene, keeping the global information as well as the relationships between the features in space, i.e., the

global structure of the environment. The results on nine patterns showed that with the help of isomorphism, one can manipulate the physical environment without changing its combinatorial structure and improve the speed and accuracy of collective decisions. The latter is associated with a decrease in the complexity of the problem in terms of introduced metrics and, hence, in the options' costs due to the spatial transformation of the patterns and, thereby, modulation of positive feedback.

Our second goal was to design generic individual decision-making rules for collective decision-making that can be robust across different environmental patterns and a number of options ($n > 2$). To the extent that agents holding preferences can manipulate social bias and, hence, collective decisions (as in Chapter 3), we have argued that sample bias imposed by the physical environment can be resolved in a social space at the level of disagreement between the agents. In Chapter 5, we developed the belief-based decision-making framework based on the Dempster–Shafer evidence theory (DST), which allows handling of uncertain and imprecise information. As such, it implies the ability to integrate evidence from multiple sources without prior knowledge of their distributions, considering not only mutually exclusive options but also the grouped ones. In this regard, we extended our benchmark set of collective perception scenarios proposed in Chapter 4 for $n > 2$ colours and conducted a comparative study of twelve fusion operators designed for one-off combinations of two independent beliefs. The latter enables agents to incorporate evidence while on the go, as soon as it is received or assessed from the social and physical surroundings, respectively. Simulation results have demonstrated that small swarms of up to 20 individuals employing evidence theory can successfully aggregate personal beliefs to collectively assess the environments with spatial correlations of the features. In particular, fusion operators designed to deal with opposing evidence have been shown to be effective in forming a trustworthy swarm, robust across a variety of spatial environmental patterns. In this context, we showed that proportional conflict redistribution of incoming evidence to unions of options allows a collective to successfully resolve conflict across clustered regions of features up to $n \leq 5$. The obtained result is the subject of the speed-accuracy trade-off, as a high level of collective accuracy is achieved at the expense of consensus time.

Using the belief-based decision-making model developed in Chapter 4, we also studied which information type is best to exchange to achieve more accurate collective decisions. For this purpose, we defined and compared three types of learning mechanisms, namely *individual*, *social* and *collective* learning, which differ in the type of communicated evidence. The results indicated the superiority of social learning over collective and individual types. In this regard, we have found out that sharing of direct evidence (albeit biased/noisy) from the physical environment (referred to as *social* learning) produces the same or more robust collective performance than sharing of the cumulative evidence of the agents (referred to as *collective* learning). The variability mainly depends on the applied fusion operator and the underlying environmental pattern. Overall, social learning can also produce less communication overhead than the collective approach, due to the exchange of only one mass (belief) value in the context of considered belief-based decision-making, which gives it another advantage to be employed in the distributed real robotic system. Although individual learning has demonstrated itself as the least effective, it has been shown to support the function of the direct modulation of positive feedback in both social and collective learning. That is, the agent's personal estimate

of the environment is also directly integrated into the agent’s belief (referred to as *individual* learning) and not only in the direct modulation of the positive feedback as in Chapter 3. As a result of these mechanisms’ coupling, we demonstrated that as the agent directly accumulates the evidence from physical and social environments over time, the collective can come up with more accurate decisions.

Finally, a secondary goal was to preserve the modularity of the best-of- n framework without major modifications of its design to ensure the generality of the proposed methodologies. For this purpose, we concentrated on the framework’s high-level procedures as in Figure 2.3 rather than specific low-level controllers, such as the motion of the agents. The latter, however, can impact the quality of the information assessed by individuals from the environment, especially in the presence of spatial correlations. In this regard, the question is how to aggregate the information and what to exchange to obtain a precise collective estimate. The current thesis proposes solutions to this question by mainly focusing on the design of the “Decision()” block, where an agent reconsiders its existing mental states. In particular, we demonstrated how, exclusively by means of individual decision-making mechanisms, one can obtain accurate and robust collective decisions without tweaking of the “Modulation()” block across different environmental patterns.

6.2 Limitations and Future Research Directions

The collective decision-making algorithms presented in this thesis include two behavioural phases prior to decision-making: exploration and dissemination. Their duration, i.e., the time during which an agent explores the options and then participates in the dissemination process, is defined through the modulation of positive feedback. Although the time for switching between the phases impacts the speed and accuracy of the decision-making strategy, it is highly dependent on the characteristics of the physical environment as well as on robots’ specifications. Since the environment is assumed to be a priori unknown to the designer, tuning the parameters for direct modulation and, hence, phases’ duration in advance becomes problematic. As mentioned at the end of the previous section, in the current study we did not tweak the mechanism of direct modulation of positive feedback and concentrated on the decision-making component, using default and the same modulation parameters across different environments. For instance, in the considered collective perception scenario, the exploration time is independent of the chosen option. While this is feasible in the case of the random distribution of the features, when the features are clustered, the exploration time can vary depending on the initial spatial position of an agent. In this regard, short exploration time can reduce the accuracy and the long one can lead to a low consensus speed. Future research can look towards developing adaptive timing of the phases with regard to the assessed information about the features. To that end, each agent can assess the scattering of the options and incorporate it into its quality estimate similar to how the biological systems weigh multiple criteria when deciding for the best alternative (Detrain and Deneubourg, 2002).

As part of future work, one can also seek ways to improve the performance of the proposed decision-making operators within the framework, specifically to decrease the variance in the collective performance. For instance, this can be addressed by incorporating a modulation of the *negative feedback*, which, according to Talamali *et al.* (2020),

has been shown to be effective, either alone or in combination with *positive feedback*, in reducing deviations from the target distribution in colony foraging performance.

Further studies exploring the issue of scalability for $n > 2$ options are suggested. In particular, the preference-based decision-making introduced in Chapter 3 can be extended to study the case of the best-of- n problem with $n > 2$ by considering the generalisation of the Ising model known as the Potts model (Martin, 1991). In this regard, the development of specific dynamic task allocation techniques, such as those described in (Ebert *et al.*, 2018), can assist the scalability issue for larger number of options by allowing agents to explore alternatives independently of their initial choice allocations. However, the question remains of how many options are in fact feasible in the real-world applications of collective perception scenario, additionally requiring further user studies. As one of the promising examples of such a real-world application, one can consider weed monitoring (Albani *et al.*, 2017). In addition, the validation of the developed methodologies on other application scenarios of the best-of- n problem besides collective perception is of future interest, including robotic implementations.

Considering learning mechanisms introduced in Chapter 5, as one of the possible extensions, one can investigate the balance of collective, social, and individual information while combining the evidence. For this purpose, one can consider the weighting of different types of evidence in the fusion process. So far, the collective and social learning mechanisms of the evidence update studied in the current work integrate individual estimates and those acquired from others in an equal proportion. It would be interesting to study which weightings are performing well in which environments and how they change across different feature distributions.

While the current thesis focuses on the design of high-level procedures, such as an individual decision-making mechanism, another possibility for future work is to develop adaptive movement routines for better exploration of the options. In the context of the collective perception scenario, one can consider the development of directed motion procedures based on the agent's decisions with regard to the assessment of the spatial distribution of the features. For this purpose, one can try to employ collective Levy walk (Khaluf *et al.*, 2018) or Brownian motion procedures, which allow for analytical design support (Hamann and Wörn, 2007) and, thus, can be compatible with compartmental modelling approach for the best-of- n problem as by Valentini (2017). Also, it could be interesting to examine how the propagation of information responds to different communication models in the context of the proposed methodologies.

Furthermore, the presented frameworks in the current work operate based on the assumption that the full set of possible options is given a priori. In future, the preliminary exploration process determining the alternatives can be added. In particular, the framework introduced in Chapter 5 can be modified to operate without any knowledge about the frame of discernment, which can be dynamically built up as the options discovered (Smarandache and Dezert, 2012). Such an ability to incorporate a dynamic frame fusion will make it appealing for further applications, which require constant exploration of the environment or/and characterised by dynamic changes, where options can evolve (appear or disappear) within time. While the consensus achievement in the current work is considered as reaching a state of full certainty in a particular outcome, in the future one can seek to implement individual response thresholds (Sumpter, 2006) in the belief fusion process as the stop criteria when enough evidence is found. In this way,

one can also control the responsiveness of the system to the possible dynamic changes in the environment.

Finally, in this dissertation, we have treated preferences and beliefs as independent mental states of an agent interacting separately with its opinion (see Figure 1.1). In the future, one can aim to design a generalised decision-making framework that also includes interactions between preferences and beliefs (Rouahi *et al.*, 2018) and study its implications on collective behaviour in the context of the best-of- n problem. As our findings indicate, in this regard, it is important to note that while an agent's enhanced mental capacity can lead to better and more robust collective decisions across environmental settings, it also imposes larger computational demands at the individual level.

Overall, the author hopes that the findings and insights gained in the current work can be helpful for the further development of robust collective decision-making strategies in artificial distributed cognitive systems.

List of Figures

1.1	Mental states of different confidence levels. <i>Preferences</i> represent pre-opinions and coevolve with the opinions themselves together in a closed-loop. Depending on the amount of justification, <i>beliefs</i> can pass into <i>opinions</i> or <i>knowledge</i> . Opinions, beliefs, and knowledge can be considered as <i>information</i>	7
2.1	Classification of the best-of- n problem.	16
2.2	(a) Multi-agent simulation: environment and agents, (b) Spatial distribution of 20 individuals resulting from their movements during 400 seconds: result over 1 run, (c) result over 100 runs. Pictures (a) and (c) are taken from (Bartashevich and Mostaghim, 2021).	19
2.3	General framework. Figure adapted from (Valentini, 2017).	24
3.1	Example of a two-dimensional Ising model configuration on a square lattice Λ_4 . Each spin is interacting with its neighbouring spins in the von Neumann neighbourhood (depicted in magenta colour).	32
3.2	Activation function according to Equation 3.11.	37
3.3	Consensus time ($T_N^{correct}$) and exit probability (E_N) over density ρ_{un} of unbiased individuals in the swarm for each value of the nonlinearity parameter β (top headings). Shaded areas represent the 95% confidence interval. Task difficulty: $\rho_b^* = 0.92$. Top plot is from (Bartashevich and Mostaghim, 2019b).	42
3.4	Exit probability (E_N) as a function of the task difficulty ρ_b^* . Configuration of parameters: $\rho_{un} = 0$, $\beta = 4.5$. Shaded areas represent the 95% confidence interval.	44
3.5	Consensus time ($T_N^{correct}$) as a function of the task difficulty ρ_b^* . Configuration of parameters: $\rho_{un} = 0$, $\beta = 4.5$. Shaded areas represent the 95% confidence interval.	45
3.6	Exit probability (E_N) as a function of the task difficulty ρ_b^* for the environments with the prevailing colour ‘black’ and ‘white’ on the left-hand and on the right-hand side, respectively. Shaded areas represent the 95% confidence interval.	47
3.7	Consensus time ($T_N^{correct}$) and exit probability (E_N) as a function of the initial number $E_a(0)$ of individuals with opinion a for $\rho_b^* \in \{0.52, 0.92\}$. Bottom plots: DMMD - \square , DMVD - \diamond , Static - Δ , Adaptive - \circ . Error bars indicate the standard error for the E_N , considering sample as binomial random variables.	49
3.8	Smoothed conditional means of consensus time ($T_N^{correct}$) and exit probability (E_N) as a function of the proportion of unbiased individuals in the swarm for different distance-weightings, i.e., $\{d_E^{-1}, d_E^{-2}\}$. The notion of d_E^0 (solid line) corresponds to the non-distance-based case. Configuration of parameters: $\rho_b^* = 0.92$, $\beta = 4.5$	50
4.1	Example of two collective perception scenarios with the same colour proportions $\rho = 0.92$ (52% white and 48% black cells in the grids).	55

4.2	Example of different environment representations as isomorphic incidence structures (Bartashevich and Mostaghim, 2019c).	57
4.3	Binary-featured pattern samples with $\rho_b^* = 0.92$ (Bartashevich and Mostaghim, 2019a).	59
4.4	Scatter diagrams of the patterns' metrics' statistics over 100 generations "before" (left-hand side) and "after" applying isomorphism (right-hand side). The figure is adapted from (Bartashevich and Mostaghim, 2019a). The same colour of points denotes that they belong to the same pattern group. . . .	61
4.5	Consensus time ($T_N^{correct}$) and exit probability (E_N) as a function of task difficulty ρ_b^* for each pattern. Dashed (red), solid (green) and dash-dotted (blue) lines correspond to the DMVD, DMMD and DC strategies, respectively. Shaded areas represent 95% confidence interval.	63
4.6	Consensus time ($T_N^{correct}$) and exit probability (E_N) within patterns "before" (left-hand side) and "after" applying isomorphism (right-hand side) for $\rho_b^* = 0.52$. The curves over box-plots are fitted via local weighted regression. Shaded areas represent 95% confidence interval.	65
4.7	The same analysis as in Figure 4.6 but for the "task difficulty" of $\rho_b^* = 0.92$	65
4.8	The heatmaps of significance levels (denoted by asterisks * - $p < .05$, ** - $p < .01$, *** - $p < .001$) according to the Mann-Whitney U-test for the difference in the performance of the decision policies across the patterns. The lower (LT) and the upper triangular (UT) parts of the matrices correspond to the performance on the patterns "before" and "after" isomorphic changes, respectively (top row: $\rho_b^* = 0.52$; bottom row: $\rho_b^* = 0.92$). The diagonal elements demonstrate how isomorphism affects the performance of a given policy on a single pattern. Non-significant results are denoted by circles of varying sizes and colours that depict the exact p -values.	66
4.9	The heatmaps of significance levels (denoted by asterisks * - $p < .05$, ** - $p < .01$, *** - $p < .001$) according to the Mann-Whitney U-test for the difference in the performance of the decision policy with itself between the easiest and the hardest settings of ρ_b^* on each pattern. The circle indicates a statistically non-significant result.	67
4.10	The heatmaps of significance levels (denoted by asterisks * - $p < .05$, ** - $p < .01$, *** - $p < .001$) according to the Mann-Whitney U-test for the pairwise comparison in the performance of the decision policies. The lower triangular (LT) part of the matrices corresponds to the results on the given pattern "before", and the upper one - to the results "after" applying isomorphism, respectively (top row: $\rho_b^* = 0.52$; bottom row: $\rho_b^* = 0.92$). Non-significant results are denoted by circles of varying sizes and colours that depict the exact p -values.	67
5.1	Samples of the patterns for different amount of options $n = \{3,5,8,10\}$ and $\rho \in \{0.67,0.93\}$	72
5.2	Scatter diagrams of the statistics over 100 runs for patterns' characteristics. Left: $\rho = 0.67$. Right: $\rho = 0.93$	74
5.3	The results for collective learning in the population of $N = 20$ agents for $\rho = 0.67$ and $n = 3$ (statistics of 100 runs). Samples of the corresponding patterns are illustrated in (a) on the right	91

5.4	The results for individual learning in the population of $N = 20$ agents for $\rho = 0.67$ and $n = 3$ (statistics of 100 runs)	95
5.5	The results for social learning in the population of $N = 20$ agents for $\rho = 0.67$ and $n = 3$ (statistics of 100 runs)	96
5.6	The results for collective learning in the population of $N = 20$ agents for $\rho = 0.93$ and $n = 3$ (statistics of 100 runs)	98
5.7	The results for individual learning in the population of $N = 20$ agents for $\rho = 0.93$ and $n = 3$ (statistics of 100 runs)	99
5.8	The results for social learning in the population of $N = 20$ agents for $\rho = 0.93$ and $n = 3$ (statistics of 100 runs)	100
5.9	Collective vs social learning (left-pink vs right-blue). Split violin plots of the average belief in the population of $N = 20$ agents after 400 iterations over 100 runs.	103
5.10	Collective vs individual learning (left-pink vs right-blue). Split violin plots of the average belief in the population of $N = 20$ agents after 400 iterations over 100 runs.	104
5.11	Social vs individual learning (left-pink vs right-blue). Split violin plots of the average belief in the population of $N = 20$ agents after 400 iterations over 100 runs.	105
5.12	Average belief (top) and success rate (bottom) over time in the population of $N = 60$ agents for $\rho = 0.67$ and $n = 3$ (Bartashevich and Mostaghim, 2021).	108
5.13	Average belief (top) and success rate (bottom) of DM5 (i.e., PCR5/6) over longer period of time (i.e., 2000 iterations) in the population of $N = 20$ agents for a variety of options $n \in \{3, 5, 8, 10\}$. Statistics of 100 runs. Learning type: collective (Bartashevich and Mostaghim, 2021).	110
B.1	Consensus time ($T_N^{correct}$) and exit probability (E_N) as a function of the task difficulty ρ_b^* . Configuration of parameters: $\rho_{un} = 0$, $\beta = 4.5$. Maximum possible communication distance between the agents $d_{max} = 5$ units. IDW1 and IDW2 indicate the inverse distance weighting with power 1 and 2, respectively, for adaptive and static policy. Shaded areas represent the 95% confidence interval.	146
B.2	Exit probability (E_N) as a function of the task difficulty ρ_b^* . Configuration of parameters: $\rho_{un} = 0$, $\beta = 4.5$. Maximum possible communication distance between the agents – top: $d_{max} = 5$ units, bottom: $d_{max} = 10$ units. IDW1 and IDW2 indicate the inverse distance weighting with power 1 and 2, respectively, for adaptive and static policy. Shaded areas represent the 95% confidence interval.	147

List of Tables

2.1	Research design.	27
3.1	Preference initialisation of six preference-based decision-making strategies with respect to the agents' initial opinions $\sigma_z \in \{+1, -1\}$	41
5.1	Algebraic properties (by rows) of fusion operators (by columns).	86
A.1	Table of default simulation parameters for collective perception scenario.	145
C.1	Collective Learning, $\rho = 0.67$: Median belief values at different run lengths. Best performance is indicated in bold font. The results which have equal medians with the best performance (in each line) are indicated by light gray color (including the best result in bold). Statistical significance is stated by two-sided pairwise Mann-Whitney-U test with p -value < 0.05.	148
C.2	Social Learning, $\rho = 0.67$: Median belief values at different run lengths. Best performance is indicated in bold font. The results which have equal medians with the best performance (in each line) are indicated by light gray color (including the best result in bold). Statistical significance is stated by two-sided pairwise Mann-Whitney-U test with p -value < 0.05.	149
C.3	Individual Learning, $\rho = 0.67$: Median belief values at different run lengths. Best performance is indicated in bold font. The results which have equal medians with the best performance (in each line) are indicated by light gray color (including the best result in bold). Statistical significance is stated by two-sided pairwise Mann-Whitney-U test with p -value < 0.05.	150
C.4	Collective Learning, $\rho = 0.93$: Median belief values at different run lengths. Best performance is indicated in bold font. The results which have equal medians with the best performance (in each line) are indicated by light gray color (including the best result in bold). Statistical significance is stated by two-sided pairwise Mann-Whitney-U test with p -value < 0.05.	151
C.5	Social Learning, $\rho = 0.93$: Median belief values at different run lengths. Best performance is indicated in bold font. The results which have equal medians with the best performance (in each line) are indicated by light gray color (including the best result in bold). Statistical significance is stated by two-sided pairwise Mann-Whitney-U test with p -value < 0.05.	152
C.6	Individual Learning, $\rho = 0.93$: Median belief values at different run lengths. Best performance is indicated in bold font. The results which have equal medians with the best performance (in each line) are indicated by light gray color (including the best result in bold). Statistical significance is stated by two-sided pairwise Mann-Whitney-U test with p -value < 0.05.	153

C.7	Median values after 10 iterations. Best performance is indicated in bold font. The results which have equal medians with the best performance (in each line) are indicated by light gray color (including the best result in bold). Statistical significance is stated by two-sided pairwise Mann-Whitney-U test with p -value < 0.05.	154
C.8	Median values after 50 iterations. Best performance is indicated in bold font. The results which have equal medians with the best performance (in each line) are indicated by light gray color (including the best result in bold). Statistical significance is stated by two-sided pairwise Mann-Whitney-U test with p -value < 0.05.	155
C.9	Median values after 100 iterations. Best performance is indicated in bold font. The results which have equal medians with the best performance (in each line) are indicated by light gray color (including the best result in bold). Statistical significance is stated by two-sided pairwise Mann-Whitney-U test with p -value < 0.05.	156
C.10	Median values after 200 iterations. Best performance is indicated in bold font. The results which have equal medians with the best performance (in each line) are indicated by light gray color (including the best result in bold). Statistical significance is stated by two-sided pairwise Mann-Whitney-U test with p -value < 0.05.	157
C.11	Median values after 300 iterations. Best performance is indicated in bold font. The results which have equal medians with the best performance (in each line) are indicated by light gray color (including the best result in bold). Statistical significance is stated by two-sided pairwise Mann-Whitney-U test with p -value < 0.05.	158
C.12	Median values after 400 iterations. Best performance is indicated in bold font. The results which have equal medians with the best performance (in each line) are indicated by light gray color (including the best result in bold). Statistical significance is stated by two-sided pairwise Mann-Whitney-U test with p -value < 0.05.	159
C.13	CL-SL, $\rho = 0.67$: p -values at different run lengths.	160
C.14	CL-IND, $\rho = 0.67$: p -values at different run lengths.	161
C.15	SL-IND, $\rho = 0.67$: p -values at different run lengths.	162
C.16	Median values after 10 iterations. Best performance is indicated in bold font. The results which have equal medians with the best performance (in each line) are indicated by light gray color (including the best result in bold). Statistical significance is stated by two-sided pairwise Mann-Whitney-U test with p -value < 0.05.	163
C.17	Median values after 50 iterations. Best performance is indicated in bold font. The results which have equal medians with the best performance (in each line) are indicated by light gray color (including the best result in bold). Statistical significance is stated by two-sided pairwise Mann-Whitney-U test with p -value < 0.05.	164

C.18	Median values after 100 iterations. Best performance is indicated in bold font. The results which have equal medians with the best performance (in each line) are indicated by light gray color (including the best result in bold). Statistical significance is stated by two-sided pairwise Mann-Whitney-U test with p -value < 0.05.	165
C.19	Median values after 200 iterations. Best performance is indicated in bold font. The results which have equal medians with the best performance (in each line) are indicated by light gray color (including the best result in bold). Statistical significance is stated by two-sided pairwise Mann-Whitney-U test with p -value < 0.05.	166
C.20	Median values after 300 iterations. Best performance is indicated in bold font. The results which have equal medians with the best performance (in each line) are indicated by light gray color (including the best result in bold). Statistical significance is stated by two-sided pairwise Mann-Whitney-U test with p -value < 0.05.	167
C.21	Median values after 400 iterations. Best performance is indicated in bold font. The results which have equal medians with the best performance (in each line) are indicated by light gray color (including the best result in bold). Statistical significance is stated by two-sided pairwise Mann-Whitney-U test with p -value < 0.05.	168
C.22	CL-SL, $\rho = 0.93$: p-values at different run lengths.	169
C.23	CL-IND, $\rho = 0.93$: p-values at different run lengths.	170
C.24	SL-IND, $\rho = 0.93$: p-values at different run lengths.	171

List of Algorithms

3.1	Preference Dynamics (Bartashevich and Mostaghim, 2019b)	38
4.1	New isomorphic matrix	57
4.2	New non-isomorphic matrix (but with the same amount of 0s and 1s) . .	58

Bibliography

- [1] A. I. Adamatzky, “Route 20, autobahn 7, and slime mold: Approximating the longest roads in usa and germany with slime mold on 3-d terrains”, *IEEE Transactions on Cybernetics*, vol. 44, no. 1, pp. 126–136, 2014 (cited on page 2).
- [2] D. Albani, J. IJsselmuiden, R. Haken, and V. Trianni, “Monitoring and mapping with robot swarms for agricultural applications”, in *2017 14th IEEE International Conference on Advanced Video and Signal Based Surveillance (AVSS)*, 2017, pp. 1–6 (cited on page 121).
- [3] G. Amdam and A. Hovland, “Measuring animal preferences and choice behavior”, *Nature Education Knowledge*, vol. 3, p. 74, Jan. 2012 (cited on page 1).
- [4] C. M. Angst, R. Agarwal, V. Sambamurthy, and K. Kelley, “Social contagion and information technology diffusion: The adoption of electronic medical records in U.S. hospitals”, *Management Science*, vol. 56, no. 8, pp. 1219–1241, 2010 (cited on page 53).
- [5] F. A. Azevedo, L. R. Carvalho, L. T. Grinberg, J. M. Farfel, R. E. Ferretti, R. E. Leite, W. J. Filho, R. Lent, and S. Herculano-Houzel, “Equal numbers of neuronal and nonneuronal cells make the human brain an isometrically scaled-up primate brain”, *Journal of Comparative Neurology*, vol. 513, no. 5, pp. 532–541, 2009 (cited on page 2).
- [6] D. Bang and C. Frith, “Making better decisions in groups”, *Royal Society Open Science*, vol. 4, 2017 (cited on page 7).
- [7] J. A. Barnett, “Computational methods for a mathematical theory of evidence”, in *Classic Works of the Dempster-Shafer Theory of Belief Functions*. Springer Berlin Heidelberg, 2008, pp. 197–216 (cited on pages 79, 115).
- [8] P. Bartashevich and S. Mostaghim, “Benchmarking collective perception: New task difficulty metrics for collective decision-making”, in *Progress in Artificial Intelligence*, Springer, 2019, pp. 699–711 (cited on pages 13, 54, 59, 61, 62).
- [9] P. Bartashevich and S. Mostaghim, “Ising model as a switch voting mechanism in collective perception”, in *Progress in Artificial Intelligence*, Springer International Publishing, 2019, pp. 617–629 (cited on pages 13, 29, 38, 42, 129).
- [10] P. Bartashevich and S. Mostaghim, “Positive impact of isomorphic changes in the environment on collective decision-making”, in *Proceedings of the Genetic and Evolutionary Computation Conference Companion*, ser. GECCO ’19, Prague, Czech Republic: ACM, 2019, pp. 105–106 (cited on pages 13, 54, 57).
- [11] P. Bartashevich and S. Mostaghim, “Multi-featured collective perception with Evidence Theory: tackling spatial correlations”, *Swarm Intelligence*, pp. 1–28, 2021 (cited on pages 13, 19, 71, 85, 90, 108, 110).

- [12] M. Beekman and T. Latty, “Brainless but Multi-Headed: Decision Making by the Acellular Slime Mould *Physarum polycephalum*”, *Journal of Molecular Biology*, vol. 427, no. 23, pp. 3734–3743, 2015 (cited on page 2).
- [13] M. Behrisch, B. Bach, N. Henry R., T. Schreck, and J.-D. Fekete, “Matrix re-ordering methods for table and network visualization”, *Comput. Graph. Forum*, vol. 35, no. 3, pp. 693–716, 2016 (cited on page 58).
- [14] M. Behrisch, B. Bach, M. Hund, M. Delz, and et al., “Magnostics: Image-based search of interesting matrix views for guided network exploration”, *IEEE Transactions on Visualization & Computer Graphics*, vol. 23, no. 1, pp. 31–40, 2017 (cited on page 58).
- [15] M. Behrisch, M. Blumenschein, N. W. Kim, L. Shao, M. El-Assady, J. Fuchs, D. Seebacher, A. Diehl, U. Brandes, H. Pfister, T. Schreck, D. Weiskopf, and D. A. Keim, “Quality metrics for information visualization”, *Computer Graphics Forum*, vol. 37, no. 3, pp. 625–662, 2018 (cited on page 58).
- [16] A. M. Berdahl, A. B. Kao, A. Flack, P. A. H. Westley, E. A. Codling, I. D. Couzin, A. I. Dell, and D. Biro, “Collective animal navigation and migratory culture: From theoretical models to empirical evidence”, *Philosophical transactions of the Royal Society of London. Series B, Biological sciences*, vol. 373, 2018 (cited on pages 8, 23).
- [17] A. Berdahl, C. J. Torney, C. C. Ioannou, J. J. Faria, and I. D. Couzin, “Emergent sensing of complex environments by mobile animal groups.”, *Science*, 2013 (cited on page 31).
- [18] T. Beth, D. Jungnickel, and H. Lenz, *Design Theory*, 2nd ed., ser. Encyclopedia of Mathematics and its Applications. Cambridge University Press, 1999, vol. II (cited on pages 55, 56).
- [19] C. Bettstetter and C. Wagner, “The spatial node distribution of the random waypoint mobility model”, in *Mobile Ad-Hoc Netzwerke, 1. Deutscher Workshop Über Mobile Ad-Hoc Netzwerke WMAN 2002*, GI, 2002, pp. 41–58 (cited on page 19).
- [20] A. R. Bilge and H. A. Taylor, “Framing the figure: Mental rotation revisited in light of cognitive strategies”, *Memory & Cognition*, vol. 45, no. 1, pp. 63–80, 2017 (cited on page 69).
- [21] C. Bonati, “The Peierls argument for higher dimensional Ising models”, *European Journal of Physics*, vol. 35, no. 3, 2014 (cited on page 33).
- [22] V. Bonifaci, K. Mehlhorn, and G. Varma, “Physarum can compute shortest paths”, *Journal of Theoretical Biology*, vol. 309, pp. 121–133, 2012 (cited on page 2).
- [23] T. Bose, A. Reina, and J. A. Marshall, “Collective decision-making”, *Current Opinion in Behavioral Sciences*, vol. 16, pp. 30–34, 2017 (cited on page 9).
- [24] M. Brambilla, E. Ferrante, M. Birattari, and M. Dorigo, “Swarm robotics: A review from the swarm engineering perspective”, *Swarm Intelligence*, vol. 7, pp. 1–41, 2013 (cited on page 9).
- [25] A. Cahen and M. Tacca, “Linking perception and cognition”, *Frontiers in Psychology*, vol. 4, p. 144, 2013 (cited on page 17).

- [26] A. Campo, S. Garnier, O. Dédriche, M. Zekkri, and M. Dorigo, “Self-organized discrimination of resources”, *PLOS ONE*, vol. 6, no. 5, pp. 1–7, 2011 (cited on page 24).
- [27] L. Chen, L. Diao, and J. Sang, “Weighted evidence combination rule based on evidence distance and uncertainty measure: An application in fault diagnosis”, *Mathematical Problems in Engineering*, 2018 (cited on page 84).
- [28] J. R. Cody, K. A. Roundtree, and J. A. Adams, “Human-collective collaborative target selection”, *Journal on Human-Robot Interaction*, vol. 10, no. 2, 2021 (cited on page 53).
- [29] J. Cody, *Discrete Consensus Decisions in Human-collective Teams*. Vanderbilt University, 2018 (cited on page 10).
- [30] M. Colosio, A. Shestakova, V. V. Nikulin, E. Blagovechtchenski, and V. Klucharev, “Neural Mechanisms of Cognitive Dissonance (Revised): An EEG Study”, *Journal of Neuroscience*, vol. 37, no. 20, pp. 5074–5083, 2017 (cited on page 6).
- [31] J. Conlisk, “Costly optimizers versus cheap imitators”, *Journal of Economic Behavior & Organization*, vol. 1, no. 3, pp. 275–293, 1980 (cited on page 8).
- [32] L. Conrard and T. J. Roper, “Consensus decision making in animals”, *Trends in Ecology & Evolution*, vol. 20, no. 8, pp. 449–456, 2005 (cited on page 9).
- [33] J. Corcoran and I. S. Hamid, “Investigating knowledge and opinion”, in. 2015, pp. 95–126 (cited on page 6).
- [34] I. D. Couzin, “Collective animal migration”, *Current Biology*, vol. 28, no. 17, R976–R980, 2018 (cited on page 3).
- [35] I. D. Couzin, C. C. Ioannou, G. Demirel, T. Gross, C. J. Torney, A. Hartnett, L. Conrard, S. A. Levin, and N. E. Leonard, “Uninformed individuals promote democratic consensus in animal groups”, *Science*, vol. 334, pp. 1578–1580, 2011 (cited on page 22).
- [36] M. Crosscombe and J. Lawry, “A model of multi-agent consensus for vague and uncertain beliefs”, *Adaptive Behavior*, vol. 24, no. 4, pp. 249–260, 2016 (cited on page 22).
- [37] M. Crosscombe and J. Lawry, “Exploiting vagueness for multi-agent consensus”, in *Multi-agent and Complex Systems*, ser. Studies in Computational Intelligence, Springer, Singapore, 2016, pp. 67–78 (cited on page 22).
- [38] M. Crosscombe, J. Lawry, and P. Bartashevich, “Evidence propagation and consensus formation in noisy environments”, in *Scalable Uncertainty Management*, Springer, 2019, pp. 310–323 (cited on pages 22, 76, 85, 86, 92, 111, 113, 115).
- [39] M. Crosscombe, J. Lawry, S. Hauert, and M. Homer, “Robust distributed decision-making in robot swarms: Exploiting a third truth state”, in *2017 IEEE/RSJ International Conference on Intelligent Robots and Systems (IROS 2017)*, Institute of Electrical and Electronics Engineers (IEEE), 2018, pp. 4326–4332 (cited on page 22).
- [40] D. L. DeAngelis and S. G. Diaz, “Decision-making in agent-based modeling: A current review and future prospectus”, *Frontiers in Ecology and Evolution*, vol. 6, pp. 1–16, 2019 (cited on page 4).

- [41] A. P. Dempster, “Upper and lower probabilities induced by a multivalued mapping”, *The Annals of Mathematical Statistics*, vol. 38, no. 2, pp. 325–339, 1967 (cited on page 80).
- [42] T. Dencœux, “Conjunctive and disjunctive combination of belief functions induced by nondistinct bodies of evidence”, *Artificial Intelligence*, vol. 172, no. 2, pp. 234–264, 2008 (cited on pages 81, 83, 85).
- [43] C. Detrain and J.-L. Deneubourg, “Complexity of environment and parsimony of decision rules in insect societies”, *The Biological Bulletin*, vol. 202, no. 3, pp. 268–274, 2002 (cited on page 120).
- [44] J. Dezert, J. Moras, and B. Pannetier, “Environment perception using grid occupancy estimation with belief functions”, in *2015 18th International Conference on Information Fusion (Fusion)*, 2015, pp. 1070–1077 (cited on page 114).
- [45] J. Dezert, A. Tchamova, D. Han, and J. Tacnet, “Why Dempster’s fusion rule is not a generalization of Bayes fusion rule”, in *Proceedings of the 16th International Conference on Information Fusion*, 2013, pp. 1127–1134 (cited on page 80).
- [46] J.-M. Drouffe and C. Godrèche, “Phase ordering and persistence in a class of stochastic processes interpolating between the Ising and voter models”, *Journal of Physics A: Mathematical and General*, vol. 32, no. 2, pp. 249–261, 1999 (cited on page 37).
- [47] B. Ducourthial and V. Cherfaoui, “Experiments with self-stabilizing distributed data fusion”, in *2016 IEEE 35th Symposium on Reliable Distributed Systems (SRDS)*, 2016, pp. 289–296 (cited on page 83).
- [48] B. Ducourthial, V. Cherfaoui, and T. Denœux, “Self-stabilizing Distributed Data Fusion”, in *14th International Symposium on Stabilization, Safety, and Security of Distributed Systems (SSS 2012)*, ser. LNCS, vol. 7596, Toronto, Canada, 2012, pp. 148–162 (cited on pages 82, 83).
- [49] A. Dussutour, T. Latty, M. Beekman, and S. J. Simpson, “Amoeboid organism solves complex nutritional challenges”, *Proceedings of the National Academy of Sciences*, vol. 107, no. 10, pp. 4607–4611, 2010 (cited on page 2).
- [50] A. G. Dyer and L. Chittka, “Bumblebees (*Bombus terrestris*) sacrifice foraging speed to solve difficult colour discrimination tasks”, *Journal of comparative physiology. A, Neuroethology, sensory, neural, and behavioral physiology*, vol. 190, no. 9, pp. 759–763, 2004 (cited on page 3).
- [51] A. G. Dyer and L. Chittka, “Fine colour discrimination requires differential conditioning in bumblebees”, *Die Naturwissenschaften*, vol. 91, no. 5, pp. 224–227, 2004 (cited on page 3).
- [52] J. T. Ebert, M. Gauci, F. Mallmann-Trenn, and R. Nagpal, “Bayes bots: Collective bayesian decision-making in decentralized robot swarms”, in *International Conference on Robotics and Automation (ICRA)*, 2020 (cited on pages 21, 56).
- [53] J. T. Ebert, M. Gauci, and R. Nagpal, “Multi-feature collective decision making in robot swarms”, in *Proceedings of the 17th International Conference on Autonomous Agents and MultiAgent Systems*, ser. AAMAS ’18, 2018, pp. 1711–1719 (cited on pages 9, 21, 76, 121).

- [54] W. Elmenreich, “An introduction to sensor fusion”, Vienna University of Technology, Institut für Technische Informatik, Tech. Rep., Nov. 2002 (cited on page 17).
- [55] L. Festinger, *A Theory of Cognitive Dissonance*. 1957 (cited on pages 5, 51, 118).
- [56] M. C. Florea, J. Dezert, P. Valin, F. Smarandache, and A.-L. Joussetme, “Adaptive combination rule and proportional conflict redistribution rule for information fusion”, *ArXiv*, vol. abs/cs/0604042, 2006 (cited on page 83).
- [57] N. R. Franks, A. Dornhaus, J. P. Fitzsimmons, and M. Stevens, “Speed versus accuracy in collective decision making”, *Proceedings of the Royal Society of London. Series B: Biological Sciences*, vol. 270, no. 1532, pp. 2457–2463, 2003 (cited on pages 3, 7, 26).
- [58] N. R. Franks, K. A. Hardcastle, S. Collins, F. D. Smith, K. M. Sullivan, E. J. Robinson, and A. B. Sendova-Franks, “Can ant colonies choose a far-and-away better nest over an in-the-way poor one?”, *Animal Behaviour*, vol. 76, no. 2, pp. 323–334, 2008 (cited on page 4).
- [59] S. Galam, “Rational group decision making: A random field ising model at $t=0$ ”, *Physica A: Statistical Mechanics and its Applications*, vol. 238, no. 1, pp. 66–80, 1997 (cited on page 31).
- [60] S. Galam, “Sociophysics: A review of galam models”, *International Journal of Modern Physics C*, vol. 19, no. 03, pp. 409–440, 2008 (cited on page 29).
- [61] B. G. Galef and K. N. Laland, “Social Learning in Animals: Empirical Studies and Theoretical Models”, *BioScience*, vol. 55, no. 6, pp. 489–499, 2005 (cited on page 23).
- [62] G. Gigerenzer and W. Gaissmaier, “Decision making: Nonrational theories”, in *International Encyclopedia of the Social Behavioral Sciences (Second Edition)*, Second Edition, Oxford: Elsevier, 2015, pp. 911–916 (cited on page 4).
- [63] C. Gini, “Measurement of inequality of incomes”, *The Economic Journal*, vol. 31, no. 121, pp. 124–126, 1921 (cited on page 73).
- [64] H. Gintis, “Why the beliefs, preferences, and constraints model?”, 2005 (cited on page 5).
- [65] H. Gintis, “The foundations of transdisciplinary behavioral science”, *Primate Neuroethology*, 2010 (cited on page 6).
- [66] A. Giusti, J. Nagi, L. Gambardella, and G. A. Di Caro, “Cooperative sensing and recognition by a swarm of mobile robots”, in *2012 IEEE/RSJ International Conference on Intelligent Robots and Systems*, IEEE, 2012, pp. 551–558 (cited on page 17).
- [67] A. Goldman and C. O’Connor, “Social epistemology”, in *The Stanford Encyclopedia of Philosophy*, Metaphysics Research Lab, Stanford University, 2019 (cited on page 23).
- [68] H.-J. Gunther, R. Riebl, L. Wolf, and C. Facchi, “Collective perception and decentralized congestion control in vehicular ad-hoc networks”, in *Proceedings of the IEEE Vehicular Networking Conference (VNC)*, 2016 (cited on page 20).

- [69] H. Hamann and H. Wörn, “A space- and time-continuous model of self-organizing robot swarms for design support”, in *First IEEE International Conference on Self-Adaptive and Self-Organizing Systems (SASO'07), Boston, USA, July 9-11*, Los Alamitos, CA: IEEE Press, 2007, pp. 23–31 (cited on page 121).
- [70] A. T. Hartnett, E. Schertzer, S. A. Levin, and I. D. Couzin, “Heterogeneous preference and local nonlinearity in consensus decision making”, *Phys. Rev. Lett.*, vol. 116, 3 2016 (cited on pages 22, 30, 37, 43, 51).
- [71] D. M. Hausman, *Preference, Value, Choice, and Welfare*. Cambridge University Press, 2012 (cited on page 6).
- [72] C. Heyes and B. Galef, “Social learning in animals: The roots of culture”, 1996 (cited on page 7).
- [73] M. Hollander, D. Wolfe, and E. Chicken, *Nonparametric Statistical Methods*, ser. Wiley Series in Probability and Statistics. Wiley, 2013 (cited on pages 61, 75).
- [74] J. A. Holyst, K. Kacperski, and F. Schweitzer, “Social impact models of opinion dynamics”, in *Annual Rev. of Comput. Phys.*, 2001, pp. 253–272 (cited on page 34).
- [75] M. Hoogendoorn, J. Treur, C. N. van der Wal, and A. van Wissen, “Modelling the interplay of emotions, beliefs and intentions within collective decision making based on insights from social neuroscience”, in *Neural Information Processing. Theory and Algorithms*, Springer Berlin Heidelberg, 2010, pp. 196–206 (cited on page 5).
- [76] W. Hoppitt and K. Laland, *Social Learning: An Introduction to Mechanisms, Methods, and Models*. Princeton University Press, 2013 (cited on page 8).
- [77] L. Huber, “Social learning in animals”, in *Encyclopedia of the Sciences of Learning*. 2012, pp. 3109–3113 (cited on page 8).
- [78] E. Ising, “Beitrag zur theorie des ferromagnetismus”, *Zeitschrift fur Physik*, vol. 31, no. 1, pp. 253–258, 1925 (cited on page 31).
- [79] S. Israel and E. Blasch, “Context assumptions for threat assessment systems”, in *Advances in Computer Vision and Pattern Recognition*. Springer, 2016, pp. 99–124 (cited on page 114).
- [80] M. Jacobs, “Accounting for changing tastes: Approaches to explaining unstable individual preferences”, *Review of Economics*, vol. 67, no. 2, pp. 121–183, 2016 (cited on page 30).
- [81] S. Janson, M. Middendorf, and M. Beekman, “Searching for a new home - scouting behavior of honeybee swarms”, *Behavioral Ecology*, vol. 18, pp. 384–392, 2007 (cited on page 4).
- [82] R. Jeanson, A. Dussutour, and V. Fourcassié, “Key factors for the emergence of collective decision in invertebrates”, *Frontiers in Neuroscience*, vol. 6, 2012 (cited on page 117).
- [83] R. Jensen, “Behaviorism, latent learning, and cognitive maps: Needed revisions in introductory psychology textbooks”, *The Behavior Analyst*, vol. 29, no. 2, pp. 187–209, 2006 (cited on page 69).

- [84] A.-L. Jousselme, D. Grenier, and E. Bosse, “A new distance between two bodies of evidence”, *Information Fusion*, vol. 2, no. 2, pp. 91–101, 2001 (cited on page 84).
- [85] A. Kacelnik, “Meanings of rationality”, in *Rational Animals?*, Oxford University Press, 2006 (cited on page 5).
- [86] O. Kanjanatarakul and T. Denoeux, “Distributed data fusion in the dempster-shafer framework”, in *12th System of Systems Engineering Conference, SoSE 2017, Waikoloa, HI, USA, June 18-21, 2017*, IEEE, 2017, pp. 1–6 (cited on page 22).
- [87] A. B. Kao, N. Miller, C. Torney, A. Hartnett, and I. D. Couzin, “Collective learning and optimal consensus decisions in social animal groups”, *PLOS Computational Biology*, vol. 10, no. 8, pp. 1–11, 2014 (cited on pages 8, 23).
- [88] F. Kaplan and P.-Y. Oudeyer, “Intrinsically motivated machines”, *50 Years of AI, Festschrift*, LNAI. 4850, pp. 304–315, 2007 (cited on page 6).
- [89] X. Ke, L. Ma, and Y. Wang, “Some notes on canonical decomposition and separability of a belief function”, in *Belief Functions: Theory and Applications*, Springer International Publishing, 2014, pp. 153–160 (cited on page 78).
- [90] R. Kennes and P. Smets, “Computational aspects of the mobius transformation”, in *Proceedings of the Sixth Annual Conference on Uncertainty in Artificial Intelligence*, ser. UAI ’90, Elsevier Science Inc., 1990, pp. 401–416 (cited on page 79).
- [91] Y. Khaluf, P. Simoens, and H. Hamann, “The neglected pieces of designing collective decision-making processes”, *Frontiers in Robotics and AI*, vol. 6, p. 16, 2019 (cited on pages 30, 76).
- [92] Y. Khaluf, S. Van Havermaet, and P. Simoens, “Collective lévy walk for efficient exploration in unknown environments”, in *Artificial Intelligence: Methodology, Systems, and Applications*, Cham: Springer International Publishing, 2018, pp. 260–264 (cited on page 121).
- [93] D. King and P. Breedon, “Towards cooperative robotic swarm recognition: Object classification and validity”, in *Advanced Design and Manufacture III*, ser. Key Engineering Materials, vol. 450, Trans. Tech. Publications Ltd, Jan. 2011, pp. 320–324 (cited on page 17).
- [94] A. Kirchner, F. Dambreville, F. Celeste, J. Dezert, and F. Smarandache, “Application of probabilistic PCR5 fusion rule for multisensor target tracking”, in *The 10th International Conference on Information Fusion*, 2007, pp. 1–8 (cited on page 114).
- [95] J. Kohlas and P.-A. Monney, “Theory of evidence —a survey of its mathematical foundations, applications and computational aspects”, *Zeitschrift für Operations Research*, vol. 39, no. 1, pp. 35–68, 1994 (cited on page 77).
- [96] G. Kohring, “Ising Models of Social Impact: the Role of Cumulative Advantage”, *Journal de Physique I*, vol. 6, no. 2, pp. 301–308, 1996 (cited on pages 34, 52).
- [97] S. Kornienko, O. Kornienko, C. Constantinescu, M. Pradier, and P. Levi, “Cognitive micro-agents: Individual and collective perception in microrobotic swarm”, in *Proceedings of IJCAI-05 Workshop on Agents in Real-Time and Dynamic Environment*, 2005 (cited on pages 17, 20).

- [98] J. Kulvicki, “Isomorphism in information carrying systems”, *Pacific Philosophical Quarterly*, vol. 85, pp. 380–395, 2004 (cited on page 55).
- [99] K. N. Laland, “Social learning strategies”, *Animal Learning and Behavior*, vol. 32, no. 1, pp. 4–14, 2004 (cited on page 23).
- [100] T. Laomettachit, T. Termsaithong, A. Sae-Tang, and O. Duangphakdee, “Decision-making in honeybee swarms based on quality and distance information of candidate nest sites”, *Journal of Theoretical Biology*, vol. 364, pp. 21–30, 2015 (cited on page 4).
- [101] B. Latané, “The psychology of social impact.”, *American Psychologist*, vol. 36, no. 4, pp. 343–356, 1981 (cited on page 33).
- [102] T. Latty and M. Beekman, “Speed-accuracy trade-offs during foraging decisions in the acellular slime mould *Physarum polycephalum*”, *Proceedings of the Royal Society B: Biological Sciences*, vol. 278, no. 1705, pp. 539–545, 2011 (cited on page 3).
- [103] C. Lee, J. Lawry, and A. Winfield, “Negative updating combined with opinion pooling in the best-of-n problem in swarm robotics”, in *Swarm Intelligence*, Springer International Publishing, 2018, pp. 97–108 (cited on pages 9, 23).
- [104] C. Lee, J. Lawry, and A. Winfield, “Combining opinion pooling and evidential updating for multi-agent consensus”, in *Proceedings of the Twenty-Seventh International Joint Conference on Artificial Intelligence, IJCAI-18*, 2018, pp. 347–353 (cited on pages 22, 115).
- [105] M. Lewenstein, A. Nowak, and B. Latané, “Statistical mechanics of social impact”, *Phys. Rev. A*, vol. 45, pp. 763–776, 2 1992 (cited on page 34).
- [106] C. Libedinsky and M. Livingstone, “Role of prefrontal cortex in conscious visual perception”, *Journal of Neuroscience*, vol. 31, no. 1, pp. 64–69, 2011 (cited on page 54).
- [107] T. M. Liggett, “Voter models”, in *Stochastic Interacting Systems: Contact, Voter and Exclusion Processes*. Springer Berlin Heidelberg, 1999, pp. 139–208 (cited on page 29).
- [108] L. Liu and R. R. Yager, “Classic Works of the Dempster-Shafer Theory of Belief Functions: An Introduction”, in *Classic Works of the Dempster-Shafer Theory of Belief Functions*. Springer Berlin Heidelberg, 2008, pp. 1–34 (cited on page 76).
- [109] N. Majcherczyk, D. J. Nallathambi, T. Antonelli, and C. Pinciroli, “Distributed data storage and fusion for collective perception in resource-limited mobile robot swarms”, *IEEE Robotics and Automation Letters*, 2021 (cited on page 17).
- [110] J. Makinson, B. Oldroyd, T. M. Schaerf, W. Wattanachaiyingcharoen, and M. Beekman, “Moving home: nest-site selection in the Red Dwarf honeybee (*Apis florea*)”, *Behavioral Ecology and Sociobiology*, vol. 65, pp. 945–958, 2010 (cited on page 4).
- [111] M. Mangel and C. W. Clark, *Dynamic Modeling in Behavioral Ecology*. Princeton University Press, 2019 (cited on page 4).

- [112] H. B. Mann and D. R. Whitney, “On a test of whether one of two random variables is stochastically larger than the other”, *The Annals of Mathematical Statistics*, vol. 18, no. 1, pp. 50–60, 1947 (cited on pages 66, 93).
- [113] J. Marshall, G. Brown, and A. Radford, “Individual confidence-weighting and group decision-making”, *Trends in ecology & evolution*, vol. 32, 2017 (cited on pages 8, 23).
- [114] A. Martin and C. Osswald, “Toward a combination rule to deal with partial conflict and specificity in belief functions theory”, *2007 10th International Conference on Information Fusion*, pp. 1–8, 2007 (cited on page 83).
- [115] A. Martin, C. Osswald, J. Dezert, and F. Smarandache, “General combination rules for qualitative and quantitative beliefs”, *Journal of Advances in Information Fusion*, vol. 3, Dec. 2008 (cited on page 21).
- [116] P. Martin, *Potts Models and Related Problems in Statistical Mechanics*, ser. Series on advances in statistical mechanics. World Scientific, 1991 (cited on page 121).
- [117] MATLAB, *version 9.5.0. (R2018b)*. Natick, Massachusetts: The MathWorks Inc., 2018 (cited on pages 59, 81).
- [118] D. C. Matz and W. Wood, “Cognitive dissonance in groups: The consequences of disagreement”, *Journal of personality and social psychology*, vol. 88, no. 1, pp. 22–37, 2005 (cited on page 6).
- [119] P. Mazdin and B. Rinner, “Coordination of mobile agents for simultaneous coverage”, in *PRIMA 2019: Principles and Practice of Multi-Agent Systems*, Cham: Springer International Publishing, 2019, pp. 170–185 (cited on page 17).
- [120] G. Morlino, V. Trianni, and E. Tuci, “Collective perception in a swarm of autonomous robots”, in *Proceedings of the International Joint Conference on Computational Intelligence*, vol. 1, SciTePress, 2010, pp. 51–59 (cited on pages 20, 21, 58).
- [121] C. K. Murphy, “Combining belief functions when evidence conflicts”, *Decis. Support Syst.*, vol. 29, no. 1, pp. 1–9, 2000 (cited on page 81).
- [122] P. Nain, D. Towsley, Benyuan Liu, and Zhen Liu, “Properties of random direction models”, in *Proceedings IEEE 24th Annual Joint Conference of the IEEE Computer and Communications Societies.*, vol. 3, 2005, pp. 1897–1907 (cited on page 19).
- [123] M. E. J. Newman and G. T. Barkema, *Monte Carlo methods in statistical physics*. Oxford, 1999 (cited on page 33).
- [124] S. C. Nicolis, N. Zabzina, T. Latty, and D. J. T. Sumpter, “Collective irrationality and positive feedback”, *PLOS ONE*, vol. 6, no. 4, pp. 1–6, 2011 (cited on pages 4, 10).
- [125] J. Nigel, “Mental imagery”, in *The Stanford Encyclopedia of Philosophy*, 2018 (cited on pages 54, 58).
- [126] A. Nowak, B. Latane, and J. Szamrej, “From private attitude to public opinion: A dynamic theory of social impact”, *Psychological Review*, vol. 97, no. 3, pp. 362–376, 1990 (cited on pages 33, 34).

- [127] M. A. Nowak, “Five rules for the evolution of cooperation”, *Science*, vol. 314, no. 5805, pp. 1560–1563, 2006 (cited on page 17).
- [128] R. Olfati-Saber and P. Jalalkamali, “Coupled distributed estimation and control for mobile sensor networks”, *IEEE Transactions on Automatic Control*, vol. 57, no. 10, pp. 2609–2614, 2012 (cited on page 17).
- [129] R. Pachella, “The interpretation of reaction time in information processing research”, *Human information processing*, p. 94, 1973 (cited on page 3).
- [130] C. A. C. Parker and H. Zhang, “Biologically inspired decision making for collective robotic systems”, in *2004 IEEE/RSJ International Conference on Intelligent Robots and Systems (IROS)*, 2004 (cited on page 9).
- [131] C. A. C. Parker and H. Zhang, “Cooperative decision-making in decentralized multiple-robot systems: The best-of- n problem”, *IEEE/ASME Transactions on Mechatronics*, vol. 14, no. 2, pp. 240–251, 2009 (cited on page 9).
- [132] C. A. C. Parker and H. Zhang, “Biologically inspired collective comparisons by robotic swarms”, *The International Journal of Robotics Research*, vol. 30, no. 5, pp. 524–535, 2011 (cited on page 9).
- [133] K. Passino and T. Seeley, “Modeling and analysis of nest-site selection by honeybee swarms: The speed and accuracy trade-off”, *Behavioral Ecology and Sociobiology*, vol. 59, pp. 427–442, 2005 (cited on pages 4, 10).
- [134] K. Passino, T. Seeley, and P. Visscher, “Swarm cognition in honey bees”, *Behavioral Ecology and Sociobiology*, vol. 62, pp. 401–414, 2008 (cited on page 4).
- [135] R. Peierls, “On ising’s model of ferromagnetism”, *Mathematical Proceedings of the Cambridge Philosophical Society*, vol. 32, no. 3, pp. 477–481, 1936 (cited on page 33).
- [136] E. Perron, D. Vasudevan, and M. Vojnovic, “Using three states for binary consensus on complete graphs”, in *IEEE INFOCOM 2009*, 2009, pp. 2527–2535 (cited on page 22).
- [137] C. J. Perry and A. B. Barron, “Honey bees selectively avoid difficult choices”, *Proceedings of the National Academy of Sciences*, vol. 110, no. 47, pp. 19 155–19 159, 2013 (cited on page 3).
- [138] A. Potemkowski, “Neurobiology of Decision Making: Methodology in Decision-Making Research. Neuroanatomical and Neurobiochemical Fundamentals”, in *Neuroeconomic and Behavioral Aspects of Decision Making*, 2017, pp. 3–18 (cited on page 2).
- [139] C. R. Reid, H. MacDonald, R. P. Mann, J. A. R. Marshall, T. Latty, and S. Garnier, “Decision-making without a brain: How an amoeboid organism solves the two-armed bandit”, *Journal of The Royal Society Interface*, vol. 13, no. 119, 2016 (cited on page 2).
- [140] A. Reina, J. A. R. Marshall, V. Trianni, and T. Bose, “Model of the best-of- n nest-site selection process in honeybees”, *Phys. Rev. E*, vol. 95, 5 2017 (cited on page 9).

- [141] A. Reina, G. Valentini, C. Fernández-Oto, M. Dorigo, and V. Trianni, “A design pattern for decentralised decision making”, *PLOS ONE*, vol. 10, no. 10, pp. 1–18, 2015 (cited on pages 10, 22).
- [142] A. Rouahi, K. B. Salah, and K. Ghédira, “Decision making: A beliefs, preferences and constraints model”, in *Belief Functions: Theory and Applications - 5th International Conference, BELIEF 2018, Compiègne, France, September 17-21, 2018, Proceedings*, ser. Lecture Notes in Computer Science, vol. 11069, 2018, pp. 217–225 (cited on pages 5, 122).
- [143] T. Sasaki and D. Biro, “Cumulative culture can emerge from collective intelligence in animal groups”, *Nature Communications*, vol. 8, no. 1, 2017 (cited on page 23).
- [144] T. Sasaki and S. C. Pratt, “The psychology of superorganisms: Collective decision making by insect societies”, *Annual Review of Entomology*, vol. 63, no. 1, pp. 259–275, 2018 (cited on pages 1, 4, 117).
- [145] T. Schmickl, C. Möslinger, and K. Crailsheim, “Collective perception in a robot swarm”, in *Proceedings of the 2nd International Conference on Swarm Robotics*, ser. SAB’06, Rome, Italy: Springer-Verlag, 2007, pp. 144–157 (cited on page 20).
- [146] K. A. Scholte and W. L. Norden, “Applying the PCR6 Rule of combination in real time classification systems”, in *2009 12th International Conference on Information Fusion*, 2009, pp. 1665–1672 (cited on page 115).
- [147] M. Schranz, M. Umlauft, M. Sende, and W. Elmenreich, “Swarm robotic behaviors and current applications”, *Frontiers in Robotics and AI*, vol. 7, 2020 (cited on pages 9, 17).
- [148] K. Sedig and R. Haworth, “Creative design of digital cognitive games: Application of cognitive toys and isomorphism”, *Bulletin of Science, Technology & Society*, vol. 32, no. 5, pp. 413–426, 2012 (cited on page 69).
- [149] K. Sentz and S. Ferson, *Combination of Evidence in Dempster-Shafer Theory*. Sandia National Laboratories, 2002 (cited on pages 22, 80).
- [150] G. Shafer, *A Mathematical Theory of Evidence*. Princeton University Press, 1976 (cited on pages 22, 78, 80, 97).
- [151] R. N. Shepard and J. Metzler, “Mental rotation of three-dimensional objects”, *Science*, vol. 171, no. 3972, pp. 701–703, 1971 (cited on page 55).
- [152] P. Simoens, M. Dragone, and A. Saffiotti, “The internet of robotic things: A review of concept, added value and applications”, *International Journal of Advanced Robotic Systems*, vol. 15, no. 1, 2018 (cited on page 20).
- [153] H. A. Simon, “Bounded rationality”, in *Utility and Probability*. 1990, pp. 15–18 (cited on page 5).
- [154] P. Skorupski, J. Spaethe, and L. Chittka, “Visual search and decision making in bees: Time, speed, and accuracy”, *Int. J. Comp. Psychol*, vol. 19, Jan. 2006 (cited on page 3).
- [155] F. Smarandache and J. Dezert, “Information fusion based on new proportional conflict redistribution rules”, in *2005 7th International Conference on Information Fusion*, vol. 2, 2005 (cited on page 81).

- [156] F. Smarandache, J. Dezert, and J. Tacnet, “Fusion of sources of evidence with different importances and reliabilities”, in *2010 13th International Conference on Information Fusion*, 2010, pp. 1–8 (cited on page 81).
- [157] F. Smarandache and J. Dezert, “Extended PCR Rules for Dynamic Frames”, in *Fusion 2012 - 15th International Conference on Information Fusion*, 2012 (cited on page 121).
- [158] F. Smarandache and J. Dezert, *Advances and Applications of DSmT for Information Fusion (Collected Works)*. USA: American Research Press, 2004 (cited on page 114).
- [159] F. Smarandache and J. Dezert, “An algorithm for quasi-associative and quasi-markovian rules of combination in information fusion”, *IRIDIA Technical Report, Université Libre de Bruxelles*, 2004 (cited on page 85).
- [160] F. Smarandache and J. Dezert, “On the consistency of PCR6 with the averaging rule and its application to probability estimation”, in *Proceedings of the 16th International Conference on Information Fusion, FUSION 2013, Istanbul, Turkey, July 9-12, 2013*, IEEE, 2013, pp. 1119–1126 (cited on page 81).
- [161] P. Smets, “The canonical decomposition of a weighted belief”, in *Proceedings of the 14th International Joint Conference on Artificial Intelligence - Volume 2*, ser. IJCAI’95, Montreal, Quebec, Canada: Morgan Kaufmann Publishers Inc., 1995, pp. 1896–1901 (cited on page 79).
- [162] P. Smets, “Analyzing the combination of conflicting belief functions”, *Information Fusion*, vol. 8, no. 4, pp. 387–412, 2007 (cited on pages 22, 79).
- [163] P. Smets and R. Kennes, “The transferable belief model”, in *Classic Works of the Dempster-Shafer Theory of Belief Functions*. Springer Berlin Heidelberg, 2008, pp. 693–736 (cited on pages 12, 78).
- [164] P. Smets, “Belief functions: The disjunctive rule of combination and the generalized bayesian theorem”, *International Journal of Approximate Reasoning*, vol. 9, no. 1, pp. 1–35, 1993 (cited on page 78).
- [165] P. L. Smith and R. Ratcliff, “Psychology and neurobiology of simple decisions”, *Trends in Neurosciences*, vol. 27, pp. 161–168, 2004 (cited on page 2).
- [166] R. Solé, M. Moses, and S. Forrest, “Liquid brains, solid brains”, *Philosophical Transactions of the Royal Society B: Biological Sciences*, vol. 374, no. 1774, 2019 (cited on page 2).
- [167] M. D. Soorati, M. Krome, M. Mora-Mendoza, J. Ghofrani, and H. Hamann, “Plasticity in collective decision-making for robots: Creating global reference frames, detecting dynamic environments, and preventing lock-ins”, in *2019 IEEE/RSJ International Conference on Intelligent Robots and Systems (IROS)*, 2019, pp. 4100–4105 (cited on page 21).
- [168] D. Stauffer, “Social applications of two-dimensional ising models”, *American Journal of Physics*, vol. 76, no. 4, pp. 470–473, 2008 (cited on page 31).
- [169] K. Steele and H. O. Stefánsson, “Decision Theory”, in *The Stanford Encyclopedia of Philosophy*, Metaphysics Research Lab, Stanford University, 2016 (cited on page 6).

- [170] P. Stegagno, C. Massidda, and H. Bülthoff, “Object recognition in swarm systems: Preliminary results”, in *Proceedings of the Workshop on the Centrality of Decentralization in Multi-Robot Systems: Holy Grail or False Idol?*, 2014, pp. 1–3 (cited on page 17).
- [171] A. Strandburg-Peshkin, D. R. Farine, I. D. Couzin, and M. C. Crofoot, “Shared decision-making drives collective movement in wild baboons”, *Science*, vol. 348, no. 6241, pp. 1358–1361, 2015 (cited on page 3).
- [172] V. Strobel, E. Castelló Ferrer, and M. Dorigo, “Managing Byzantine robots via blockchain technology in a swarm robotics collective decision making scenario”, in *Proceedings of 17th International Conference on Autonomous Agents and MultiAgent Systems*, ser. AAMAS ’18, 2018, pp. 541–549 (cited on pages 21, 29, 43, 56, 62).
- [173] V. Strobel, E. Castelló Ferrer, and M. Dorigo, “Blockchain technology secures robot swarms: A comparison of consensus protocols and their resilience to byzantine robots”, *Frontiers in Robotics and AI*, vol. 7, p. 54, 2020, ISSN: 2296-9144 (cited on page 21).
- [174] D. J. Sumpter, N. Zabzina, and S. C. Nicolis, “Six predictions about the decision making of animal and human groups”, *Managerial and Decision Economics*, vol. 33, no. 5-6, pp. 295–309, 2012 (cited on pages 4, 10).
- [175] D. Sumpter, “The principles of collective animal behaviour”, *Philosophical Transactions of the Royal Society B: Biological Sciences*, vol. 361, no. 1465, pp. 5–22, 2006 (cited on page 121).
- [176] M. S. Talamali, T. Bose, M. Haire, X. Xu, J. A. R. Marshall, and A. Reina, “Sophisticated collective foraging with minimalist agents: A swarm robotics test”, *Swarm Intelligence*, 2020 (cited on pages 10, 120).
- [177] M. S. Talamali, J. A. R. Marshall, T. Bose, and A. Reina, “Improving collective decision accuracy via time-varying cross-inhibition”, in *International Conference on Robotics and Automation, ICRA 2019, Montreal, QC, Canada, May 20-24, 2019*, IEEE, 2019, pp. 9652–9659 (cited on page 9).
- [178] M. Tennenbaum, Z. Liu, D. Hu, and A. Fernandez-Nieves, “Mechanics of fire ant aggregations”, *Nature materials*, vol. 15, 2015 (cited on page 2).
- [179] G. Thandavarayan, M. Sepulcre, and J. Gozalvez, “Generation of cooperative perception messages for connected and automated vehicles”, *IEEE Transactions on Vehicular Technology*, 2020 (cited on page 20).
- [180] J. Toran, “On the hardness of graph isomorphism”, *Society for Industrial and Applied Mathematics*, vol. 33, no. 5, pp. 1093–1108, 2004 (cited on page 58).
- [181] C. Torney, Z. Neufeld, and I. D. Couzin, “Context-dependent interaction leads to emergent search behavior in social aggregates”, *Proceedings of the National Academy of Sciences*, vol. 106, no. 52, 2009 (cited on page 31).
- [182] M. Trabattoni, G. Valentini, and M. Dorigo, “Hybrid control of swarms for resource selection”, in *Swarm Intelligence*, Springer International Publishing, 2018, pp. 57–70 (cited on pages 10, 70).

- [183] G. Valentini, D. Brambilla, H. Hamann, and M. Dorigo, “Collective perception of environmental features in a robot swarm”, in *Swarm Intelligence*, Springer, 2016, pp. 65–76 (cited on pages 17, 18, 21, 26, 43, 56, 64).
- [184] G. Valentini, *Achieving Consensus in Robot Swarms: Design and Analysis of Strategies for the best-of-n Problem*. Springer International Publishing, 2017 (cited on pages 9–11, 13, 17, 18, 22–24, 26, 29, 43, 58, 121).
- [185] G. Valentini, E. Ferrante, and M. Dorigo, “The best-of-n problem in robot swarms: Formalization, state of the art, and novel perspectives”, *Frontiers in Robotics and AI*, vol. 4, p. 9, 2017 (cited on pages 16, 17).
- [186] G. Valentini, H. Hamann, and M. Dorigo, “Self-organized collective decision making: The weighted voter model”, in *Proceedings of the 13th Int. Conf. on Autonomous Agents and Multiagent Systems*, ser. AAMAS ’14, IFAAMAS, 2014, pp. 45–52 (cited on pages 9, 22, 30).
- [187] S. Wenmackers, D. Vanpoucke, and I. Douven, “Rationality: A social-epistemology perspective”, *Frontiers in Psychology*, vol. 5, p. 581, 2014 (cited on page 23).
- [188] L. Xu, A. Krzyzak, and C. Y. Suen, “Methods of combining multiple classifiers and their applications to handwriting recognition”, *IEEE Transactions on Systems, Man, and Cybernetics*, vol. 22, no. 3, pp. 418–435, 1992 (cited on page 21).
- [189] R. Yager, “Quasi-associative operations in the combination of evidence”, *Kybernetes*, vol. 16, pp. 37–41, 1987 (cited on page 85).
- [190] L. Zhao, G. Yang, W. Wang, Y. Chen, J. P. Huang, H. Ohashi, and H. E. Stanley, “Herd behavior in a complex adaptive system”, *Proceedings of the National Academy of Sciences*, vol. 108, no. 37, pp. 15 058–15 063, 2011 (cited on page 8).
- [191] K. Zhou, A. Martin, and Q. Pan, “Evidence combination for a large number of sources”, in *2017 20th International Conference on Information Fusion (FUSION)*, 2017 (cited on page 79).
- [192] T. Ziemke, D.-A. Jirnhed, and G. Hesslow, “Internal simulation of perception: A minimal neuro-robotic model”, *Neurocomput.*, vol. 68, pp. 85–104, 2005 (cited on page 69).
- [193] M. E. Zimmerman, “Speed–accuracy tradeoff”, in *Encyclopedia of Clinical Neuropsychology*. New York, NY: Springer New York, 2011, pp. 2344–2344 (cited on page 3).
- [194] N. E. Zoghby, V. Cherfaoui, and T. Denoeux, “Evidential distributed dynamic map for cooperative perception in vanets”, in *2014 IEEE Intelligent Vehicles Symposium Proceedings*, 2014, pp. 1421–1426 (cited on page 22).
- [195] A. Zurbuchen, L. Landert, J. Klaiber, A. Müller, S. Hein, and S. Dorn, “Maximum foraging ranges in solitary bees: Only few individuals have the capability to cover long foraging distances”, *Biological Conservation - BIOL CONSERV*, vol. 143, pp. 669–676, 2010 (cited on page 4).

Parameters of Collective Perception Scenario

Parameter description	Symbol	Value
Number of cell in a grid	Γ	400
Size of a grid cell	$cell \times cell$	$1 \times 1 \text{ unit}^2$
Speed of linear motion	$ \vec{v} $	1.6 units/s ¹
Angular velocity	ω	7.5 rad/s
Agent diameter	Θ	0.7 units
Population size (default)	N	20
Maximum communication radius	d_{max}	5 units
Communication frequency	$\Delta\tau_C$	10 times per second
Exploration time	t	10 seconds

Table A.1: Table of default simulation parameters for collective perception scenario.

¹One physical second (s) is modeled by 100 iterations in the simulation and one unit corresponds to 10 cm.

Supplementary Material to Chapter 3

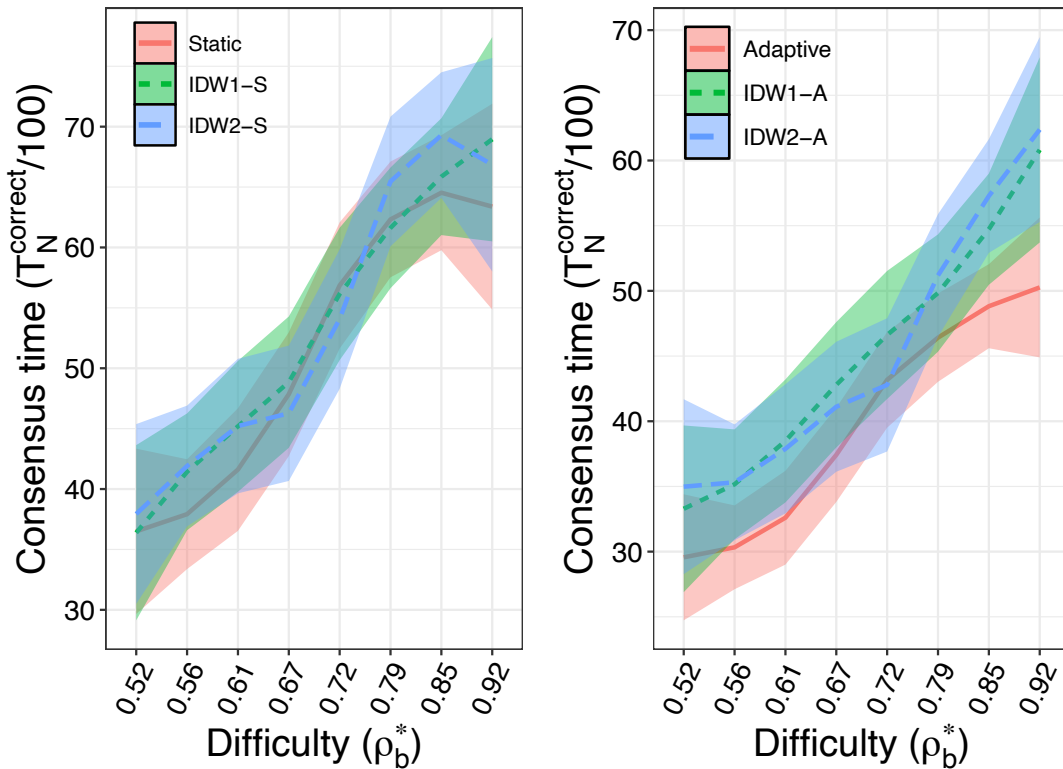


Figure B.1: Consensus time (T_N^{correct}) and exit probability (E_N) as a function of the task difficulty ρ_b^* . Configuration of parameters: $\rho_{un} = 0$, $\beta = 4.5$. Maximum possible communication distance between the agents $d_{max} = 5$ units. IDW1 and IDW2 indicate the inverse distance weighting with power 1 and 2, respectively, for adaptive and static policy. Shaded areas represent the 95% confidence interval.

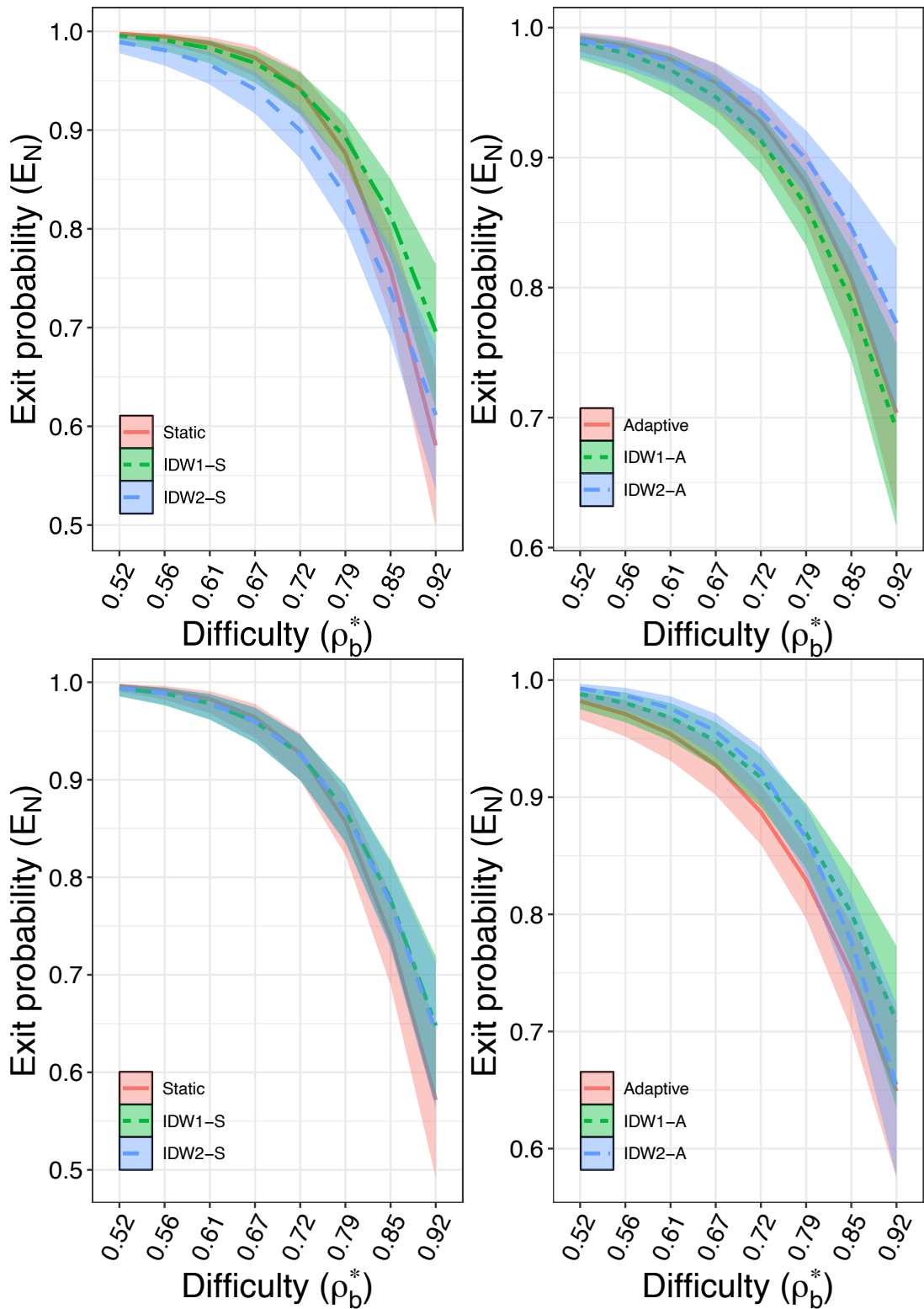


Figure B.2: Exit probability (E_N) as a function of the task difficulty ρ_b^* . Configuration of parameters: $\rho_{un} = 0$, $\beta = 4.5$. Maximum possible communication distance between the agents – top: $d_{max} = 5$ units, bottom: $d_{max} = 10$ units. IDW1 and IDW2 indicate the inverse distance weighting with power 1 and 2, respectively, for adaptive and static policy. Shaded areas represent the 95% confidence interval.

Supplementary Material to Chapter 5

C.1 Statistical Analysis of Collective, Social, and Individual Learning

Iterations	Pattern	DM1	DM2	DM3	DM4	DM5	DM6	DM7	DM8	DM9	DM10	DM11	DM12
10	Random	0.7	0.669	0.632	0.286	0.674	0.709	0.709	0.703	0.75	0.61	0.479	0.579
	Stripe	0.5	0.5	0.482	0.38	0.526	0.491	0.5	0.5	0.502	0.464	0.45	0.55
	Star	0.551	0.55	0.541	0.286	0.599	0.594	0.6	0.55	0.55	0.568	0.444	0.536
	Band	0.602	0.636	0.605	0.312	0.676	0.658	0.7	0.65	0.75	0.642	0.504	0.659
	Band-S	0.5	0.527	0.5	0.339	0.543	0.526	0.527	0.516	0.541	0.491	0.487	0.561
	Band-W	0.612	0.598	0.559	0.28	0.649	0.582	0.55	0.6	0.566	0.584	0.494	0.593
	Rec	0.5	0.5	0.55	0.327	0.519	0.521	0.5	0.5	0.5	0.5	0.429	0.5
	Random	0.7	1	1	0.33	1	0.915	0.75	0.75	0.85	1	1	1
50	Stripe	0.55	0.55	0.597	0.396	0.6	0.545	0.55	0.55	0.524	0.6	0.502	0.587
	Star	0.6	0.991	0.95	0.34	0.888	0.792	0.65	0.6	0.575	0.95	0.897	0.9
	Band	0.65	1	1	0.354	1	0.898	0.725	0.7	0.85	1	1	1
	Band-S	0.55	0.7	0.7	0.38	0.803	0.605	0.55	0.525	0.55	0.7	0.625	0.8
	Band-W	0.65	1	1	0.348	1	0.828	0.55	0.65	0.6	1	0.887	0.95
	Rec	0.55	0.668	0.7	0.39	0.681	0.557	0.507	0.5	0.5	0.69	0.522	0.65
	Random	0.7	1	1	0.321	1	0.921	0.75	0.75	0.85	1	1	1
	100	Stripe	0.55	0.616	0.605	0.394	0.654	0.501	0.55	0.55	0.527	0.625	0.546
Star		0.6	1	1	0.342	1	0.771	0.65	0.6	0.575	1	1	1
Band		0.65	1	1	0.383	1	0.877	0.725	0.7	0.85	1	1	1
Band-S		0.55	0.85	0.8	0.389	0.923	0.609	0.55	0.525	0.55	0.862	0.75	0.9
Band-W		0.65	1	1	0.342	1	0.824	0.55	0.65	0.6	1	1	1
Rec		0.55	0.8	0.85	0.389	0.834	0.545	0.525	0.5	0.5	0.85	0.55	0.825
Random		0.7	1	1	0.349	1	0.917	0.75	0.75	0.85	1	1	1
200		Stripe	0.55	0.683	0.75	0.402	0.762	0.505	0.55	0.55	0.525	0.75	0.594
	Star	0.6	1	1	0.358	1	0.769	0.65	0.6	0.575	1	1	1
	Band	0.65	1	1	0.372	1	0.895	0.725	0.7	0.85	1	1	1
	Band-S	0.55	1	1	0.38	1	0.586	0.55	0.525	0.55	1	0.937	1
	Band-W	0.65	1	1	0.377	1	0.823	0.55	0.65	0.6	1	1	1
	Rec	0.55	0.95	0.95	0.368	0.949	0.516	0.525	0.5	0.5	1	0.75	0.95
	Random	0.7	1	1	0.332	1	0.925	0.75	0.75	0.85	1	1	1
	300	Stripe	0.55	0.7	0.85	0.416	0.846	0.509	0.55	0.55	0.525	0.759	0.6
Star		0.6	1	1	0.338	1	0.794	0.65	0.6	0.6	1	1	1
Band		0.65	1	1	0.368	1	0.891	0.725	0.7	0.85	1	1	1
Band-S		0.55	1	1	0.392	1	0.572	0.55	0.525	0.55	1	1	1
Band-W		0.65	1	1	0.361	1	0.837	0.55	0.65	0.6	1	1	1
Rec		0.55	1	1	0.376	1	0.555	0.525	0.5	0.5	1	0.85	1
Random		0.7	1	1	0.356	1	0.91	0.75	0.75	0.85	1	1	1
400		Stripe	0.55	0.75	0.85	0.441	0.917	0.504	0.55	0.55	0.525	0.85	0.6
	Star	0.6	1	1	0.359	1	0.789	0.65	0.6	0.6	1	1	1
	Band	0.65	1	1	0.35	1	0.893	0.725	0.7	0.85	1	1	1
	Band-S	0.55	1	1	0.39	1	0.56	0.55	0.525	0.55	1	1	1
	Band-W	0.65	1	1	0.348	1	0.825	0.55	0.65	0.6	1	1	1
	Rec	0.55	1	1	0.367	1	0.569	0.525	0.5	0.5	1	0.975	1

Table C.1: Collective Learning, $\rho = 0.67$: Median belief values at different run lengths. Best performance is indicated in bold font. The results which have equal medians with the best performance (in each line) are indicated by light gray color (including the best result in bold). Statistical significance is stated by two-sided pairwise Mann-Whitney-U test with p -value < 0.05 .

Iterations	Pattern	DM1	DM2	DM3	DM4	DM5	DM6	DM7	DM8	DM9	DM10	DM11	DM12
10	Random	0.678	0.619	0.61	0.353	0.69	0.7	0.674	0.682	0.702	0.634	0.518	0.519
	Stripe	0.5	0.495	0.477	0.461	0.521	0.503	0.517	0.5	0.518	0.546	0.45	0.544
	Star	0.627	0.547	0.55	0.367	0.606	0.589	0.603	0.561	0.558	0.55	0.466	0.517
	Band	0.686	0.594	0.611	0.359	0.682	0.671	0.703	0.653	0.623	0.639	0.502	0.49
	Band-S	0.541	0.507	0.499	0.39	0.529	0.476	0.539	0.546	0.513	0.535	0.45	0.487
	Band-W	0.6	0.606	0.594	0.362	0.643	0.613	0.573	0.575	0.646	0.554	0.489	0.525
Rec	0.5	0.516	0.456	0.383	0.526	0.499	0.5	0.5	0.5	0.5	0.4	0.5	
50	Random	0.75	1	1	0.382	1	0.886	0.75	0.75	0.8	1	1	0.688
	Stripe	0.55	0.6	0.551	0.43	0.569	0.489	0.55	0.5	0.55	0.618	0.5	0.598
	Star	0.65	0.9	0.834	0.39	0.848	0.721	0.65	0.6	0.6	0.862	0.757	0.654
	Band	0.7	1	1	0.413	1	0.838	0.75	0.725	0.75	1	0.991	0.758
	Band-S	0.55	0.704	0.709	0.436	0.707	0.592	0.55	0.55	0.55	0.7	0.55	0.594
	Band-W	0.6	1	0.95	0.392	0.999	0.74	0.6	0.6	0.668	0.95	0.898	0.693
Rec	0.55	0.679	0.65	0.403	0.678	0.512	0.5	0.525	0.5	0.647	0.545	0.59	
100	Random	0.75	1	1	0.375	1	0.871	0.75	0.75	0.8	1	1	0.757
	Stripe	0.55	0.66	0.573	0.446	0.644	0.507	0.55	0.5	0.55	0.652	0.5	0.6
	Star	0.65	1	1	0.419	1	0.687	0.65	0.6	0.6	1	0.955	0.668
	Band	0.7	1	1	0.388	1	0.828	0.75	0.725	0.75	1	1	0.757
	Band-S	0.55	0.85	0.9	0.431	0.875	0.556	0.55	0.55	0.55	0.824	0.661	0.639
	Band-W	0.6	1	1	0.379	1	0.744	0.6	0.6	0.675	1	1	0.778
Rec	0.55	0.823	0.849	0.388	0.779	0.498	0.5	0.525	0.5	0.8	0.639	0.66	
200	Random	0.75	1	1	0.387	1	0.874	0.75	0.75	0.8	1	1	0.732
	Stripe	0.55	0.8	0.712	0.461	0.703	0.472	0.55	0.5	0.55	0.75	0.591	0.709
	Star	0.65	1	1	0.399	1	0.673	0.65	0.6	0.6	1	1	0.739
	Band	0.7	1	1	0.398	1	0.831	0.75	0.725	0.75	1	1	0.737
	Band-S	0.55	1	1	0.435	1	0.582	0.55	0.55	0.55	1	0.75	0.826
	Band-W	0.6	1	1	0.41	1	0.758	0.55	0.6	0.675	1	1	0.731
Rec	0.55	0.95	1	0.405	0.933	0.552	0.5	0.525	0.5	0.975	0.787	0.8	
300	Random	0.75	1	1	0.403	1	0.899	0.75	0.75	0.8	1	1	0.76
	Stripe	0.55	0.9	0.757	0.44	0.741	0.524	0.55	0.5	0.55	0.9	0.6	0.772
	Star	0.65	1	1	0.404	1	0.708	0.65	0.6	0.6	1	1	0.743
	Band	0.7	1	1	0.429	1	0.828	0.75	0.725	0.75	1	1	0.738
	Band-S	0.55	1	1	0.441	1	0.544	0.525	0.55	0.55	1	0.85	0.825
	Band-W	0.6	1	1	0.394	1	0.751	0.55	0.6	0.675	1	1	0.808
Rec	0.55	1	1	0.415	1	0.531	0.5	0.525	0.5	1	0.914	0.818	
400	Random	0.75	1	1	0.386	1	0.886	0.775	0.75	0.8	1	1	0.77
	Stripe	0.55	0.9	0.9	0.446	0.781	0.54	0.55	0.5	0.55	0.95	0.6	0.763
	Star	0.65	1	1	0.398	1	0.681	0.65	0.6	0.6	1	1	0.7
	Band	0.7	1	1	0.407	1	0.832	0.75	0.725	0.75	1	1	0.767
	Band-S	0.55	1	1	0.441	1	0.57	0.5	0.55	0.55	1	1	0.868
	Band-W	0.6	1	1	0.398	1	0.753	0.55	0.6	0.675	1	1	0.792
Rec	0.55	1	1	0.394	1	0.553	0.5	0.525	0.5	1	1	0.843	

Table C.2: Social Learning, $\rho = 0.67$: Median belief values at different run lengths. Best performance is indicated in bold font. The results which have equal medians with the best performance (in each line) are indicated by light gray color (including the best result in bold). Statistical significance is stated by two-sided pairwise Mann-Whitney-U test with p -value < 0.05 .

Iterations	Pattern	DM1	DM2	DM3	DM4	DM5	DM6	DM7	DM8	DM9	DM10	DM11	DM12
10	Random	0.486	0.478	0.495	0.242	0.488	0.448	0.505	0.512	0.401	0.463	0.423	0.489
	Stripe	0.5	0.5	0.5	0.337	0.5	0.457	0.5	0.5	0.5	0.5	0.507	0.5
	Star	0.504	0.453	0.459	0.268	0.52	0.445	0.498	0.5	0.432	0.47	0.473	0.477
	Band	0.508	0.493	0.471	0.261	0.512	0.443	0.469	0.498	0.418	0.493	0.462	0.494
	Band-S	0.5	0.494	0.492	0.32	0.489	0.425	0.5	0.5	0.474	0.508	0.5	0.47
	Band-W	0.5	0.481	0.497	0.25	0.498	0.412	0.522	0.498	0.45	0.458	0.474	0.5
Rec	0.5	0.5	0.45	0.335	0.5	0.441	0.496	0.5	0.477	0.5	0.485	0.498	
50	Random	0.5	0.55	0.55	0.284	0.55	0.615	0.55	0.55	0.45	0.5	0.635	0.55
	Stripe	0.55	0.525	0.55	0.424	0.5	0.462	0.525	0.5	0.5	0.5	0.55	0.55
	Star	0.55	0.5	0.55	0.317	0.55	0.532	0.55	0.55	0.45	0.55	0.558	0.5
	Band	0.55	0.55	0.55	0.286	0.55	0.584	0.5	0.5	0.45	0.55	0.644	0.55
	Band-S	0.5	0.525	0.5	0.393	0.55	0.496	0.55	0.525	0.5	0.55	0.55	0.5
	Band-W	0.55	0.55	0.55	0.297	0.55	0.535	0.55	0.525	0.5	0.525	0.6	0.55
Rec	0.5	0.55	0.5	0.354	0.5	0.442	0.5	0.5	0.5	0.55	0.5	0.5	
100	Random	0.5	0.55	0.55	0.281	0.55	0.637	0.55	0.55	0.45	0.5	0.65	0.55
	Stripe	0.55	0.525	0.55	0.418	0.5	0.483	0.525	0.5	0.5	0.5	0.55	0.55
	Star	0.55	0.5	0.55	0.307	0.55	0.554	0.55	0.55	0.45	0.55	0.6	0.5
	Band	0.55	0.55	0.55	0.298	0.55	0.637	0.5	0.5	0.45	0.55	0.667	0.55
	Band-S	0.525	0.525	0.5	0.372	0.55	0.463	0.55	0.525	0.5	0.55	0.55	0.5
	Band-W	0.55	0.55	0.55	0.315	0.55	0.57	0.55	0.525	0.5	0.525	0.6	0.55
Rec	0.5	0.55	0.5	0.355	0.5	0.44	0.5	0.5	0.5	0.55	0.5	0.5	
200	Random	0.5	0.55	0.55	0.274	0.55	0.67	0.55	0.55	0.45	0.5	0.65	0.55
	Stripe	0.55	0.525	0.55	0.39	0.5	0.479	0.525	0.5	0.5	0.5	0.55	0.55
	Star	0.55	0.5	0.55	0.31	0.55	0.544	0.55	0.55	0.45	0.55	0.6	0.5
	Band	0.55	0.55	0.55	0.303	0.55	0.634	0.5	0.5	0.45	0.55	0.7	0.55
	Band-S	0.525	0.525	0.5	0.392	0.55	0.482	0.55	0.525	0.5	0.55	0.55	0.5
	Band-W	0.55	0.55	0.55	0.319	0.55	0.555	0.55	0.525	0.5	0.525	0.6	0.55
Rec	0.5	0.55	0.5	0.359	0.5	0.458	0.5	0.5	0.5	0.55	0.5	0.5	
300	Random	0.5	0.55	0.55	0.285	0.55	0.666	0.55	0.55	0.45	0.5	0.65	0.55
	Stripe	0.55	0.525	0.55	0.415	0.5	0.473	0.525	0.5	0.5	0.5	0.55	0.55
	Star	0.55	0.5	0.55	0.306	0.55	0.546	0.55	0.55	0.45	0.55	0.6	0.5
	Band	0.55	0.55	0.55	0.301	0.55	0.622	0.5	0.5	0.45	0.55	0.7	0.55
	Band-S	0.525	0.525	0.5	0.366	0.55	0.497	0.55	0.525	0.5	0.55	0.55	0.5
	Band-W	0.55	0.55	0.55	0.298	0.55	0.573	0.55	0.525	0.5	0.525	0.6	0.55
Rec	0.5	0.55	0.5	0.355	0.5	0.448	0.5	0.5	0.5	0.55	0.5	0.5	
400	Random	0.5	0.55	0.55	0.272	0.55	0.678	0.55	0.55	0.45	0.5	0.65	0.55
	Stripe	0.55	0.525	0.55	0.405	0.5	0.482	0.525	0.5	0.5	0.5	0.55	0.55
	Star	0.55	0.5	0.55	0.298	0.55	0.532	0.55	0.55	0.45	0.55	0.6	0.5
	Band	0.55	0.55	0.55	0.297	0.55	0.638	0.5	0.5	0.45	0.55	0.7	0.55
	Band-S	0.525	0.525	0.5	0.378	0.55	0.475	0.55	0.525	0.5	0.55	0.55	0.5
	Band-W	0.55	0.55	0.55	0.315	0.55	0.574	0.55	0.525	0.5	0.525	0.6	0.55
Rec	0.5	0.55	0.5	0.368	0.5	0.429	0.5	0.5	0.5	0.55	0.5	0.5	

Table C.3: Individual Learning, $\rho = 0.67$: Median belief values at different run lengths. Best performance is indicated in bold font. The results which have equal medians with the best performance (in each line) are indicated by light gray color (including the best result in bold). Statistical significance is stated by two-sided pairwise Mann-Whitney-U test with p -value < 0.05.

Iterations	Pattern	DM1	DM2	DM3	DM4	DM5	DM6	DM7	DM8	DM9	DM10	DM11	DM12
10	Random	0.451	0.4	0.347	0.174	0.453	0.434	0.35	0.4	0.442	0.321	0.228	0.399
	Stripe	0.4	0.35	0.4	0.251	0.417	0.349	0.4	0.35	0.395	0.362	0.3	0.4
	Star	0.4	0.329	0.343	0.197	0.385	0.376	0.45	0.386	0.35	0.301	0.298	0.422
	Band	0.451	0.351	0.386	0.205	0.454	0.419	0.4	0.466	0.505	0.348	0.238	0.414
	Band-S	0.4	0.334	0.329	0.235	0.389	0.349	0.372	0.414	0.4	0.35	0.3	0.366
	Band-W	0.4	0.371	0.344	0.191	0.472	0.346	0.403	0.45	0.429	0.316	0.302	0.454
Rec	0.35	0.345	0.315	0.243	0.379	0.366	0.362	0.4	0.359	0.325	0.3	0.4	
50	Random	0.45	0.835	0.595	0.186	0.776	0.803	0.35	0.45	0.45	0.614	0.478	0.534
	Stripe	0.4	0.455	0.5	0.277	0.522	0.397	0.4	0.35	0.4	0.45	0.421	0.462
	Star	0.4	0.473	0.415	0.206	0.453	0.438	0.45	0.4	0.375	0.442	0.375	0.562
	Band	0.45	0.632	0.8	0.217	0.91	0.719	0.4	0.475	0.55	0.706	0.549	0.688
	Band-S	0.4	0.45	0.4	0.247	0.589	0.423	0.4	0.45	0.4	0.425	0.404	0.398
	Band-W	0.4	0.656	0.478	0.223	0.77	0.462	0.4	0.45	0.45	0.526	0.511	0.675
Rec	0.35	0.376	0.428	0.25	0.411	0.364	0.375	0.4	0.4	0.35	0.377	0.499	
100	Random	0.45	1	1	0.181	1	0.799	0.35	0.45	0.45	1	0.999	0.901
	Stripe	0.4	0.55	0.6	0.285	0.6	0.38	0.4	0.35	0.4	0.55	0.492	0.563
	Star	0.4	0.575	0.382	0.211	0.612	0.495	0.45	0.4	0.375	0.564	0.486	0.75
	Band	0.45	1	1	0.212	1	0.739	0.4	0.475	0.55	1	0.866	1
	Band-S	0.4	0.6	0.45	0.24	0.763	0.408	0.4	0.45	0.4	0.45	0.45	0.463
	Band-W	0.4	0.917	0.713	0.208	0.951	0.488	0.4	0.45	0.45	0.71	0.603	0.825
Rec	0.35	0.425	0.5	0.237	0.498	0.397	0.375	0.4	0.4	0.406	0.446	0.568	
200	Random	0.45	1	1	0.185	1	0.82	0.35	0.45	0.45	1	1	1
	Stripe	0.4	0.7	0.75	0.282	0.788	0.38	0.4	0.35	0.4	0.725	0.511	0.65
	Star	0.4	0.905	0.579	0.187	0.65	0.479	0.45	0.4	0.375	0.888	0.569	1
	Band	0.45	1	1	0.212	1	0.773	0.4	0.475	0.55	1	1	1
	Band-S	0.4	0.724	0.599	0.261	0.947	0.391	0.4	0.45	0.4	0.452	0.581	0.6
	Band-W	0.4	1	1	0.234	1	0.49	0.4	0.45	0.45	1	0.943	1
Rec	0.35	0.425	0.6	0.243	0.612	0.405	0.375	0.4	0.4	0.647	0.45	0.873	
300	Random	0.45	1	1	0.178	1	0.833	0.35	0.45	0.45	1	1	1
	Stripe	0.4	0.847	0.85	0.273	0.85	0.39	0.4	0.35	0.4	0.8	0.55	0.7
	Star	0.4	1	0.979	0.2	0.719	0.523	0.45	0.4	0.375	1	0.95	1
	Band	0.45	1	1	0.211	1	0.782	0.4	0.475	0.55	1	1	1
	Band-S	0.4	0.825	0.625	0.259	1	0.415	0.4	0.45	0.4	0.649	0.55	0.737
	Band-W	0.4	1	1	0.199	1	0.541	0.4	0.45	0.45	1	1	1
Rec	0.35	0.624	0.785	0.242	0.679	0.334	0.375	0.4	0.4	0.728	0.6	0.95	
400	Random	0.45	1	1	0.2	1	0.821	0.35	0.45	0.45	1	1	1
	Stripe	0.4	0.88	0.85	0.28	0.944	0.381	0.4	0.35	0.4	0.9	0.572	0.775
	Star	0.4	1	1	0.216	0.885	0.472	0.45	0.4	0.375	1	1	1
	Band	0.45	1	1	0.197	1	0.755	0.4	0.475	0.55	1	1	1
	Band-S	0.4	0.975	0.675	0.257	1	0.405	0.4	0.45	0.4	0.578	0.7	0.85
	Band-W	0.4	1	1	0.216	1	0.489	0.4	0.45	0.45	1	1	1
Rec	0.35	0.75	0.946	0.251	0.83	0.363	0.375	0.4	0.4	0.95	0.547	1	

Table C.4: Collective Learning, $\rho = 0.93$: Median belief values at different run lengths. Best performance is indicated in bold font. The results which have equal medians with the best performance (in each line) are indicated by light gray color (including the best result in bold). Statistical significance is stated by two-sided pairwise Mann-Whitney-U test with p -value < 0.05 .

Iterations	Pattern	DM1	DM2	DM3	DM4	DM5	DM6	DM7	DM8	DM9	DM10	DM11	DM12
10	Random	0.457	0.373	0.372	0.208	0.443	0.372	0.45	0.438	0.437	0.348	0.228	0.381
	Stripe	0.4	0.399	0.347	0.309	0.385	0.363	0.4	0.4	0.35	0.35	0.3	0.356
	Star	0.397	0.313	0.318	0.197	0.353	0.366	0.399	0.4	0.362	0.372	0.26	0.345
	Band	0.403	0.351	0.343	0.225	0.474	0.325	0.462	0.44	0.45	0.3	0.252	0.344
	Band-S	0.397	0.382	0.392	0.264	0.415	0.324	0.4	0.4	0.4	0.351	0.3	0.372
	Band-W	0.402	0.368	0.328	0.238	0.41	0.371	0.401	0.45	0.4	0.298	0.303	0.354
	Rec	0.369	0.35	0.301	0.253	0.392	0.326	0.377	0.392	0.35	0.35	0.294	0.351
50	Random	0.5	0.789	0.743	0.203	0.77	0.611	0.45	0.45	0.5	0.702	0.437	0.398
	Stripe	0.4	0.5	0.443	0.304	0.46	0.365	0.4	0.4	0.4	0.456	0.398	0.44
	Star	0.4	0.445	0.413	0.217	0.423	0.41	0.4	0.4	0.4	0.486	0.336	0.419
	Band	0.45	0.685	0.654	0.267	0.758	0.574	0.5	0.5	0.5	0.56	0.454	0.394
	Band-S	0.4	0.525	0.453	0.292	0.566	0.366	0.4	0.4	0.4	0.45	0.415	0.415
	Band-W	0.45	0.597	0.49	0.252	0.639	0.433	0.4	0.45	0.41	0.501	0.443	0.375
	Rec	0.4	0.404	0.316	0.248	0.508	0.34	0.4	0.4	0.35	0.415	0.364	0.332
100	Random	0.5	1	1	0.191	1	0.657	0.45	0.45	0.5	1	0.601	0.415
	Stripe	0.4	0.623	0.5	0.307	0.549	0.398	0.4	0.4	0.4	0.573	0.421	0.561
	Star	0.4	0.536	0.423	0.25	0.538	0.426	0.4	0.4	0.4	0.529	0.372	0.453
	Band	0.45	1	0.872	0.234	0.996	0.592	0.5	0.5	0.5	0.974	0.515	0.43
	Band-S	0.4	0.608	0.546	0.285	0.67	0.395	0.4	0.4	0.4	0.535	0.449	0.387
	Band-W	0.45	0.701	0.497	0.246	0.711	0.434	0.4	0.45	0.425	0.674	0.595	0.391
	Rec	0.4	0.427	0.369	0.265	0.522	0.383	0.4	0.4	0.35	0.522	0.444	0.443
200	Random	0.5	1	1	0.194	1	0.661	0.45	0.45	0.5	1	0.878	0.399
	Stripe	0.4	0.75	0.55	0.321	0.689	0.383	0.4	0.4	0.4	0.7	0.515	0.625
	Star	0.4	0.655	0.516	0.236	0.616	0.399	0.4	0.4	0.4	0.61	0.417	0.397
	Band	0.45	1	1	0.226	1	0.539	0.5	0.5	0.5	1	0.804	0.364
	Band-S	0.4	0.8	0.728	0.305	0.792	0.422	0.4	0.4	0.4	0.741	0.501	0.42
	Band-W	0.45	1	0.611	0.259	0.963	0.429	0.4	0.45	0.425	0.895	0.65	0.433
	Rec	0.4	0.595	0.534	0.245	0.623	0.34	0.4	0.4	0.35	0.658	0.449	0.483
300	Random	0.5	1	1	0.196	1	0.668	0.45	0.45	0.5	1	1	0.46
	Stripe	0.4	0.85	0.636	0.29	0.73	0.35	0.4	0.4	0.4	0.75	0.5	0.6
	Star	0.4	0.83	0.608	0.242	0.631	0.453	0.4	0.4	0.4	0.626	0.355	0.404
	Band	0.45	1	1	0.241	1	0.543	0.45	0.5	0.5	1	1	0.397
	Band-S	0.4	0.9	0.9	0.291	0.916	0.41	0.4	0.4	0.4	0.922	0.573	0.496
	Band-W	0.45	1	0.95	0.255	1	0.413	0.4	0.45	0.425	1	0.825	0.396
	Rec	0.4	0.793	0.723	0.255	0.676	0.356	0.4	0.4	0.35	0.842	0.51	0.409
400	Random	0.5	1	1	0.203	1	0.631	0.45	0.45	0.5	1	1	0.373
	Stripe	0.4	0.95	0.75	0.296	0.769	0.378	0.4	0.4	0.4	0.762	0.6	0.701
	Star	0.4	0.98	0.704	0.228	0.716	0.407	0.4	0.4	0.4	0.684	0.421	0.4
	Band	0.45	1	1	0.238	1	0.531	0.45	0.5	0.5	1	1	0.441
	Band-S	0.4	1	1	0.289	1	0.395	0.4	0.4	0.4	1	0.65	0.585
	Band-W	0.45	1	1	0.258	1	0.396	0.4	0.45	0.425	1	1	0.384
	Rec	0.4	0.871	0.7	0.26	0.73	0.377	0.4	0.4	0.35	0.938	0.628	0.516

Table C.5: Social Learning, $\rho = 0.93$: Median belief values at different run lengths. Best performance is indicated in bold font. The results which have equal medians with the best performance (in each line) are indicated by light gray color (including the best result in bold). Statistical significance is stated by two-sided pairwise Mann-Whitney-U test with p -value < 0.05 .

Iterations	Pattern	DM1	DM2	DM3	DM4	DM5	DM6	DM7	DM8	DM9	DM10	DM11	DM12
10	Random	0.351	0.339	0.348	0.156	0.352	0.275	0.354	0.38	0.312	0.36	0.283	0.378
	Stripe	0.399	0.393	0.395	0.255	0.399	0.333	0.4	0.35	0.384	0.365	0.381	0.39
	Star	0.35	0.349	0.347	0.168	0.373	0.29	0.347	0.345	0.348	0.351	0.334	0.355
	Band	0.385	0.373	0.364	0.174	0.388	0.308	0.362	0.382	0.316	0.353	0.307	0.375
	Band-S	0.38	0.353	0.35	0.211	0.372	0.329	0.376	0.35	0.35	0.36	0.353	0.35
	Band-W	0.398	0.392	0.39	0.175	0.383	0.321	0.399	0.394	0.363	0.39	0.376	0.388
Rec	0.35	0.365	0.349	0.215	0.353	0.285	0.357	0.35	0.35	0.365	0.358	0.374	
50	Random	0.35	0.4	0.4	0.163	0.4	0.338	0.375	0.4	0.365	0.4	0.371	0.4
	Stripe	0.4	0.4	0.4	0.274	0.4	0.336	0.4	0.35	0.4	0.4	0.4	0.4
	Star	0.35	0.4	0.375	0.174	0.4	0.325	0.35	0.35	0.379	0.4	0.4	0.35
	Band	0.4	0.4	0.4	0.175	0.4	0.359	0.4	0.4	0.35	0.4	0.4	0.4
	Band-S	0.4	0.4	0.4	0.242	0.399	0.338	0.4	0.4	0.35	0.4	0.4	0.397
	Band-W	0.4	0.4	0.4	0.207	0.4	0.345	0.4	0.4	0.4	0.4	0.4	0.4
Rec	0.35	0.4	0.35	0.233	0.4	0.33	0.375	0.375	0.35	0.4	0.4	0.4	
100	Random	0.35	0.4	0.4	0.16	0.4	0.375	0.375	0.4	0.372	0.4	0.4	0.4
	Stripe	0.4	0.4	0.4	0.281	0.4	0.341	0.4	0.35	0.4	0.4	0.4	0.4
	Star	0.35	0.4	0.375	0.195	0.4	0.344	0.35	0.35	0.398	0.4	0.4	0.35
	Band	0.4	0.4	0.4	0.183	0.4	0.354	0.4	0.4	0.35	0.4	0.449	0.4
	Band-S	0.4	0.4	0.4	0.236	0.4	0.325	0.4	0.4	0.35	0.4	0.4	0.4
	Band-W	0.4	0.4	0.4	0.199	0.4	0.348	0.4	0.4	0.4	0.4	0.4	0.4
Rec	0.35	0.4	0.35	0.21	0.4	0.327	0.375	0.375	0.35	0.4	0.4	0.4	
200	Random	0.35	0.4	0.4	0.156	0.4	0.365	0.375	0.4	0.375	0.4	0.442	0.4
	Stripe	0.4	0.4	0.4	0.281	0.4	0.333	0.4	0.35	0.4	0.4	0.4	0.4
	Star	0.35	0.4	0.375	0.184	0.4	0.334	0.35	0.35	0.4	0.4	0.4	0.35
	Band	0.4	0.4	0.4	0.186	0.4	0.371	0.4	0.4	0.35	0.4	0.45	0.4
	Band-S	0.4	0.4	0.4	0.244	0.4	0.336	0.4	0.4	0.35	0.4	0.4	0.4
	Band-W	0.4	0.4	0.4	0.206	0.4	0.331	0.4	0.4	0.4	0.4	0.4	0.4
Rec	0.35	0.4	0.35	0.219	0.4	0.315	0.375	0.375	0.35	0.4	0.4	0.4	
300	Random	0.35	0.4	0.4	0.157	0.4	0.382	0.375	0.4	0.375	0.4	0.425	0.4
	Stripe	0.4	0.4	0.4	0.277	0.4	0.339	0.4	0.35	0.4	0.4	0.4	0.4
	Star	0.35	0.4	0.375	0.187	0.4	0.323	0.35	0.35	0.4	0.4	0.4	0.35
	Band	0.4	0.4	0.4	0.173	0.4	0.368	0.4	0.4	0.35	0.4	0.45	0.4
	Band-S	0.4	0.4	0.4	0.234	0.4	0.325	0.4	0.4	0.35	0.4	0.4	0.4
	Band-W	0.4	0.4	0.4	0.189	0.4	0.327	0.4	0.4	0.4	0.4	0.4	0.4
Rec	0.35	0.4	0.35	0.237	0.4	0.326	0.375	0.375	0.35	0.4	0.4	0.4	
400	Random	0.35	0.4	0.4	0.161	0.4	0.377	0.375	0.4	0.375	0.4	0.425	0.4
	Stripe	0.4	0.4	0.4	0.276	0.4	0.341	0.4	0.35	0.4	0.4	0.4	0.4
	Star	0.35	0.4	0.375	0.21	0.4	0.351	0.35	0.35	0.4	0.4	0.4	0.35
	Band	0.4	0.4	0.4	0.184	0.4	0.364	0.4	0.4	0.35	0.4	0.45	0.4
	Band-S	0.4	0.4	0.4	0.257	0.4	0.351	0.4	0.4	0.35	0.4	0.4	0.4
	Band-W	0.4	0.4	0.4	0.205	0.4	0.33	0.4	0.4	0.4	0.4	0.4	0.4
Rec	0.35	0.4	0.35	0.226	0.4	0.316	0.375	0.375	0.35	0.4	0.4	0.4	

Table C.6: Individual Learning, $\rho = 0.93$: Median belief values at different run lengths. Best performance is indicated in bold font. The results which have equal medians with the best performance (in each line) are indicated by light gray color (including the best result in bold). Statistical significance is stated by two-sided pairwise Mann-Whitney-U test with p -value < 0.05 .

C.2 Statistical comparison - I: Collective, Social, and Individual Learning

	Random	Stripe	Star	Band	Band-S	Band-W	Rec
CL-DM1	0.7	0.5	0.551	0.602	0.5	0.612	0.5
SL-DM1	0.678	0.5	0.627	0.686	0.541	0.6	0.5
IND-DM1	0.486	0.5	0.504	0.508	0.5	0.5	0.5
CL-DM2	0.669	0.5	0.55	0.636	0.527	0.598	0.5
SL-DM2	0.619	0.495	0.547	0.594	0.507	0.606	0.516
IND-DM2	0.478	0.5	0.453	0.493	0.494	0.481	0.5
CL-DM3	0.632	0.482	0.541	0.605	0.5	0.559	0.55
SL-DM3	0.61	0.477	0.55	0.611	0.499	0.594	0.456
IND-DM3	0.495	0.5	0.459	0.471	0.492	0.497	0.45
CL-DM4	0.286	0.38	0.286	0.312	0.339	0.28	0.327
SL-DM4	0.353	0.461	0.367	0.359	0.39	0.362	0.383
IND-DM4	0.242	0.337	0.268	0.261	0.32	0.25	0.335
CL-DM5	0.674	0.526	0.599	0.676	0.543	0.649	0.519
SL-DM5	0.69	0.521	0.606	0.682	0.529	0.643	0.526
IND-DM5	0.488	0.5	0.52	0.512	0.489	0.498	0.5
CL-DM6	0.709	0.491	0.594	0.658	0.526	0.582	0.521
SL-DM6	0.7	0.503	0.589	0.671	0.476	0.613	0.499
IND-DM6	0.448	0.457	0.445	0.443	0.425	0.412	0.441
CL-DM7	0.709	0.5	0.6	0.7	0.527	0.55	0.5
SL-DM7	0.674	0.517	0.603	0.703	0.539	0.573	0.5
IND-DM7	0.505	0.5	0.498	0.469	0.5	0.522	0.496
CL-DM8	0.703	0.5	0.55	0.65	0.516	0.6	0.5
SL-DM8	0.682	0.5	0.561	0.653	0.546	0.575	0.5
IND-DM8	0.512	0.5	0.5	0.498	0.5	0.498	0.5
CL-DM9	0.75	0.502	0.55	0.75	0.541	0.566	0.5
SL-DM9	0.702	0.518	0.558	0.623	0.513	0.646	0.5
IND-DM9	0.401	0.5	0.432	0.418	0.474	0.45	0.477
CL-DM10	0.61	0.464	0.568	0.642	0.491	0.584	0.5
SL-DM10	0.634	0.546	0.55	0.639	0.535	0.554	0.5
IND-DM10	0.463	0.5	0.47	0.493	0.508	0.458	0.5
CL-DM11	0.479	0.45	0.444	0.504	0.487	0.494	0.429
SL-DM11	0.518	0.45	0.466	0.502	0.45	0.489	0.4
IND-DM11	0.423	0.507	0.473	0.462	0.5	0.474	0.485
CL-DM12	0.579	0.55	0.536	0.659	0.561	0.593	0.5
SL-DM12	0.519	0.544	0.517	0.49	0.487	0.525	0.5
IND-DM12	0.489	0.5	0.477	0.494	0.47	0.5	0.498

Table C.7: Median values after 10 iterations. Best performance is indicated in bold font. The results which have equal medians with the best performance (in each line) are indicated by light gray color (including the best result in bold). Statistical significance is stated by two-sided pairwise Mann-Whitney-U test with p -value < 0.05.

	Random	Stripe	Star	Band	Band-S	Band-W	Rec
CL-DM1	0.7	0.55	0.6	0.65	0.55	0.65	0.55
SL-DM1	0.75	0.55	0.65	0.7	0.55	0.6	0.55
IND-DM1	0.5	0.55	0.55	0.55	0.5	0.55	0.5
CL-DM2	1	0.55	0.991	1	0.7	1	0.668
SL-DM2	1	0.6	0.9	1	0.704	1	0.679
IND-DM2	0.55	0.525	0.5	0.55	0.525	0.55	0.55
CL-DM3	1	0.597	0.95	1	0.7	1	0.7
SL-DM3	1	0.551	0.834	1	0.709	0.95	0.65
IND-DM3	0.55	0.55	0.55	0.55	0.5	0.55	0.5
CL-DM4	0.33	0.396	0.34	0.354	0.38	0.348	0.39
SL-DM4	0.382	0.43	0.39	0.413	0.436	0.392	0.403
IND-DM4	0.284	0.424	0.317	0.286	0.393	0.297	0.354
CL-DM5	1	0.6	0.888	1	0.803	1	0.681
SL-DM5	1	0.569	0.848	1	0.707	0.999	0.678
IND-DM5	0.55	0.5	0.55	0.55	0.55	0.55	0.5
CL-DM6	0.915	0.545	0.792	0.898	0.605	0.828	0.557
SL-DM6	0.886	0.489	0.721	0.838	0.592	0.74	0.512
IND-DM6	0.615	0.462	0.532	0.584	0.496	0.535	0.442
CL-DM7	0.75	0.55	0.65	0.725	0.55	0.55	0.507
SL-DM7	0.75	0.55	0.65	0.75	0.55	0.6	0.5
IND-DM7	0.55	0.525	0.55	0.5	0.55	0.55	0.5
CL-DM8	0.75	0.55	0.6	0.7	0.525	0.65	0.5
SL-DM8	0.75	0.5	0.6	0.725	0.55	0.6	0.525
IND-DM8	0.55	0.5	0.55	0.5	0.525	0.525	0.5
CL-DM9	0.85	0.524	0.575	0.85	0.55	0.6	0.5
SL-DM9	0.8	0.55	0.6	0.75	0.55	0.668	0.5
IND-DM9	0.45	0.5	0.45	0.45	0.5	0.5	0.5
CL-DM10	1	0.6	0.95	1	0.7	1	0.69
SL-DM10	1	0.618	0.862	1	0.7	0.95	0.647
IND-DM10	0.5	0.5	0.55	0.55	0.55	0.525	0.55
CL-DM11	1	0.502	0.897	1	0.625	0.887	0.522
SL-DM11	1	0.5	0.757	0.991	0.55	0.898	0.545
IND-DM11	0.635	0.55	0.558	0.644	0.55	0.6	0.5
CL-DM12	1	0.587	0.9	1	0.8	0.95	0.65
SL-DM12	0.688	0.598	0.654	0.758	0.594	0.693	0.59
IND-DM12	0.55	0.55	0.5	0.55	0.5	0.55	0.5

Table C.8: Median values after 50 iterations. Best performance is indicated in bold font. The results which have equal medians with the best performance (in each line) are indicated by light gray color (including the best result in bold). Statistical significance is stated by two-sided pairwise Mann-Whitney-U test with p -value<0.05.

	Random	Stripe	Star	Band	Band-S	Band-W	Rec
CL-DM1	0.7	0.55	0.6	0.65	0.55	0.65	0.55
SL-DM1	0.75	0.55	0.65	0.7	0.55	0.6	0.55
IND-DM1	0.5	0.55	0.55	0.55	0.525	0.55	0.5
CL-DM2	1	0.616	1	1	0.85	1	0.8
SL-DM2	1	0.66	1	1	0.85	1	0.823
IND-DM2	0.55	0.525	0.5	0.55	0.525	0.55	0.55
CL-DM3	1	0.605	1	1	0.8	1	0.85
SL-DM3	1	0.573	1	1	0.9	1	0.849
IND-DM3	0.55	0.55	0.55	0.55	0.5	0.55	0.5
CL-DM4	0.321	0.394	0.342	0.383	0.389	0.342	0.389
SL-DM4	0.375	0.446	0.419	0.388	0.431	0.379	0.388
IND-DM4	0.281	0.418	0.307	0.298	0.372	0.315	0.355
CL-DM5	1	0.654	1	1	0.923	1	0.834
SL-DM5	1	0.644	1	1	0.875	1	0.779
IND-DM5	0.55	0.5	0.55	0.55	0.55	0.55	0.5
CL-DM6	0.921	0.501	0.771	0.877	0.609	0.824	0.545
SL-DM6	0.871	0.507	0.687	0.828	0.556	0.744	0.498
IND-DM6	0.637	0.483	0.554	0.637	0.463	0.57	0.44
CL-DM7	0.75	0.55	0.65	0.725	0.55	0.55	0.525
SL-DM7	0.75	0.55	0.65	0.75	0.55	0.6	0.5
IND-DM7	0.55	0.525	0.55	0.5	0.55	0.55	0.5
CL-DM8	0.75	0.55	0.6	0.7	0.525	0.65	0.5
SL-DM8	0.75	0.5	0.6	0.725	0.55	0.6	0.525
IND-DM8	0.55	0.5	0.55	0.5	0.525	0.525	0.5
CL-DM9	0.85	0.527	0.575	0.85	0.55	0.6	0.5
SL-DM9	0.8	0.55	0.6	0.75	0.55	0.675	0.5
IND-DM9	0.45	0.5	0.45	0.45	0.5	0.5	0.5
CL-DM10	1	0.625	1	1	0.862	1	0.85
SL-DM10	1	0.652	1	1	0.824	1	0.8
IND-DM10	0.5	0.5	0.55	0.55	0.55	0.525	0.55
CL-DM11	1	0.546	1	1	0.75	1	0.55
SL-DM11	1	0.5	0.955	1	0.661	1	0.639
IND-DM11	0.65	0.55	0.6	0.667	0.55	0.6	0.5
CL-DM12	1	0.6	1	1	0.9	1	0.825
SL-DM12	0.757	0.6	0.668	0.757	0.639	0.778	0.66
IND-DM12	0.55	0.55	0.5	0.55	0.5	0.55	0.5

Table C.9: Median values after 100 iterations. Best performance is indicated in bold font. The results which have equal medians with the best performance (in each line) are indicated by light gray color (including the best result in bold). Statistical significance is stated by two-sided pairwise Mann-Whitney-U test with p -value < 0.05.

	Random	Stripe	Star	Band	Band-S	Band-W	Rec
CL-DM1	0.7	0.55	0.6	0.65	0.55	0.65	0.55
SL-DM1	0.75	0.55	0.65	0.7	0.55	0.6	0.55
IND-DM1	0.5	0.55	0.55	0.55	0.525	0.55	0.5
CL-DM2	1	0.683	1	1	1	1	0.95
SL-DM2	1	0.8	1	1	1	1	0.95
IND-DM2	0.55	0.525	0.5	0.55	0.525	0.55	0.55
CL-DM3	1	0.75	1	1	1	1	0.95
SL-DM3	1	0.712	1	1	1	1	1
IND-DM3	0.55	0.55	0.55	0.55	0.5	0.55	0.5
CL-DM4	0.349	0.402	0.358	0.372	0.38	0.377	0.368
SL-DM4	0.387	0.461	0.399	0.398	0.435	0.41	0.405
IND-DM4	0.274	0.39	0.31	0.303	0.392	0.319	0.359
CL-DM5	1	0.762	1	1	1	1	0.949
SL-DM5	1	0.703	1	1	1	1	0.933
IND-DM5	0.55	0.5	0.55	0.55	0.55	0.55	0.5
CL-DM6	0.917	0.505	0.769	0.895	0.586	0.823	0.516
SL-DM6	0.874	0.472	0.673	0.831	0.582	0.758	0.552
IND-DM6	0.67	0.479	0.544	0.634	0.482	0.555	0.458
CL-DM7	0.75	0.55	0.65	0.725	0.55	0.55	0.525
SL-DM7	0.75	0.55	0.65	0.75	0.55	0.55	0.5
IND-DM7	0.55	0.525	0.55	0.5	0.55	0.55	0.5
CL-DM8	0.75	0.55	0.6	0.7	0.525	0.65	0.5
SL-DM8	0.75	0.5	0.6	0.725	0.55	0.6	0.525
IND-DM8	0.55	0.5	0.55	0.5	0.525	0.525	0.5
CL-DM9	0.85	0.525	0.575	0.85	0.55	0.6	0.5
SL-DM9	0.8	0.55	0.6	0.75	0.55	0.675	0.5
IND-DM9	0.45	0.5	0.45	0.45	0.5	0.5	0.5
CL-DM10	1	0.75	1	1	1	1	1
SL-DM10	1	0.75	1	1	1	1	0.975
IND-DM10	0.5	0.5	0.55	0.55	0.55	0.525	0.55
CL-DM11	1	0.594	1	1	0.937	1	0.75
SL-DM11	1	0.591	1	1	0.75	1	0.787
IND-DM11	0.65	0.55	0.6	0.7	0.55	0.6	0.5
CL-DM12	1	0.725	1	1	1	1	0.95
SL-DM12	0.732	0.709	0.739	0.737	0.826	0.731	0.8
IND-DM12	0.55	0.55	0.5	0.55	0.5	0.55	0.5

Table C.10: Median values after 200 iterations. Best performance is indicated in bold font. The results which have equal medians with the best performance (in each line) are indicated by light gray color (including the best result in bold). Statistical significance is stated by two-sided pairwise Mann-Whitney-U test with p -value<0.05.

	Random	Stripe	Star	Band	Band-S	Band-W	Rec
CL-DM1	0.7	0.55	0.6	0.65	0.55	0.65	0.55
SL-DM1	0.75	0.55	0.65	0.7	0.55	0.6	0.55
IND-DM1	0.5	0.55	0.55	0.55	0.525	0.55	0.5
CL-DM2	1	0.7	1	1	1	1	1
SL-DM2	1	0.9	1	1	1	1	1
IND-DM2	0.55	0.525	0.5	0.55	0.525	0.55	0.55
CL-DM3	1	0.85	1	1	1	1	1
SL-DM3	1	0.757	1	1	1	1	1
IND-DM3	0.55	0.55	0.55	0.55	0.5	0.55	0.5
CL-DM4	0.332	0.416	0.338	0.368	0.392	0.361	0.376
SL-DM4	0.403	0.44	0.404	0.429	0.441	0.394	0.415
IND-DM4	0.285	0.415	0.306	0.301	0.366	0.298	0.355
CL-DM5	1	0.846	1	1	1	1	1
SL-DM5	1	0.741	1	1	1	1	1
IND-DM5	0.55	0.5	0.55	0.55	0.55	0.55	0.5
CL-DM6	0.925	0.509	0.794	0.891	0.572	0.837	0.555
SL-DM6	0.899	0.524	0.708	0.828	0.544	0.751	0.531
IND-DM6	0.666	0.473	0.546	0.622	0.497	0.573	0.448
CL-DM7	0.75	0.55	0.65	0.725	0.55	0.55	0.525
SL-DM7	0.75	0.55	0.65	0.75	0.525	0.55	0.5
IND-DM7	0.55	0.525	0.55	0.5	0.55	0.55	0.5
CL-DM8	0.75	0.55	0.6	0.7	0.525	0.65	0.5
SL-DM8	0.75	0.5	0.6	0.725	0.55	0.6	0.525
IND-DM8	0.55	0.5	0.55	0.5	0.525	0.525	0.5
CL-DM9	0.85	0.525	0.6	0.85	0.55	0.6	0.5
SL-DM9	0.8	0.55	0.6	0.75	0.55	0.675	0.5
IND-DM9	0.45	0.5	0.45	0.45	0.5	0.5	0.5
CL-DM10	1	0.759	1	1	1	1	1
SL-DM10	1	0.9	1	1	1	1	1
IND-DM10	0.5	0.5	0.55	0.55	0.55	0.525	0.55
CL-DM11	1	0.6	1	1	1	1	0.85
SL-DM11	1	0.6	1	1	0.85	1	0.914
IND-DM11	0.65	0.55	0.6	0.7	0.55	0.6	0.5
CL-DM12	1	0.8	1	1	1	1	1
SL-DM12	0.76	0.772	0.743	0.738	0.825	0.808	0.818
IND-DM12	0.55	0.55	0.5	0.55	0.5	0.55	0.5

Table C.11: Median values after 300 iterations. Best performance is indicated in bold font. The results which have equal medians with the best performance (in each line) are indicated by light gray color (including the best result in bold). Statistical significance is stated by two-sided pairwise Mann-Whitney-U test with p -value < 0.05.

	Random	Stripe	Star	Band	Band-S	Band-W	Rec
CL-DM1	0.7	0.55	0.6	0.65	0.55	0.65	0.55
SL-DM1	0.75	0.55	0.65	0.7	0.55	0.6	0.55
IND-DM1	0.5	0.55	0.55	0.55	0.525	0.55	0.5
CL-DM2	1	0.75	1	1	1	1	1
SL-DM2	1	0.9	1	1	1	1	1
IND-DM2	0.55	0.525	0.5	0.55	0.525	0.55	0.55
CL-DM3	1	0.85	1	1	1	1	1
SL-DM3	1	0.9	1	1	1	1	1
IND-DM3	0.55	0.55	0.55	0.55	0.5	0.55	0.5
CL-DM4	0.356	0.441	0.359	0.35	0.39	0.348	0.367
SL-DM4	0.386	0.446	0.398	0.407	0.441	0.398	0.394
IND-DM4	0.272	0.405	0.298	0.297	0.378	0.315	0.368
CL-DM5	1	0.917	1	1	1	1	1
SL-DM5	1	0.781	1	1	1	1	1
IND-DM5	0.55	0.5	0.55	0.55	0.55	0.55	0.5
CL-DM6	0.91	0.504	0.789	0.893	0.56	0.825	0.569
SL-DM6	0.886	0.54	0.681	0.832	0.57	0.753	0.553
IND-DM6	0.678	0.482	0.532	0.638	0.475	0.574	0.429
CL-DM7	0.75	0.55	0.65	0.725	0.55	0.55	0.525
SL-DM7	0.775	0.55	0.65	0.75	0.5	0.55	0.5
IND-DM7	0.55	0.525	0.55	0.5	0.55	0.55	0.5
CL-DM8	0.75	0.55	0.6	0.7	0.525	0.65	0.5
SL-DM8	0.75	0.5	0.6	0.725	0.55	0.6	0.525
IND-DM8	0.55	0.5	0.55	0.5	0.525	0.525	0.5
CL-DM9	0.85	0.525	0.6	0.85	0.55	0.6	0.5
SL-DM9	0.8	0.55	0.6	0.75	0.55	0.675	0.5
IND-DM9	0.45	0.5	0.45	0.45	0.5	0.5	0.5
CL-DM10	1	0.85	1	1	1	1	1
SL-DM10	1	0.95	1	1	1	1	1
IND-DM10	0.5	0.5	0.55	0.55	0.55	0.525	0.55
CL-DM11	1	0.6	1	1	1	1	0.975
SL-DM11	1	0.6	1	1	1	1	1
IND-DM11	0.65	0.55	0.6	0.7	0.55	0.6	0.5
CL-DM12	1	0.85	1	1	1	1	1
SL-DM12	0.77	0.763	0.7	0.767	0.868	0.792	0.843
IND-DM12	0.55	0.55	0.5	0.55	0.5	0.55	0.5

Table C.12: Median values after 400 iterations. Best performance is indicated in bold font. The results which have equal medians with the best performance (in each line) are indicated by light gray color (including the best result in bold). Statistical significance is stated by two-sided pairwise Mann-Whitney-U test with p -value<0.05.

C.2.1 Collective vs Social Learning, $\rho = 0.67$

Iterations	Pattern	DM1	DM2	DM3	DM4	DM5	DM6	DM7	DM8	DM9	DM10	DM11	DM12
10	Random	7.8e-01	9.6e-01	8.1e-01	7.4e-07	3.7e-01	5.5e-01	9.6e-01	8.7e-01	8.9e-01	4.2e-01	9.8e-02	9.9e-01
	Stripe	4.9e-01	4.6e-01	3.5e-01	2.1e-07	4.5e-01	5.5e-01	7.2e-01	7.9e-01	5.5e-01	1.4e-02	5.9e-01	3.6e-01
	Star	5.3e-02	9.3e-01	4.6e-01	2.0e-06	3.6e-01	5.8e-01	4.2e-01	1.3e-01	4.0e-01	6.2e-01	2.1e-01	8.0e-01
	Band	1.5e-01	8.1e-01	7.3e-01	8.0e-05	5.0e-01	5.4e-01	7.6e-01	4.4e-01	1.0e+00	3.0e-01	5.3e-01	1.0e+00
	Band-S	3.1e-01	4.7e-01	7.3e-01	5.7e-04	6.4e-01	9.7e-01	4.4e-01	3.0e-01	6.4e-01	1.7e-01	9.1e-01	1.0e+00
	Band-W	7.7e-01	2.6e-01	1.3e-01	6.8e-06	6.6e-01	3.7e-01	1.2e-01	9.1e-01	3.6e-02	8.4e-01	1.5e-01	1.0e+00
Rec	3.5e-01	1.2e-01	9.4e-01	3.2e-03	2.3e-01	7.5e-01	5.0e-01	1.6e-01	3.1e-01	7.0e-01	8.7e-01	5.9e-01	
50	Random	1.8e-01	8.5e-01	5.5e-01	3.0e-04	6.5e-01	1.0e+00	6.2e-01	3.8e-01	5.6e-01	7.0e-01	1.0e+00	1.0e+00
	Stripe	5.0e-01	1.2e-01	4.0e-01	2.1e-02	8.9e-01	1.0e+00	7.5e-01	8.5e-01	4.7e-01	5.9e-02	5.6e-01	6.4e-01
	Star	7.8e-02	9.8e-01	1.0e+00	1.5e-04	7.3e-01	9.8e-01	3.1e-01	2.4e-01	2.6e-01	8.7e-01	9.6e-01	1.0e+00
	Band	5.0e-02	9.6e-01	9.4e-01	6.3e-04	9.9e-01	1.0e+00	3.9e-01	3.7e-01	9.8e-01	6.9e-01	1.0e+00	1.0e+00
	Band-S	3.6e-01	6.5e-01	2.8e-01	8.5e-05	9.9e-01	9.0e-01	5.2e-01	3.1e-01	8.3e-01	3.6e-01	9.9e-01	1.0e+00
	Band-W	8.3e-01	6.9e-01	9.8e-01	6.2e-05	8.4e-01	1.0e+00	1.9e-01	9.8e-01	8.1e-02	7.8e-01	3.5e-01	1.0e+00
Rec	4.0e-01	4.7e-01	7.6e-01	6.2e-02	5.8e-01	9.6e-01	7.5e-01	2.8e-01	3.8e-01	9.7e-01	5.8e-01	8.4e-01	
100	Random	1.8e-01	3.2e-01	1.6e-01	3.1e-04	3.4e-01	1.0e+00	6.2e-01	3.8e-01	5.6e-01	9.1e-01	8.7e-01	1.0e+00
	Stripe	5.0e-01	1.1e-01	5.8e-01	1.6e-03	8.6e-01	2.3e-01	7.8e-01	8.5e-01	4.8e-01	7.9e-02	7.4e-01	5.0e-01
	Star	7.7e-02	9.2e-01	9.5e-01	2.1e-07	9.1e-01	1.0e+00	2.7e-01	2.4e-01	2.6e-01	6.9e-01	9.9e-01	1.0e+00
	Band	5.0e-02	7.7e-01	4.9e-01	2.2e-01	9.2e-01	1.0e+00	4.2e-01	3.8e-01	9.8e-01	1.9e-01	8.9e-01	1.0e+00
	Band-S	3.6e-01	6.2e-01	8.2e-02	1.4e-03	9.6e-01	1.0e+00	5.7e-01	3.1e-01	8.3e-01	4.1e-01	9.5e-01	1.0e+00
	Band-W	8.3e-01	1.6e-01	8.6e-01	1.3e-03	9.1e-01	1.0e+00	2.7e-01	9.8e-01	7.3e-02	5.5e-01	5.6e-01	1.0e+00
Rec	4.0e-01	2.5e-01	4.7e-01	2.3e-01	6.3e-01	9.7e-01	7.5e-01	2.9e-01	4.0e-01	9.2e-01	7.3e-02	9.9e-01	
200	Random	1.8e-01	7.9e-02	4.5e-02	9.6e-04	7.9e-02	1.0e+00	5.1e-01	3.8e-01	5.6e-01	8.4e-01	1.6e-01	1.0e+00
	Stripe	5.0e-01	5.1e-02	3.6e-01	1.6e-04	9.8e-01	9.1e-01	7.9e-01	8.5e-01	4.6e-01	1.2e-01	4.6e-01	8.1e-01
	Star	7.7e-02	7.2e-01	8.3e-01	1.5e-03	1.0e+00	1.0e+00	2.3e-01	2.4e-01	2.6e-01	2.2e-01	8.8e-01	1.0e+00
	Band	5.0e-02	2.8e-01	4.8e-01	2.5e-03	7.2e-01	1.0e+00	5.3e-01	3.8e-01	9.8e-01	8.1e-03	7.2e-01	1.0e+00
	Band-S	3.6e-01	5.8e-01	4.2e-01	9.2e-04	9.9e-01	6.4e-01	6.4e-01	3.1e-01	8.3e-01	3.3e-01	9.9e-01	1.0e+00
	Band-W	8.3e-01	1.2e-02	3.5e-01	5.0e-03	1.0e+00	1.0e+00	4.0e-01	9.8e-01	7.2e-02	8.3e-01	7.6e-01	1.0e+00
Rec	4.0e-01	2.0e-01	3.9e-01	2.4e-01	6.1e-01	1.2e-01	7.5e-01	2.9e-01	4.0e-01	6.6e-01	2.3e-01	1.0e+00	
300	Random	1.8e-01	7.9e-02	4.5e-02	5.8e-05	7.9e-02	1.0e+00	4.6e-01	3.8e-01	5.6e-01	8.4e-01	1.6e-01	1.0e+00
	Stripe	5.0e-01	7.8e-02	2.4e-01	5.9e-03	9.9e-01	3.0e-01	7.9e-01	8.5e-01	4.6e-01	6.1e-02	6.8e-01	8.8e-01
	Star	7.7e-02	4.0e-01	8.1e-01	7.3e-05	9.7e-01	1.0e+00	2.2e-01	2.4e-01	2.7e-01	1.9e-02	8.4e-01	1.0e+00
	Band	5.0e-02	2.8e-01	2.1e-01	2.6e-05	1.6e-01	1.0e+00	6.6e-01	3.8e-01	9.8e-01	2.0e-03	1.6e-01	1.0e+00
	Band-S	3.6e-01	7.3e-01	3.9e-01	1.4e-03	9.7e-01	9.2e-01	7.4e-01	3.1e-01	8.3e-01	3.0e-01	9.9e-01	1.0e+00
	Band-W	8.3e-01	2.2e-02	2.8e-02	5.3e-03	1.0e+00	1.0e+00	6.2e-01	9.8e-01	7.2e-02	8.5e-01	1.0e+00	1.0e+00
Rec	4.0e-01	8.9e-02	6.1e-01	6.8e-03	5.8e-01	9.7e-01	7.6e-01	2.9e-01	4.0e-01	7.1e-01	4.0e-02	1.0e+00	
400	Random	1.8e-01	7.9e-02	4.5e-02	5.5e-03	7.9e-02	1.0e+00	3.9e-01	3.8e-01	5.6e-01	8.4e-01	1.6e-01	1.0e+00
	Stripe	5.0e-01	5.0e-02	2.0e-01	3.4e-02	9.9e-01	9.7e-02	8.4e-01	8.5e-01	4.6e-01	7.8e-02	5.5e-01	9.7e-01
	Star	7.7e-02	3.8e-01	6.7e-01	2.3e-03	8.8e-01	1.0e+00	1.7e-01	2.4e-01	2.7e-01	5.0e-02	5.9e-01	1.0e+00
	Band	5.0e-02	2.8e-01	2.1e-01	3.1e-04	1.6e-01	1.0e+00	7.2e-01	3.8e-01	9.8e-01	2.0e-03	1.6e-01	1.0e+00
	Band-S	3.6e-01	7.1e-01	2.6e-01	4.7e-03	1.0e+00	4.9e-01	8.1e-01	3.1e-01	8.3e-01	3.6e-01	9.7e-01	1.0e+00
	Band-W	8.3e-01	2.2e-02	2.8e-02	2.9e-04	1.0e+00	1.0e+00	7.5e-01	9.8e-01	7.2e-02	8.0e-01	1.0e+00	1.0e+00
Rec	4.0e-01	4.2e-02	7.5e-01	2.3e-01	3.3e-01	8.8e-01	7.6e-01	2.9e-01	4.0e-01	5.1e-01	6.1e-02	1.0e+00	

Table C.13: CL-SL, $\rho = 0.67$: p-values at different run lengths.

C.2.2 Collective vs Individual Learning, $\rho = 0.67$

Iterations	Pattern	DM1	DM2	DM3	DM4	DM5	DM6	DM7	DM8	DM9	DM10	DM11	DM12
10	Random	1.0e+00	9.9e-01	1.0e+00									
	Stripe	9.3e-01	3.3e-01	1.1e-01	9.9e-01	7.1e-01	9.6e-01	7.5e-01	9.5e-01	9.1e-01	1.1e-01	4.2e-04	8.6e-01
	Star	1.0e+00	1.0e+00	1.0e+00	9.9e-01	1.0e+00	1.0e+00	1.0e+00	9.9e-01	1.0e+00	1.0e+00	2.1e-01	1.0e+00
	Band	1.0e+00											
	Band-S	9.1e-01	8.9e-01	9.3e-01	9.0e-01	1.0e+00	1.0e+00	1.0e+00	8.1e-01	9.6e-01	1.0e+00	2.1e-01	3.0e-01
	Band-W	1.0e+00	1.0e+00	1.0e+00	9.8e-01	1.0e+00	1.0e+00	8.4e-01	1.0e+00	1.0e+00	1.0e+00	1.0e+00	4.2e-01
Rec	8.5e-01	1.9e-01	9.6e-01	5.3e-01	8.3e-01	1.0e+00	9.3e-01	6.8e-01	9.3e-01	3.3e-01	2.8e-03	6.8e-01	
50	Random	1.0e+00											
	Stripe	7.7e-01	9.0e-01	9.6e-01	1.4e-01	1.0e+00	1.0e+00	5.8e-01	9.3e-01	8.0e-01	9.6e-01	2.4e-01	9.8e-01
	Star	9.9e-01	1.0e+00	9.7e-01	1.0e+00	1.0e+00	1.0e+00						
	Band	1.0e+00											
	Band-S	8.0e-01	1.0e+00	1.0e+00	6.4e-01	1.0e+00	1.0e+00	6.2e-01	8.5e-01	1.0e+00	1.0e+00	1.0e+00	1.0e+00
	Band-W	1.0e+00	1.0e+00	1.0e+00	1.0e+00	1.0e+00	1.0e+00	5.0e-01	1.0e+00	1.0e+00	1.0e+00	1.0e+00	1.0e+00
Rec	6.5e-01	1.0e+00	1.0e+00	9.4e-01	1.0e+00	1.0e+00	8.9e-01	5.3e-01	8.6e-01	1.0e+00	6.6e-01	1.0e+00	
100	Random	1.0e+00											
	Stripe	7.5e-01	9.7e-01	9.9e-01	1.3e-01	1.0e+00	7.9e-01	5.9e-01	9.2e-01	8.0e-01	1.0e+00	5.2e-01	9.9e-01
	Star	9.9e-01	1.0e+00	1.0e+00	1.0e+00	1.0e+00	1.0e+00	1.0e+00	9.8e-01	1.0e+00	1.0e+00	1.0e+00	1.0e+00
	Band	1.0e+00											
	Band-S	8.0e-01	1.0e+00	1.0e+00	9.1e-01	1.0e+00	1.0e+00	6.2e-01	8.6e-01	1.0e+00	1.0e+00	1.0e+00	1.0e+00
	Band-W	1.0e+00	1.0e+00	1.0e+00	9.9e-01	1.0e+00	1.0e+00	5.0e-01	1.0e+00	1.0e+00	1.0e+00	1.0e+00	1.0e+00
Rec	6.4e-01	1.0e+00	1.0e+00	9.2e-01	1.0e+00	1.0e+00	8.9e-01	5.4e-01	8.7e-01	1.0e+00	9.5e-01	1.0e+00	
200	Random	1.0e+00											
	Stripe	7.5e-01	9.8e-01	1.0e+00	8.6e-01	1.0e+00	9.8e-01	5.7e-01	9.2e-01	7.8e-01	1.0e+00	8.5e-01	1.0e+00
	Star	9.9e-01	1.0e+00	1.0e+00	1.0e+00	1.0e+00	1.0e+00	1.0e+00	9.8e-01	1.0e+00	1.0e+00	1.0e+00	1.0e+00
	Band	1.0e+00											
	Band-S	8.0e-01	1.0e+00	1.0e+00	5.0e-01	1.0e+00	1.0e+00	6.3e-01	8.6e-01	1.0e+00	1.0e+00	1.0e+00	1.0e+00
	Band-W	1.0e+00	1.0e+00	1.0e+00	1.0e+00	1.0e+00	1.0e+00	5.0e-01	1.0e+00	1.0e+00	1.0e+00	1.0e+00	1.0e+00
Rec	6.4e-01	1.0e+00	1.0e+00	8.9e-01	1.0e+00	1.0e+00	8.9e-01	5.4e-01	8.7e-01	1.0e+00	1.0e+00	1.0e+00	
300	Random	1.0e+00											
	Stripe	7.5e-01	9.9e-01	1.0e+00	5.4e-01	1.0e+00	9.7e-01	5.7e-01	9.2e-01	7.8e-01	1.0e+00	9.5e-01	1.0e+00
	Star	9.9e-01	1.0e+00	1.0e+00	9.9e-01	1.0e+00	1.0e+00	1.0e+00	9.8e-01	1.0e+00	1.0e+00	1.0e+00	1.0e+00
	Band	1.0e+00											
	Band-S	8.0e-01	1.0e+00	1.0e+00	9.2e-01	1.0e+00	1.0e+00	6.3e-01	8.5e-01	1.0e+00	1.0e+00	1.0e+00	1.0e+00
	Band-W	1.0e+00	1.0e+00	1.0e+00	1.0e+00	1.0e+00	1.0e+00	5.0e-01	1.0e+00	1.0e+00	1.0e+00	1.0e+00	1.0e+00
Rec	6.4e-01	1.0e+00	1.0e+00	9.8e-01	1.0e+00	1.0e+00	8.9e-01	5.4e-01	8.7e-01	1.0e+00	1.0e+00	1.0e+00	
400	Random	1.0e+00											
	Stripe	7.5e-01	9.9e-01	1.0e+00	1.0e+00	1.0e+00	9.3e-01	5.7e-01	9.2e-01	7.8e-01	1.0e+00	9.8e-01	1.0e+00
	Star	9.9e-01	1.0e+00	1.0e+00	1.0e+00	1.0e+00	1.0e+00	1.0e+00	9.8e-01	1.0e+00	1.0e+00	1.0e+00	1.0e+00
	Band	1.0e+00											
	Band-S	8.0e-01	1.0e+00	1.0e+00	9.7e-01	1.0e+00	1.0e+00	6.3e-01	8.5e-01	1.0e+00	1.0e+00	1.0e+00	1.0e+00
	Band-W	1.0e+00	1.0e+00	1.0e+00	1.0e+00	1.0e+00	1.0e+00	5.0e-01	1.0e+00	1.0e+00	1.0e+00	1.0e+00	1.0e+00
Rec	6.4e-01	1.0e+00	1.0e+00	9.1e-01	1.0e+00	1.0e+00	8.9e-01	5.4e-01	8.7e-01	1.0e+00	1.0e+00	1.0e+00	

Table C.14: CL-IND, $\rho = 0.67$: p-values at different run lengths.

C.2.3 Social vs Individual Learning, $\rho = 0.67$

Iterations	Pattern	DM1	DM2	DM3	DM4	DM5	DM6	DM7	DM8	DM9	DM10	DM11	DM12
10	Random	1.0e+00	7.5e-01										
	Stripe	9.3e-01	3.8e-01	1.5e-01	1.0e+00	7.3e-01	9.8e-01	5.0e-01	7.9e-01	8.6e-01	9.5e-01	3.4e-04	8.9e-01
	Star	1.0e+00	5.3e-01										
	Band	1.0e+00											
	Band-S	9.9e-01	9.0e-01	7.5e-01	1.0e+00	1.0e+00	1.0e+00	8.8e-01	9.9e-01	1.0e+00	7.1e-01	2.7e-02	8.5e-01
	Band-W	1.0e+00	7.9e-01										
Rec	9.1e-01	6.9e-01	4.0e-01	1.0e+00	9.5e-01	1.0e+00	9.3e-01	9.2e-01	9.8e-01	1.6e-01	8.6e-06	6.4e-01	
50	Random	1.0e+00											
	Stripe	7.7e-01	1.0e+00	9.7e-01	8.8e-01	9.6e-01	9.5e-01	2.9e-01	6.3e-01	8.1e-01	1.0e+00	1.3e-01	9.3e-01
	Star	1.0e+00											
	Band	1.0e+00											
	Band-S	9.3e-01	1.0e+00	1.0e+00	1.0e+00	1.0e+00	1.0e+00	6.3e-01	9.6e-01	9.9e-01	1.0e+00	8.1e-01	9.7e-01
	Band-W	1.0e+00	1.0e+00	1.0e+00	1.0e+00	1.0e+00	1.0e+00	9.3e-01	1.0e+00	1.0e+00	1.0e+00	1.0e+00	1.0e+00
Rec	7.4e-01	1.0e+00	1.0e+00	1.0e+00	1.0e+00	1.0e+00	6.4e-01	7.8e-01	9.2e-01	1.0e+00	6.5e-01	9.8e-01	
100	Random	1.0e+00											
	Stripe	7.5e-01	1.0e+00	9.8e-01	9.8e-01	1.0e+00	9.2e-01	2.7e-01	6.1e-01	8.0e-01	1.0e+00	2.5e-01	1.0e+00
	Star	1.0e+00											
	Band	1.0e+00											
	Band-S	9.3e-01	1.0e+00	1.0e+00	1.0e+00	1.0e+00	1.0e+00	5.7e-01	9.6e-01	9.9e-01	1.0e+00	1.0e+00	1.0e+00
	Band-W	1.0e+00	1.0e+00	1.0e+00	1.0e+00	1.0e+00	1.0e+00	8.9e-01	1.0e+00	1.0e+00	1.0e+00	1.0e+00	1.0e+00
Rec	7.2e-01	1.0e+00	1.0e+00	9.8e-01	1.0e+00	1.0e+00	6.6e-01	7.8e-01	9.2e-01	1.0e+00	1.0e+00	1.0e+00	
200	Random	1.0e+00											
	Stripe	7.4e-01	1.0e+00	1.0e+00	1.0e+00	1.0e+00	6.8e-01	2.4e-01	6.0e-01	8.0e-01	1.0e+00	9.5e-01	1.0e+00
	Star	1.0e+00											
	Band	1.0e+00											
	Band-S	9.3e-01	1.0e+00	1.0e+00	1.0e+00	1.0e+00	1.0e+00	4.9e-01	9.6e-01	9.9e-01	1.0e+00	1.0e+00	1.0e+00
	Band-W	1.0e+00	1.0e+00	1.0e+00	1.0e+00	1.0e+00	1.0e+00	7.7e-01	1.0e+00	1.0e+00	1.0e+00	1.0e+00	1.0e+00
Rec	7.2e-01	1.0e+00	1.0e+00	9.8e-01	1.0e+00	1.0e+00	6.6e-01	7.7e-01	9.2e-01	1.0e+00	1.0e+00	1.0e+00	
300	Random	1.0e+00											
	Stripe	7.4e-01	1.0e+00	1.0e+00	9.9e-01	1.0e+00	9.9e-01	2.4e-01	6.0e-01	7.9e-01	1.0e+00	8.5e-01	1.0e+00
	Star	1.0e+00											
	Band	1.0e+00											
	Band-S	9.3e-01	1.0e+00	1.0e+00	1.0e+00	1.0e+00	1.0e+00	3.6e-01	9.6e-01	9.9e-01	1.0e+00	1.0e+00	1.0e+00
	Band-W	1.0e+00	1.0e+00	1.0e+00	1.0e+00	1.0e+00	1.0e+00	5.2e-01	1.0e+00	1.0e+00	1.0e+00	1.0e+00	1.0e+00
Rec	7.2e-01	1.0e+00	1.0e+00	1.0e+00	1.0e+00	1.0e+00	6.4e-01	7.7e-01	9.2e-01	1.0e+00	1.0e+00	1.0e+00	
400	Random	1.0e+00											
	Stripe	7.4e-01	1.0e+00	1.0e+00	1.0e+00	1.0e+00	1.0e+00	1.9e-01	6.0e-01	7.9e-01	1.0e+00	9.9e-01	1.0e+00
	Star	1.0e+00											
	Band	1.0e+00											
	Band-S	9.3e-01	1.0e+00	1.0e+00	1.0e+00	1.0e+00	1.0e+00	2.6e-01	9.6e-01	9.9e-01	1.0e+00	1.0e+00	1.0e+00
	Band-W	1.0e+00	1.0e+00	1.0e+00	1.0e+00	1.0e+00	1.0e+00	3.2e-01	1.0e+00	1.0e+00	1.0e+00	1.0e+00	1.0e+00
Rec	7.2e-01	1.0e+00	1.0e+00	9.8e-01	1.0e+00	1.0e+00	5.9e-01	7.7e-01	9.2e-01	1.0e+00	1.0e+00	1.0e+00	

Table C.15: SL-IND, $\rho = 0.67$: p-values at different run lengths.

C.3 Statistical comparison - II: Collective, Social, and Individual Learning

	Random	Stripe	Star	Band	Band-S	Band-W	Rec
CL-DM1	0.451	0.4	0.4	0.451	0.4	0.4	0.35
SL-DM1	0.457	0.4	0.397	0.403	0.397	0.402	0.369
IND-DM1	0.351	0.399	0.35	0.385	0.38	0.398	0.35
CL-DM2	0.4	0.35	0.329	0.351	0.334	0.371	0.345
SL-DM2	0.373	0.399	0.313	0.351	0.382	0.368	0.35
IND-DM2	0.339	0.393	0.349	0.373	0.353	0.392	0.365
CL-DM3	0.347	0.4	0.343	0.386	0.329	0.344	0.315
SL-DM3	0.372	0.347	0.318	0.343	0.392	0.328	0.301
IND-DM3	0.348	0.395	0.347	0.364	0.35	0.39	0.349
CL-DM4	0.174	0.251	0.197	0.205	0.235	0.191	0.243
SL-DM4	0.208	0.309	0.197	0.225	0.264	0.238	0.253
IND-DM4	0.156	0.255	0.168	0.174	0.211	0.175	0.215
CL-DM5	0.453	0.417	0.385	0.454	0.389	0.472	0.379
SL-DM5	0.443	0.385	0.353	0.474	0.415	0.41	0.392
IND-DM5	0.352	0.399	0.373	0.388	0.372	0.383	0.353
CL-DM6	0.434	0.349	0.376	0.419	0.349	0.346	0.366
SL-DM6	0.372	0.363	0.366	0.325	0.324	0.371	0.326
IND-DM6	0.275	0.333	0.29	0.308	0.329	0.321	0.285
CL-DM7	0.35	0.4	0.45	0.4	0.372	0.403	0.362
SL-DM7	0.45	0.4	0.399	0.462	0.4	0.401	0.377
IND-DM7	0.354	0.4	0.347	0.362	0.376	0.399	0.357
CL-DM8	0.4	0.35	0.386	0.466	0.414	0.45	0.4
SL-DM8	0.438	0.4	0.4	0.44	0.4	0.45	0.392
IND-DM8	0.38	0.35	0.345	0.382	0.35	0.394	0.35
CL-DM9	0.442	0.395	0.35	0.505	0.4	0.429	0.359
SL-DM9	0.437	0.35	0.362	0.45	0.4	0.4	0.35
IND-DM9	0.312	0.384	0.348	0.316	0.35	0.363	0.35
CL-DM10	0.321	0.362	0.301	0.348	0.35	0.316	0.325
SL-DM10	0.348	0.35	0.372	0.3	0.351	0.298	0.35
IND-DM10	0.36	0.365	0.351	0.353	0.36	0.39	0.365
CL-DM11	0.228	0.3	0.298	0.238	0.3	0.302	0.3
SL-DM11	0.228	0.3	0.26	0.252	0.3	0.303	0.294
IND-DM11	0.283	0.381	0.334	0.307	0.353	0.376	0.358
CL-DM12	0.399	0.4	0.422	0.414	0.366	0.454	0.4
SL-DM12	0.381	0.356	0.345	0.344	0.372	0.354	0.351
IND-DM12	0.378	0.39	0.355	0.375	0.35	0.388	0.374

Table C.16: Median values after 10 iterations. Best performance is indicated in bold font. The results which have equal medians with the best performance (in each line) are indicated by light gray color (including the best result in bold). Statistical significance is stated by two-sided pairwise Mann-Whitney-U test with p -value < 0.05.

	Random	Stripe	Star	Band	Band-S	Band-W	Rec
CL-DM1	0.45	0.4	0.4	0.45	0.4	0.4	0.35
SL-DM1	0.5	0.4	0.4	0.45	0.4	0.45	0.4
IND-DM1	0.35	0.4	0.35	0.4	0.4	0.4	0.35
CL-DM2	0.835	0.455	0.473	0.632	0.45	0.656	0.376
SL-DM2	0.789	0.5	0.445	0.685	0.525	0.597	0.404
IND-DM2	0.4	0.4	0.4	0.4	0.4	0.4	0.4
CL-DM3	0.595	0.5	0.415	0.8	0.4	0.478	0.428
SL-DM3	0.743	0.443	0.413	0.654	0.453	0.49	0.316
IND-DM3	0.4	0.4	0.375	0.4	0.4	0.4	0.35
CL-DM4	0.186	0.277	0.206	0.217	0.247	0.223	0.25
SL-DM4	0.203	0.304	0.217	0.267	0.292	0.252	0.248
IND-DM4	0.163	0.274	0.174	0.175	0.242	0.207	0.233
CL-DM5	0.776	0.522	0.453	0.91	0.589	0.77	0.411
SL-DM5	0.77	0.46	0.423	0.758	0.566	0.639	0.508
IND-DM5	0.4	0.4	0.4	0.4	0.399	0.4	0.4
CL-DM6	0.803	0.397	0.438	0.719	0.423	0.462	0.364
SL-DM6	0.611	0.365	0.41	0.574	0.366	0.433	0.34
IND-DM6	0.338	0.336	0.325	0.359	0.338	0.345	0.33
CL-DM7	0.35	0.4	0.45	0.4	0.4	0.4	0.375
SL-DM7	0.45	0.4	0.4	0.5	0.4	0.4	0.4
IND-DM7	0.375	0.4	0.35	0.4	0.4	0.4	0.375
CL-DM8	0.45	0.35	0.4	0.475	0.45	0.45	0.4
SL-DM8	0.45	0.4	0.4	0.5	0.4	0.45	0.4
IND-DM8	0.4	0.35	0.35	0.4	0.4	0.4	0.375
CL-DM9	0.45	0.4	0.375	0.55	0.4	0.45	0.4
SL-DM9	0.5	0.4	0.4	0.5	0.4	0.41	0.35
IND-DM9	0.365	0.4	0.379	0.35	0.35	0.4	0.35
CL-DM10	0.614	0.45	0.442	0.706	0.425	0.526	0.35
SL-DM10	0.702	0.456	0.486	0.56	0.45	0.501	0.415
IND-DM10	0.4	0.4	0.4	0.4	0.4	0.4	0.4
CL-DM11	0.478	0.421	0.375	0.549	0.404	0.511	0.377
SL-DM11	0.437	0.398	0.336	0.454	0.415	0.443	0.364
IND-DM11	0.371	0.4	0.4	0.4	0.4	0.4	0.4
CL-DM12	0.534	0.462	0.562	0.688	0.398	0.675	0.499
SL-DM12	0.398	0.44	0.419	0.394	0.415	0.375	0.332
IND-DM12	0.4	0.4	0.35	0.4	0.397	0.4	0.4

Table C.17: Median values after 50 iterations. Best performance is indicated in bold font. The results which have equal medians with the best performance (in each line) are indicated by light gray color (including the best result in bold). Statistical significance is stated by two-sided pairwise Mann-Whitney-U test with p -value < 0.05.

	Random	Stripe	Star	Band	Band-S	Band-W	Rec
CL-DM1	0.45	0.4	0.4	0.45	0.4	0.4	0.35
SL-DM1	0.5	0.4	0.4	0.45	0.4	0.45	0.4
IND-DM1	0.35	0.4	0.35	0.4	0.4	0.4	0.35
CL-DM2	1	0.55	0.575	1	0.6	0.917	0.425
SL-DM2	1	0.623	0.536	1	0.608	0.701	0.427
IND-DM2	0.4	0.4	0.4	0.4	0.4	0.4	0.4
CL-DM3	1	0.6	0.382	1	0.45	0.713	0.5
SL-DM3	1	0.5	0.423	0.872	0.546	0.497	0.369
IND-DM3	0.4	0.4	0.375	0.4	0.4	0.4	0.35
CL-DM4	0.181	0.285	0.211	0.212	0.24	0.208	0.237
SL-DM4	0.191	0.307	0.25	0.234	0.285	0.246	0.265
IND-DM4	0.16	0.281	0.195	0.183	0.236	0.199	0.21
CL-DM5	1	0.6	0.612	1	0.763	0.951	0.498
SL-DM5	1	0.549	0.538	0.996	0.67	0.711	0.522
IND-DM5	0.4	0.4	0.4	0.4	0.4	0.4	0.4
CL-DM6	0.799	0.38	0.495	0.739	0.408	0.488	0.397
SL-DM6	0.657	0.398	0.426	0.592	0.395	0.434	0.383
IND-DM6	0.375	0.341	0.344	0.354	0.325	0.348	0.327
CL-DM7	0.35	0.4	0.45	0.4	0.4	0.4	0.375
SL-DM7	0.45	0.4	0.4	0.5	0.4	0.4	0.4
IND-DM7	0.375	0.4	0.35	0.4	0.4	0.4	0.375
CL-DM8	0.45	0.35	0.4	0.475	0.45	0.45	0.4
SL-DM8	0.45	0.4	0.4	0.5	0.4	0.45	0.4
IND-DM8	0.4	0.35	0.35	0.4	0.4	0.4	0.375
CL-DM9	0.45	0.4	0.375	0.55	0.4	0.45	0.4
SL-DM9	0.5	0.4	0.4	0.5	0.4	0.425	0.35
IND-DM9	0.372	0.4	0.398	0.35	0.35	0.4	0.35
CL-DM10	1	0.55	0.564	1	0.45	0.71	0.406
SL-DM10	1	0.573	0.529	0.974	0.535	0.674	0.522
IND-DM10	0.4	0.4	0.4	0.4	0.4	0.4	0.4
CL-DM11	0.999	0.492	0.486	0.866	0.45	0.603	0.446
SL-DM11	0.601	0.421	0.372	0.515	0.449	0.595	0.444
IND-DM11	0.4	0.4	0.4	0.449	0.4	0.4	0.4
CL-DM12	0.901	0.563	0.75	1	0.463	0.825	0.568
SL-DM12	0.415	0.561	0.453	0.43	0.387	0.391	0.443
IND-DM12	0.4	0.4	0.35	0.4	0.4	0.4	0.4

Table C.18: Median values after 100 iterations. Best performance is indicated in bold font. The results which have equal medians with the best performance (in each line) are indicated by light gray color (including the best result in bold). Statistical significance is stated by two-sided pairwise Mann-Whitney-U test with p -value<0.05.

	Random	Stripe	Star	Band	Band-S	Band-W	Rec
CL-DM1	0.45	0.4	0.4	0.45	0.4	0.4	0.35
SL-DM1	0.5	0.4	0.4	0.45	0.4	0.45	0.4
IND-DM1	0.35	0.4	0.35	0.4	0.4	0.4	0.35
CL-DM2	1	0.7	0.905	1	0.724	1	0.425
SL-DM2	1	0.75	0.655	1	0.8	1	0.595
IND-DM2	0.4	0.4	0.4	0.4	0.4	0.4	0.4
CL-DM3	1	0.75	0.579	1	0.599	1	0.6
SL-DM3	1	0.55	0.516	1	0.728	0.611	0.534
IND-DM3	0.4	0.4	0.375	0.4	0.4	0.4	0.35
CL-DM4	0.185	0.282	0.187	0.212	0.261	0.234	0.243
SL-DM4	0.194	0.321	0.236	0.226	0.305	0.259	0.245
IND-DM4	0.156	0.281	0.184	0.186	0.244	0.206	0.219
CL-DM5	1	0.788	0.65	1	0.947	1	0.612
SL-DM5	1	0.689	0.616	1	0.792	0.963	0.623
IND-DM5	0.4	0.4	0.4	0.4	0.4	0.4	0.4
CL-DM6	0.82	0.38	0.479	0.773	0.391	0.49	0.405
SL-DM6	0.661	0.383	0.399	0.539	0.422	0.429	0.34
IND-DM6	0.365	0.333	0.334	0.371	0.336	0.331	0.315
CL-DM7	0.35	0.4	0.45	0.4	0.4	0.4	0.375
SL-DM7	0.45	0.4	0.4	0.5	0.4	0.4	0.4
IND-DM7	0.375	0.4	0.35	0.4	0.4	0.4	0.375
CL-DM8	0.45	0.35	0.4	0.475	0.45	0.45	0.4
SL-DM8	0.45	0.4	0.4	0.5	0.4	0.45	0.4
IND-DM8	0.4	0.35	0.35	0.4	0.4	0.4	0.375
CL-DM9	0.45	0.4	0.375	0.55	0.4	0.45	0.4
SL-DM9	0.5	0.4	0.4	0.5	0.4	0.425	0.35
IND-DM9	0.375	0.4	0.4	0.35	0.35	0.4	0.35
CL-DM10	1	0.725	0.888	1	0.452	1	0.647
SL-DM10	1	0.7	0.61	1	0.741	0.895	0.658
IND-DM10	0.4	0.4	0.4	0.4	0.4	0.4	0.4
CL-DM11	1	0.511	0.569	1	0.581	0.943	0.45
SL-DM11	0.878	0.515	0.417	0.804	0.501	0.65	0.449
IND-DM11	0.442	0.4	0.4	0.45	0.4	0.4	0.4
CL-DM12	1	0.65	1	1	0.6	1	0.873
SL-DM12	0.399	0.625	0.397	0.364	0.42	0.433	0.483
IND-DM12	0.4	0.4	0.35	0.4	0.4	0.4	0.4

Table C.19: Median values after 200 iterations. Best performance is indicated in bold font. The results which have equal medians with the best performance (in each line) are indicated by light gray color (including the best result in bold). Statistical significance is stated by two-sided pairwise Mann-Whitney-U test with p -value < 0.05.

	Random	Stripe	Star	Band	Band-S	Band-W	Rec
CL-DM1	0.45	0.4	0.4	0.45	0.4	0.4	0.35
SL-DM1	0.5	0.4	0.4	0.45	0.4	0.45	0.4
IND-DM1	0.35	0.4	0.35	0.4	0.4	0.4	0.35
CL-DM2	1	0.847	1	1	0.825	1	0.624
SL-DM2	1	0.85	0.83	1	0.9	1	0.793
IND-DM2	0.4	0.4	0.4	0.4	0.4	0.4	0.4
CL-DM3	1	0.85	0.979	1	0.625	1	0.785
SL-DM3	1	0.636	0.608	1	0.9	0.95	0.723
IND-DM3	0.4	0.4	0.375	0.4	0.4	0.4	0.35
CL-DM4	0.178	0.273	0.2	0.211	0.259	0.199	0.242
SL-DM4	0.196	0.29	0.242	0.241	0.291	0.255	0.255
IND-DM4	0.157	0.277	0.187	0.173	0.234	0.189	0.237
CL-DM5	1	0.85	0.719	1	1	1	0.679
SL-DM5	1	0.73	0.631	1	0.916	1	0.676
IND-DM5	0.4	0.4	0.4	0.4	0.4	0.4	0.4
CL-DM6	0.833	0.39	0.523	0.782	0.415	0.541	0.334
SL-DM6	0.668	0.35	0.453	0.543	0.41	0.413	0.356
IND-DM6	0.382	0.339	0.323	0.368	0.325	0.327	0.326
CL-DM7	0.35	0.4	0.45	0.4	0.4	0.4	0.375
SL-DM7	0.45	0.4	0.4	0.45	0.4	0.4	0.4
IND-DM7	0.375	0.4	0.35	0.4	0.4	0.4	0.375
CL-DM8	0.45	0.35	0.4	0.475	0.45	0.45	0.4
SL-DM8	0.45	0.4	0.4	0.5	0.4	0.45	0.4
IND-DM8	0.4	0.35	0.35	0.4	0.4	0.4	0.375
CL-DM9	0.45	0.4	0.375	0.55	0.4	0.45	0.4
SL-DM9	0.5	0.4	0.4	0.5	0.4	0.425	0.35
IND-DM9	0.375	0.4	0.4	0.35	0.35	0.4	0.35
CL-DM10	1	0.8	1	1	0.649	1	0.728
SL-DM10	1	0.75	0.626	1	0.922	1	0.842
IND-DM10	0.4	0.4	0.4	0.4	0.4	0.4	0.4
CL-DM11	1	0.55	0.95	1	0.55	1	0.6
SL-DM11	1	0.5	0.355	1	0.573	0.825	0.51
IND-DM11	0.425	0.4	0.4	0.45	0.4	0.4	0.4
CL-DM12	1	0.7	1	1	0.737	1	0.95
SL-DM12	0.46	0.6	0.404	0.397	0.496	0.396	0.409
IND-DM12	0.4	0.4	0.35	0.4	0.4	0.4	0.4

Table C.20: Median values after 300 iterations. Best performance is indicated in bold font. The results which have equal medians with the best performance (in each line) are indicated by light gray color (including the best result in bold). Statistical significance is stated by two-sided pairwise Mann-Whitney-U test with p -value<0.05.

	Random	Stripe	Star	Band	Band-S	Band-W	Rec
CL-DM1	0.45	0.4	0.4	0.45	0.4	0.4	0.35
SL-DM1	0.5	0.4	0.4	0.45	0.4	0.45	0.4
IND-DM1	0.35	0.4	0.35	0.4	0.4	0.4	0.35
CL-DM2	1	0.88	1	1	0.975	1	0.75
SL-DM2	1	0.95	0.98	1	1	1	0.871
IND-DM2	0.4	0.4	0.4	0.4	0.4	0.4	0.4
CL-DM3	1	0.85	1	1	0.675	1	0.946
SL-DM3	1	0.75	0.704	1	1	1	0.7
IND-DM3	0.4	0.4	0.375	0.4	0.4	0.4	0.35
CL-DM4	0.2	0.28	0.216	0.197	0.257	0.216	0.251
SL-DM4	0.203	0.296	0.228	0.238	0.289	0.258	0.26
IND-DM4	0.161	0.276	0.21	0.184	0.257	0.205	0.226
CL-DM5	1	0.944	0.885	1	1	1	0.83
SL-DM5	1	0.769	0.716	1	1	1	0.73
IND-DM5	0.4	0.4	0.4	0.4	0.4	0.4	0.4
CL-DM6	0.821	0.381	0.472	0.755	0.405	0.489	0.363
SL-DM6	0.631	0.378	0.407	0.531	0.395	0.396	0.377
IND-DM6	0.377	0.341	0.351	0.364	0.351	0.33	0.316
CL-DM7	0.35	0.4	0.45	0.4	0.4	0.4	0.375
SL-DM7	0.45	0.4	0.4	0.45	0.4	0.4	0.4
IND-DM7	0.375	0.4	0.35	0.4	0.4	0.4	0.375
CL-DM8	0.45	0.35	0.4	0.475	0.45	0.45	0.4
SL-DM8	0.45	0.4	0.4	0.5	0.4	0.45	0.4
IND-DM8	0.4	0.35	0.35	0.4	0.4	0.4	0.375
CL-DM9	0.45	0.4	0.375	0.55	0.4	0.45	0.4
SL-DM9	0.5	0.4	0.4	0.5	0.4	0.425	0.35
IND-DM9	0.375	0.4	0.4	0.35	0.35	0.4	0.35
CL-DM10	1	0.9	1	1	0.578	1	0.95
SL-DM10	1	0.762	0.684	1	1	1	0.938
IND-DM10	0.4	0.4	0.4	0.4	0.4	0.4	0.4
CL-DM11	1	0.572	1	1	0.7	1	0.547
SL-DM11	1	0.6	0.421	1	0.65	1	0.628
IND-DM11	0.425	0.4	0.4	0.45	0.4	0.4	0.4
CL-DM12	1	0.775	1	1	0.85	1	1
SL-DM12	0.373	0.701	0.4	0.441	0.585	0.384	0.516
IND-DM12	0.4	0.4	0.35	0.4	0.4	0.4	0.4

Table C.21: Median values after 400 iterations. Best performance is indicated in bold font. The results which have equal medians with the best performance (in each line) are indicated by light gray color (including the best result in bold). Statistical significance is stated by two-sided pairwise Mann-Whitney-U test with p -value < 0.05.

C.3.1 Collective vs Social Learning, $\rho = 0.93$

Iterations	Pattern	DM1	DM2	DM3	DM4	DM5	DM6	DM7	DM8	DM9	DM10	DM11	DM12
10	Random	8.5e-01	5.3e-01	7.9e-02	2.8e-03	6.0e-01	9.5e-01	5.2e-02	4.5e-01	4.4e-01	4.4e-01	5.3e-01	8.1e-01
	Stripe	6.6e-01	1.3e-01	9.8e-01	1.0e-05	9.6e-01	5.9e-01	4.0e-01	2.0e-02	9.2e-01	9.0e-01	3.6e-01	5.6e-01
	Star	7.8e-01	4.5e-01	8.6e-01	1.9e-01	9.3e-01	9.5e-01	9.6e-01	3.7e-01	5.4e-01	2.0e-02	9.0e-01	9.9e-01
	Band	9.6e-01	7.2e-01	9.4e-01	4.6e-02	6.7e-01	9.9e-01	1.1e-01	5.8e-01	9.1e-01	8.9e-01	1.3e-01	9.7e-01
	Band-S	5.7e-01	5.0e-02	9.6e-02	5.2e-02	3.8e-01	5.5e-01	1.5e-01	3.0e-01	4.2e-01	5.6e-01	5.7e-01	2.1e-01
	Band-W	4.1e-01	6.0e-01	6.3e-01	3.0e-03	9.8e-01	2.3e-01	6.6e-01	3.0e-01	7.0e-01	7.1e-01	4.2e-01	1.0e+00
50	Rec	9.6e-02	2.5e-02	4.3e-01	5.0e-01	1.8e-01	5.2e-01	2.6e-01	8.7e-01	9.1e-01	3.0e-01	6.8e-01	9.8e-01
	Random	6.9e-01	8.1e-01	1.2e-01	2.8e-02	3.2e-01	1.0e+00	2.5e-02	4.4e-01	1.1e-01	3.8e-01	8.2e-01	7.1e-01
	Stripe	5.4e-01	5.6e-02	1.0e+00	1.2e-01	9.6e-01	8.0e-01	4.5e-01	4.3e-02	9.3e-01	3.0e-01	8.2e-01	8.1e-01
	Star	7.5e-01	6.0e-01	6.6e-01	1.5e-01	8.8e-01	7.5e-01	9.0e-01	3.6e-01	4.9e-01	1.3e-01	7.9e-01	9.9e-01
	Band	9.1e-01	4.0e-01	9.4e-01	1.5e-03	9.9e-01	1.0e+00	8.7e-02	4.4e-01	6.5e-01	7.9e-01	8.4e-01	9.9e-01
	Band-S	6.0e-01	2.6e-02	1.5e-01	2.1e-02	9.4e-01	9.9e-01	2.4e-01	3.9e-01	4.3e-01	8.9e-02	6.0e-01	1.1e-01
100	Band-W	3.6e-01	8.5e-01	4.8e-01	2.7e-03	1.0e+00	5.7e-01	6.7e-01	2.0e-01	8.4e-01	5.3e-01	9.2e-01	1.0e+00
	Rec	1.0e-01	2.0e-01	9.7e-01	3.9e-01	9.8e-02	7.1e-01	2.0e-01	8.1e-01	8.4e-01	1.2e-01	4.5e-01	1.0e+00
	Random	6.9e-01	6.6e-01	6.1e-02	1.9e-01	5.8e-02	1.0e+00	2.8e-02	4.5e-01	1.2e-01	1.7e-01	1.0e+00	7.9e-01
	Stripe	5.3e-01	7.6e-02	9.9e-01	5.5e-02	9.7e-01	3.3e-01	4.7e-01	3.4e-02	9.4e-01	1.9e-01	6.5e-01	8.4e-01
	Star	7.5e-01	8.6e-01	4.7e-01	2.6e-04	9.0e-01	9.7e-01	8.9e-01	3.6e-01	5.0e-01	3.6e-01	9.7e-01	9.9e-01
	Band	9.1e-01	2.2e-01	9.4e-01	8.8e-02	9.6e-01	1.0e+00	1.0e-01	4.3e-01	6.4e-01	4.9e-01	1.0e+00	9.9e-01
200	Band-S	6.1e-01	1.4e-01	1.2e-01	7.8e-04	8.6e-01	5.6e-01	2.7e-01	3.9e-01	4.0e-01	1.3e-01	6.0e-01	4.6e-01
	Band-W	3.6e-01	9.3e-01	9.7e-01	1.4e-03	1.0e+00	9.9e-01	7.2e-01	2.1e-01	8.3e-01	8.8e-01	7.6e-01	1.0e+00
	Rec	1.1e-01	1.9e-01	9.4e-01	1.0e-01	1.7e-01	4.5e-01	2.0e-01	8.2e-01	8.6e-01	1.3e-01	4.6e-01	9.9e-01
	Random	6.9e-01	1.5e-01	1.5e-03	1.6e-01	1.3e-03	1.0e+00	3.1e-02	4.5e-01	1.2e-01	8.5e-02	1.0e+00	8.4e-01
	Stripe	5.3e-01	2.6e-01	9.9e-01	7.6e-03	1.0e+00	3.7e-01	5.2e-01	3.4e-02	9.4e-01	5.5e-01	6.6e-01	9.4e-01
	Star	7.5e-01	7.7e-01	4.9e-01	4.0e-05	5.3e-01	9.9e-01	8.5e-01	3.6e-01	5.0e-01	5.8e-01	9.9e-01	9.8e-01
300	Band	9.1e-01	6.5e-02	5.1e-01	2.2e-02	6.0e-01	1.0e+00	1.4e-01	4.3e-01	6.4e-01	2.0e-01	1.0e+00	9.8e-01
	Band-S	6.0e-01	2.4e-01	4.7e-02	2.3e-02	9.4e-01	3.6e-01	3.4e-01	3.9e-01	4.0e-01	6.6e-02	6.0e-01	6.1e-01
	Band-W	3.6e-01	9.1e-01	1.0e+00	3.9e-02	1.0e+00	1.0e+00	8.3e-01	2.1e-01	8.3e-01	9.4e-01	1.0e+00	1.0e+00
	Rec	1.0e-01	1.8e-01	7.1e-01	2.1e-01	2.3e-01	9.6e-01	1.8e-01	8.2e-01	8.6e-01	2.2e-01	5.4e-01	9.9e-01
	Random	6.9e-01	9.9e-02	7.9e-05	8.5e-03	7.0e-04	1.0e+00	2.9e-02	4.5e-01	1.2e-01	4.5e-02	1.0e+00	8.4e-01
	Stripe	5.3e-01	2.2e-01	9.6e-01	8.9e-02	9.9e-01	9.5e-01	6.0e-01	3.4e-02	9.4e-01	7.0e-01	6.2e-01	9.8e-01
400	Star	7.5e-01	8.0e-01	4.2e-01	4.0e-03	3.3e-01	9.9e-01	8.4e-01	3.6e-01	5.0e-01	5.5e-01	1.0e+00	9.9e-01
	Band	9.1e-01	2.5e-02	1.3e-01	7.6e-03	2.2e-01	1.0e+00	2.1e-01	4.3e-01	6.4e-01	2.0e-01	1.0e+00	9.8e-01
	Band-S	6.0e-01	1.9e-01	2.6e-02	6.1e-03	8.8e-01	8.5e-01	4.8e-01	3.9e-01	4.0e-01	1.2e-01	4.7e-01	6.8e-01
	Band-W	3.6e-01	8.5e-01	1.0e+00	2.2e-03	1.0e+00	1.0e+00	8.8e-01	2.1e-01	8.3e-01	9.4e-01	1.0e+00	1.0e+00
	Rec	1.0e-01	2.9e-01	6.3e-01	1.3e-01	2.7e-01	3.3e-01	1.7e-01	8.2e-01	8.6e-01	1.8e-01	7.4e-01	9.9e-01
	Random	6.9e-01	9.9e-02	7.9e-05	3.6e-01	1.9e-04	1.0e+00	2.5e-02	4.5e-01	1.2e-01	4.5e-02	9.9e-01	8.5e-01
400	Stripe	5.3e-01	2.0e-01	9.1e-01	7.0e-02	9.9e-01	6.7e-01	6.3e-01	3.4e-02	9.4e-01	6.5e-01	4.5e-01	9.6e-01
	Star	7.5e-01	7.7e-01	3.5e-01	1.7e-01	3.7e-01	9.8e-01	8.2e-01	3.6e-01	5.0e-01	4.3e-01	1.0e+00	9.9e-01
	Band	9.1e-01	1.6e-02	8.8e-02	1.8e-03	1.7e-01	1.0e+00	2.8e-01	4.3e-01	6.4e-01	1.3e-01	9.9e-01	9.8e-01
	Band-S	6.0e-01	1.6e-01	1.7e-02	4.2e-03	9.0e-01	5.5e-01	5.7e-01	3.9e-01	4.0e-01	9.5e-02	6.6e-01	6.2e-01
	Band-W	3.6e-01	7.8e-01	9.9e-01	4.1e-03	1.0e+00	1.0e+00	9.4e-01	2.1e-01	8.3e-01	8.8e-01	1.0e+00	1.0e+00
	Rec	1.0e-01	3.3e-01	7.0e-01	7.8e-02	3.9e-01	5.1e-01	1.7e-01	8.2e-01	8.6e-01	1.4e-01	3.8e-01	9.9e-01

Table C.22: CL-SL, $\rho = 0.93$: p-values at different run lengths.

C.3.2 Collective vs Individual Learning, $\rho = 0.93$

Iterations	Pattern	DM1	DM2	DM3	DM4	DM5	DM6	DM7	DM8	DM9	DM10	DM11	DM12
10	Random	1.0e+00	9.7e-01	4.0e-01	9.9e-01	9.8e-01	1.0e+00	7.6e-01	9.4e-01	1.0e+00	2.8e-01	2.8e-03	7.2e-01
	Stripe	4.4e-01	5.7e-02	3.6e-01	4.7e-01	9.3e-01	9.4e-01	1.4e-01	3.5e-01	6.7e-01	6.3e-01	4.1e-05	6.8e-01
	Star	1.0e+00	1.2e-01	5.6e-01	1.0e+00	5.3e-01	1.0e+00	1.0e+00	9.2e-01	7.8e-01	1.2e-01	1.8e-02	9.9e-01
	Band	1.0e+00	5.2e-01	8.6e-01	1.0e+00	1.0e+00	1.0e+00	8.0e-01	9.9e-01	1.0e+00	3.9e-01	6.4e-06	9.6e-01
	Band-S	9.0e-01	9.3e-02	1.7e-01	9.8e-01	9.3e-01	9.7e-01	8.0e-01	9.8e-01	1.0e+00	9.3e-02	5.0e-03	4.3e-01
	Band-W	6.6e-01	1.8e-01	1.7e-02	9.9e-01	1.0e+00	9.2e-01	9.4e-01	9.9e-01	1.0e+00	4.4e-03	2.9e-04	1.0e+00
Rec	6.1e-01	5.2e-04	3.0e-02	9.8e-01	8.5e-01	9.9e-01	5.0e-01	9.6e-01	9.6e-01	1.0e-02	1.3e-03	8.6e-01	
50	Random	1.0e+00	1.0e+00	9.5e-01	9.8e-01	1.0e+00	1.0e+00	5.1e-01	9.2e-01	9.9e-01	1.0e+00	9.8e-01	7.1e-01
	Stripe	2.2e-01	9.9e-01	1.0e+00	7.3e-01	1.0e+00	1.0e+00	6.3e-02	3.0e-01	6.5e-01	9.8e-01	8.6e-01	1.0e+00
	Star	9.7e-01	9.3e-01	8.9e-01	9.7e-01	9.7e-01	1.0e+00	1.0e+00	8.3e-01	6.3e-01	8.6e-01	3.6e-01	1.0e+00
	Band	1.0e+00	9.8e-01	1.0e+00	1.0e+00	1.0e+00	1.0e+00	4.8e-01	9.8e-01	1.0e+00	1.0e+00	9.9e-01	1.0e+00
	Band-S	6.5e-01	8.8e-01	8.5e-01	8.4e-01	1.0e+00	1.0e+00	7.3e-01	9.4e-01	1.0e+00	8.9e-01	8.6e-01	5.6e-01
	Band-W	5.0e-01	1.0e+00	9.0e-01	8.7e-01	1.0e+00	1.0e+00	7.7e-01	9.5e-01	9.9e-01	9.8e-01	1.0e+00	1.0e+00
Rec	4.4e-01	2.3e-01	9.5e-01	8.3e-01	9.5e-01	9.8e-01	2.6e-01	9.3e-01	8.7e-01	3.8e-01	4.2e-01	1.0e+00	
100	Random	1.0e+00	1.0e+00	1.0e+00	9.8e-01	1.0e+00	1.0e+00	5.6e-01	9.2e-01	9.9e-01	1.0e+00	1.0e+00	8.1e-01
	Stripe	2.2e-01	1.0e+00	1.0e+00	4.0e-01	1.0e+00	9.9e-01	5.2e-02	2.8e-01	6.5e-01	1.0e+00	1.0e+00	1.0e+00
	Star	9.6e-01	1.0e+00	5.9e-01	8.9e-01	9.9e-01	1.0e+00	1.0e+00	8.2e-01	5.7e-01	9.7e-01	1.0e+00	9.9e-01
	Band	1.0e+00	1.0e+00	1.0e+00	1.0e+00	1.0e+00	1.0e+00	4.7e-01	9.8e-01	1.0e+00	1.0e+00	1.0e+00	9.9e-01
	Band-S	6.4e-01	1.0e+00	8.7e-01	5.4e-01	1.0e+00	1.0e+00	7.2e-01	9.3e-01	1.0e+00	7.4e-01	9.8e-01	7.1e-01
	Band-W	4.9e-01	1.0e+00	1.0e+00	4.8e-01	1.0e+00	1.0e+00	7.7e-01	9.5e-01	9.9e-01	1.0e+00	1.0e+00	1.0e+00
Rec	4.6e-01	6.2e-01	1.0e+00	9.5e-01	9.8e-01	1.0e+00	2.6e-01	9.3e-01	8.7e-01	8.3e-01	9.4e-01	9.9e-01	
200	Random	1.0e+00	1.0e+00	1.0e+00	1.0e+00	1.0e+00	1.0e+00	5.7e-01	9.2e-01	9.8e-01	1.0e+00	1.0e+00	8.4e-01
	Stripe	2.2e-01	1.0e+00	1.0e+00	6.7e-01	1.0e+00	9.9e-01	5.2e-02	2.9e-01	6.4e-01	1.0e+00	1.0e+00	1.0e+00
	Star	9.6e-01	1.0e+00	9.5e-01	7.4e-01	1.0e+00	1.0e+00	1.0e+00	8.2e-01	5.5e-01	9.6e-01	1.0e+00	9.8e-01
	Band	1.0e+00	1.0e+00	1.0e+00	9.9e-01	1.0e+00	1.0e+00	4.7e-01	9.8e-01	1.0e+00	1.0e+00	1.0e+00	9.8e-01
	Band-S	6.3e-01	1.0e+00	9.1e-01	9.5e-01	1.0e+00	1.0e+00	7.2e-01	9.2e-01	1.0e+00	7.9e-01	1.0e+00	7.7e-01
	Band-W	4.9e-01	1.0e+00	1.0e+00	9.9e-01	1.0e+00	1.0e+00	7.7e-01	9.5e-01	9.9e-01	1.0e+00	1.0e+00	1.0e+00
Rec	4.5e-01	5.9e-01	1.0e+00	9.8e-01	1.0e+00	1.0e+00	2.6e-01	9.3e-01	8.6e-01	9.8e-01	9.9e-01	9.9e-01	
300	Random	1.0e+00	1.0e+00	1.0e+00	9.9e-01	1.0e+00	1.0e+00	5.7e-01	9.2e-01	9.8e-01	1.0e+00	1.0e+00	8.4e-01
	Stripe	2.2e-01	1.0e+00	1.0e+00	2.4e-01	1.0e+00	1.0e+00	5.2e-02	2.9e-01	6.4e-01	1.0e+00	1.0e+00	1.0e+00
	Star	9.6e-01	1.0e+00	9.6e-01	9.2e-01	9.9e-01	1.0e+00	1.0e+00	8.2e-01	5.5e-01	9.1e-01	1.0e+00	9.9e-01
	Band	1.0e+00	1.0e+00	1.0e+00	1.0e+00	1.0e+00	1.0e+00	4.7e-01	9.8e-01	1.0e+00	1.0e+00	1.0e+00	9.8e-01
	Band-S	6.3e-01	1.0e+00	9.5e-01	9.8e-01	1.0e+00	1.0e+00	7.2e-01	9.2e-01	1.0e+00	6.1e-01	1.0e+00	7.0e-01
	Band-W	4.9e-01	1.0e+00	1.0e+00	9.1e-01	1.0e+00	1.0e+00	7.7e-01	9.5e-01	9.9e-01	1.0e+00	1.0e+00	1.0e+00
Rec	4.5e-01	8.3e-01	1.0e+00	6.4e-01	1.0e+00	9.1e-01	2.6e-01	9.3e-01	8.6e-01	9.9e-01	1.0e+00	9.9e-01	
400	Random	1.0e+00	1.0e+00	1.0e+00	1.0e+00	1.0e+00	1.0e+00	5.7e-01	9.2e-01	9.8e-01	1.0e+00	1.0e+00	8.4e-01
	Stripe	2.2e-01	1.0e+00	1.0e+00	5.7e-01	1.0e+00	1.0e+00	5.2e-02	2.9e-01	6.3e-01	1.0e+00	1.0e+00	1.0e+00
	Star	9.6e-01	1.0e+00	9.5e-01	9.6e-01	1.0e+00	1.0e+00	1.0e+00	8.2e-01	5.5e-01	8.9e-01	1.0e+00	9.9e-01
	Band	1.0e+00	1.0e+00	1.0e+00	9.1e-01	1.0e+00	1.0e+00	4.7e-01	9.8e-01	1.0e+00	1.0e+00	1.0e+00	9.8e-01
	Band-S	6.3e-01	1.0e+00	9.0e-01	6.8e-01	1.0e+00	1.0e+00	7.2e-01	9.2e-01	1.0e+00	7.6e-01	1.0e+00	6.9e-01
	Band-W	4.9e-01	1.0e+00	1.0e+00	9.2e-01	1.0e+00	1.0e+00	7.7e-01	9.5e-01	9.9e-01	1.0e+00	1.0e+00	1.0e+00
Rec	4.5e-01	8.2e-01	1.0e+00	9.1e-01	1.0e+00	1.0e+00	2.6e-01	9.3e-01	8.6e-01	9.4e-01	1.0e+00	9.9e-01	

Table C.23: CL-IND, $\rho = 0.93$: p-values at different run lengths.

C.3.3 Social vs Individual Learning, $\rho = 0.93$

Iterations	Pattern	DM1	DM2	DM3	DM4	DM5	DM6	DM7	DM8	DM9	DM10	DM11	DM12
10	Random	1.0e+00	9.1e-01	9.0e-01	1.0e+00	1.0e+00	1.0e+00	1.0e+00	9.9e-01	1.0e+00	4.2e-01	5.7e-04	3.9e-01
	Stripe	2.6e-01	4.9e-01	1.8e-03	1.0e+00	3.6e-01	9.2e-01	2.0e-01	9.7e-01	1.3e-01	1.4e-01	4.7e-04	6.4e-01
	Star	9.6e-01	1.1e-01	7.7e-02	1.0e+00	4.5e-02	9.9e-01	9.8e-01	9.8e-01	8.5e-01	8.6e-01	4.0e-05	2.5e-01
	Band	7.1e-01	2.8e-01	1.8e-01	1.0e+00	1.0e+00	8.8e-01	1.0e+00	9.9e-01	1.0e+00	1.6e-02	4.9e-04	2.9e-01
	Band-S	8.4e-01	7.1e-01	8.5e-01	1.0e+00	9.7e-01	9.3e-01	9.8e-01	9.9e-01	1.0e+00	6.1e-02	2.6e-03	7.8e-01
	Band-W	7.8e-01	7.9e-02	4.3e-03	1.0e+00	9.1e-01	9.8e-01	8.3e-01	1.0e+00	9.9e-01	1.6e-04	9.1e-04	2.9e-01
Rec	9.5e-01	1.1e-01	4.4e-02	9.8e-01	9.7e-01	9.9e-01	7.9e-01	7.3e-01	6.3e-01	9.0e-02	4.1e-05	1.0e-01	
50	Random	1.0e+00	9.7e-01	1.0e+00	1.0e+00	9.7e-01	2.3e-01						
	Stripe	1.8e-01	1.0e+00	5.7e-01	9.6e-01	1.0e+00	1.0e+00	5.9e-02	9.2e-01	1.1e-01	1.0e+00	4.2e-01	9.9e-01
	Star	8.1e-01	9.9e-01	8.6e-01	1.0e+00	8.9e-01	1.0e+00	9.6e-01	9.6e-01	6.9e-01	9.9e-01	4.6e-02	9.0e-01
	Band	7.8e-01	1.0e+00	1.0e+00	1.0e+00	1.0e+00	1.0e+00	1.0e+00	9.9e-01	1.0e+00	1.0e+00	8.6e-01	7.3e-01
	Band-S	5.3e-01	1.0e+00	1.0e+00	1.0e+00	1.0e+00	9.4e-01	9.2e-01	9.6e-01	1.0e+00	9.9e-01	6.9e-01	9.7e-01
	Band-W	7.2e-01	1.0e+00	9.5e-01	1.0e+00	1.0e+00	1.0e+00	5.8e-01	9.9e-01	9.3e-01	9.6e-01	8.8e-01	2.0e-01
Rec	9.0e-01	4.8e-01	1.1e-01	8.7e-01	1.0e+00	8.8e-01	6.5e-01	6.7e-01	5.5e-01	9.2e-01	5.6e-01	8.8e-02	
100	Random	1.0e+00	1.0e+00	1.0e+00	9.9e-01	1.0e+00	1.0e+00	1.0e+00	9.7e-01	1.0e+00	1.0e+00	1.0e+00	7.7e-01
	Stripe	1.8e-01	1.0e+00	1.0e+00	9.4e-01	1.0e+00	1.0e+00	3.9e-02	9.3e-01	9.1e-02	1.0e+00	9.3e-01	1.0e+00
	Star	8.1e-01	1.0e+00	9.7e-01	1.0e+00	1.0e+00	1.0e+00	9.8e-01	9.5e-01	6.4e-01	1.0e+00	4.3e-01	9.7e-01
	Band	7.7e-01	1.0e+00	1.0e+00	1.0e+00	1.0e+00	1.0e+00	1.0e+00	9.9e-01	9.9e-01	1.0e+00	1.0e+00	7.1e-01
	Band-S	5.2e-01	1.0e+00	1.0e+00	1.0e+00	1.0e+00	1.0e+00	8.9e-01	9.5e-01	1.0e+00	9.8e-01	9.9e-01	4.6e-01
	Band-W	7.0e-01	1.0e+00	9.1e-01	1.0e+00	1.0e+00	1.0e+00	4.9e-01	9.9e-01	9.3e-01	1.0e+00	1.0e+00	2.8e-01
Rec	9.0e-01	8.5e-01	7.3e-01	1.0e+00	1.0e+00	1.0e+00	6.6e-01	6.8e-01	5.2e-01	1.0e+00	9.7e-01	7.7e-01	
200	Random	1.0e+00	9.7e-01	1.0e+00	1.0e+00	1.0e+00	6.7e-01						
	Stripe	1.8e-01	1.0e+00	1.0e+00	1.0e+00	1.0e+00	1.0e+00	3.2e-02	9.3e-01	8.8e-02	1.0e+00	1.0e+00	1.0e+00
	Star	8.1e-01	1.0e+00	9.9e-01	1.0e+00	1.0e+00	1.0e+00	9.8e-01	9.5e-01	6.2e-01	1.0e+00	6.8e-01	7.1e-01
	Band	7.7e-01	1.0e+00	1.0e+00	1.0e+00	1.0e+00	1.0e+00	9.9e-01	9.9e-01	1.0e+00	1.0e+00	1.0e+00	2.9e-01
	Band-S	5.2e-01	1.0e+00	1.0e+00	1.0e+00	1.0e+00	1.0e+00	8.6e-01	9.5e-01	1.0e+00	1.0e+00	1.0e+00	6.6e-01
	Band-W	6.9e-01	1.0e+00	9.8e-01	1.0e+00	1.0e+00	1.0e+00	3.0e-01	9.9e-01	9.3e-01	9.9e-01	1.0e+00	7.5e-01
Rec	9.0e-01	9.8e-01	1.0e+00	1.0e+00	1.0e+00	9.9e-01	6.7e-01	6.8e-01	5.0e-01	1.0e+00	9.9e-01	9.3e-01	
300	Random	1.0e+00	9.7e-01	1.0e+00	1.0e+00	1.0e+00	9.8e-01						
	Stripe	1.8e-01	1.0e+00	1.0e+00	7.9e-01	1.0e+00	7.2e-01	2.3e-02	9.3e-01	8.8e-02	1.0e+00	1.0e+00	1.0e+00
	Star	8.1e-01	9.9e-01	1.0e+00	1.0e+00	1.0e+00	1.0e+00	9.9e-01	9.5e-01	6.2e-01	9.9e-01	1.8e-01	8.2e-01
	Band	7.7e-01	1.0e+00	1.0e+00	1.0e+00	1.0e+00	1.0e+00	9.8e-01	9.9e-01	1.0e+00	1.0e+00	1.0e+00	7.1e-01
	Band-S	5.2e-01	1.0e+00	1.0e+00	1.0e+00	1.0e+00	1.0e+00	7.6e-01	9.5e-01	1.0e+00	1.0e+00	1.0e+00	8.2e-01
	Band-W	6.9e-01	1.0e+00	1.0e+00	1.0e+00	1.0e+00	1.0e+00	2.1e-01	9.9e-01	9.3e-01	1.0e+00	1.0e+00	3.0e-01
Rec	9.0e-01	1.0e+00	1.0e+00	9.1e-01	1.0e+00	9.8e-01	6.8e-01	6.8e-01	5.0e-01	1.0e+00	9.9e-01	6.4e-01	
400	Random	1.0e+00	9.7e-01	1.0e+00	1.0e+00	1.0e+00	2.4e-01						
	Stripe	1.8e-01	1.0e+00	1.0e+00	9.5e-01	1.0e+00	9.8e-01	1.9e-02	9.3e-01	8.5e-02	1.0e+00	1.0e+00	1.0e+00
	Star	8.1e-01	9.9e-01	1.0e+00	1.0e+00	1.0e+00	9.9e-01	9.9e-01	9.5e-01	6.2e-01	1.0e+00	6.6e-01	7.6e-01
	Band	7.7e-01	1.0e+00	1.0e+00	1.0e+00	1.0e+00	1.0e+00	9.6e-01	9.9e-01	1.0e+00	1.0e+00	1.0e+00	9.6e-01
	Band-S	5.2e-01	1.0e+00	1.0e+00	1.0e+00	1.0e+00	1.0e+00	6.8e-01	9.5e-01	1.0e+00	1.0e+00	1.0e+00	9.9e-01
	Band-W	6.9e-01	1.0e+00	1.0e+00	1.0e+00	1.0e+00	1.0e+00	9.2e-02	9.9e-01	9.3e-01	1.0e+00	1.0e+00	6.0e-01
Rec	9.0e-01	1.0e+00	1.0e+00	9.9e-01	1.0e+00	1.0e+00	6.8e-01	6.8e-01	5.0e-01	1.0e+00	1.0e+00	9.4e-01	

Table C.24: SL-IND, $\rho = 0.93$: p-values at different run lengths.

Ehrenerklärung

Ich versichere hiermit, dass ich die vorliegende Arbeit ohne unzulässige Hilfe Dritter und ohne Benutzung anderer als der angegebenen Hilfsmittel angefertigt habe; verwendete fremde und eigene Quellen sind als solche kenntlich gemacht. Insbesondere habe ich nicht die Hilfe eines kommerziellen Promotionsberaters in Anspruch genommen. Dritte haben von mir weder unmittelbar noch mittelbar geldwerte Leistungen für Arbeiten erhalten, die im Zusammenhang mit dem Inhalt der vorgelegten Dissertation stehen.

Ich habe insbesondere nicht wissentlich:

- Ergebnisse erfunden oder widersprüchliche Ergebnisse verschwiegen,
- statistische Verfahren absichtlich missbraucht, um Daten in ungerechtfertigter Weise zu interpretieren,
- fremde Ergebnisse oder Veröffentlichungen plagiiert,
- fremde Forschungsergebnisse verzerrt wiedergegeben.

Mir ist bekannt, dass Verstöße gegen das Urheberrecht Unterlassungs- und Schadensersatzansprüche des Urhebers sowie eine strafrechtliche Ahndung durch die Strafverfolgungsbehörden begründen kann. Die Arbeit wurde bisher weder im Inland noch im Ausland in gleicher oder ähnlicher Form als Dissertation eingereicht und ist als Ganzes auch noch nicht veröffentlicht.

Magdeburg, den 21.06.2021

Palina Bartashevich